Analysis of Changes in the Potato Leaf Proteome Triggered by Phosphite Reveals Functions Associated with Induced Resistance Against *Phytophthora infestans*

by

Sanghyun Lim

Submitted in partial fulfilment of the requirements

for the degree of Doctor of Philosophy

at

Dalhousie University
Halifax, Nova Scotia
November 2012

DALHOUSIE UNIVERSITY

DEPARTMENT OF BIOLOGY

The undersigned hereby certify that they have read and recommend to the Faculty of Graduate Studies for acceptance a thesis entitled "Analysis of Changes in the Potato Leaf Proteome Triggered by Phosphite Reveals Functions Associated with Induced Resistance Against *Phytophthora infestans*" by Sanghyun Lim in partial fulfilment of the requirements for the degree of Doctor of Philosophy.

Dated: November 13, 2012

External Examiner: _____

Research Co-Supervisors: _____

Examining Committee: _____

_____

Departmental Representative: _____

DALHOUSIE UNIVERSITY

DATE: November 13, 2012

AUTHOR: Sanghyun Lim

TITLE: Analysis of Changes in the Potato Leaf Proteome Triggered by Phosphite Reveals Functions Associated with Induced Resistance Against *Phytophthora infestans*

DEPARTMENT OR SCHOOL: Department of Biology

DEGREE: PhD CONVOCATION: May YEAR: 2013

_____

Signature of Author

Table of Contents

List of Tables

List of Figures

Abstract

Exogenous chemicals can be used to stimulate induced resistance (IR), a process related to increased disease resistance of susceptible plants against a broad range of pathogens. The identification of molecular components related to IR provides an understanding of the mechanisms related to host resistance to pathogens. Environmentally friendly phosphite (Phi)-based fungicides are increasingly used in controlling oomycete pathogens such as *Phytophthora infestans*, causing late blight of potatoes and other solanaceous crops. Their efficacy was clearly proven by field trials carried out by a group of researchers led by Wang-Pruski. Nevertheless, the molecular mechanisms responsible for stimulation of IR by Phi-based fungicides have not been fully documented.

In this study, 93 differentially regulated proteins (62 up-regulated and 31 down-regulated proteins) in Phi-treated potato leaves were identified by iTRAQ-based quantitative proteomics. The majority of these differentially regulated proteins have not been previously reported. Identification of the differentially regulated proteins revealed two major molecular mechanisms related to defense and metabolism for energy generation. Defense mechanisms include the hypersensitive response (HR), reactive oxygen species pathway, salicylic acid-dependent pathway, and antimicrobial activities. Energy generating metabolisms include glycolysis, photosynthesis, and starch degradation.

Four days post inoculation with *P. infestans*, the abundance of 16 of the 93 differentially regulated proteins increased significantly in the Phi-treated plants compared with that of the control plants. On the other hand, the abundance of 9 of the 93 differentially regulated proteins was decreased in the Phi-treated plants compared to that of the control plants. The abundance of the remaining 68 differentially regulated proteins was unchanged for both challenged Phi-treated and control plants. This suggests that pre-activation of proteins in Phi-treated sample before infection is essential to increase the levels of host resistance to the pathogen. Many of the 68 differentially regulated proteins that did not change after infection play roles in HR. These proteins include cathepsin B, cysteine protease inhibitors, and proteins involved in reactive oxygen species and salicylic acid pathways. Callose deposition and subcellular changes related to HR were observed in the Phi-treated plants, indicating that Phi-responsive proteins facilitate the activation of HR against the pathogen.

List of Abbreviations Used

ABA, abscisic acid
ALD, fructose-phosphate aldolase
Avr, avirulence
BABA, β-aminobutyric acid
BABA-IR, β-aminobutyric acid-induced resistance
BTH, benzo-(1,2,3)-thiadiazole-7-carbothioic acid S-methyl ester
CaM, calmodulin
CathB, cathepsin B
CDPK, calcium-dependent protein kinase
CIP, International Potato Center
Con, control
CPI, cysteine protease inhibitor
cv, cultivar
dpi, days post inoculation
EDS1, enhanced disease susceptibility1
EST, expression sequence tags
ET, ethylene
ETI, effector-triggered immunity
ETS, effector-triggered susceptibility
FAO, Food and Agriculture Organization of the United Nations
Fd, ferredoxin
FDR, false discovery rate
FRAC, Fungicide resistance action committee
GAPDH, glyceraldehyde-3-phosphate dehydrogenase
GLP, germin-like protein
GM, genetically modified
GO, Gene Ontology
GOGAT, glutamate synthase
GPI, glucose-6-phosphate isomerase
GS, glutamine synthetase
GST, glutathione S-transferase
GWD, α-glucan water dikinase
HR, hypersensitive response
ICS1, isochorismate synthase 1
IPM, integrated pest management
IR, induced resistance
ISR, induced systemic resistance
iTRAQ, isobaric tag relative and absolute quantification
JA, jasmonic acid
KAT2, 3-ketoacyl-CoA thiolase 2
L, liter
MAMPs, microbe-associated molecular patterns
MAP, mitogen-activated protein

MDHAR, monodehydroascorbate reductase
MRM, multiple reaction monitoring
mTRAQ, MRM Tags for Relative and Absolute Quantification
MudPIT, multidimensional protein identification technology
NPR1, NONEXPRESSOR of PR1
PAD4, phytoalexin deficient 4
PAMPs, pathogen-associated molecular patterns
PCD, programmed cell death
PEPC, phosphoenolpyruvate carboxylases
PG, polygalacturonase
PGI, polygalacturonase inhibitor
PGPE, plant growth-promoting rhizobacteria
PGPF, plant growth-promoting fungi
Phi, phosphite
Phi-IR, phosphite-induced resistance
PK, pyruvate kinase
PMRA, Pest Management Regulatory Agency
PR, pathogenesis-related
PRRs, pattern recognition receptors
PR-2, β-1,3-glucanase
PR-3, chitinase
PR-5, thaumatin/osmotin-like protein
PR-9, peroxidase
PTI, PAMP-triggered immunity
PVPP, polyvinyl polypyrrolidone
P5CR, pyrroline-5-carboxylate reductase
P5CS, pyrroline-5-carboxylate synthetase
P5C, pyrroline-5-carboxylate
R, resistance
ROS, reactive oxygen species
RuBisCO, ribulose bisphosphate carboxylase/oxygenase
SA, salicylic acid
SAR, systemic acquired resistance
SCX, strong cation exchange
SEM, scanning electron microscopy
TC, tentative consensus sequences
TCA, tricarboxylic acid
TEM, transmission electron microscopy
TF, transcription factor
TPI, triosephosphate isomerase
US EPA, United States Environmental Protection Agency
2-D GE, two-dimensional gel electrophoresis
2-D LC-MS/MS, two-dimensional liquid chromatography tandem mass spectrometry

Chapter 1. Introduction

Abstract

Plants exposed to pathogens trigger a recognition response, resulting in activation of well-coordinated genes involved in the defense responses. Defects in rapid recognition of pathogens result in the delay of activation or inactivation of the defense responses, rendering the plants susceptible to infection. For susceptible plants, defense responses can be bolstered by pre-treatments with inducing agents before pathogen invasion. Such immunity is called induced resistance (IR), a process related to the increased levels of disease resistance that protects plants against a broad range of pathogens. Cultivated potato (*Solanum tuberosum* L.) is an economically important crop, the world's 4th largest economically important food crop, is susceptible to many oomycetes, including *Phytophthora infestans* (Mont.) de Bary. Pathogens causing diseases can be controlled mainly by fungicides. Environmentally friendly phosphite (salts of phosphorous acid; Phi)-based fungicides are increasingly being used as alternative fungicides in controlling oomycete pathogens. The complex modes of action of Phi are dependent on its concentration. Higher levels of Phi have a direct inhibitory effect on the pathogens' growth and development. Lower concentrations of Phi boost plant resistance to pathogens by inducing plant defense responses associated with IR. However, the defense mechanisms involved in Phi-IR at the molecular level have not been well documented. An improved understanding of Phi-IR will provide added incentive for the use of Phi-based fungicides as an alternative strategy in controlling plant diseases.

1.1 Potato

Potato (*Solanum tuberosum* L.) is grown worldwide, with average annual yields of 325 million tons (FAOSTAT, 2011). Potato cultivation originated in South America and the potato was introduced to Europe in the 1500s. Potatoes are grown in over 160 countries under diverse climate conditions (Spooner *et al*., 2005). The potato is a nutrient dense crop that is high in carbohydrates and proteins and low in fat. Potatoes are excellent sources of vitamin C and potassium and supply a variety of dietary nutrients, such as vitamin B, magnesium, and phosphorus. The potato also contains polyphenolic antioxidant compounds, which can contribute to the reduction of inflammation, cancers, cardiovascular disease, and diabetes. Potatoes are prepared by several means, including baking, boiling, and frying (Camire *et al*., 2009).

The United Nations promotes cultivation of potatoes in developing countries for their nutritional value, their ability to adapt to diverse environments, and their ability to be grown in readily adopted farming systems (Diallo *et al*., 2011). Worldwide production of potatoes is increasing annually, except in Europe, with moderate increases in total production (Mullins *et al*., 2006; FAOSTAT, 2011). However, potato plants are susceptible to numerous pathogens, resulting in the reduction of potato yield. For instance, late blight caused by the oomycete *Phytophthora infestans* (Mont.) de Bary is the most serious disease worldwide. Bacterial wilt caused by *Ralstonia solanacearum* Smith leads to severe loss of production. Various viruses, such as potato virus Y and potato leafroll virus, are able to reduce yield by 50 percent. Colorado potato beetle (*Leptinotarsa decemlineata* Say) has recently shown strong resistance to insecticides. The potato cyst nematode (*Globodera rostochiensis* Wollenweber) is a serious soil pest. Potato pests and

pathogens result in annual losses of 25% (FAOSTAT, 2008; Diallo *et al*., 2011). Potato late blight alone causes over $3 billion in annual losses worldwide (Fry, 2008).

The control of potato diseases relies mainly on the application of pesticides, but intensive use of pesticides is linked to toxicity to humans and damage to the environment (FAOSTAT, 2008; Fry, 2008). Therefore, the Food and Agriculture Organization of the United Nations (FAO) and the International Potato Center (CIP) support pest control by Integrated Pest Management (IPM). IPM urges the use of biopesticides with lower toxicity, which is one alternative to improve ecosystem health (FAOSTAT, 2008). In addition, genetically modified (GM) potatoes such as the *Bt* potato that expresses the *Bacillus thuringiensis* Berliner toxin are resistant to the Colorado potato beetle. Another GM potato line generated to boost plant immunity overexpresses the resistance (*R*) gene *Rpi-blb1* from *Solanum bulbocastanum* Dunal to become resistant to *P. infestans* (Mullins *et al*., 2006). However, these lines are still not permitted in developed countries for potato production.

1.1.1 Oomycetes Causing Plant Diseases

Oomycetes, fungi-like organisms that are evolutionarily more closely related to brown algae, are economically important pathogens causing devastating diseases in a broad-spectrum of horticultural, ornamental, and forest species. Oomycetes of the genera *Phythophthora spp*. such as *P. infestans*, *P. ramorum*, *P. cinnamomi*, *P. erythroseptica* and *P. palmivora* causing diseases, such as late blight, sudden oak death, root rot, pink rot, and cocoa stem canker, respectively, are widespread across North America, Europe,

Australia, South Africa, and Asia (Daniel and Guest, 2006; Balci *et al*., 2007; Cahill *et al*., 2008; King *et al*., 2010; McMahon *et al*., 2010).

Cultivated potato is susceptible to the oomycete *Phytophthora infestans* which causes late blight. Potato late blight resulted in a 25% reduction of the population of Ireland in the 1840s. Two major events, the great famine in Ireland caused by potato late blight and the destruction of grapes caused by the oomycete *Plasmopara viticola*, led to the development of plant pathology (Guest and Grant, 1991). Even today, potato late blight still causes enormous economic damage.

1.1.2 Life Cycle of *Phytophthora infestans*

Phytophthora infestans has both asexual and sexual life cycles. The asexual cycle facilitates rapid population growth on a limited host range, such as Solanaceous species that include potatoes and tomatoes. Sporangia (2n: diploid) are formed on sporangiophores during periods of high humidity and are then dispersed by wind and water. They germinate either via a germ tube at 18 ºC - 24 ºC or by releasing zoospores at relatively low temperatures (8 ºC - 18 ºC). Encysted zoospores penetrate host tissues via a germ tube. Continued fungal growth establishes a biotrophic (growing on living host tissues) relationship for at least the first 2 days after infection, during which no visible disease symptoms are apparent. After that, a necrotrophic (killing the host and then feeding on its contents) relationship is formed, leading to the production of lesions in host tissues. Individual lesions can be the source of production of 100,000 - 300,000 sporangia per day. The sporangia are capable of dispersing over long distances by wind, resulting in rapid epidemic development under conducive conditions (Fry, 2008). Tubers can be

infected when sporangia are washed down from parts above ground, such as foliage and stems, during rain events. Sporangia (directly or indirectly via zoospores) infect tubers when soil conditions are wet and cool. *P. infestans* can overwinter in potato tubers and culls. Sporangiophores terminating in sporangia can form on infected tubers in spring to provide initial inoculum for disease development in a particular growing season (Judelson, 1997; Fry, 2008).

For sexual reproduction, A1 and A2 mating types that produce compatible mating hormones are required. In response to the hormones that have not been identified yet, the fusion of an oogonium (n) and antheridium (n) leads to the formation of an oospore (2n), generating a new strain. Germinating oospores produce a sporangium (2n), thus re-establishing the asexual cycle (Judelson, 1997; Fry, 2008). In Canada prior to 1994, the US-1 strain (A1 mating type) of *P. infestans* was predominant. By 1995, the US-8 (A2 mating type) genotype dominated populations of the pathogen in Canada outside British Columbia and Alberta. In 1996, a new A2 mating type was found in British Columbia (Peters *et al*., 1999). During 2009 and 2010, US-8 dominated populations of the pathogen in potatoes and tomatoes in Quebec, New Brunswick, and Prince Edward Island, while US-11, US-23, and US-24 (A1 mating types) dominated in Manitoba, Saskatchewan, and Alberta (Kawchuk *et al*., 2012).

1.1.3 Fungicides Controlling Plant Diseases

P. infestans is most often controlled in potato agriculture by the application of fungicides (Fry, 2008). Bordeaux mixture, a mixture of copper sulfate and calcium hydroxide discovered by Millardet in 1885, was an effective fungicide for 90 years

against grapevine downy mildew and late blight foliar diseases. However, it was not effective against soil-borne diseases, such as pink rot and leak tuber rot, which are caused by *P. erythroseptica* Pethybr. and *Pythium ultimum* Trow, respectively (Guest and Grant, 1991). The phenylamide-based systemic fungicide metalaxyl introduced in the 1970s was highly effective at controlling both foliar and soil-borne diseases caused by oomycetes. Metalaxyl acts as an RNA synthesis inhibitor to prevent mycelial growth and haustoria formation of *P. infestans* (Matheron and Porchas, 2000). However, a strain of *P. infestans* resistant to metalaxyl was reported in Europe in 1981, in Canada and the US in the 1990s and thereafter worldwide. This resulted in the loss of effective late blight disease control, especially against tuber blight (Dowley and O'Sullivan, 1981; Goodwin *et al*., 1994). To date, chlorothalonil (54.0% active ingredient), a protectant fungicide known as Bravo^{TM}, is commonly used to control potato late blight in Canada and the US. However, concerns have been raised about its long-term use related to impacts on human health and the environment since it was classified as a group of probable human carcinogens by the United States Environmental Protection Agency (US EPA). In addition, chlorothalonil (1.2 L/ha) can only be used to control foliar pathogens and is less directly able to control tuber blight (Caux *et al*., 1996).

1.2 Plant Innate Immunity

In nature, plants are constantly exposed to complex environments. When plants encounter pathogens, the recognition of conserved microbial structures or effectors secreted by pathogens occurs through surveillance systems. The term 'innate immunity' has been described as '…the surveillance system that detects the presence and nature of

the infection and provides the first line of host defense…' (Medzhitov, 2001). The presence or absence of inheritably determined surveillance systems in the form of receptors in plants is a key to trigger appropriate and rapid host defense responses (Ryan *et al*., 2007). The detection of pathogens by plant receptors activates plant defense responses rapidly to limit the growth of pathogens, rendering plants resistant to the pathogens, hence an incompatible interaction. However, certain pathogens have evolved effectors to escape this recognition by plants. Defects in recognition of pathogens by the plants result in the delay of activation or inactivation of plant defense responses, rendering plants susceptible to infection by the pathogens, hence a compatible interaction (Jones and Dangl, 2006; Rasmussen *et al*., 2012).

In general, plants monitor the presence of pathogens with two layers of receptors; pattern recognition receptors (PRRs) and resistance (R) proteins (Figure 1.1). At first, plants respond against foreign invaders by recognizing their conserved structures known as microbe- or pathogen-associated molecular patterns (MAMPs or PAMPs). MAMPs and PAMPs, more generally known as elicitors, are recognized by the first layer of receptors (PRRs). The plants that have PPRs corresponding to the MAMPs or PAMPs can generate PAMP-triggered immunity (PTI) (Figure 1.1). PTI protects plants from a majority of pathogens because PAMPs are essential components of pathogens (Nurnberger and Kemmerling, 2006).

The second layer of plant receptors encoded by *R* genes recognizes pathogen effectors (Figure 1.1). Most, if not all, biotrophic pathogens releases their effectors into plant cells. The effectors target multiple plant proteins to inhibit plant defense signaling pathways, resulting in suppression of PTI. These pathogens can successfully disable PTI,

the first level of plant immunity, by using their effector proteins. For such pathogens, plants that have R proteins corresponding to the effectors generate effector-triggered immunity (ETI), resulting in a higher amplitude of defense (Figure 1.1). It is important to note that effector proteins of pathogens can evolve rapidly to escape recognition; therefore, plant R proteins should co-evolve in order to maintain their resistance function. The breakdown of this balance will result in susceptibility of the plant against the pathogen (Jones and Dangl, 2006).

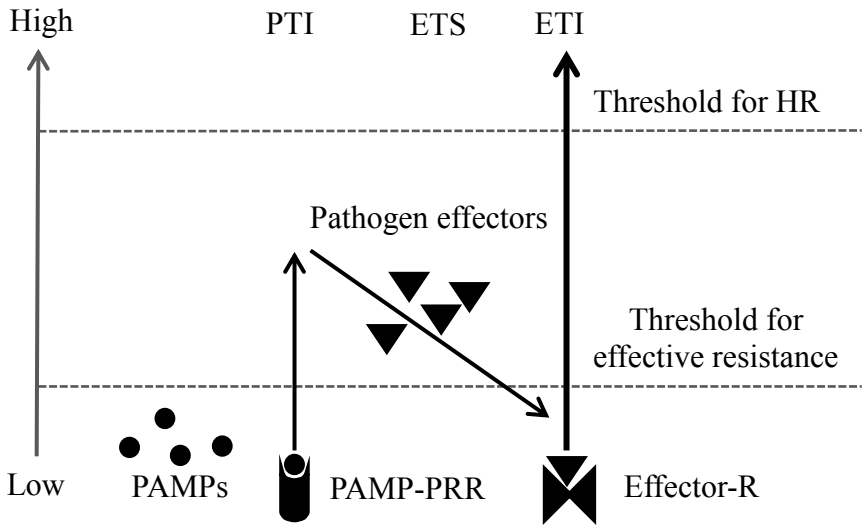

Figure 1.1. The amplitude of defense by PTI and ETI. The recognition of PAMPs (circles) by PRRs activates PTI. The amplitude of defense passes a threshold for effective resistance. Successful pathogens secrete effector proteins (triangles) to suppress PTI, causing effector-triggered susceptibility (ETS). The recognition of one effector via R protein triggers ETI which passes a threshold for HR. This figure is modified from Jones and Dangl, 2006.

1.2.1 PAMP-Triggered Immunity

Pathogen recognition receptors in plants recognize PAMPs, such as cell wall fragments (chitin and beta-1,3-glucan oligomers), flagellin, and elongation factor Tu, at

local infection sites (Zipfel *et al*., 2006; Nurnberger and Kemmerling, 2006; Iriti and Faoro, 2009). After the recognition event, plants turn on signaling pathways, leading to the activation of defense responses in mediating PTI; the amplitude of defense by PTI passes a threshold for effective resistance to the pathogens recognized by PRRs (Figure 1.1). For example, the chitin elicitor-binding protein in *Arabidopsis* recognizes chitosan, a pathogen cell wall component, leading to the activation of the mitogen-activated protein (MAP) kinase signaling pathway. The pathway activates defense responses such as callose deposition, generation of Ca^{2+} and reactive oxygen species (ROS), production of the plant hormones jasmonic acid (JA) and abscisic acid (ABA), and accumulation of phytoalexin (Iriti and Faoro, 2009). These defense responses are associated with cell wall reinforcement, expression of defense-related genes, production of antimicrobial substances, and initiation of the hypersensitive response (HR) for effective resistance (Pieterse *et al*., 2009). HR leads to a rapid host cell death at local infection sites in order to inhibit the growth of biotrophs growing on living host tissues (Mur *et al*., 2008).

In PAMP-triggered immunity, hydrolases and hydrolase inhibitors are important players for effective resistance. After pathogen recognition, plants secrete hydrolases, such as beta-1,3-glucanase and chitinase, to degrade components of the pathogen cell wall, which is one of the PAMP-triggered defense responses. The degraded cell wall fragments are used as PAMPs to further boost PTI. In the 'arms race' of defense and counter-defense during pathogen infection, pathogens also secrete numerous cell wall degrading enzymes, such as polygalacturonase and pectate lyase, to break down the structure of the plant cell wall. Plants, therefore, secrete hydrolase inhibitors, such as polygalacturonase inhibitor protein, to degrade enzymes secreted by the pathogens

(Lagaert *et al*., 2009). Shetty *et al*. (2009) identified that the degree of expression of hydrolase genes at the transcription level was higher in resistant plants than in susceptible plants. Thus, the recognition of a pathogen boosts levels of hydrolases and hydrolase inhibitors in plants and the abundance in levels of these proteins is associated with disease resistance.

In nature, most plants are resistant to the majority of pathogens. It, therefore, indicates that PRRs are universal receptors in plants and PAMP-triggered defense responses are effective for resistance to a vast majority of pathogens. Nonetheless, certain pathogens suppress PTI by using their effector proteins (Jones and Dangl, 2006). For instance, in potatoes, a PRR recognizes the PAMP, Pep-13, which is a highly conserved 13-amino acid fragment within the cell wall transglutaminase of *Phythophthora* species (Brunner *et al*., 2002). The detection of Pep-13 in potatoes triggers PTI including activation of both SA and JA signaling pathways, H_2O_2 accumulation, expression of defense-related genes, and the hypersensitive response (Halim *et al*., 2004, 2009). However, *P. infestans* is still able to colonize potato plants, causing diseases. This is explained by effectors secreted from *P. infestans* that suppress PTI [effector-triggered susceptibility (ETS)] (Figure 1.1; Halim *et al*., 2009).

1.2.2 Effector-Triggered Immunity

Pathogen effector proteins play roles in suppressing PTI as well as facilitating infection processes. Bacterial effectors AvrE and HopPtoM suppress PAMP-triggered defense responses, such as salicylic acid (SA)-dependent systemic acquired resistance (SAR) and callose deposition, resulting in suppression of SA-dependent gene expression

and promotion of necrosis (Debroy *et al*., 2004). Pathogen effector proteins facilitate infection processes by being involved in adhesion to the plant cell, promotion of pathogen dispersal, and degradation of plant physical barriers, rendering plants susceptible (Hein *et al*., 2009).

The recognition of pathogen effectors by plant R proteins, the secondary surveillance system, can activate ETI. As shown in Figure 1.1, interactions of a pathogen effector, so-called avirulence (Avr) protein, with a corresponding plant R protein trigger ETI, a higher amplitude of defense than PTI. ETI is activated by R-Avr interactions known as gene-for-gene interactions; therefore, R proteins are specific receptors, in contrast to PRRs that detect general and essential components of pathogens. In many cases, ETI can result in the hypersensitive response (Figure 1.1); it is one of the strongest components for disease resistance. The recognition of pathogens by R proteins rapidly induces the key events of HR; as early events, rapid production of reactive oxygen species and increases in levels of Ca^{2+} concentrations in the host cytoplasm occur (Wojtaszek, 1997). NADPH oxidase is the key enzyme for ROS burst. Virus-induced gene silencing of this enzyme in *Nicotiana benthamiana* Domin reduced ROS generation, leading to a decrease in level of resistance to *P. infestans* (Yoshioka *et al*., 2003). The transient expression of calmodulin, a Ca^{2+} binding protein, in pepper leaves displayed HR-like cell death upon infection (Choi *et al*., 2009). Transgenic potato expressing a calcium-dependent protein kinase (*CDPK*) gene that includes a calmodulin-like domain showed the phosphorylation of NADPH oxidase by StCDPK. The phosphorylated NADPH oxidase induced a ROS burst, triggering HR by ROS and Ca^{2+}-dependent manners for resistance to the biotrophic stage of *P. infestans* (Kobayashi *et al*., 2012).

Beside the involvement of Ca^{2+} and ROS, HR is triggered by changes in ion fluxes and pH, and accumulation of SA (Jabs, 1999; Durrant and Dong, 2004; Garcia-Brugger *et al*., 2006).

In addition to the direct interaction of an R protein corresponding to an Avr protein, indirect recognition of Avr proteins by R proteins has also been identified in plants (Chisholm *et al*., 2006). For instance, the effector protein AVR2 from *Cladosporium fulvum* (Cooke) Arx acts as a protease inhibitor against plant cysteine protease RCR3. The R protein Cf-2 in tomato plants (*Solanum lycopersicum* L.) detects the complex of AVR2 and RCR3 and this recognition activates Cf-2 dependent defense responses, leading to HR in plants (Rooney *et al*., 2005).

1.2.3 Fast-Evolving Effectors

To escape the plant surveillance system by R proteins and/or suppress plant defense responses, pathogen effectors can evolve quickly. Tian *et al*. (2007) demonstrated that in order to to inhibit the activity of host proteases, EPIC1 to EPIC4, a new family of Extracellular Protease Inhibitor with a Cystatin-like domain, from *P. infestans* interacts with PIP1, *Phytophthora* Inhibited Protease 1, in tomato plants. The presence of *epiC1* and *epiC2* in *P. infestans* but not in other *Phytophthora* species, such as *P. sojae* and *P. ramorum*, indicated that effectors in *P. infestans* evolve relatively rapidly (Tian *et al*., 2007). For fast-evolving effectors, plant proteins co-evolve accordingly. Kaschani *et al*. (2010) discovered the cysteine protease C14, a new target of EPIC1 and EPIC2, in tomato and a closely related potato. In contrast to the C14 with conserved sequences in tomato plants, C14 is under diversifying selection in wild potato

species (*Solanum demissum* Lindl. and *Solanum verrucosum* Schltdl.) resistant to *P. infestans* (Kaschani *et al*., 2010).

In the 'arms race' of defense and counter-defense during plant-pathogen interactions, many plant proteases play roles in *R* gene-mediated HR and the action of proteolysis (Shindo and van der Hoorn, 2008). Proteases, such as aspartic protease, and cathepsin B that is classified as a cysteine protease, in potato plants are up-regulated during *P. infestans* infection (Avrova *et al*., 1999, 2004; Guevara *et al*., 2002). Induction of their expression is higher and faster in a resistant potato cultivar than in a susceptible cultivar (Avrova *et al*., 2004; Guevara *et al*., 2002). Overexpression of C14, a cysteine protease, overcomes the action of AVRblb2, a cysteine protease inhibitor, resulting in increased levels of resistance to *P. infestans* (Bozkurt *et al*., 2011). Therefore, the degree of their induction is associated with levels of resistance, indicating that the activity of host proteases could modulate defense (Tian *et al*., 2007).

1.3 Plant Acquired Resistance

Since susceptible plants do not have surveillance R proteins corresponding to the pathogen effectors, they are unable to activate rapid and intense defense responses to specific pathogens. For susceptible plants, certain chemicals can boost PTI nad ETI in innate immunity. Such a response in plants is similar to vaccination in humans and is, therefore, named acquired resistance or induced resistance (Uknes *et al*., 1992). Applications of inducing agents turn on genes involved in defense mechanisms, leading to increased levels of resistance in susceptible plants. The amplitude of defense responses associated with acquired resistance is sometimes lower than that of defense response

elicited by R proteins (Oostendorp *et al*., 2001). However, acquired resistance confers enhanced resistance in plants against a broader range of pathogens (Hammerschmidt *et al*., 2001). Understanding how to boost levels of resistance in susceptible plants by pre-treatment with inducing agents could be incorporated in disease management strategies.

1.3.1 The Concept of Induced Resistance

The concept of "immunization" or "acquired resistance" in plants was first reported by Chester (1933). It is based on the experiment using tobacco infected with tobacco mosaic virus. After infection, these plants exhibited resistance against secondary infection by different viruses as well as other pathogens. In addition, both infected areas and uninfected distant cells in the infected tobacco leaves showed resistance. Several decades later, a framework of such resistance called systemic acquired resistance was established (Ross, 1961; Kuc, 1982; Sticher *et al*., 1997). The term "induced resistance" for plants was established at the First International Symposium on Induced Resistance to Plant Disease (Hammerschmidt *et al*., 2001).

Induced resistance (IR) is defined as systemically enhanced defensive capacity activated by the application of inducers such as microbes, organic compounds, and pesticides (van Loon *et al*., 1998). For example, the application of salicylic acid (SA) or SA analogs activates systemic acquired resistance (SAR) in susceptible plants. SAR is a component of PTI and ETI; the recognition of pathogens by plant surveillance systems at local infection sites activates SA-dependent SAR, leading to the expression of pathogenesis-related (*PR*) genes in uninfected distant healthy cells. The rapid expression of a subset of *PR* genes has been considered one of the important indicators in resistant

plants (de Jong *et al*., 2004; Ahn *et al*., 2005). Therefore, the identification of molecular components involved in IR and the linking of the components with defense mechanisms in mediating PTI and ETI, provide information about defense responses which are delayed or inactivated in susceptible plants.

1.3.2 Three Types of Induced Resistance

Based on different hormone-dependent signaling pathways, three types of IR, β-aminobutyric acid (BABA)-induced resistance, induced systemic resistance, and systemic acquired resistance have been documented to date (Goellner and Conrath, 2008).

Plant hormones are essential and act as primary signals to induce and regulate plant defense responses (Halim *et al*., 2009; Verhage *et al*., 2010). In general, SA-dependent defense responses are effective in controlling biotrophic pathogens, while JA-dependent signaling pathways are effective in controlling necrotrophic pathogens (Halim *et al*., 2007). SA-dependent HR, a programmed host cell death, restricts the growth of biotrophic pathogens, whereas host cell death facilitates the infection of necrotrophic pathogens (Govrin and Levine, 2000).

1.3.2.1 β-Aminobutyric Acid (BABA)-Induced Resistance

β-aminobutyric acid (BABA)-induced resistance (BABA-IR) is elicited by the chemical, β-aminobutyric acid. BABA-IR protects *Arabidopsis* mutants that are defective in JA/ET-dependent signaling pathways, but not in the SA-dependent signaling pathway against *Botrytis cinerea* (De Bary) Whetzel. SA is, therefore, required to activate BABA-IR against *B. cinerea* (Zimmerli *et al*., 2001). In another case, BABA treatment of

Arabidopsis mutants, impaired in JA- or SA-dependent signaling pathways, were found to confer effective protection against the necrotrophic fungi *Alternaria brassicicola* (Schwein.) Wittshire and *Monographella cucumerina* (Lindf.) Arx. However, the BABA-IR is not effective in ABA-deficient mutants against these pathogens. It has been suggested that ABA is essential to activate BABA-triggered defense responses against pathogens (Ton and Mauch-Mani, 2004). Other mutant analysis demonstrated that BABA-IR involves enhanced SA-dependent cell death and ABA-dependent callose deposition for effective resistance against the oomycete *Hyalopernospora parasitica* (Pers.) Constant. (Ton *et al*., 2005). BABA-treated potato plants showed increased levels of resistance against *P. infestans* (Cohen, 2002). BABA-IR is effective in transgenic potato plants impaired in the JA biosynthesis pathway, but not in their ability to accumulate SA (Eschen-Lippold *et al*., 2010). In potato plants, SA is required to activate BABA-IR involved in increases in levels of SA-dependent β-1,3-glucanase, aspartyl protease as well as phenol, and phytoalexins (Andreu *et al*., 2006). Taken together, SA and/or ABA are required to induce defense responses involved in BABA-IR in *Arabidopsis* for disease resistance depending on the pathogen species.

1.3.2.2 Induced Systemic Resistance

Induced systemic resistance (ISR) is triggered by plant growth-promoting rhizobacteria (PGPR) and fungi (PGPF), which are beneficial soil-borne microorganisms. Applications of non-pathogenic soil-borne microbes have increased the levels of disease resistance in aboveground plant tissues against pathogens (van Loon *et al*., 1998). Tomato plants treated with the PGPRs *Bacillus pumilus* SE34 and *Pseudomonas*

fluorescens 89B61 were found to show enhanced resistance to *P. infestans*. JA-insensitive tomato mutant *def1* and ethylene (ET)-insensitive tomato mutant *Nr* were unable to activate ISR upon PGPR infection (Yan *et al*., 2002). JA and ET are required for the activation of ISR-dependent defense signaling pathways, in contrast to SA and/or ABA that act as central player(s) in the regulation of BABA-IR. The increased level of resistance elicited by PGPRs was similar to that of resistance triggered by BABA (Pieterse *et al*., 2009).

In plant-PGPR interactions, plants recognize PAMPs of rhizobacteria, leading to an activation of PAMP-triggered defense responses before infection with other pathogens. After the recognition of rhizobacteria, plants activate the expression of the *MYB72* gene, a key component of ISR. MYB72 activates the expression of transcription factors *MYC2* and *EREBP* genes to turn on JA- and ET-dependent defense-related genes (van der Ent *et al*., 2009). A transcriptome analysis of ISR triggered by PGPR *Pseudomonas fluorescens* WCS417r revealed that the majority of the 81 PGPR-responsive genes in *Arabidopsis* were regulated by JA and/or ET (Verhagen *et al*., 2004). ISR, therefore, is effective against pathogens that can be controlled by JA- and ET-dependent defense responses (Pieterse *et al*., 2009).

Pathogenesis-related (PR) genes can be classified into basic and acidic isoforms. ISR triggers the expression of basic pathogenesis-related (PR) proteins such as basic PR-1 and basic PR-5 via JA-/ET-dependent pathways. Basic and acidic PR proteins in plants have similar amino acid sequences. However, basic PR proteins mostly have additional sequences at the C-terminal, indicating slightly higher molecular weight (van Loon and van Strien, 1999). Basic PR proteins are secreted to vacuole. In contrast to acidic PR

proteins are expressed via SA-dependent pathway related to the other type of induced resistance, systemic acquired resistance. The acidic PR proteins are secreted to apoplast (Riviere *et al*., 2008).

1.3.2.3 Systemic Acquired Resistance

Systemic acquired resistance (SAR) can be induced by SA or SA analogues such as benzo-(1,2,3)-thiadiazole-7-carbothioic acid S-methyl ester (BTH) and 2,6-dichloroisonicotinic acid (INA). SA-treated plant leaves transmit a signal(s) to trigger systemic immunity. A mobile signal induces the accumulation of SA, which binds to ROS scavenging enzymes, resulting in increased levels of ROS. Ultimately, a systemic defense response is transferred from the SA-treated leaf to the untreated leaf, which is called systemic acquired resistance (Ryals *et al*., 1994). It has been demonstrated that SA is required for the establishment of SAR by *Arabidopsis NahG* mutants. The *NahG* mutants overexpress the bacterial salicylate hydroxylase gene (the gene product converts SA into catechol) and are unable to accumulate SA. The *NahG* mutants are incapable of activating SAR, resulting in susceptiblility to bacterial and fungal pathogens (Delaney *et al*., 1994).

The molecular mechanism of SAR has been well documented (Oostendorp *et al*., 2001). SA application or pathogen recognition by R proteins activates the triacyl-glycerol lipase EDS1. EDS1 is required to express isochorismate synthase 1 (*ICS1*) and *EDS5* (Durrant and Dong, 2004; Wiermer *et al*., 2005). In *Arabidopsis*, ICS1 is required for SA synthesis via the isochorismate pathway (Wildermuth *et al*., 2001). EDS5 is a transporter that transports intermediates involved in SA biosynthesis. SA binds to ROS scavenging

enzymes, such as ascorbate peroxidase and catalase, leading to inhibition of the activity of the enzymes, resulting in increase in H_2O_2 concentration (Wendehenne *et al*., 1998). NPR1 (NONEXPRESSOR of PR1), a key regulator of SAR (Cao *et al*., 1997), is controlled by alterations in the cellular redox state. NPR1 forms inactive oxidized oligomers in the cytosol. During pathogen infection, SA accumulation-mediated changes convert the inactive oligomers into the active monomeric forms. The active NPR1 is then transported into the nucleus where it interacts with a transcription factor TGA in order to express many *PR* and secretory genes (Pieterse and van Loon, 2004). These gene products have antimicrobial activity with properties of pathogen cell wall degradation (Durrant and Dong, 2004). The transcription factor WRKY is also required to express *PR* genes (Eulgem and Somssich, 2007). In contrast to TGA and WRKY, SNI1 is a negative regulator of *PR* genes (Li *et al*., 1999; Desveaux *et al*., 2004). SAR is characterized by sustained resistance in plants that lasts between a few weeks to a few months in order to cope with secondary infections (Kuc, 1987; Durrant and Dong, 2004). SAR is effective against pathogens that can be controlled by SA-dependent defense responses (Pieterse *et al*., 2009). However, pre-treatment with BTH (1.5 mM) was not able to protect susceptible potato cv. Bintje from *P. infestans*, while BABA (1 mM) application was found to protect potato cv. Bintje with increased level of resistance similar to that of resistance shown by the resistant potato cv. Matilda (Si-Ammour *et al*., 2003). The expression of the *PR-1* gene in potato plants grown in field conditions was not long-lasting, indicating that field-grown potatoes were less sensitive to BTH (Navarre and Mayo, 2004).

1.4 Environmentally Friendly Agrochemical Phosphite

Enhanced resistance in plants conferred by inducing agents has led to the development of a series of inducing agents for field application. Many chemical agents are toxic to human health and the environment, and selecting an environmentally friendly agent is the key. Phosphites, salts of phosphorous acid, are one of these that have been used for over four decades and they continue to draw attention for their applications as fungicides.

1.4.1 Phosphite: an Alternative Fungicide

Phosphite (salts of phosphorous acid; Phi), the reduced form of phosphate, is an oxyanion of phosphorous acid (H_3PO_3). When phosphorous acid is dissolved in water, the strong acid form called phosphonic acid is produced. Alkali metal salts, such as potassium or aluminum ions, are added to make its pH neutral because the strong acid itself is harmful to plant tissues. The addition of potassium hydroxide forms the resulting solution called potassium phosphite or mono- and di-potassium salts of phosphorous acid. Another resulting solution called fosetyl-Al is formed by the addition of aluminum ions (Guest and Grant, 1991).

Phosphite was discovered by Rhone-Poulenc laboratories in France in the 1970s as a systemic antifungal agent. It is absorbed across membranes on plant foliage and stems with great mobility and solubility. Phi, a phloem-mobile molecule, can be applied via foliar spray or stem injection. Therefore, foliar applications of Phi-based fungicides with systemic properties were found to reduce foliar as well as root diseases (Guest and Grant, 1991). In addition, Phi-based fungicides are very safe and environmentally

friendly biopesticides as classified by the US EPA (Lobato *et al*., 2008). As well, the Fungicide Resistance Action Committee (FRAC) classified Phi into group 33; fungicides with low risk of resistance development (www.frac.info). Phi has drawn significant attention recently in Canada as an alternative fungicide because of its good environmental profile. Health Canada's Pest Management Regulatory Agency (PMRA) reported that Phi does not present an unacceptable risk to humans and the environment (http://publications.gc.ca/collections/collection_2010/arla-pmra/H113-26-2010-9-eng.pdf). Integrated pest management (IPM) is a philosophy that addresses pest control by way of the safest and most effective methods, while reducing pesticide use. In IPM programs, Phi is regarded as an attractive alternative to promote the reduction of the use of toxic fungicides (Mayton *et al*., 2008).

1.4.2 The Efficacy of Phosphite Against Oomycetes and Other Fungal Pathogens

Phosphite-based fungicides are increasingly being used in controlling oomycete pathogens such as the late blight agent, *P. infestans*, and *P. erythroseptica*, which causes pink rot. The fungicides are also used to control *Pseudoperonospora humuli* (Miyabe & Takah.) G. W. Wilson, which causes downy mildew in grape production (http://www.omafra.gov.on.ca/english/crops/updates/tfgrape/tfgrape20120622.htm). Johnson *et al*. (2004) assessed the efficacy of a commercial version of Phi (Phostrol™ containing 53.6% mono- and di-basic sodium, potassium, and ammonium salts of phosphorous acid; Nufarm Americas Inc., USA) for control of tuber rot caused by *P. infestans* and *P. erythroseptica*. Mean incidence and severity of late blight and pink rot in tubers, from potatoes pre-treated with Phi twice at the rates of 7.49 kg active

ingredient/hectare, were less than that of tubers from control potato plants. Miller and Miller (2011) reported that applications of potatoes with Phostrol twice (8 pint/acre) for late blight and three times (10 pint/acre) for pink rot provided significant tuber protection from these diseases. Post-harvest applications of Phostrol resulted in 14% late blight and 10% pink rot symptoms after 77 days in storage when compared to untreated potato tubers showing 90% late blight and 61% pink rot symptoms (Woodell *et al*., 2005).

Seed tubers and potato foliage pre-treated with Agro-EMCODI SA (Agro-EMCODI, Argentina) containing calcium and potassium salts of phosphorous acid were also evaluated (Lobato *et al*., 2008). At the rate of 1% (v/v) of the commercial product equivalent to 3 L/hectare, Phi-treated seed tubers were conferred a high level of protection against *P. infestans*, while excellent protection of potato foliage was provided by 4 applications at the rate of 2% of the commercial product. In contrast to the systemic fungicide Phi, protectant fungicides, such as chlorothalonil (Bravo^{TM}) or Mancozeb (Dithane^{TM} or Manzate^{TM}), are applied to potato plants on average 10 times during the growing season in Canada (Wang-Pruski *et al*., 2010; Garron *et al*., 2012).

Phosphite-based fungicides are also effective in controlling other pathogens such as the fungi *Microdochium nivale* (Schaffnit) E. Mull. and *Venturia pirina* Aderh (Dempsey *et al*., 2011; Percival and Noviss, 2010). Dempsey *et al*. (2011) presented that Phi-treated turfgrass enhanced levels of host resistance against *M. nivale*. In this case, Phi levels remained between 3000 – 4000 ppm in plant leaves after spraying for 3 weeks. As dose-dependent manners, 100 µg/ml of Phi fully inhibited the growth of *M. nivale* and 38 µg/ml of Phi showed the growth inhibition of half of pathogens *in vitro* assay. Percival and Noviss (2010) reported that Phi is effective in controlling *Venturia pirina* causing

pear scab. In this case, Phi (300 g phosphorous acid of Phoenix^{TM}/L) showed significant reduction of infection in pear plants under field conditions. Other evidence for suppression of fungal potato diseases, such as early blight (*Alternaria solani*) and silver scurf (*Helminthosporium solani*), has been obtained in recent years (personal coomunication; R. D. Peters, Agriculture and Agri-Food Canada, Charlottetown, PE).

Wang-Pruski *et al*. (2010) conducted three-year field trials to evaluate the efficacy of Phi (Confine containing 45.8% mono- and di-potassium salts of phosphorous acid; Winfield Solutions LLC., USA) on potato foliar late blight in Prince Edward Island, Canada. Analysis of disease severity showed that leaves from potato plants, pre-treated with Phi five times in 2007, and 2008 and six times in 2009 at the rate of 5.8 L product/hectare, had significantly less disease than leaves from untreated plants. The combined applications of Phi and chlorothalonil provided better disease suppression than the application of Phi or chlorothalonil alone. The severity of the infection, assessed 4 days post infection (dpi) by determining the percentage of diseased foliar area, was approximately 20% in control samples and about 5% in Phi-treated samples (Wang-Pruski *et al*., 2010).

1.4.3 Direct Mode of Action of Phosphite

The mode of action of Phi is complex (Massound *et al*., 2012). Studies reported so far indicated that the complex mode of action is dependent on Phi concentration: higher levels of Phi have a direct inhibitory effect on various fungi and fungi-like organisms, such as oomycetes and other species (Fenn and Coffey, 1984). The direct mode of action of Phi resulted in the inhibition of germination, zoospore production and

mycelia growth of *Phytophthora cinnamomi* (Cohen and Coffey, 1986; Guest and Bompeix, 1990; Wilkinson *et al*., 2001). After the addition of Phi in a culture medium, changes in levels of gene expression in *P. cinnamomi* were reported (King *et al*., 2010). Genes involved in cell wall biosynthesis of the pathogen, such as cellulose synthase and glycan synthase, were repressed in a medium with Phi (40 µg/ml), while the expression of the genes was not significantly changed in a medium containing relatively lower 5 µg/ml Phi. Four days after the addition of Phi (40 µg/ml), about 70% of *P. cinnamomi* growth was inhibited in the medium. These results suggested that Phi directly suppressed cell wall biosynthesis of the pathogen. The relatively low Phi concentration (5 µg/ml) may not have been sufficient to have a direct inhibitory effect on the pathogen (Wong *et al*., 2009; King *et al*., 2010).

1.4.4 Indirect Mode of Action of Phosphite

In contrast to the direct mode of action of Phi, lower concentrations of Phi are related to an indirect mode whereby plant defense responses associated with induced resistance are involved (Coffey and Joseph, 1985; Jackson *et al*., 2000). Studies on Phi-IR suggested that Phi turns on more than one defense signaling pathway in plants and the indirect mode of action of Phi contributes to pathogen inhibition more than the direct mode of action (Daniel and Guest, 2006). Previous studies revealed Phi-triggered biochemical changes (Nemestothy and Guest, 1990; Jackson *et al*. 2000). Based on defense-related genes involved in resistance to *P. infestans*, the degree of expression of several genes in Phi-treated plants was investigated (Andreu *et al*., 2006; Eshraghi *et al*., 2011). Molecular mechanisms underlying the indirect mode of action of Phi on the

inhibition of *P. infestans* are not well established (Daniel and Guest, 2006; Massoud *et al*., 2012).

1.4.4.1 Phi-Triggered Biochemical Changes

Phi-treated plants were found to accumulate phytoalexins, phenols, ethylene, callose, hydrogen peroxide, pectin, and superoxide. Tobacco cultivar (cv.) NC2326 became resistant to *P. nicotianae* by rapid induction of accumulation of sesquiterpenoid phytoalexins (antimicrobial substances) in the area of penetrated sites. Upon treatment of cv. NC2326 with mevinolin, an inhibitor of sesquiterpenoid biosynthesis, the plant became susceptible to *P. nicotianae*. However, pre-treatment with Phi in NC2326, followed by mevinolin exposure, did not increase its susceptibility. In addition, applications of tobacco cv. Hicks susceptible to *P. nicotianae* with Phi increased levels of phytoalexins, suggesting that Phi turns on more than one defense response (Nemestothy and Guest, 1990).

Phenolic compounds play a role in providing physical and chemical barriers to pathogen growth at infection sites. The compounds are produced via the phenylpropanoid pathway and are derived from the amino acids phenylalanine and tyrosine (Candela *et al*., 1995). To investigate the phenylpropanoid pathway behind Phi protection, Jackson *et al*. (2000) measured the activities of two enzymes, 4-coumarate coenzyme A ligase and cinnamyl alcohol dehydrogenase, involved in the phenylpropanoid pathway. Increased activities and accumulation of phenols were identified in Phi-treated *Eucalyptus marginata*, an Australian native tree, after infection with *P. cinnamomi*. In *Lambertia Formosa-P. cinnamomi* interactions, the activity of another enzyme, phenylalanine

ammonia lyase, involved in the phenylpropanoid pathway was increased in Phi-treated trees at 24 h after infection with *P. cinnamomi* (Suddaby *et al*., 2008). In potato-*P. infestans* pathosystems, Phi-treated potatoes cv. Kennebec had increased amounts of phenol and phytoalexin after pathogen infection (Andreu *et al*., 2006).

In addition to the accumulation of phytoalexins and phenols, Phi applications to tobacco susceptible to *P. nicotianae* increased levels of ethylene (Nemestothy and Guest, 1990). Under light microscopy, releases of superoxide, rapid cytoplasmic aggregation and nuclear migration were observed in Phi-treated tobacco against *P. nicotianae* and Phi-treated *Arabidopsis* against *P. palmivora* (Guest, 1986; Daniel and Guest, 2006). Recently, Phi-treated *Arabidopsis* leaves showed more rapid and intense callose deposition and hydrogen peroxide production than untreated leaves upon infection with *P. cinnamomi* (Eshraghi *et al*., 2011). Olivieri *et al*. (2012) reported increased pectin, one of the components of primary cell wall, in periderm and cortex in tubers obtained from Phi-treated potatoes.

1.4.4.2 Up-Regulated Genes in Phi-Treated Plants

The degree of expression of β-1,3-glucanase and aspartic protease genes was identified in potato cultivars conferring different degrees of field resistance to *P. infestans* (Guevara *et al*., 2002; Tonon *et al*., 2002). The increased levels of polygalacturonase-inhibiting protein and proteinase inhibitor in potato plants also contributed to resistance to *P. infestans* (Machinandiarena *et al*., 2001).

Andreu *et al*. (2006) identified an increase in abundance of β-1,3-glucanase and aspartic protease at the protein level in tubers from Phi-treated potato cv. Kennebec by

western blotting. Increased abundance and/or activities of polygalacturonase-inhibiting protein and proteinase inhibitor in tubers obtained from Phi-treated potatoes were identified upon infection with *Fusarium solani* (Olivieri *et al*., 2012).

Plant hormones play a central role in the expression of defense-related genes. It is well known that *PR1*, *PR5*, and *NPR1* are markers involved in salicylic acid pathways, while *THI2.1* and *PDF1.2* are involved in jasmonic acid/ethylene pathways in *Arabidopsis* (Turner *et al*., 2002). Recently, Eshraghi *et al*. (2011) investigated the expression of the five defense-related genes at the transcription level by using quantitative real-time reverse transcription polymerase chain reaction. Phi-treated *Arabidopsis* was found to show enhanced expression of the five genes via SA- or JA/ET-dependent pathways. But against Eshraghi, in *Arabidopsis*, it was "SA-dependent rather than JA or ET dependent and PR1a expression was induced indicating a similarity to SAR with SA-dependent priming" (Massound *et al*., 2012).

1.4.4.3 Phi-Induced Resistance in *Arabidopsis*

Recently, Massound *et al*. (2012) reported Phi-IR in *Arabidopsis* infected with the oomycete *Hyaloperonospore arabidopsidis*. In *Arabidopsis-H. arabidopsidis* interactions, low concentrations (10 mM) of Phi stimulated plant defense responses to enhance host resistance in comparison to high doses of Phi (50 mM or greater) which shows direct antimicrobial activity. Low doses of Phi were given to six individual mutants that were defective of jasmonic acid-dependent signaling pathway (*jar1-1*), or ethylene-dependent signaling pathway (*ein2-1*), abscisic acid biosynthetic pathway (*aba1-5*), reactive oxygen species production (*atrbohD*), and phytoalexins accumulation (*pad3-1* and *f6'h1-1*). The

results showed that Phi induced the resistance of these mutant plants to the pathogen. Also, two mutants impaired in salicylic acid (SA)-dependent signaling pathway (*npr1-1*) or SA-defective plants (*sid2-1*, NahG) were treated by Phi. In this case, Phi did not induce the resistance of these mutant plants to the pathogen.

At the gene expression level, Massound *et al*. (2012) identified the up-regulation of phytoalexin deficient 4 (PAD4) and enhanced disease susceptibility1 (EDS1) genes involved in the SA signaling pathway. In addition, pathogenesis-related (PR1) gene, a marker gene of SA-dependent signaling pathway, was also up-regulated by Phi. It was known that the MAP kinase MPK4 regulates the expression of *PAD4* and *EDS1* negatively (Petersen *et al*., 2000). Therefore, the authors examined MPK4 and confirmed that MPK4 phosphorylation and accumulation at the protein level were decreased in Phi-treated *Arabidopsis*. This indicated that low concentrations of Phi triggers SA accumulation and SA-dependent signaling pathway. Induced resistance mechanisms are conserved across dicots (Zimmerli *et al*., 2001; Yan *et al*., 2002; Eschen-Lippold *et al*., 2010). Phi-IR in *Arabidopsis* could be directly relevant to the effects found in other plants, such as potatoes. Interestingly, Eshraghi *et al*. (2011) reported that the involvement of jasmonic acid-dependent pathway in Phi-treated *Arabidopsis* upon infection with the hemibiotrophic oomycete *Phytophthora cinnamomi*. Therefore, broad defense responses could be activated in Phi-treated plants upon hemibiotrophic pathogens, such as *P. infestans*.

1.5 Conclusion

Imperfect surveillance systems in plants lead to slow or diminished defense responses, rendering plants susceptible to pathogens. Potato plants are susceptible to numerous pathogens, resulting in losses of approximately 25% of production worldwide. Chronic application of fungicides currently used to control oomycete diseases should be reduced due to toxicity to humans and damage to the environment. The environmentally friendly biopesticide, phosphite, is regarded as a potential alternative fungicide against oomycetes. Phi has complex mode of actions that are dependent on its concentration. It is known that lower levels of Phi trigger plant defense responses via negative regulation of MPK4 and primes SA dependent resistance against oomycetes, leading to increased levels of resistance against pathogens. The induced resistance elicited by inducing chemicals, such as Phi, increases levels of resistance in plants. Therefore, understanding of Phi-IR is a critical step in disease management. However, the defense mechanisms involved in Phi-IR at the molecular level remained to be investigated.

1.6 Hypothesis

In order to investigate the mode of actions of phosphite related to the increased resistance to late blight in potatoes, it is hypothesized that applications of phosphite to potato leaves will trigger changes in the expression levels of a series of genes in both the cell wall and cytoplasm.

The following objectives were designed to test this hypothesis.

Objective 1: Establish an effective method to isolate a large number of potato leaf proteins from the cell wall and cytoplasm.

Objective 2: Identify Phi-responsive leaf proteins and analyze their changes in abundance upon pathogen infection using proteomics.

Objective 3: Investigate functions of candidate proteins for their contributions to the induced late blight suppression in potato leaves.

Chapter 2. Protein Profiling in Potato (*Solanum tuberosum* L.) Leaf Tissues by Differential Centrifugation

Abstract

Foliar diseases, such as late blight, result in serious threats to potato production. As such, potato leaf tissue becomes an important substrate to study biological processes, such as plant defense responses to infection. Nonetheless, the potato leaf proteome remains poorly characterized. Here, we report protein profiling of potato leaf tissues using a modified differential centrifugation approach to separate the leaf tissues into cell wall and cytoplasmic fractions. This method helps to increase the number of identified proteins, including targeted putative cell wall proteins. The method allowed for the identification of 1484 non-redundant potato leaf proteins, of which 364 and 447 were reproducibly identified proteins in the cell wall and cytoplasmic fractions, respectively. Reproducibly identified proteins corresponded to over 70% of proteins identified in each replicate. A diverse range of proteins was identified based on their theoretical p*I* values, molecular masses, functional classification, and biological processes. Such a protein extraction method is effective for the establishment of a highly qualified proteome profile.

Published; Sanghyun Lim, Kenneth Chisholm, Robert H. Coffin, Rick D. Peters, Khalil I. Al-Mughrabi, Gefu Wang-Pruski, Devanand M. Pinto. 2012. Journal of Proteome Research 11: 2594 – 2601

2.1 Introduction

Technologies within the realm of proteomics can identify a large number of proteins in a single analysis and can reveal dynamic changes resulting from internal and external stimuli. In potatoes (*Solanum tuberosum* L.), the fourth largest food crop with annual world production of 329 million tons (FAO, 2008), proteomics has been used to study potato tuber after-cooking darkening, potato tuber development, proteins in potato tubers, and potato skins (Lehesranta *et al*., 2006; Lehesranta *et al*., 2007; Agrawal *et al*., 2008; Barel and Ginzberg, 2008; Chaves *et al*., 2009; Murphy *et al*., 2010). Since many pathogens, such as *Phytophthora infestans* (Mont.) de Bary, infect leaf tissues, a study of biological activities in potato leaves using proteomics becomes important (Arbogast *et al*., 1999; Conrath *et al*., 2003; Liu and Halterman, 2009). Liu and Halterman (2009) detected approximately 500 potato leaf protein spots by phenol extraction of whole leaf tissue using two-dimensional gel electrophoresis (2-D GE). Two other reported protein profiles of potato shoots and petioles under salt stress and varying photoperiods, respectively, have been performed using 2-D GE (Aghaei *et al*., 2008; Shah *et al*., 2011). Only 322 and 125 proteins were identified in these reports (Aghaei *et al*., 2008; Shah *et al*., 2011).

The key issue facing construction of a high quality protein profile of potato leaf tissue is the immense complexity of the plant proteome. This is further complicated by the presence of highly abundant proteins, such as ribulose bisphosphate carboxylase/oxygenase (RuBisCO) in leaf tissues (Lee *et al*., 2007). This complexity makes reproducible proteomic profiling by shotgun proteomic techniques very challenging. Lee et al. (2007) applied two shotgun techniques, multidimensional protein identification technology (MudPIT) and 1-D gel-LC-MS/MS. The authors successfully

identified 2342 non-redundant Arabidopsis leaf proteins by the combination of two shotgun techniques using 6 different extraction buffers. However, the authors suggested the development of a simple method for a better leaf proteomic analysis is needed.

Subcellular fractionation of whole tissue homogenates by centrifugation at different forces could be used to isolate various organelles and thereby enhance the detection of a wide range of leaf proteins (Lee and Cooper, 2006). According to the density of the subcellular contents, for example, a pellet obtained by relatively low force such as 1,000x g will contain nuclei, cell walls and chloroplasts (Lee and Cooper, 2006), whereas a pellet obtained by higher forces, such as 200,000x g will contain intracellular vesicles (Sachs *et al*., 2008). Subcellular fractionation is especially effective at removing highly abundant proteins such as RuBisCO that are present in chloroplasts of plant leaf cells (De Godoy *et al*., 2006; Lee *et al*., 2007). Lee and Cooper (2006) used differential centrifugation to isolate *Arabidopsis* leaf proteins. A total of 1204 non-redundant leaf proteins were identified in three different fractions with two biological replicates. They demonstrated that differential centrifugation recovered more diverse proteins than a crude extraction method which only identified 594 non-redundant proteins in *Arabidopsis* leaves (Lee and Cooper, 2006). Protein profiles have also been established by isolating specific organelles, such as vacuoles, chloroplasts, plasma membranes and cell walls, prior to proteomic analysis (Ferro *et al*., 2003; Carter *et al*., 2004; Tanaka *et al*., 2004; Feiz *et al*., 2006). Feiz et al. (2006) established a method to purify plant cell walls using an acidic acetate buffer in order to maintain interactions between polysaccharides and cell wall proteins. The authors were able to extract approximately 100 cell wall proteins using $CaCl_2$ and LiCl buffers.

The aim of this work was to establish a simple, highly reproducible method to construct a high coverage protein profile of potato leaf tissue. We established a fractionation strategy using differential centrifugation to separate the pellet (cell wall fraction) and the supernatant (cytoplasmic fraction) from potato leaf tissues. We also applied a further purification procedure in the pelleted cell wall fraction following the differential centrifugation. We confirmed that the identified potato leaf proteins in the two fractions covered a diverse range. Proteomic analysis of leaf samples obtained from three field replicated plots resulted in over 70% of the same proteins being identified in at least two of the replicates. This rate is very high, especially the samples were produced in the field conditions (Lucker *et al*., 2009; Muetzelburg *et al*., 2009). Therefore, this method can be used for successful construction of a protein profile in potato leaf tissues to study potato leaf physiology, biochemical aspects of abiotic stress and potato-pathogen interactions.

2.2 Materials and Methods

2.2.1 Plant Materials

Potato var. 'Russet Burbank' seed tubers were planted in late May with 30 cm plant spacing and 40 cm in-row spacing in plot islands. The research plots were located at Cavendish Farms Research Field, Summerside, Prince Edward Island, Canada. The plots from which leaves were excised for this study were part of a larger trial for management of potato late blight with fungicides. The trial was arranged in a completely randomized block design with four replicates. Only the 'control' plots receiving no fungicide inputs during the growing season were sampled for the purpose of this study. In early August,

four fully-expended leaves from four individual plants in each replicate plot were collected and frozen immediately in liquid nitrogen. In this study, three field replicates were used for protein profiling.

2.2.2 Isolation of Proteins from the Cell Wall Fraction

Proteins from each biological replicate, which consisted of four leaves from four individual plants, were extracted using the procedure outlined in Figure 2.1. The extraction method was based on the method of Feiz et al. (2006) with some modifications. These include the use of a MOPS/KOH buffer for grinding leaf tissues to maintain a neutral pH as opposed to using an acidic acetate buffer, and the use of trichloroacetic acid (TCA) for precipitation after $CaCl_2$ extraction. Four grams of potato leaves from each replicate were ground on ice in 10 mL MOPS/KOH grinding buffer [50 mM MOPS/KOH, pH 7.5, 5 mM EDTA, 1 mM PMSF, 330 mM sucrose, 5 mM DTT, 0.6% polyvinyl polypyrrolidone (PVPP), and 10 µL mL^{-1} protease inhibitor cocktail (Sigma, Kikuchi *et al*., 2006)]. The homogenate was centrifuged at 1,500x g for 10 min at 4 ºC. The supernatant was used to extract soluble (cytoplasmic) proteins as described in the next section. The pellet was incubated in 10 mL acetate buffer (5 mM acetate buffer, pH 4.6, 0.4 M sucrose, 2 mM PMSF, 0.6% PVPP, 0.2% (v/v) protease inhibitor cocktail) on ice for 30 min with shaking and then centrifuged at 1,500x g for 10 min at 4 ºC. The pellet was resuspended in 10 mL purification buffer (5 mM acetate buffer, pH 4.6, 0.2% (v/v) protease inhibitor cocktail) containing 0.6 M sucrose. After centrifugation at 1,500x g for 10 min at 4 ºC, the pellet was resuspended in 10 mL of the same buffer but containing 1 M sucrose in order to remove organelles less dense than polysaccharides within cell walls

(Feiz *et al*., 2006) and then centrifuged at 1,500x g. The pellet was then dissolved and vortexed with the extraction buffer (5 mM acetate buffer, pH 4.6, 0.1% (v/v) protease inhibitor cocktail, 0.2 M $CaCl_2$) for 10 min at 4 ºC and then was centrifuged at 10,000x g for 20 min at 4 ºC. TCA was added to the supernatant to a final concentration of 10%. The mixture was inverted, vortexed, and stored at -20 ºC for 30 min. The pellet was then resuspended in the urea buffer (8 M urea, 100 mM Tris-HCl, pH 8.5) and stored at -80 ºC until further use

.

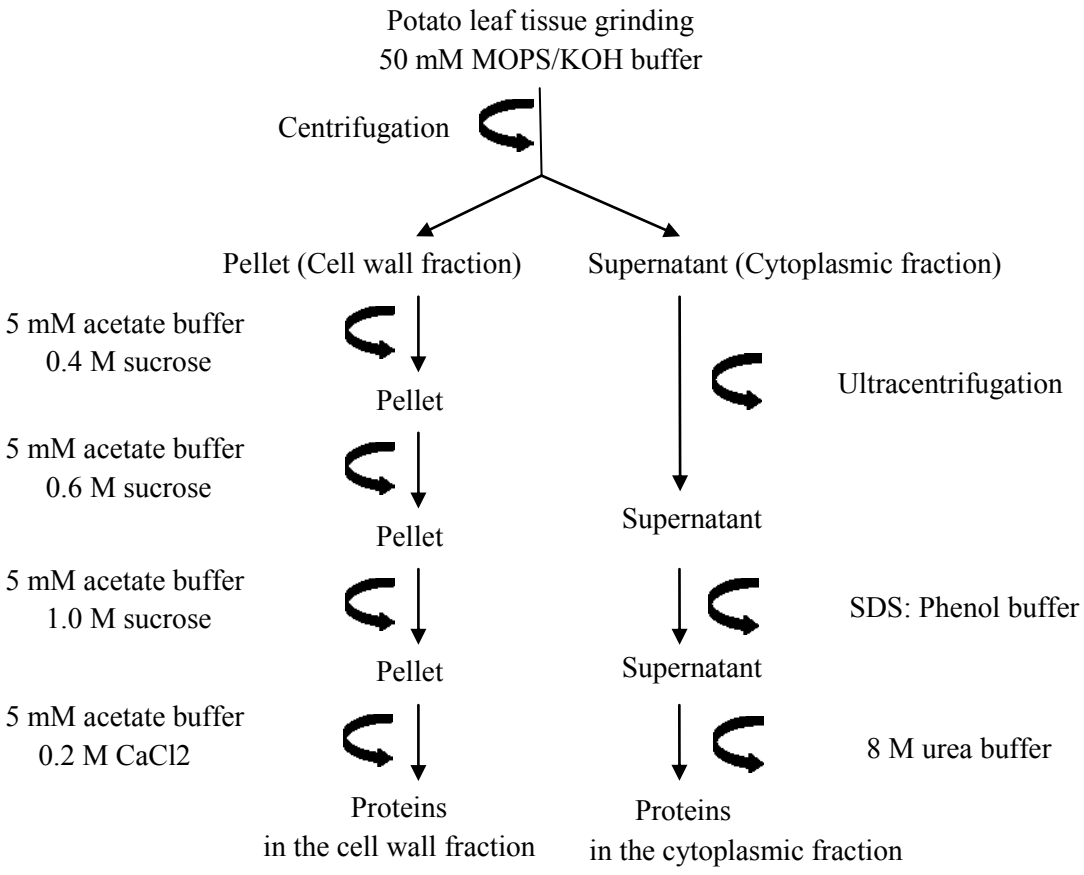

Figure 2.1. Description of the steps involved in protein extraction from the cell wall and the cytoplasmic fractions of the same potato leaf tissue by differential centrifugation.

2.2.3 Isolation of Proteins from the Cytoplasmic Fraction

For the cytoplasmic fraction, the use of another buffer was considered. SDS/phenol extraction of recalcitrant plant tissues including leaves (Wang *et al*., 2006) was employed with addition of an ultracentrifugation step. The supernatant obtained above was ultracentrifuged at 100,000x g for 1 hour (Figure 2.1) to remove plasma membrane and microsomes. TCA was added in the supernatant to a final concentration of 10%, mixed by vortexing and kept at -20 ºC for 30 min. It was centrifuged at 16,000x g for 5 min at 4 ºC and the pellet was successively washed with 80% methanol, 0.1 M ammonium acetate and finally 80% acetone. The pellet was air dried and resuspended with 400 µL SDS buffer (30% sucrose, 2% SDS, 0.1 M Tris-HCl, pH 8.0, 5% *β*-mercaptoethanol) and then 400 µL phenol (pH 8.0, Sigma) was added. The mixture was inverted and incubated at room temperature for 5 min. After centrifugation at room temperature at 8,000x g for 10 min, 400 µL upper phenol phase was transferred to a new tube that was filled with 100% methanol containing 0.1 M ammonium acetate. It was stored for 30 min at -20 ºC and was centrifuged at 16,000x g for 5 min at 4 ºC and then the pellet was washed with 100% methanol and 80% acetone, successively. The pellet was resuspended in the urea buffer (8 M urea, 100 mM Tris-HCl, pH 8.5) and stored at -80 ºC until further use. All chemicals were purchased from Sigma-Aldrich (St. Louis, MO, USA).

2.2.4 Protein Digestion

The extracted proteins from the two fractions were quantified by Bradford assay (Bradford, 1976). One hundred micrograms of cell wall proteins and 500 micrograms of cytoplasmic proteins were reduced with 5 mM DTT for 30 min at 60 ºC, alkylated with 15 mM iodoacetamide for 30 min at room temperature in the dark and then digested with trypsin (1:50 w/w trypsin/protein ratio; Promega, Madison, WI, USA) at 37 ºC overnight. Digested polypeptides were desalted using C18 Sep-Pak cartridge (Waters, Milford, MA, USA) using 0.5 mL 50% acetonitrile and then 0.5 mL 100% acetonitrile for peptide elution.

2.2.5 Two-Dimensional LC-MS/MS

Two-dimensional liquid chromatography tandem mass spectrometry (2-D LC-MS/MS) was performed using an Agilent 1100 LC coupled with a 4000 Q-TRAP mass spectrometer (Applied Biosystems Inc, Foster City, CA, USA). The peptides were fractionated by strong cation exchange (SCX) using a 100 mm x 2.1 mm^2 polysulfoetyl A column (PolyLC, Columbia, MD, USA) into 30 fractions at a flow rate of 0.2 mL min^{-1} using a linear gradient from 10 to 600 mM ammonium formate over 70 min. Each fraction was dried by speed vacuum and redissolved in 25 µL of mobile phase A (0.1 % formic acid in water). Peptides in each fraction were separated by reversed-phase liquid chromatography on an Agilent 1100 CapLC equipped with a 150 mm x 0.1 mm monolithic C18 (Phenomenex, CA, USA) coupled to a 4000 Q-TRAP mass spectrometer. An electrospray voltage of 5500 V was applied to the 30 µm spray tip (New Objectives, MA, USA). A linear gradient from mobile phase A (5% acetonitrile, 0.2% formic acid) to

mobile phase B (80% acetonitrile, 0.2% formic acid) over 50 min was applied at the flow rate of 2 μL min^{-1}. MS/MS spectra from the mass spectrometry were collected by information dependent acquisition.

2.2.6 Protein Identification

Proteins were identified based on the MS/MS spectra searched against the potato gene index database (http://compbio.dfci.harvard.edu/cgi-bin/tgi/gimain.pl?gudb=potato; release 12.0) including 61,372 unique expressed sequence tags (ESTs) sequences by using the Mascot v. 2.1.0 search engine (http://matrixscience.com, Matrix Science, London, UK). All the proteins were identified using this database before the potato genome sequence was published (The potato genome sequencing consortium, 2011). The search parameters included fixed cysteine carbamido-methylation, variable methionine oxidation, a maximum of one missed tryptic cleavage site, peptide tolerance of ±1.2 Da, and MS/MS tolerance of ±0.8 Da. A significance threshold of $p < 0.05$ and an ions score of 30 or greater in Mascot for an MS/MS match were used. Proteins matched with at least one unique peptide were considered. The mass window for precursor ion selection is 3 Da. Rolling collision energy is calculated by $(slope)^{*(M/Z)} + (intercept)$. For +2 ion, 0.044 slope and 5.500 intercept and for +3 ion, 0.029 slope and 3.850 intercept were used. False discovery rate for the estimate of false positives among the matched peptides was performed in the decoy (reversed) database (Wright *et al*., 2009).

2.2.7 Bioinformatic Analysis

SignalP server was used to predict the presence and location of cleavage sites for a signal peptide (http://www.cbs.dtu.dk/services/SignalP/; Bendtsen *et al*., 2004). Functional categories established by Bevan *et al*. (1998) were used to analyze molecular functions for the identified proteins. Cytoscape (Cline *et al*., 2007) software was used to classify the identified proteins into biological processes. The Cytoscape plugin BiNGO (Maere *et al*., 2005) was used to perform gene ontology (GO) enrichment analysis. In this study, GO annotation files against Arabidopsis available at NCBI (http://www.geneontology.org/GO.downloads.annotations.shtml) were used. Arabodopsis TAIR identifiers on GO annotation files were matched with each potato protein TC (tentative consensus) number against the potato gene index database.

2.3 Results and Discussion

2.3.1 Establishment of Potato Leaf Protein Profiles

Proteomic analysis of the cell wall fraction from three independent biological replicates was performed, resulting in the identification of 420, 391, and 442 proteins in each replicate (Mascot score > 30, $p \leq 0.05$) when searched against the potato gene index database (Figure 2.2A). The false discovery rates (FDR) were 2.4%, 1.3%, and 1.2%, respectively. Proteins detected in at least 2 of 3 replicates defined as reproducibly identified proteins were investigated to estimate the variance among the three biological replicates grown in the field. A total of 364 reproducibly identified proteins in the cell wall fraction were identified, corresponding to 70%, 71%, and 74% of the identified proteins in three replicates, respectively (Figure 2.2A, Appendix A). These reproducibly

identified proteins such as peroxidases, osmotins, and beta-1,3-glucosidase could be relatively high abundant proteins in leaf tissues. They may be involved in essential functions such as metabolism and defense responses in leaves. A total of 354 proteins appeared in only one of the three replicates (Figure 2.2A). Many of them were detected by a single peptide, suggesting that they may be relatively low abundant leaf proteins and therefore, difficult to extract.

Proteomic analysis of the cytoplasmic fractions resulted in the identification of 544, 506 and 525 proteins with 1.8, 1.7, and 1.8% FDRs, respectively, in the three biological replicates (Figure 2.2B). Of these, 72%, 72%, and 65% of the identified proteins in three replicates, respectively, were reproducibly identified proteins (Figure 2.2B, Appendix B). In total, 447 reproducibly identified proteins were identified in the cytoplasmic fraction. A total of 475 proteins were identified only in one of the three replicates.

This high reproducibility represents one of the most consistent methods for proteomic profiling of plant leaf tissues reported to date. In total, 1484 non-redundant proteins were identified from both the cell wall and cytoplasmic fractions of the three replicates. The potato gene index database we used was constructed using expression sequence tags (ESTs) to form tentative consensus sequences (TC). Therefore, the number of 1484 non-redundant proteins might be overestimated because more than one TC might be part of the same gene that encodes a protein. The potato genome was not completely sequenced at the time the data was processed. Nonetheless, the unified dataset indicates the highest number of potato leaf proteins ever reported. Using differential centrifugation, Lee and Cooper (2006) reported the identification of 1204 non-redundant Arabidopsis

leaf proteins (genome completely sequenced) from three fractions of two biological replicates, although they did not determine the reproducibility of the procedure. For the pellet fractions, the authors used *n*-dodecyl β-D-maltoside (DDM) buffer to extract proteins, especially membrane proteins. In contrast, in this study we used $CaCl_2$ buffer to extract proteins in the pellet for putative cell wall proteins. The use of $CaCl_2$ buffer helped to extract more putative cell wall proteins than the other buffers (Lee and Cooper, 2006). It is worthwhile to note that the higher number of proteins we obtained (1484) could also be the result of the developmental stage of the potato leaves, MS equipment we used, and richer genomic databases available for better protein identification.

The theoretical p*I* of the reproducibly identified leaf proteins from the two fractions varied from 4.05 (TC166407) to 11.26 (TC165127) (Figure 2.3A). The average p*I* of the reproducibly identified proteins identified from both the cell wall and cytoplasmic fractions was more than 8.1. The theoretical molecular mass of the reproducibly identified proteins in both fractions ranged from 8.9 kDa (AM907859) to 187 kDa (TC165690) (Figure 2.3B). Proteins of low molecular weight, defined as less than 40 kDa, comprised half of the reproducibly identified proteins in the cell wall fraction. Proteins identified in the cell wall fraction are relatively basic and of lower mass than those in the cytoplasmic fraction. However, the theoretical p*I* must be taken as indicative and the molecular mass may be underestimated because the database used did not contain full-length gene coding sequence. Nonetheless, the range of molecular masses reported here is very similar to the range of masses for the Arabidopsis leaf proteins identified by Lee et al. (2007) Therefore, the distribution of the detected potato leaf proteins for a range of biological and metabolic processes, such as cellular processes,

response to abiotic and biotic stimulus, defense responses, energy pathway, and protein metabolism, may indicate similar distribution with Arabidopsis leaf proteins.

(a)

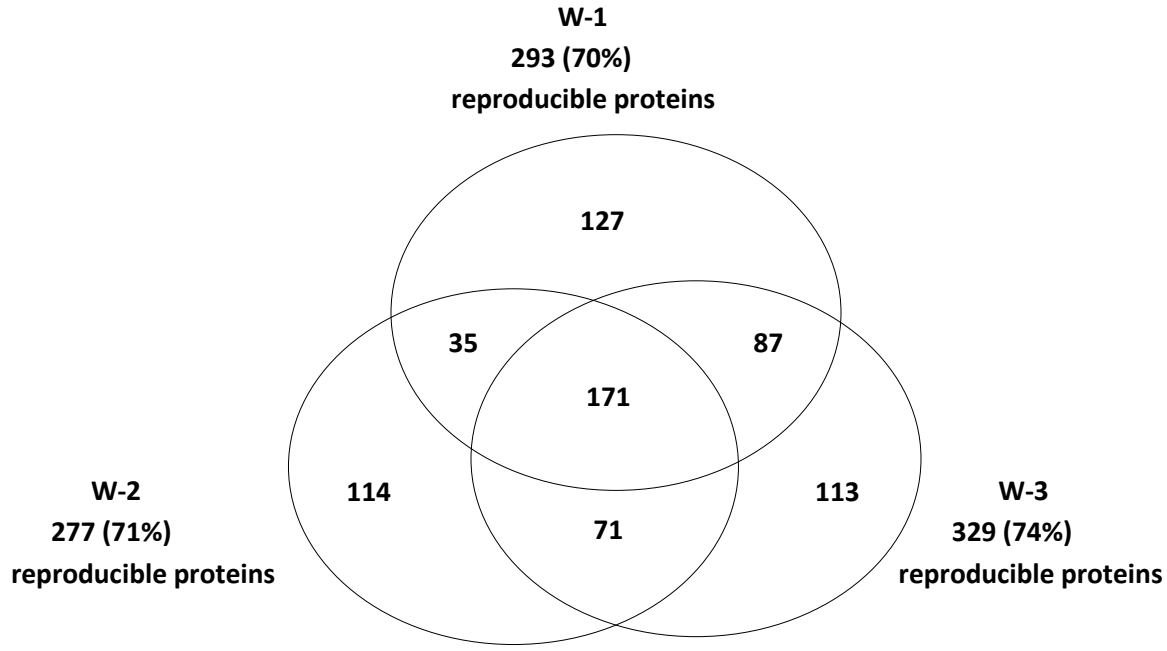

(b)

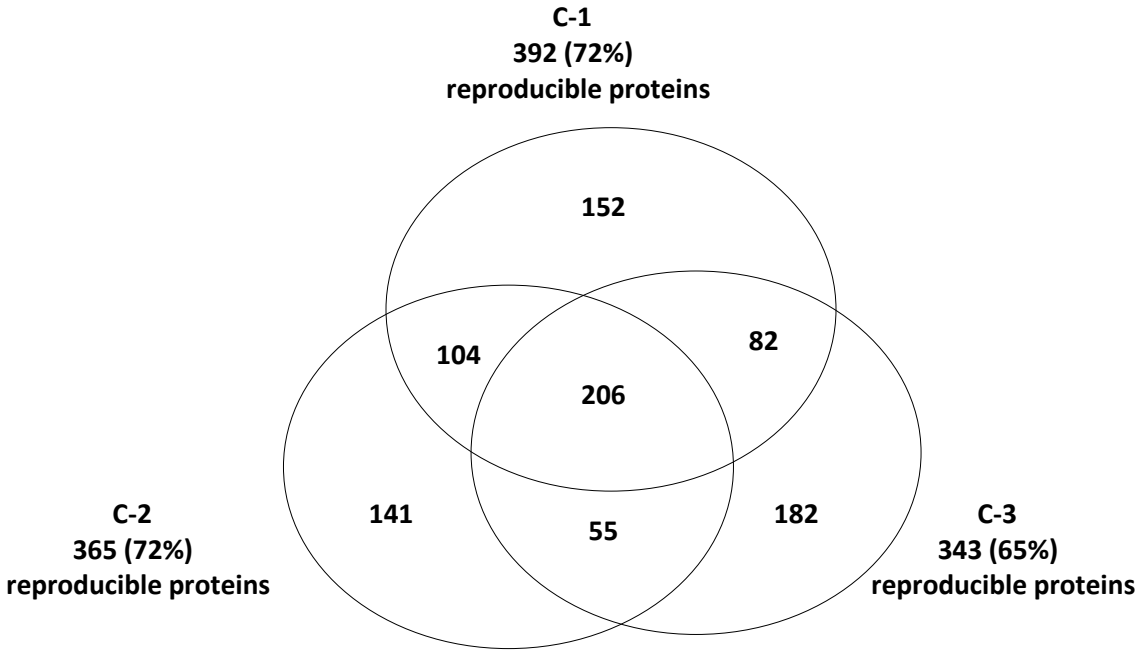

Figure 2.2. Venn diagrams showing the numbers of reproducibly identified proteins detected in the two fractions of the three biological replicates. (a) Numbers of proteins in the cell wall fraction. W: cell wall fraction. W-1, W-2, and W-3: three independent biological replicates. (b) Numbers of proteins in the cytoplasmic fraction. C: cytoplasmic fraction. C-1, C-2, C-3: three independent biological replicates. The number shared by the two circles indicates the number of the same proteins found in the two replicates. The number shared by all three circles indicates the number of proteins found in all three replicates.

(a)

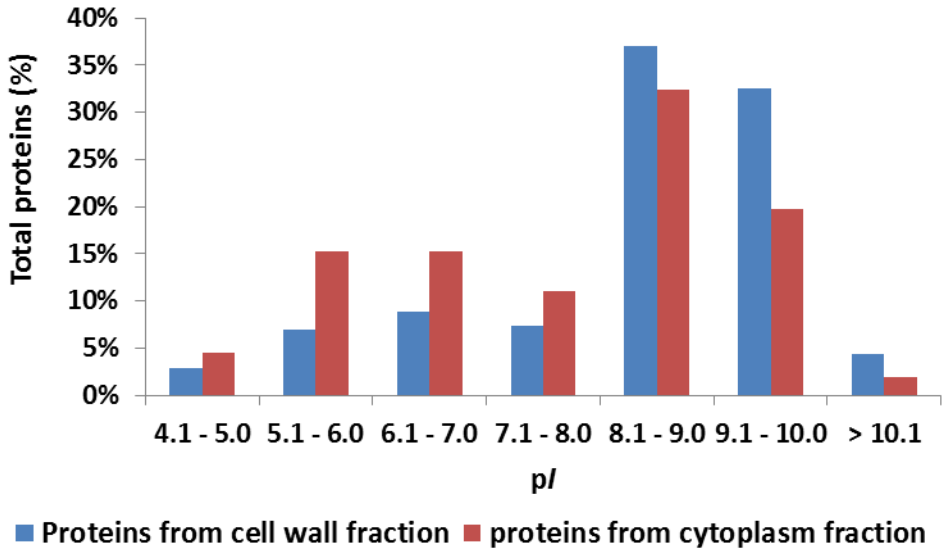

(b)

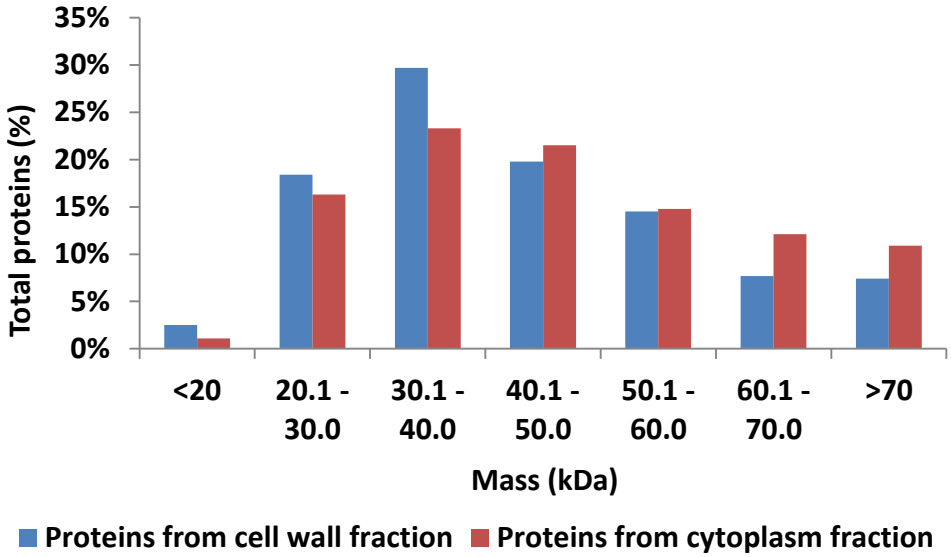

Figure 2.3. The theoretical p*I* values and molecular masses of reproducibly identified proteins identified from the two fractions. (a) The p*I* values of the reproducibly identified proteins. X-axis represents p*I* values ranging from 4.1 to 10.0 and beyond. Y-axis represents protein proportions. (b) The molecular masses in kDa of the reproducibly identified proteins. X-axis represents molecular masses ranging from less than 20.0 kDa to more than 70.0 kDa. Y-axis represents protein proportions.

2.3.2 Classification of the Proteins based on Their Molecular Functions

The reproducibly identified proteins from the two fractions were classified into functional categories based on the criteria established by Bevan et al. (1998). The proteins were functionally assigned based on published literature. The reproducibly identified proteins in both fractions were assigned to 10-11 functional categories (Figure 2.4). The proteins that could not be assigned a function are grouped into the unknown functional group. Metabolism and defense were the most common functional categories in both fractions, containing the two highest numbers of proteins. Using the sequenced potato genome we took all 91 proteins with unknown functions and analyzed by BLASTN (http://solanaceae.plantbiology.msu.edu/integrated_searches.shtml) (The potato genome sequencing consortium, 2011). Of these 91 proteins, 73 of them were reclassified. Interestingly, three of the 73 proteins were classified as having an intracellular traffic function. None of the previously classified proteins belonged to this category. The functions of only 18 of the 91 unknown proteins still remain to be determined. Therefore, this new database can act as the basis for future investigations of the potato proteome.

It is believed that most of the canonical cell wall proteins contain an N-terminal secretory signal peptide that is responsible for extracellular and apoplastic destinations of the proteins via ER-Golgi. However, several studies indicated that only half of proteins extracted by isolation of pure cell walls have a secretory signal peptide (Chivasa *et al*.,

2002; Watson *et al*., 2004). Feiz et al. (2006) isolated pure cell walls from *Arabidopsis thaliana* hypocotyls and identified 65 cell wall proteins with a signal peptide by $CaCl_2$ buffer (Feiz *et al*., 2006). Another study carried out by Goulet et al. (2010) showed that most proteins located in the cell wall and apoplast of *Nicotiana benthamiana* leaves are involved in defense and cell wall modification. In this study, therefore, in order to examine the proteins for their cell wall location, we analyzed all 115 proteins from the defense and cell wall modification functional categories. Eighty four of the 115 proteins (73%) possessed secretory signal peptides (Appendix A). Some of the remaining 31 proteins may be cell wall proteins lacking a signal peptide that are targeted to the cell wall via a non-classical pathway (Jamet *et al*., 2006; Kwon *et al*., 2008). However, due to the limited knowledge of the non-classical pathway, we were not able to pinpoint which proteins are cell wall associated proteins. Also, many proteins, for example, thaumatin-like protein, glutathione-S-transferase, and superoxide dismutase, found in the cell wall fraction would be expected to belong to the cytoplasmic fraction based on their biochemical functions. In addition, some proteins identified in the cell wall fraction are involved in glycolysis and the TCA cycle in mitochondria. These results indicate that, even at a low force of 1,500x g, the cell wall fraction could be contaminated by some proteins of other organelles (Lee and Cooper, 2006). Nevertheless, this method provided the identification of a large number of putative cell wall proteins in the cell wall fraction (Feiz *et al*., 2006).

The differential centrifugation approach helped to remove highly abundant RuBisCO proteins in the cell wall fraction. RuBisCO proteins comprise up to 50% of the soluble leaf proteins and are located in the plastids (Spreitzer and Salvucci, 2002). Simple

centrifugation at 1,500x g could exclude the majority of the chloroplasts from the cell wall fraction. Two RuBisCO proteins, ribulose bisphosphate carboxylase small chain 1 (TC167578), and ribulose bisphosphate carboxylase large chain precursor (TC163152), were found in the cell wall fraction (Appendix A), which were identified by 18 unique peptides. However, 10 RuBisCO proteins (Appendix B) which were identified by 93 unique peptides were found in the cytoplasmic fraction.

The diversity of the proteins characterized using this differential centrifugation method is higher than that obtained from the crude extraction method (Lee and Cooper, 2006). In this study, diverse defense-related proteins were represented in both fractions (Appendix A and B), because of their defined functions in each location. In the cell wall fraction, PR protein families (van Loon *et al*., 2006) were identified as the largest group in the defense category. In the cytoplasmic fraction, reactive oxygen species (ROS)-related proteins were identified as the largest group in the category, suggesting that defense-related proteins in the two fractions could play different roles in defense mechanisms. In the cell wall modification category, 34 proteins, including xylosidases and pectin acetylesterases, were identified in the cell wall fraction, whereas, in the cytoplasmic fraction, 24 proteins such as glucosidases and amylases primarily related to carbohydrate modification processes (Goulet *et al*., 2010) were identified. This may indicate cooperation of these proteins in the cell wall modification function. Proteins involved in signal transduction, such as five acid phosphatases with a signal peptide that play a role in extracellular signal mediation (Chivasa *et al*., 2002) were identified in the cell wall fraction, whereas, eight 14-3-3 proteins involved in signaling events related to transcriptional control (Watson *et al*., 2004) were identified in the cytoplasmic fraction.

In the cytoplasmic fraction, 42% of the reproducibly identified proteins (189) were assigned to the metabolism category. These proteins play roles in various processes of carbohydrate, amino acid, nucleotide, and vitamin metabolism. These metabolic processes occur in organelles such as the cytosol, chloroplast, mitochondria, and peroxisome. In addition, vacuolar targeting proteins and nuclear proteins were identified in the cytoplasmic fraction.

(a)

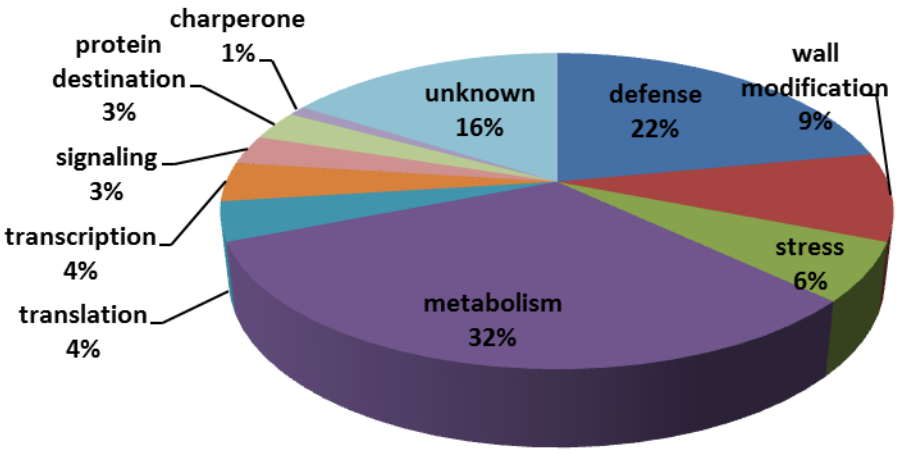

(b)

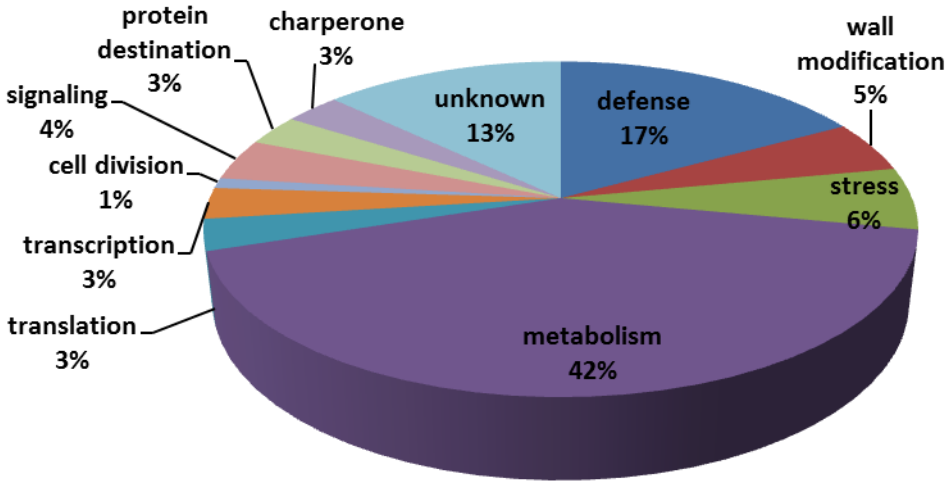

Figure 2.4. Categorization based on molecular functions of the reproducibly identified proteins from the two fractions of potato leaf tissues. (a) Classification of functions of the leaf proteins identified in the cell wall fraction. (b) Classification of functions of the leaf proteins identified in the cytoplasmic fraction.

2.3.3 Classification of the Proteins based on Their Biological Processes

To investigate the diverse roles of proteins obtained from the two fractions, the identified proteins were analyzed for their biological processes using Gene Ontology (GO) (http://www.geneontology.org). GO annotation was performed using Cytoscape with the BiNGO plugin (Cline *et al*., 2007). In some cases, proteins were classified into more than one category reflecting their role in multiple biological processes. In both fractions, the top 25 biological processes represented, based on the order of protein cluster frequency which is a percentage of proteins annotated to a biological process, are described in Figure 2.5. Proteins involved in metabolic process, cellular process, primary metabolic process, cellular metabolic process, response to stimulus, and macromolecular metabolic process, were highly represented in both fractions, although 4 out of 25

biological processes were represented differently in the fractions (Figure 2.5 A and B). In total, the 364 reproducibly identified proteins in the cell wall fraction were associated with 126 biological processes and the 447 reproducibly identified proteins in the cytoplasmic fraction were associated with 209 biological processes.

Of the 126 biological processes corresponding to proteins identified in the cell wall fraction, 32 biological processes, such as cell wall organization, cell-wall loosening, cell wall metabolic process, hemicellulose metabolic process, xyloglucan metabolic process, and xylan catabolic process were identified in only the cell wall fraction. Of 209 biological processes involving proteins in the cytoplasmic fraction, a total of 116 categories, such as starch, sucrose, and vitamin metabolic processes, nitrogen and sulfur compounds, amino acid, nucleoside, and polysaccharide biosynthetic processes, aerobic respiration, and chloroplast organization, were identified in only the cytoplasmic fraction. Classification of biological processes based on GO ontology using Cytoscape supported the identification of diverse leaf proteins from the two fractions.

In summary, the differential centrifugation method described here provided an effective way to reduce sample complexity with simple and effective depletion of high abundance proteins in plant leaf tissues. The employed method also provided high (~70%) reproducibility of proteins identified from biological replicates grown in a field. Potato leaf protein profiling by this simple differential centrifugation method provided increased coverage of the potato leaf proteome. In addition, the use of proper buffers using $CaCl_2$ and SDS/phenol for cell wall and cytoplasmic fractions, respectively, helped to increase the coverage of leaf proteins. Potato leaf protein profiling using the described method is a first step toward successful investigation of biological functions at the

proteomic level. The technique can also be implemented for comparative proteomics to study potato leaf biology, growth, development, and responses to abiotic or biotic stresses.

(a)

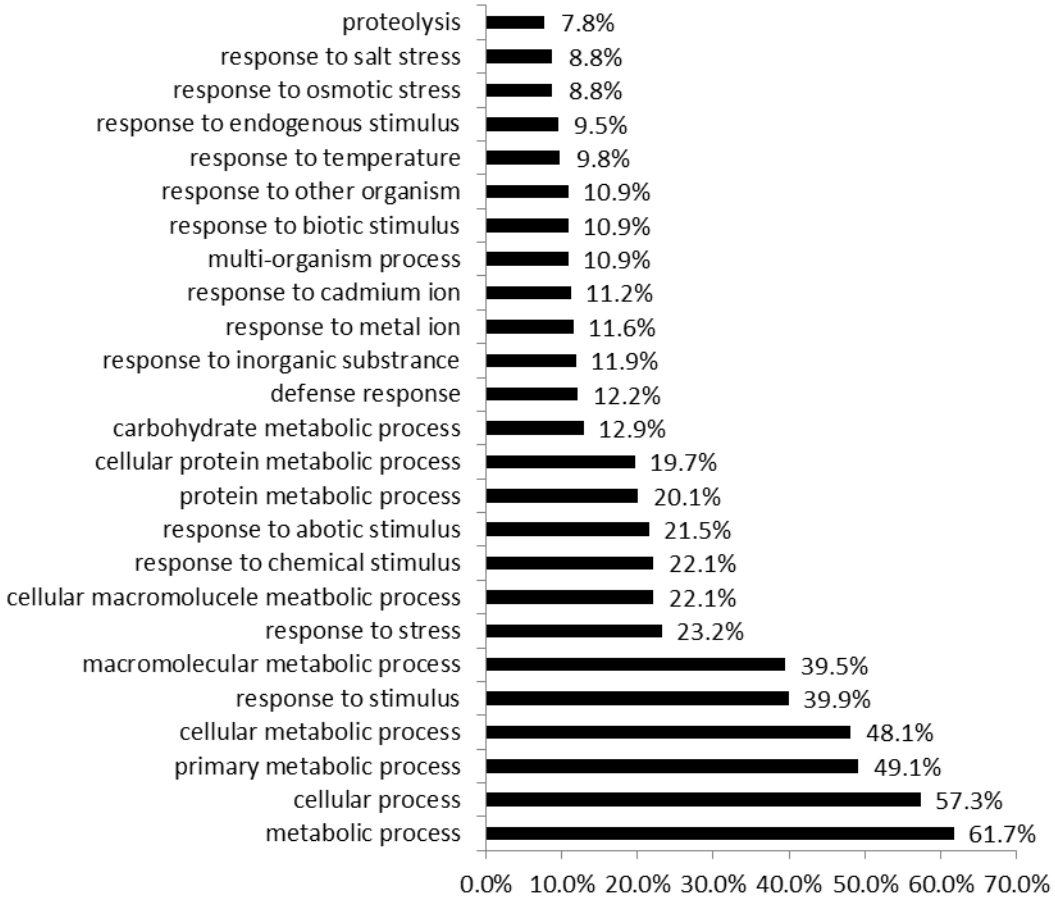

(b)

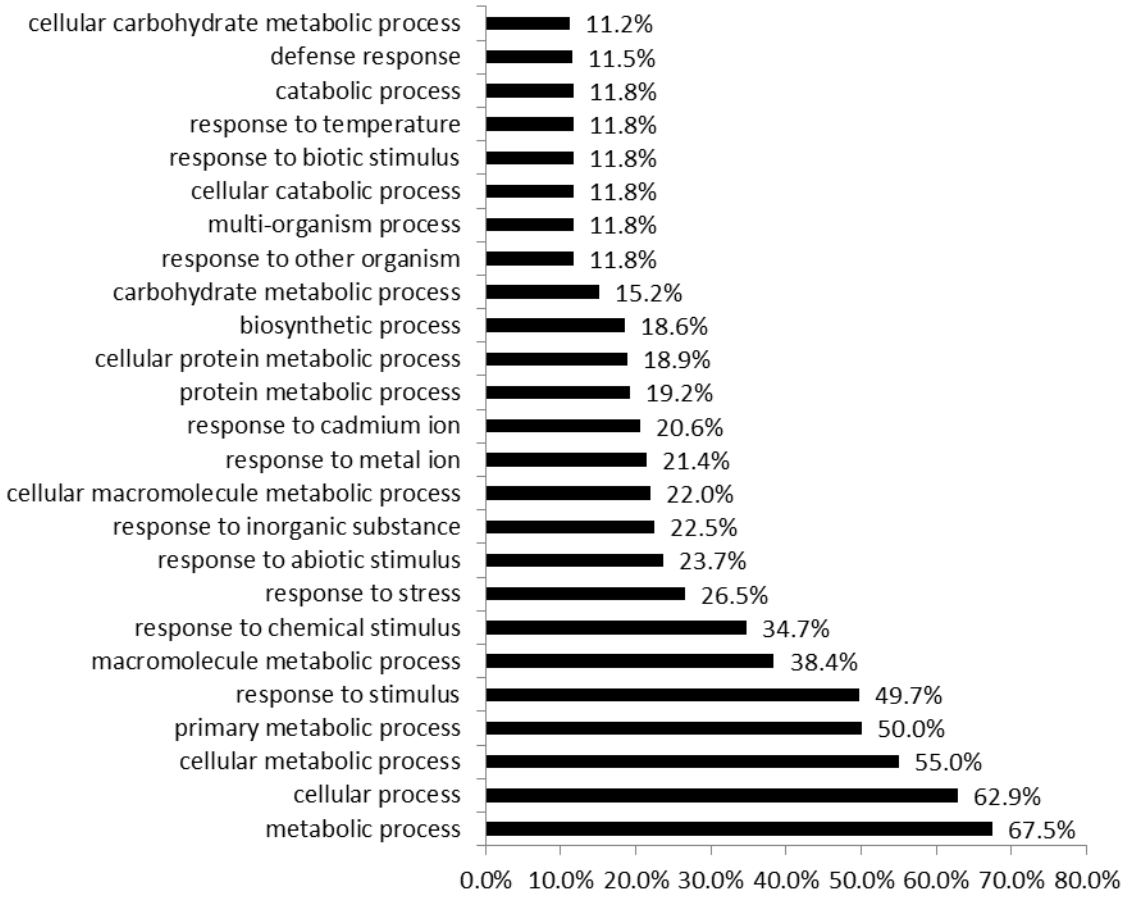

Figure 2.5. The distribution of top 25 biological process categories based on protein cluster frequencies. (a) The distribution of biological processes involved in proteins identified in the cell wall fraction. (b) The distribution of biological processes involved in proteins identified in the cytoplasmic fraction. Y-axis represents biological process category, X-axis represents protein cluster frequency assigned to each category.

Chapter 3. Proteomics Analysis Suggests Broad Functional Changes in Potato Leaves Triggered by Phosphite and a Complex Indirect Mode of Action Against *Phytophthora infestans*

Abstract

Phosphite (salts of phosphorous acid; Phi)-based fungicides are increasingly used in controlling oomycete pathogens, such as the late blight agent *Phytophthora infestans*. In plants, low amounts of Phi induce pathogen resistance through an indirect mode of action. We used iTRAQ-based quantitative proteomics to investigate the effects of phosphite on potato plants before and after infection with *P. infestans*. Ninety-three (62 up-regulated and 31 down-regulated) differentially regulated proteins were identified in the leaf proteome of Phi-treated potato plants. Four days post inoculation with *P. infestans*, 16 of the 31 down-regulated proteins remained down-regulated and 42 of the 62 up-regulated proteins remained up-regulated, including 90% of the defense proteins. This group includes pathogenesis-related, stress-responsive, and detoxification-related proteins. This finding suggests broad effects of Phi on plant defense mechanisms and metabolism. Further investigations using a callose deposition assay and microscopic imaging were undertaken to study leaf tissues after infection. One defense response observed was the activation of the hypersensitive response in Phi-treated potato leaves against *P. infestans*. This study currently represents the most comprehensive analysis of the indirect mode of action of Phi.

3.1 Introduction

The capability of plants to resist biotic and abiotic stresses can be enhanced by treatment with chemicals such as β-aminobutyric acid (BABA) or benzo (1,2,3)-thiadiazole-7-carbothioic acid *S*-methyl ester (BTH) (Goellner and Conrath, 2008). These chemicals pre-activate defense responses and increase disease resistant levels against a broad range of pathogens through a process described as induced resistance (IR) (Oostendorp *et al*., 2001; Zimmerli *et al*., 2001; Shimono *et al.,* 2007). Significant efforts have been made to identify the molecular components related to IR (Ton *et al*., 2005; Shimono *et al.,* 2007). Ton *et al*. (2005) found that IR triggered by BABA was associated with changes in the expression of three genes, including a cyclin-dependent kinase-like protein, a polyphosphoinositide phosphatase, and the abscisic acid biosynthetic enzyme zeaxanthin epoxidase. The diversity of functions of these genes suggested that broader defense responses are activated in relation to IR. Shimono *et al*. (2007) found that WRKY45, a transcription factor dependent on the systemic acquired resistance (SAR) signaling pathway in rice, is induced after the BTH application provides enhanced resistance against the rice blast fungus. These findings support the paradigm that triggering IR in plants by agrochemicals enhances pathogen resistance. This strategy provides an alternative to conventional fungicides used for controlling plant diseases (Ahn *et al*., 2005).

The cultivated potato (*Solanum tuberosum* L.) is the fourth-largest food crop in the world. It is susceptible to the oomycete *Phytophthora infestans* that causes late blight, the most devastating disease of potatoes. The intensive use of fungicides to control late blight raises concerns regarding their impact on human health and the environment (Fry,

2008). Also, *P. infestans* is a fast evolving, highly adaptive pathogen (Tian *et al*., 2007). These adaptive features of *P. infestans* led to the occurrence in the early 1990s of new strains resistant to metalaxyl, one of the most effective fungicides used for controlling late blight Goodwin *et al*., 1994). Various salts of phosphorous acid (phosphite; Phi) are increasingly being used as alternative fungicides since they are considered more environmentally friendly (Lobato *et al*., 2008; Mayton *et al*., 2008). Phi is a systemic, phloem-mobile fungicide used to control foliar as well as soil-borne diseases caused by various oomycete species in agricultural, horticultural and forestry settings (Guest and Grant, 1991; Balci *et al*., 2007; Cahill *et al*., 2008). In contrast to many other fungicides, Phi can be degraded to naturally occurring phosphates by soil microorganisms possessing the enzyme phosphite dehydrogenase (Relyea and van der Donk, 2005).

Although the inhibitory effects of Phi on oomycetes are well documented (Fenn and Coffey, 1984; Jackson *et al*., 2000), its mode of actions at the molecular level are not fully understood (Massound *et al*., 2012). Phi has complex modes of action. Phi can directly affect the mycelial growth of *Phytophthora* species (Fenn and Coffey, 1984; Guest and Bompeix, 1990). Phi also can indirectly trigger plant defense responses (Nemestothy and Guest, 1990; Jackson *et al*., 2000). Studies by Nemestothy and Guest (1990) have shown that Phi treatment was associated with cell wall reinforcement with lignin and phenolic compounds in Phi-treated tobacco infected with *P. nicotiana*. Other studies also showed that following Phi application, *P. infestans*-challenged potato plants displayed increased production of antimicrobial compounds, such as phytoalexins (Andreu *et al*., 2006). Phi-treated *Arabidopsis* challenged by *P. palmivora* responded with increased reactive oxygen species (ROS) production, rapid cytoplasmic aggregation

and nuclear migration (Daniel and Guest, 2006), while *P. cinnamomi* enhanced the expression of five defense genes whose products are involved in the salicylic acid (SA), jasmonic acid (JA) and ethylene (ET) pathways (Eshraghi *et al*., 2011). A slightly different pathosystem, consisting of Phi-treated *Arabidopsis* and the biotrophic oomycete *Hyaloperonospora*, was used recently to demonstrate that IR occurs *via* SA-dependent signaling pathways rather than through JA- and ET-dependent pathways (Massoud *et al*., 2012). Although these studies represent significant contributions to the identification of specific molecular components involved in phosphite-induced resistance (Phi-IR) against *Phytophthora* species, a more comprehensive view of the targets and mechanisms related to the indirect mode of action of Phi is needed.

The aim of this study was to determine the protein population in potato leaves that is responsive to Phi treatments before and after infection with *P. infestans*. We used a quantitative proteomics approach with iTRAQ (isobaric Tag for Relative and Absolute Quantification) reagents to establish four protein profiles, from which 93 differentially regulated proteins were identified. Subsequently, multiple reaction monitoring (MRM), a targeted method for quantification of specific proteins, was used to perform technical validation of these differentially regulated proteins. The functions of up-regulated proteins in Phi-treated sample identified through proteomics as well as the cytological observations suggest a strong HR component in the Phi-IR in potato leaves against *P. infestans*.

3.2 Materials and Methods

3.2.1 Plant Materials and Treatments

Potato (*Solanum tuberosum* L.) cultivar 'Russet Burbank' seed tubers were planted in the research field of Cavendish Farms (New Annan, Prince Edward Island, Canada) in late May (Wang-Pruski *et al*., 2010). The trial was arranged in a completely randomized block design with four replications. The experimental treatments consisted of field applications of either water (Con; control) or 5.8 liters/ha Confine^{TM} (Phi; treated) in 250 liter water/ha. Confine^{TM} was obtained from Winfield Solutions LLC, St. Paul, MN via The Agronomy Company of Canada Ltd, Thorndale, ON. Confine^{TM} is a fungicide containing 45.8% mono- and di-potassium salts of phosphorous acid. Treatments were applied weekly except for a two-week interval between the first and the second treatments. Fungicide applications were made with a tractor mounted commercial sprayer. In total, 5 treatments (applications of water or fungicide) were applied before sampling. In early August, three days after the last treatment, 4 individual water- or Confine^{TM}-treated plants were harvested. One fully extended healthy (no insect damage to plants) leaf from each of water- or Confine^{TM}-treated plants was collected. In total, four leaves from four different plants (Con or Phi) per replicate were collected, wrapped in aluminum foil, and dipped immediately into liquid nitrogen. The entire time from detaching to freezing was less than 3 min. Leaf samples were named Con-0 and Phi-0, respectively (Figure 3.1). No late blight was observed in the region during the season.

For the cytological observations, potato cv. 'Russet Burbank' seed tubers were planted in pots and the pots were arranged in a completely randomized block design with four replications. They were grown in a growth chamber at 24ºC with 16 h light and at 16ºC with 8 h dark cycle. When plants were two months old, they were treated with water

or Confine™ (0.4 mL/20 mL water) one day before sampling. Two healthy leaves of control or Phi-treated plants from each of four replicates were collected.

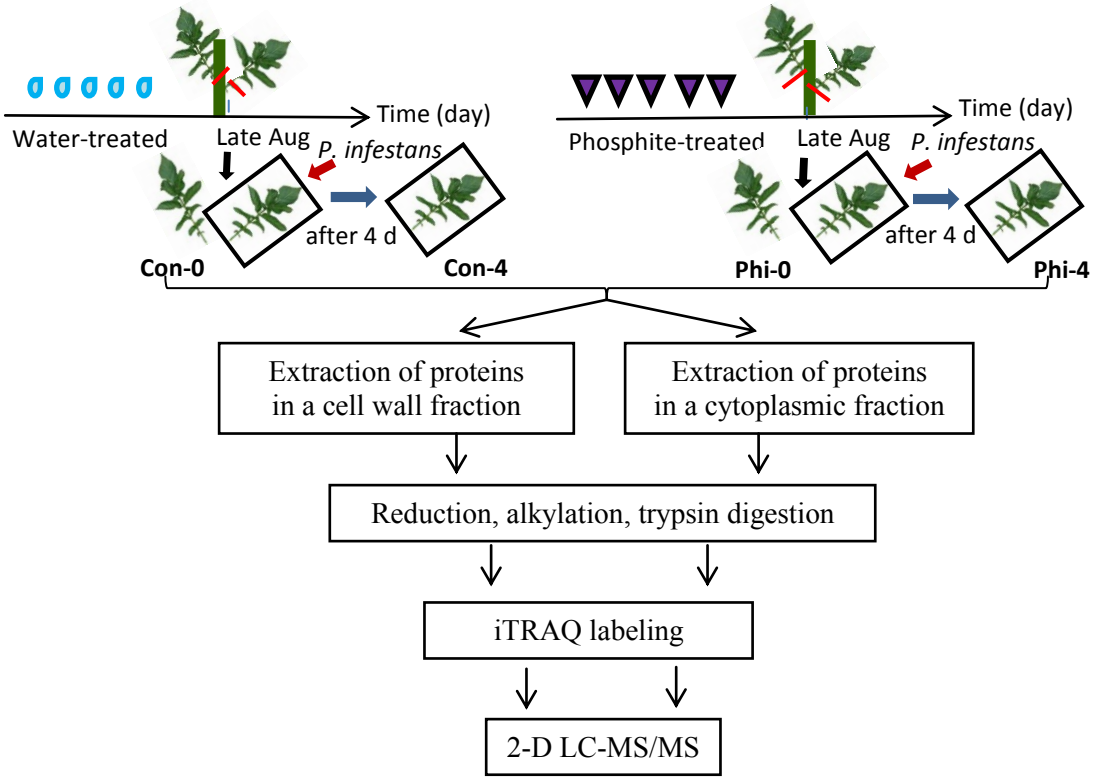

Figure 3.1. Overview of potato leaf sampling and iTRAQ experiment.

3.2.2 *Phytophthora infestans* Inoculation

From the field trial, a second leaf was detached from the same plants and inoculated with 1 mL of a sporangial suspension (50,000 sporangia/ml) of *P. infestans* using an atomized sprayer. The isolate used for inoculation was obtained locally (Prince Edward Island, Canada) and was determined to be of the US-8 genotype (A2 mating type), the most prevalent genotype of the pathogen in eastern Canada for the past decade

(Peters *et al*., 2001). Each inoculated leaf was placed on wet paper in a Ziploc bag and incubated in a growth chamber at 16ºC with 12 h light and 12 h dark cycle. The severity of the infection on the control and Phi-treated leaves was estimated based on the percentage of diseased leaf area (James 1971). Four days post inoculation (dpi) leaf samples labeled Con-4 and Phi-4 were collected (Figure 3.1) and frozen in liquid nitrogen. Each detached leaf obtained from the growth chamber for the cytological observations was inoculated and incubated the same way as for the field samples.

3.2.3 Protein Extraction and iTRAQ Labeling

Three of the four field replicates of the four different types of leaf samples (Con-0, Phi-0, Con-4, and Phi-4) were used for protein profiling. Potato leaf proteins were separated by centrifugation into cell wall and cytoplasmic fractions, and extracted based on a published method (Lim *et al*., 2012). One hundred microgram of protein extract from each of the two subcellular fractions was dissolved in 20 μL of iTRAQ dissolution buffer (Applied Biosystems, Foster City, CA, USA). Protein denaturation, reduction, blocking of cysteine residues, and digestion were performed according to the iTRAQ manufacturer's protocol. Tags used were 114 Da for Con-0, 115 Da for Phi-0, 116 Da for Con-4, and 117 Da for Phi-4. After labeling for 1 h, peptides from all four samples were combined and desalted using a C18 Sep-Pak cartridge (Waters, Milford, MA, USA). The peptides were fractionated into 30 fractions by strong cation exchange using a 100 mm × 2.1 mm^2 polysulfoethyl A column (PolyLC, Columbia, MD, USA) (Lim *et al*., 2012). Peptides in each fraction was then separated on a NanoAcquity UPLC system (Waters, Milford, MA, USA) with a C18 column coupled to a QTOF Premier mass spectrometer

(Waters, Milford, MA, USA) equipped with a nano electrospray source. A linear gradient from mobile phase A (5% acetonitrile, 0.1% formic acid) to mobile phase B (85% acetonitrile, 0.1% formic acid) over 60 min was applied at the flow rate of 500 nl/min. MS/MS was conducted by data-directed analysis acquisition of the three most intense peaks with a charge state of 2+ or 3+ in the MS spectra. Lockspray was used at a constant flow of 2 µl/min of 200 fM/µl Glu-Fibrinogen B (Sigma-Aldrich), scanning every 20 s.

3.2.4 Protein Identification

Raw data processing from the MS/MS peak lists was performed using the Proteinlynx software (Waters, Milford, MA, USA) with default parameters for MS and MS/MS (Murphy and Pinto, 2010). Mascot (v2.1.0, Matrix Science, London, UK) was used to search the peak list against two databases, the Potato Genome Sequencing Consortium database and Potato Gene Index database (Lim *et al*., 2012) and to generate iTRAQ reporter ion intensities. Peptide ratios were average normalized and peptide ratios identified from the Con-0 sample were selected as the denominator to compare the relative abundance of each protein. Protein ratios were calculated using the weighted average by Mascot. In order to reduce variability between replicates due to sample preparation, a normalization procedure was applied. In this case, means of the iTRAQ 115/114 ratios of proteins that were not significantly differentially regulated ($0.75 \leq$ fold change ≤ 1.4) in each replicate were calculated (Table 3.1). The calculated mean of iTRAQ 115/114 ratios in each replicate were set to 1 and then, iTRAQ 115/114 ratios of all other differentially regulated proteins were normalized accordingly. MultiExperment Viewer (MeV) software v4.8 (http://www.tm4.org/mev.html) was used to generate a

heatmap representing relative abundance of proteins. Protein ratios generated by Mascot were converted to $\log_2$ ratios to generate a heatmap.

Table 3.1. Normalization of means of iTRAQ 115/114 ratio from two fractions of the three replicates

Criteria for normalization	Replicate	iTRAQ 115/114 ratios
Means of proteins in 0.75 ≤ fold change ≤ 1.4	W-2	1
	W-3	0.98
	W-4	1
	C-2	1.07
	C-3	1.04
	C-4	0.95
After means of iTRAQ 115/114 ratios set to 1	W-2	1
	W-3	1
	W-4	1
	C-2	1
	C-3	1
	C-4	1

W, wall fraction; C, cytoplasmic fraction; 2, 3, 4, three different biological replicates.

3.2.5 Scanning Electron Microscopy

Scanning electron microscopy (SEM), Transmission electron microscopy (TEM), and callose visualization were performed using the control and Phi-treated detached leaves collected at 5 dpi. Leaf pieces in 100% ethanol were placed in a critical point dryer (Bomar SPC-900, Bomar Company, Tacoma, Washington, USA). The ethanol was replaced with liquid CO_2 by rinsing 3 times for 30 min, then the chamber was heated to 42 °C and the pressure was allowed to rise to ~1350 psi. At this point, the temperature was maintained at 42 °C and the pressure was released slowly (100 psi/min) until

atmospheric pressure was reached. The samples were then mounted on carbon tape and coated with gold/palladium using a Polaron SC-7620 sputter coater (Polaron, Quorum Technologies, East Sussex, UK). The samples were examined and images were taken using a Hitachi S3000N Scanning Electron Microscope (Hitachi, Ibaraki-Ken, Japan).

3.2.6 Transmission Electron Microscopy

Leaf pieces (2 x 2 mm) were fixed with 3% glutaraldehyde in 0.1 M cacodylate buffer (pH 7.4) at room temperature for 2 h. Samples were washed with the cacodylate buffer for 15 min twice, post-fixed with 1% osmium tetroxide in cacodylate buffer for 90 min, washed with a cacodylate buffer and dehydrated by a graded series of ethanol for 15 min/each. Samples were then dehydrated with 100% ethanol three times for 15 min/each, transferred to acetone and infiltrated through an epon-acetone resin mixture series. Embedding was done in fresh 100% resin at 45 °C for 24 h, and at 60 °C for 24 h for polymerization. Ultrathin (80 nm) sections (Reichert ultracuts) were cut and examined under TEM (Hitachi 7500) and then photographed using a Bioscan camera with Gatan software.

3.2.7 Callose Deposition

Leaf pieces were gradually dehydrated and re-hydrated via gradually decreased concentrations of ethanol. Samples were stained in 0.05% aniline blue in 0.15 M KH_2PO_4, pH 9.5 overnight and then de-stained in 0.15 M KH_2PO_4, pH 9.5 (Bhadauria *et al*., 2010). De-stained samples were mounted in 30% glycerol on glass slides and examined using a UV epifluorescence microscope (DMRE, Leica Wetzler, Germany). Callose was

observed using the excitation filter BP 340-380 nm and emission filter LP 425 nm (Pasqualini *et al*., 2003). A light microscope was used to examine the infected area on leaf pieces. All images were acquired and processed using the software, Compix Simple PCI (JH Technologies, San Jose, USA).

3.2.8 mTRAQ Labeling and MRM

One hundred microgram of proteins from two biological replicates of Con-0 and Phi-0 samples was labeled with mass differential Tags for Relative and Absolute Quantification (mTRAQ) light and heavy reagents, respectively. Labeling with mTRAQ reagents was performed according to the mTRAQ manufacturer's protocol (Applied Biosystems, Foster City, CA, USA). The labeled peptides from the two samples were combined and desalted using C18 SepPak cartridges (Waters, Milford, MA, USA). 1-D LC-MS/MS was performed using an Agilent 1100 capillary HPLC (Agilent, Santa Clara, CA, USA) coupled to a 4000 Q-TRAP mass spectrometer (Applied Biosystems, USA). Reversed-phase liquid chromatography was conducted using a 100 μm × 150 mm^2 monolithic C18 column (Phenomenex, CA, USA). A linear gradient from mobile A (5% acetonitrile, 0.1% formic acid) to mobile B (90% acetonitrile, 0.1% formic acid) over 50 min was applied at the flow rate of 2 μl/min. MRM acquisition and MRM-triggered MS/MS acquisition were followed by the method described by Murphy and Pinto (2010). MRM transitions of a peptide for each of the 15 proteins (13 up-regulated and 2 down-regulated proteins) were assessed. The average of peak areas generated by the 3 or 4 MRM transitions of each peptide provided the relative abundance of each protein in Con-

0 and Phi-0 leaves. MultiQuant (v1.1, Applied Biosystems, USA) was used to integrate peak areas of MRM chromatograms using the parameters of Murphy and Pinto (2010).

3.3 Results

3.3.1 Profiling Potato Leaf Proteins

Proteomic profiles were established using four different groups of plant leaf samples grown in field trials in 2007 (Wang-Pruski *et al*., 2010): two groups of uninoculated samples, Phi treatment (Phi-0) and untreated control leaves (Con-0), and two groups of 4 days post inoculation (dpi) samples, Phi-4 and Con-4. At 4 dpi, Phi-treated samples showed significantly less late blight development when compared with control leaves (Figure 3.2; Wang-Pruski *et al*., 2010).

Proteomics analysis was used to identify cell wall and cytoplasmic leaf proteins regulated by Phi application and their changes in abundance upon infection with *P. infestans*. Proteomic analysis of the cell wall fraction provided a total of 843 iTRAQ-labeled non-redundant proteins. The number of proteins identified in each replicate was 639, 620 and 552, respectively (Figure 3.3a). False discovery rates (FDR) were estimated as 0.3%, 0.3%, and 0.4% at the peptide identity level in each replicate, respectively. Proteomic analysis of the cytoplasmic fraction provided a total number of 1094 iTRAQ-labeled non-redundant proteins. The number of proteins identified in each replicate was 561, 684 and 773, respectively (Figure 3.3b). FDR were estimated as 0.5%, 0.3%, and 0.3% in each replicate, respectively.

Proteins identified in at least two of the three independent biological replicates, which are referred to as reproducibly identified proteins (Berg *et al*., 2006; Lim *et al*.,

2012), were selected for quantitative comparative analysis. In total, 83%, 85%, and 89% of the identified proteins in the cell wall fractions of the three replicates, respectively, were reproducibly identified proteins, while 81%, 76%, and 70% of the identified proteins in the cytoplasmic fractions of the three replicates, respectively, were reproducibly identified proteins. In total, 1172 reproducibly identified proteins, 577 proteins from the cell wall fraction (Appendix C) and 595 proteins from the cytoplasmic fraction (Appendix D), were used for further analyses.

(a)

(b)

Figure 3.2. Degree of late blight symptoms in leaves of the control and Phi-treated plants. Four leaves detached from control or Phi-treated potato cv. Russet Burbank

inoculated by *P. infestans*. Pictures were taken 4 days post inoculation. (a) Infected control potato leaves. (b) Infected Phi-treated potato leaves.

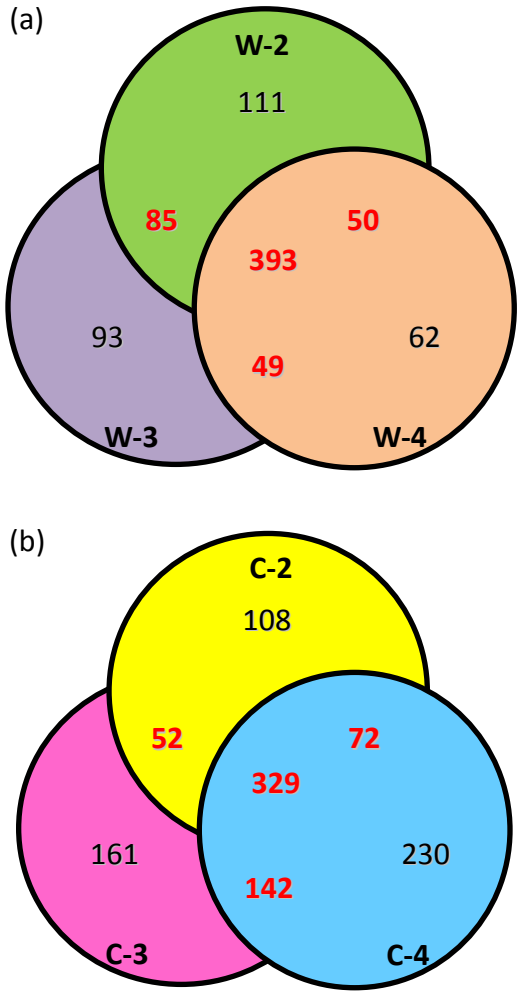

Figure 3.3. Numbers of iTRAQ-labeled proteins identified in the three replicates. Each colored circle represents the proteins from one replicate. The four numbers included in each circle represent the numbers of proteins that are found only in this replicate (black) or commonly found in two or three replicates (red). (a) Numbers of iTRAQ-labeled proteins identified in the cell wall fraction of three biological replicates. The cell wall fraction from the three biological replicates resulted in the identification of 647 (W-2), 637 (W-3), and 552 (W-4) proteins in each replicate, respectively. (b) Numbers of iTRAQ-labeled proteins identified the cytoplasmic fraction. The cytoplasmic fraction from the three biological replicates resulted in the identification of 561 (C-2), 684 (C-3), and 773 (C-4) proteins, respectively. W, wall fraction; 2, 3, 4, three different biological replicates; C, cytoplasmic fraction.

3.3.2 Identification of Differentially Regulated Proteins in Phi-Treated Sample

To identify differentially regulated proteins in Phi-treated sample in the absence of *P. infestans*, the iTRAQ 115/114 (Phi-0/Con-0) ratio of 1172 reproducibly identified proteins was investigated. A 1.4-fold change cut-off was used to define proteins that are significantly up-regulated in Phi-treated sample. This threshold was selected based on other reports (Zhu *et al*., 2009; Wang *et al*., 2012). Similarly, a fold change threshold of 0.75 was used to define significant down-regulation. The fold change of the proteins was converted to $\log_2$ expression data to generate a heatmap representing differentially regulated proteins in Phi-treated sample using the MeV (v4.8) software (Saeed *et al*., 2006).

A total of 62 different proteins were found to be up-regulated in the Phi-treated sample (ratios of Phi-0/Con-0 in Table 3.2; Figure 3.4a). Thirty three proteins were obtained from the cell wall fraction and 39 were obtained from the cytoplasmic fraction. Among them, 10 proteins were found in both the cell wall and cytoplasmic fractions. A total of 31 proteins were found to be down-regulated in the Phi-treated sample (ratios of Phi-0/Con-0 in Table 3.3; Figure 3.4b). Thirty-one proteins were found to be down-regulated proteins. Thirteen proteins were identified in the cell wall fraction and 18 proteins were found in the cytoplasmic fraction, but none in both fractions. In summary, 7.9% (93 of 1172 proteins) of reproducibly identified proteins were regulated in the Phi-treated sample.

Table 3.2. Up-Regulated Proteins in Phi-Treated Sample in the Absence of *P. infestans* (Phi-0/Con-0) and Their Changes in the Presence of *P. infestans* (Phi-4/Phi-0)

Accession no	Protein identification	Phi-0/ Con-0	Phi-4/ Phi-0	Con-4/ Con-0	Phi-4/ Con-4	Functions	Signal peptide
TC176356[w]	Basic PR-1 protein	2.84*	4.05	11.88	0.93	Defense	Yes
TC169479[c]	Basic PR-1 protein	1.81	7.53	9.97	1.30	Defense	Yes
TC169479[w]	Basic PR-1 protein	3.32	3.31	14.55	0.74	Defense	Yes
TC168375[w]	PR-1 protein	1.55	3.30	4.98	0.88	Defense	Yes
TC170396[c]	PR-1 protein	1.68	5.23	4.84	1.58	Defense	Yes
TC170396[w]	PR-1 protein	1.83	3.34	6.31	0.86	Defense	Yes
TC172275[c]	PR protein P2 (PR-4)	1.79	4.96	6.75	1.22	Defense	No
TC172275[w]	PR protein P2 (PR-4)	1.63	1.65	2.44	1.14	Defense	No
TC173865[c]	Beta-1,3 glucanase (PR-2)	1.82	1.71	2.81	0.85	Defense	Yes
TC163195[c]	Beta-1,3 glucanase (PR-2)	1.82	1.94	2.62	1.19	Defense	Yes
TC175030[w]	Beta-1,3-1,4-glucanase	1.43	0.55	0.83	0.88	Defense	No
TC168318[c]	Class II chitinase (PR-3)	1.46	1.50	2.50	0.92	Defense	Yes
TC168318[w]	Class II chitinase (PR-3)	1.41	0.98	2.56	0.68	Defense	Yes
CK263954[c]	Class II chitinase (PR-3)	1.48	1.85	2.17	1.10	Defense	Yes
CK263954[w]	Class II chitinase (PR-3)	1.53	0.97	2.65	0.72	Defense	Yes
TC168794[c]	Class II chitinase (PR-3)	1.41	3.40	5.08	0.93	Defense	No
TC163769[c]	Acidic endochitinase	1.44	1.47	2.99	0.58	Defense	Yes
TC163769[w]	Acidic endochitinase	1.58	0.64	1.45	0.67	Defense	Yes
TC163429[w]	Endochitinase	1.44	0.96	1.61	0.87	Defense	Yes
TC189821[w]	Thaumatin-like protein (PR-5)	1.82	1.00	2.12	0.83	Defense	No
TC169893[w]	Thaumatin-like protein (PR-5)	1.63	1.11	1.98	0.86	Defense	No
TC172434[c]	Peroxidase (PR-9)	1.52	1.68	2.38	1.25	Defense	Yes
TC172434[w]	Peroxidase (PR-9)	1.43	1.10	1.71	1.00	Defense	Yes
TC169870[c]	Peroxidase (PR-9)	1.73	1.71	2.61	1.10	Defense	No
TC164504[w]	Peroxidase (PR-9)	1.71	2.35	5.75	0.43	Defense	Yes
TC186921[c]	Glutathione S-transferase	1.50	1.20	1.84	0.99	Defense	No
TC186921[w]	Glutathione S-transferase	1.46	0.92	2.02	0.63	Defense	No
TC177499[c]	Glutathione S-transferase	1.41	1.25	1.74	1.01	Defense	Yes
TC176436[w]	Monodehydroascorbate reductase	1.41	0.87	1.45	0.87	Defense	No
TC186221[w]	Putative heat shock protein	1.63	1.47	1.02	2.35	Defense	No
TC182291[w]	Osmotin-like protein (PR-5)	1.72	6.77	15.27	0.75	Defense	Yes
TC165487[c]	Osmotin-like protein (PR-5)	1.48	7.93	10.39	1.08	Defense	Yes
TC165487[w]	Osmotin-like protein (PR-5)	1.70	5.75	13.10	0.74	Defense	Yes
TC163374[w]	Osmotin-like protein (PR-5)	1.99	20.85	36.58	0.81	Defense	Yes
TC171679[w]	Osmotin-like protein (PR-5)	1.56	6.61	13.62	0.75	Defense	Yes

Table 3.2. (*Continued*)

Accession no	Protein identification	Phi-0/ Con-0	Phi-4/ Phi-0	Con-4/ Con-0	Phi-4/ Con-4	Functions	Signal peptide
TC179738[w]	GDSL-motif lipase	1.40	0.78	0.42	2.41	Defense	Yes
TC189750[w]	Wound-induced protein WIN1	1.49	9.21	13.17	1.14	Defense	Yes
TC182527[c]	Wound-induced proteinase inhibitor 1	1.44	1.53	1.24	1.77	Defense	No
TC173874[c]	Germin-like protein (PR-16)	1.48	1.43	3.56	0.65	Defense	Yes
TC176976[c]	Cathepsin B	1.39	1.74	2.15	1.12	Defense	Yes
TC172593[c]	Cysteine proteinase 3	1.45	1.33	2.04	0.95	Defense	Yes
TC181645[w]	Cysteine protease inhibitor 9	1.79	0.38	0.55	1.16	Defense	Yes
TC166886[w]	Cysteine protease inhibitor 7	2.04	0.34	0.51	1.44	Defense	Yes
TC166762[c]	Cysteine protease inhibitor 1	1.46	0.79	0.70	1.63	Defense	Yes
TC166762[w]	Cysteine protease inhibitor 1	1.55	0.36	0.64	0.87	Defense	
TC186600[c]	60S acidic ribosomal protein	1.78	0.89	1.11	1.44	P.S.	
TC186583[c]	Ribosome recycling factor	1.58	0.73	1.06	1.03	P.S.	
TC180423[c]	Acidic ribosomal protein	1.40	1.10	2.15	0.74	P.S.	
TC178608[c]	40S ribosomal protein S16	1.44	1.54	1.51	1.49	P.S.	
TC165455[c]	60S ribosomal protein L13	1.68	1.37	1.95	0.85	P.S.	
TC165221[c]	30S ribosomal protein S9	2.14	0.43	0.50	1.45	P.S.	
TC163292[c]	Elongation factor 1-alpha	1.40	1.28	1.98	0.92	P.S.	
CV470531[c]	Elongation factor TuB	1.47	0.84	1.21	0.97	P.S.	
TC164403[c]	60S ribosomal protein L1	1.40	1.29	1.53	1.17	P.S.	
TC166345[c]	Biotin carboxylase	1.44	0.73	0.72	1.07	Metabolism	
TC183342[c]	3-ketoacyl-CoA thiolase 2	1.76	2.01	4.20	0.79	Metabolism	
TC165530[c]	Adenylyl-sulfate reductase	1.52	0.25	0.25	1.58	Metabolism	
TC165467[c]	Pyrroline-5-carboxylate reductase	1.45	n/a**	1.67	n/a	Metabolism	
TC163648[c]	Serine hydroxymethyltransferase	1.43	0.76	1.33	0.77	Metabolism	
TC194216[w]	G3PDH	1.40	0.73	0.59	1.33	Energy	
TC166486[w]	G3PDH	1.72	0.54	0.75	1.17	Energy	
TC181183[w]	G3PDH	1.47	0.86	1.36	0.93	Energy	
TC165027[w]	Succinyl-CoA ligase	2.27	1.03	2.90	0.74	Energy	
TC163506[w]	Triosephosphate isomerase	1.56	0.47	0.81	0.83	Energy	
TC168258[c]	Calmodulin-5/6/7/8	2.06	0.95	1.23	1.54	S.T.	
TC166307[c]	Calmodulin-5/6/7/8	1.40	1.12	1.23	1.39	S.T.	
TC172096[c]	Histidine triad (HIT) protein	1.43	0.81	0.89	1.41	S.T.	
TC180805[w]	Threonine endopeptidase	2.20	0.44	1.68	0.41	P.D.	
TC167954[w]	Aminopeptidase	1.90	0.44	0.86	1.01	P.D.	
TC165237[c]	BTF3-like transcription factor	1.46	0.88	1.17	1.05	Transcription	
TC168485[c]	Putative uncharacterized protein	1.43	1.02	1.28	1.13	Unknown	
TC164517[c]	Putative uncharacterized protein	2.15	0.35	0.66	1.00	Unknown	

c, the cytoplasmic fraction; w, the cell wall fraction.
* Average of iTRAQ ratios of each protein identified in at least two of three different biological replicates.
** n/a, not available because the ratio of the protein was identified in only one of the three biological replicate.
P.S., Protein synthesis; S.T., Signal transduction; P.D., Protein destination.

Table 3.3. Down-Regulated Proteins in Phi-Treated Sample in the Absence of *P. infestans* (Phi-0/Con-0) and Their Changes in the Presence of *P. infestans* (Phi-4/Phi-0)

Accession no	Protein identification	Phi-0/ Con-0	Phi-4/ Phi-0	Con-4/ Con-0	Phi-4/ Con-4	Function
TC163042[c]	Phosphoenolpyruvate carboxylase	0.50	1.85	0.88	1.04	Energy
TC181436[c]	Phosphoenolpyruvate carboxylase	0.64	1.62	1.05	0.97	Energy
TC164001[w]	Oxygen-evolving enhancer protein	0.65	0.52	0.40	0.81	Energy
TC163384[w]	Oxygen-evolving enhancer protein 1	0.75	0.49	0.48	0.76	Energy
CK257172[w]	Pyruvate dehydrogenase	0.69	0.93	0.45	1.46	Energy
TC171649[c]	Pyruvate kinase	0.58	2.52	1.19	1.28	Energy
TC168267[w]	Fructose-bisphosphate aldolase	0.61	0.83	0.47	0.97	Energy
TC164121[w]	Fructose-bisphosphate aldolase	0.67	0.67	0.51	0.87	Energy
TC163071[c]	Glucose-6-phosphate isomerase	0.67	1.62	0.96	1.05	Energy
TC167284[c]	6-phosphogluconate dehydrogenase	0.71	1.52	0.78	1.49	Energy
TC191617[w]	Phosphoribulokinase	0.71	1.22	0.86	1.16	Energy
TC165919[c]	Alpha-glucan phosphorylase	0.41	2.40	0.86	1.19	Metabolism
TC165690[c]	Alpha-glucan phosphorylase	0.72	1.07	0.67	1.10	Metabolism
TC163028[c]	Alpha-glucan water dikinase	0.64	1.47	0.56	2.15	Metabolism
TC163054[c]	Sucrose synthase 2	0.53	3.68	2.19	0.91	Metabolism
TC179073[w]	Ferredoxin	0.63	0.67	0.64	0.61	Metabolism
TC169318[c]	Glutamate synthase	0.46	1.50	0.55	1.04	Metabolism
TC164369[c]	Alanine aminotransferase	0.72	0.67	0.48	0.98	Metabolism
TC163367[c]	Aminotransferase 2	0.74	0.82	0.58	0.95	Metabolism
TC163226[c]	Glycine dehydrogenase	0.69	0.91	0.60	1.05	Metabolism
TC190989[c]	Thaumatin-like protein	0.61	1.70	1.41	0.66	Defense
TC189821[c]	Thaumatin-like protein	0.63	1.82	1.87	0.53	Defense
TC165098[c]	Glutathione S-transferase	0.75	1.57	0.97	1.21	Defense
TC172573[w]	Polygalacturonase inhibitor protein	0.65	1.41	0.50	2.02	Defense
TC181534[c]	Elongation factor EF-2	0.62	2.02	0.94	1.25	P.S.
TC164483[c]	Ribosomal protein L3-like	0.72	1.08	0.72	1.08	P.S.
TC169973[w]	40S ribosomal protein S12	0.74	0.95	0.39	1.81	P.S.
TC164185[w]	Histone H1	0.74	1.03	0.75	0.99	Transcription
EG015239[w]	Small nuclear ribonucleoprotein	0.61	1.63	n/a	n/a	Transcription
EG016190[w]	Multiprotein bridging factor 1c	0.72	1.18	0.89	1.00	S.T.
TC175288[w]	Proteasome subunit alpha type-6	0.72	1.07	0.53	1.42	P.D.

c, the cytoplasmic fraction; w, the cell wall fraction.

* Average of iTRAQ ratios of each protein identified in at least two of three different biological replicates.

** n/a, not available because the ratio of the protein was identified in only one of the three biological replicate.

P.S., Protein synthesis; S.T., Signal transduction; P.D., Protein destination.

(a)

TC169479W Basic PR-1 protein
TC176356 Basic PR-1 protein
TC165027 Succinyl-CoA ligase
TC180805 Threonine endopeptidase
TC164517 Putative uncharacterized protein
TC165221 30S ribosomal protein S9
TC168258 Calmodulin-5/6/7/8
TC166886 Cysteine protease inhibitor 7
TC163374 Osmotin-like protein
TC167954 Aminopeptidase
TC170396W PR-1 protein
TC173865 Beta-1 3-glucanase
TC189821W Thaumatin-like protein
TC163195 Beta-1 3-glucanase
TC169479C Basic PR-1 protein
TC181645 Cysteine protease inhibitor 9
TC172275C PR protein P2
TC186600 60S acidic ribosomal protein
TC183342 3-ketoacyl-CoA thiolase 2
TC169870 Peroxidase
TC166486 Glyceraldehyde 3-phosphate dehydrogenase
TC182291 Osmotin-like protein
TC164504 Peroxidase
TC165487W Osmotin-like protein
TC170396C PR-1 protein
TC165455 60S ribosomal protein L13
TC186221 Putative heat shock protein
TC172275W PR protein P2
TC169893 Thaumatin-like protein
TC163769W Acidic endochitinase
TC186583 Ribosome recycling factor
TC163506 Triosephosphate isomerase
TC171679 Osmotin-like protein
TC168375 PR-1 protein
TC166762W Cysteine protease inhibitor 1
CK263954W Class II chitinase
TC165530 Adenylyl-sulfate reductase
TC172434C Peroxidase
TC186921C Glutathione S-transferase
TC189750 Wound-induced protein WIN1
TC165487C Osmotin-like protein
TC173874 Germin-like protein
CK263954C Class II chitinase
TC181183 Glyceraldehyde 3-phosphate dehydrogenase
CV470531 Elongation factor TuB
TC168318C Class II chitinase
TC186921W Glutathione S-transferase
TC166762C Cysteine protease inhibitor 1
TC165237 BTF3-like transcription factor
TC165467 Pyrroline-5-carboxylate reductase
TC172593 Cysteine proteinase 3
TC163429 Endochitinase
TC166345 Biotin carboxylase
TC163769C Acidic endochitinase
TC178608 40S ribosomal protein S16
TC182527 Wound-induced proteinase inhibitor 1
TC172434W Peroxidase
TC172096 Histidine triad (HIT) protein
TC175030 Beta-1 3-1 4-glucanase
TC168485 Putative uncharacterized protein
TC163648 Serine hydroxymethyltransferase
TC177499 Glutathione S-transferase
TC168794 Class V Chitinase
TC168318W Class II chitinase
TC176436 Monodehydroascorbate reductase
TC194216 Glyceraldehyde 3-phosphate dehydrogenase
TC180423 Acidic ribosomal protein
TC166307 Calmodulin-5/6/7/8
TC179738 GDSL-motif lipase
TC163292 Elongation factor 1-alpha
TC164403 60S ribosomal protein L1
TC176976 Cathepsin B

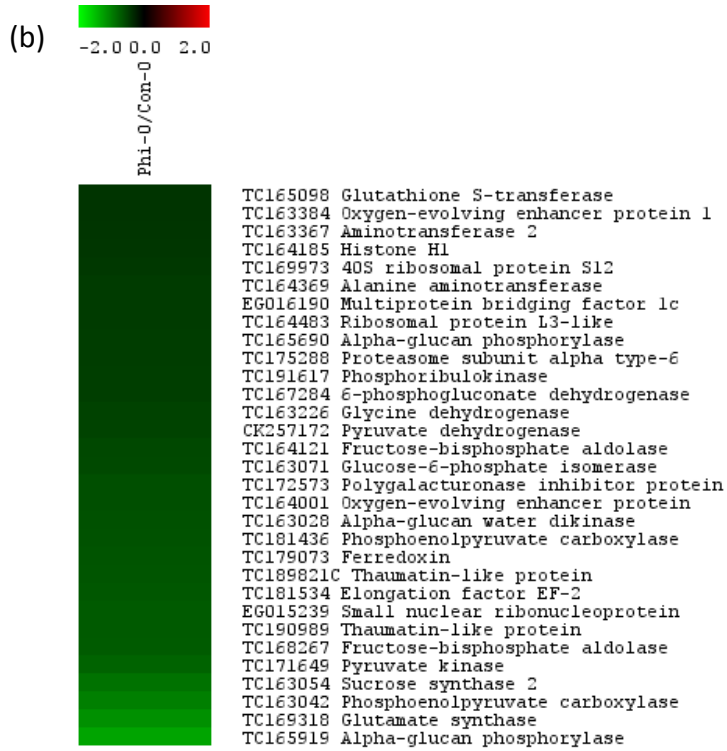

Figure 3.4. Heatmaps representing differentially regulated proteins in Phi-treated sample. The proteins are ordered based on the magnitude of induction or repression. (a) A heatmap shows up-regulated proteins in the absence of *P. infestans*. The proteins are more abundant in Phi-treated leaves than the control leaves. (b) A heatmap shows down-regulated proteins in the absence of *P. infestans*. The proteins are less abundant in Phi-treated leaves than the control leaves. C or W next to TC number means fraction. C, cytoplasmic fraction; W, cell wall fraction.

The 62 up-regulated and 31 down-regulated proteins were categorized into 8 and 7 functional groups, respectively (Figure 3.5), based on Bevan *et al*. (1998). Of the 62 up-regulated proteins, 35 proteins were related to defense functions. This group was comprised of 22 pathogenesis-related (PR) proteins, 5 proteases/protease inhibitors, 5 stress-responsive proteins, and 3 detoxification-related proteins. PR proteins, such as acidic PR-1, β-1,3-glucanase (PR-2), chitinase (PR-3), thaumatin/osmotin-like protein (PR-5), and peroxidase (PR-9) were up-regulated in the Phi-treated sample (Table 2), represented the most abundant group in the defense category of the up-regulated proteins.

Using SignalP software (Bendtsen *et al*., 2004), we found that 25 of these 35 proteins had a signal peptide at their N-terminus; therefore, they corresponded to putative secretory proteins (Table 2). Proteome analysis revealed 7 reactive oxygen species (ROS)-related proteins were up-regulated. These were glutathione S-transferases (GST), monodehydroascorbate reductase (MDHAR), peroxidases and germin-like protein (GLP) (Table 2). GSTs and MDHAR involved in the ROS scavenging system control the level of ROS for ROS homeostasis. Peroxidase and GLP with superoxide dismutase or oxalate oxidase activity contribute to the production of ROS (Mittler, 2002). The up-regulation of these proteins indicates that changes in ROS levels occur in Phi-treated plants. Increased H_2O_2 serves as a secondary messenger to activate defense responses such as cell wall reinforcement. Three up-regulated peroxidases were identified in this study; two of them were class III peroxidases that have a signal peptide (Table 2). Class III peroxidase-mediated H_2O_2-dependent cross-linking of cell wall components reinforces cell walls through the formation of physical barriers composed of lignification or suberization (Almagro *et al*., 2009). In this study, cathepsin B and cysteine protease inhibitors that are associated with HR were also up-regulated.

The second most abundant functional group among the 62 up-regulated proteins was associated with protein synthesis (Figure 3.5a). Metabolism- and energy-related proteins involved in glycolysis and amino acid metabolism formed the third group. The putative functions of 2 up-regulated proteins were not known. In contrast to up-regulated proteins in the Phi-treated sample, 20 of the 31 down-regulated proteins were classified into metabolism and energy functions, such as starch metabolism, amino acid metabolism,

photosynthesis, glycolysis and tricarboxylic acid (TCA) cycle. The second most abundant group (4 proteins) was associated with defense (Figure 3.5b).

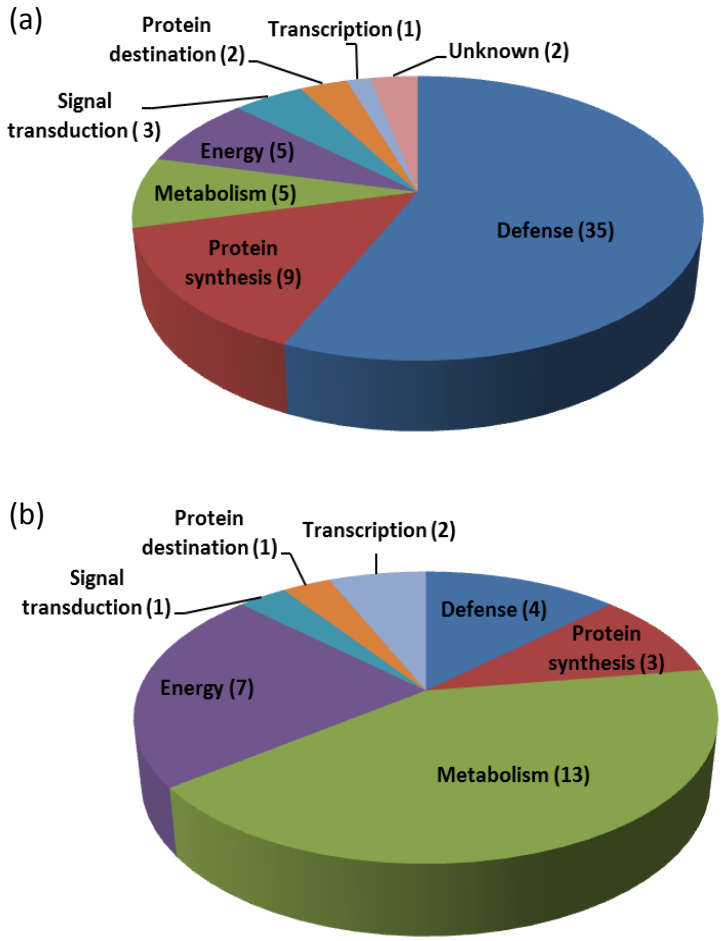

Figure 3.5. Functional classification of differentially regulated proteins. (a) Functional groups assigned to the 62 up-regulated proteins. (b) Functional groups assigned to the 31 down-regulated proteins. Numbers in parenthesis indicate a number of proteins classified into a functional category.

3.3.3 Identification of Changes in Abundance of the Differentially Regulated Proteins in Infected Phi-Treated Sample

The relative abundance of the 62 up-regulated and 31 down-regulated proteins in the Phi-treated leaves in the presence of *P. infestans* at 4 dpi (ratios of Phi-4/Phi-0 in Tables 2 and 3), was depicted in heatmaps (Figure 3.6). After 4 dpi, the relative abundance of 24 of the 62 up-regulated proteins was further increased based on the fold change criteria (group 1, Figure 3.6a). Twenty one of these 24 proteins have defense-related functions; they were 17 PR proteins, 3 stress-responsive proteins and 1 protease. The relative abundance of 23 of the 62 up-regulated proteins was unchanged or changed insignificantly in the presence of the pathogen (group 2, Figure 3.6a). Ten of the proteins have defense functions, 5 proteins were related protein synthesis, 3 for metabolism, 3 for signal transduction, 1 for transcription, and 1 with unknown function. Lastly, the relative abundance of 15 of the 62 up-regulated proteins was found to be decreased at 4 dpi (group 3, Figure 3.6a). These 15 proteins were comprised of proteins in the following functional classes: defense function (4 proteins), glycolysis (3 proteins), metabolism (2 proteins), sulfur assimilation pathway (1 protein), protein synthesis (2 proteins), protein destination (2 proteins), and unknown function (1 protein). Of the 4 defense-related proteins, 3 were different cysteine protease inhibitors and the remaining protein was a beta-1,3-1,4-glucanase.

In the presence of *P. infestans*, the abundance of 15 of the 31 down-regulated proteins was up-regulated (group 1, Figure 3.6b). These were the proteins found to be involved in starch/sucrose metabolism, pyruvate metabolism, and defense. The abundance of 11 of the 31 down-regulated proteins did not show significant changes

(group 2, Figure 3.6b), whereas the relative abundance of 5 of the 31 down-regulated proteins involved in photosynthesis and amino acid metabolism was further decreased (group 3, Fig.ure 3.6b).

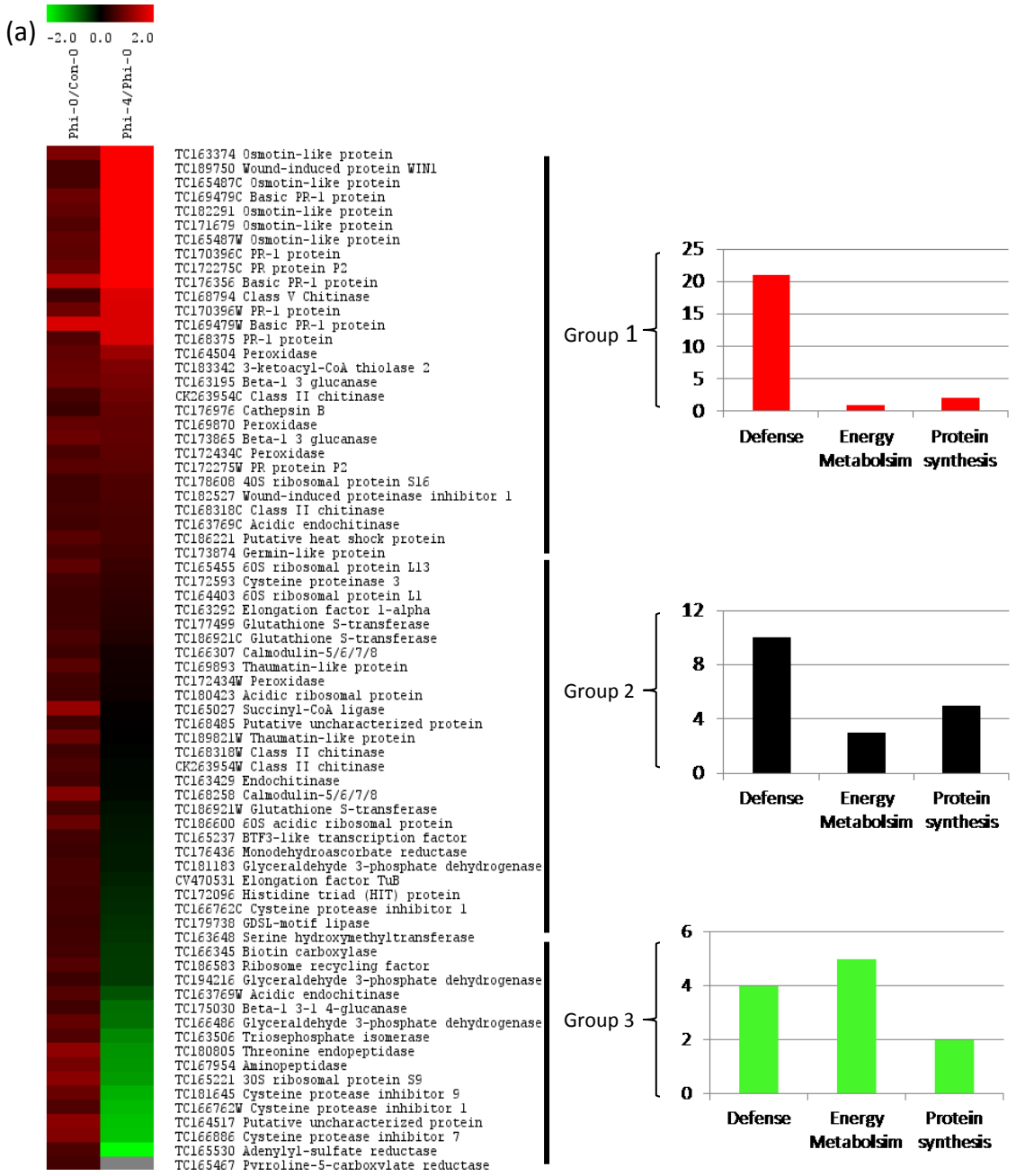

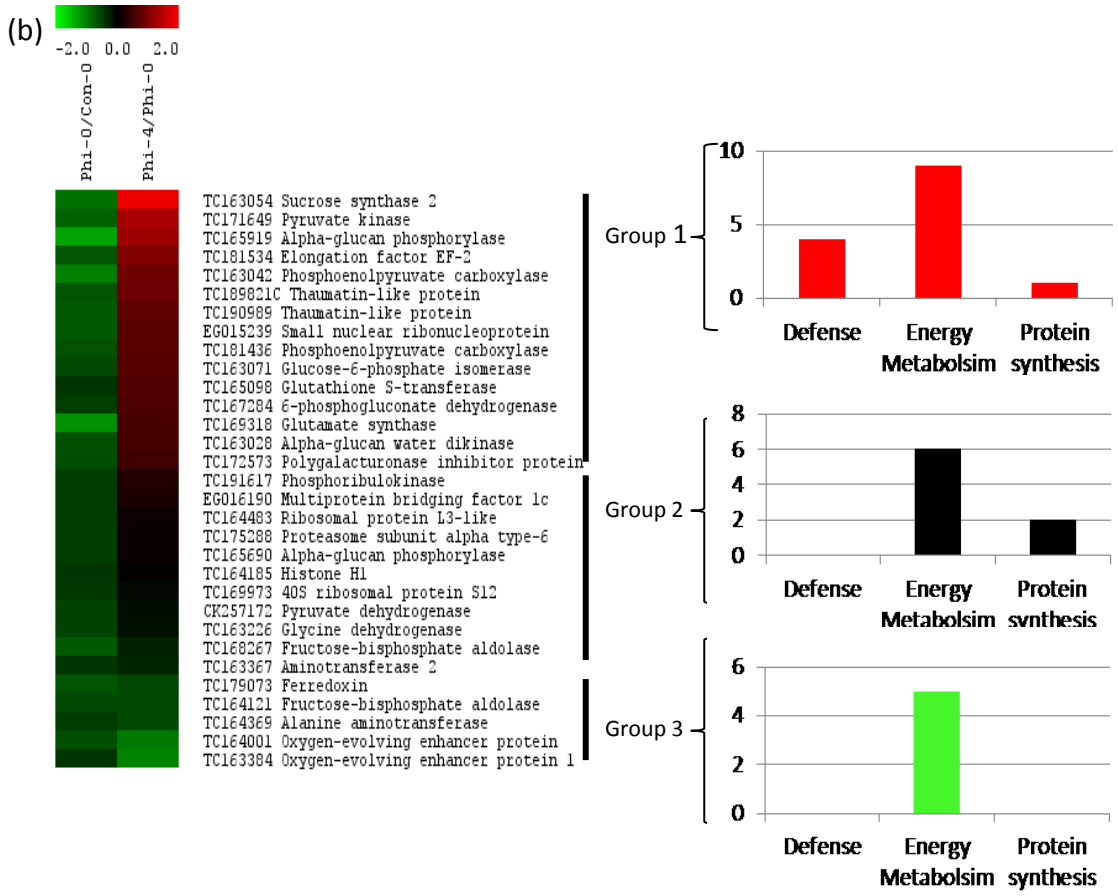

Figure 3.6. Changes in abundance of the differentially regulated proteins in infected Phi-treated sample. (a) Changes in abundance of the 62 up-regulated proteins in the presence of *P. infestans*. Left column in the heatmap shows the up-regulated proteins before infection. The value of each protein was calculated by the ratio of Phi-0/Con-0. Right column in the heatmap shows the changes in abundance of the up-regulated proteins at 4 dpi. The value was calculated by the ratio of Phi-4/Phi-0. The columns on the right of the figure were grouped based on the ratio of Phi-4/Phi-0. The number of proteins in the three largest functional groups was shown. Group 1 indicates proteins showing further increase in abundance 4 days after infection. Group 2 indicates proteins showing insignificant changes. Group 3 indicates proteins showing down-regulation at 4 dpi. (b) Changes in abundance of the 31 down-regulated proteins in the presence of *P. infestans*. Left column in the heatmap shows the down-regulated proteins before infection. The value of each protein was calculated by the ratio of Phi-0/Con-0. Right column in the heatmap shows the changes in abundance of the down-regulated proteins at 4 dpi. The value was calculated by the ratio of Phi-4/Phi-0. The columns on the right of the figure were grouped based on the ratio of Phi-4/Phi-0. Group 1 indicates proteins showing further increase in abundance 4 days after infection. Group 2 indicates proteins showing insignificant changes. Group 3 indicates proteins showing down-regulation at 4 dpi.

3.3.4 Identification of Proteins Showing Differential Abundance in Both Infected Phi-Treated and Infected Control Samples

In order to estimate the suppressive effects of Phi on *P. infestans* development in potato leaves, the relative abundance of the 93 proteins in both infected Phi-treated leaves (Phi-4) and infected control leaves (Con-4) were calculated (ratios of Phi-4/Con-4 in Tables 2 and 3, Figure 3.7). Proteins showing differential abundance in both infected samples may be the key components involved in Phi-IR against late blight in potatoes.

From the 62 up-regulated proteins, 10 proteins were more abundant in infected Phi-treated sample (Phi-4) than in infected control sample (Con-4) (group 1, Figure 3.7a). These proteins are responsible for defense (4 proteins), protein synthesis (3 proteins), signal transduction (2 proteins), and metabolism (1 protein). The majority (45 of 62 proteins) of the proteins showed no significant changes in both infected samples (group 2, Figure 3.7a). The other 7 proteins were less abundant in Phi-4 samples when compared to Con-4 samples (group 3, Figure 3.7a). They play roles in defense (4 proteins), metabolism (1 protein), protein synthesis (1 protein), and protein destination (1 protein).

From the 31 down-regulated proteins, the abundance of 6 proteins were found to be elevated in Phi-4 (group 1, Figure 3.7b). They are involved in energy (2 proteins), metabolism (1 protein), defense (1 protein), protein synthesis (1 protein), and protein destination (1 protein). The majority (22 of 31 proteins) of the proteins showed no significant changes in both infected samples (group 2, Figure 3.7b). The other 3 proteins, ferredoxin in metabolism and two thaumatin-like proteins in defense, were less abundant in Phi-4 than Con-4 samples (group 3, Figure 3.7b). The Phi-4/Con-4 ratio data indicate

that the abundance of most of the 93 proteins in infected Phi-treated leaves was similar to the abundance observed in infected control leaves at 4 dpi with *P. infestans*.

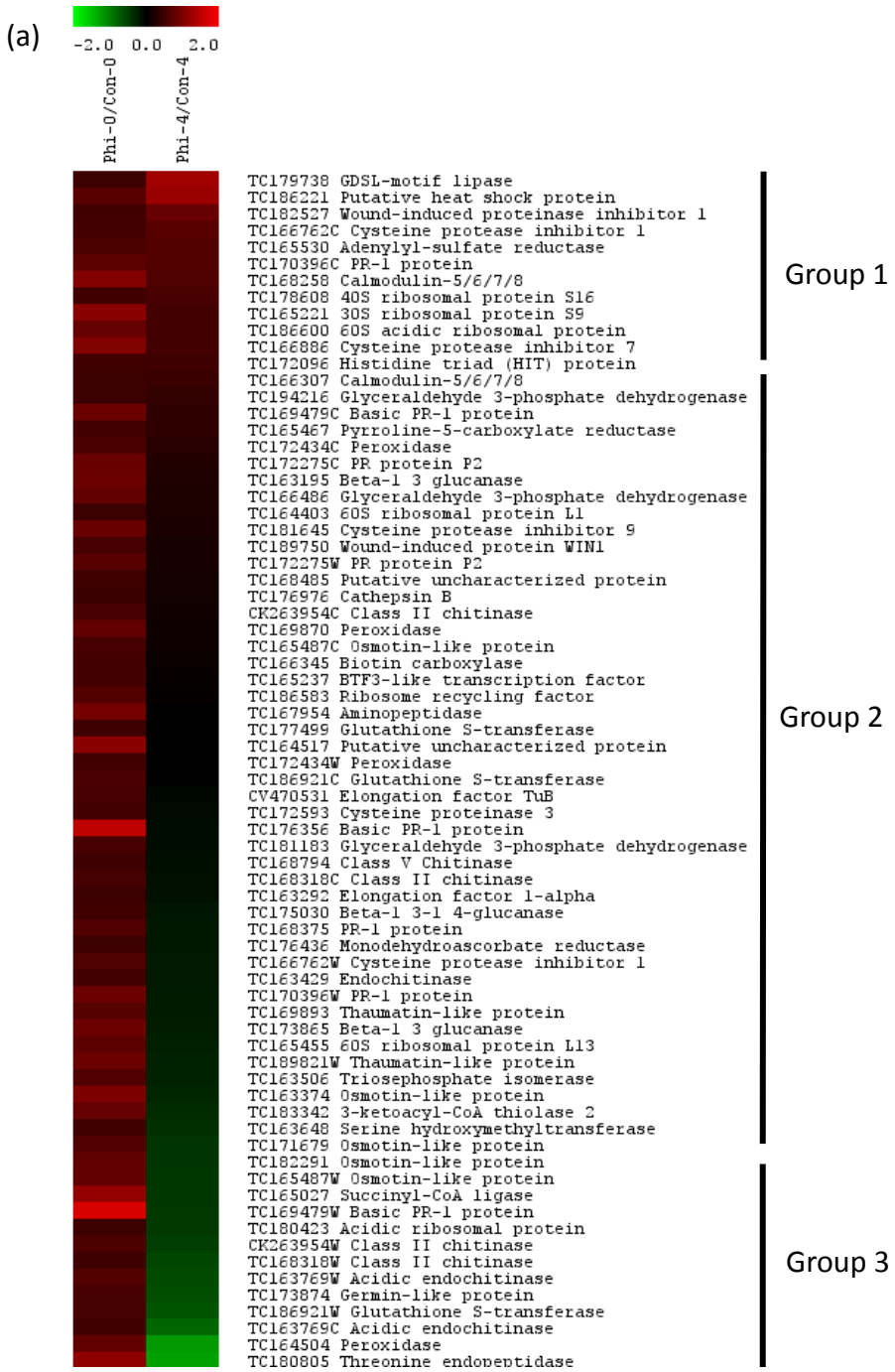

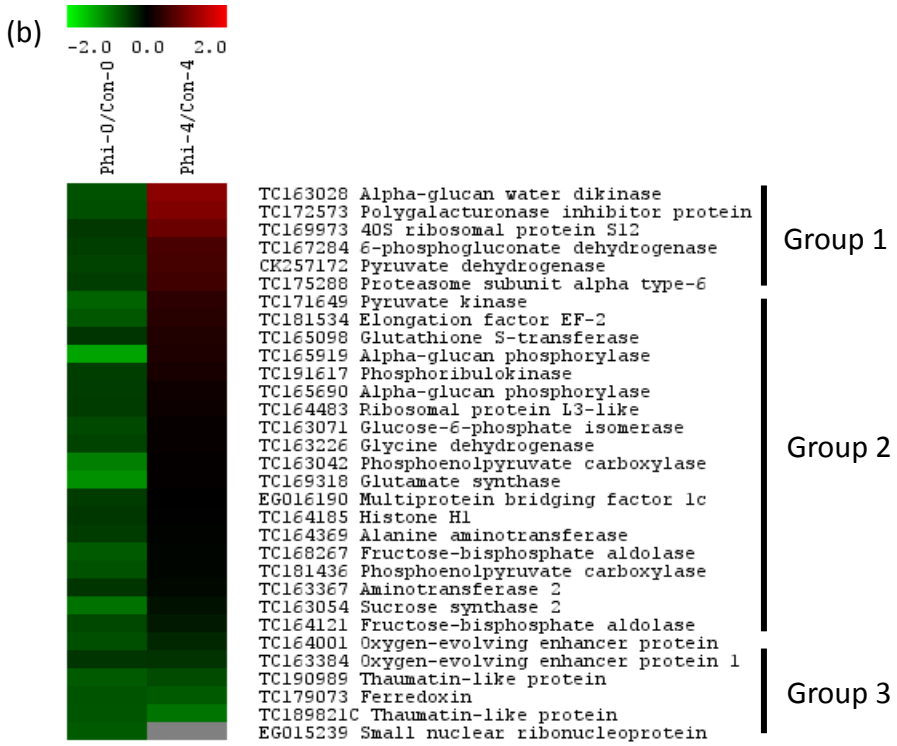

Figure 3.7. Differential abundance of the 93 proteins in infected Phi-treated and infected control samples. (a) Differential expression of the 62 up-regulated proteins in infected Phi-treated and infected control samples at 4 dpi. Left column in the heatmap shows the up-regulated proteins before infection. The value of each protein was calculated by the ratio of Phi-0/Con-0. Right column in the heatmap shows abundance of the proteins in infected Phi-treated and infected control samples at 4 dpi. The value was calculated by the ratio of Phi-4/Con-4. Three groups were represented based on the ratio of Phi-4/Con-4. Group 1 indicates proteins that were more abundant in Phi-treated leaves than the control leaves after infection. Group 2 indicates proteins that were similar levels in abundance in both infected Phi-treated and infected control leaves. Group 3 indicates proteins that were less abundant in Phi-treated leaves than the control leaves after infection. (b) Differential expression of the 31 down-regulated proteins in infected Phi-treated and infected control samples at 4 dpi. Left column in the heatmap shows the down-regulated proteins before infection. The value of each protein was calculated by the ratio of Phi-0/Con-0. Right column in the heatmap shows abundance of the proteins in infected Phi-treated and infected control samples. The value was calculated by the ratio of Phi-4/Con-4. Three groups were represented based on the ratio of Phi-4/Con-4. Group 1 indicates proteins that were more abundant in Phi-treated leaves than the control leaves after infection. Group 2 indicates proteins that were similar levels in abundance in both infected Phi-treated and infected control leaves. Group 3 indicates proteins that were less abundant in Phi-treated leaves than the control leaves after infection.

3.3.5 Microscopic Analyses of Phi-Treated and Control Potato Leaves Infected with *P. infestans*

Some of the defense-related proteins identified in this study, such as glutathione S-transferases, monodehydroascorbate reductase, and germin-like protein, are involved in reactive oxygen species (ROS) scavenging and H_2O_2 production. Large increases in H_2O_2 trigger local responses that lead to hypersensitive response (HR), a form of programmed cell death (PCD) (Almagro *et al*., 2009). Therefore, to investigate whether Phi-treated potato leaf cells undergo HR upon infection, cell death symptoms were examined. Cell death symptoms on leaves from Phi-treated plants were extremely limited and delayed at 4 - 6 dpi in comparison to the control leaves (Figure 3.8). Under scanning electron microscopy (SEM), we could find obvious extracellular pathogen growth (sporangiophores with sporangia) on the control leaves at 5 dpi, but no apparent plant epidermal cell death symptoms were found (Figure 3.9a and 3.9c). As opposed to the control leaves, collapsed epidermal cells were observed in Phi-treated plants at 5 dpi, but with no apparent escaping hyphae or sporangia around dead cells (Figure 3.9b and 3.9d). This suggests that the infection was restricted to a limited area and development of *P. infestans* was suppressed.

Observation using transmission electron microscopy (TEM) revealed ultrastructural differences in Phi-treated leaf tissues versus the control leaf tissues after the infection. At 5 dpi, the infected area of the control samples showed many cells with disrupted nuclear membranes and chloroplasts in different stages of degeneration, e.g. with reduced thylakoids and the disappearance of grana (Figure 3.10a, 3.10b, and 3.10c). In contrast, analysis of the infected area of Phi-treated samples revealed cells exhibiting

typical morphologic changes associated with PCD such as chromatin margination and condensation, and irregular nuclear envelope (Figure 3.10b). Further, thylakoids and stacked grana had the tendency to remain intact until chloroplasts were enveloped (Figure 3.10d and 3.10f). In addition, many cells from Phi-treated samples displayed vacuolization (Figure 3.10f). These are typical evidence of cells undergoing PCD (Coll *et al*., 2011).

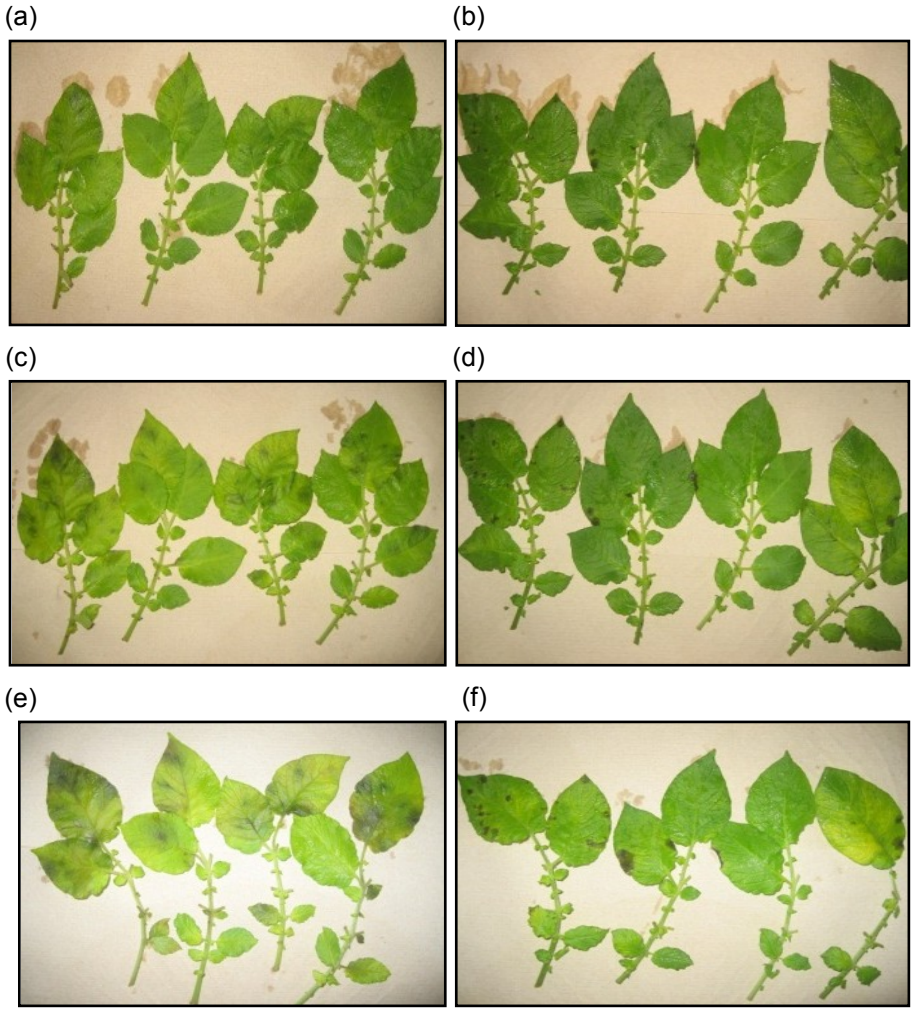

Figure 3.8. Observation of disease development symptoms on the infected control and infected Phi-treated leaves. (a) Untreated control potato leaves 4 dpi. (b) Phi-

treated potato leaves 4 dpi. (c) Untreated potato leaves 5 dpi. (d) Phi-treated potato leaves 5 dpi. (e) Untreated potato leaves 6 dpi. (f) Phi-treated potato leaves 6 dpi.

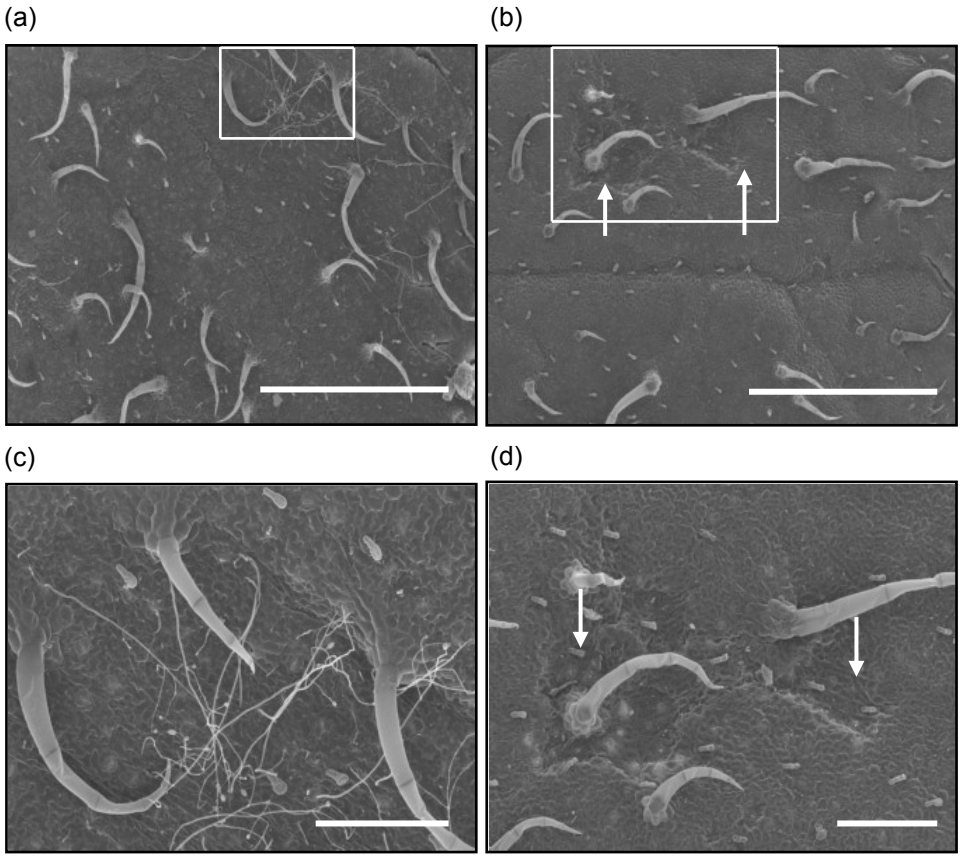

Figure 3.9. Scanning electron microscopy images representing the control and Phi-treated potato leaves at 5 dpi. (a) Leaf surface of the control leaf sample. *P. infestans* was found on the control leaf sample. (b) Leaf surface of the Phi-treated leaf sample. Collapsed cell areas (arrows) on Phi-treated leaf samples. (c) High magnification of rectangular area on (a) showing *P. infestans* observed. (d) High magnification of rectangular area on (b) showing collapsed cells (arrows) on Phi-treated leaf. Bar = 2 mm for images of (a) and (b). Bar = 500 μm for images of (c) and (d).

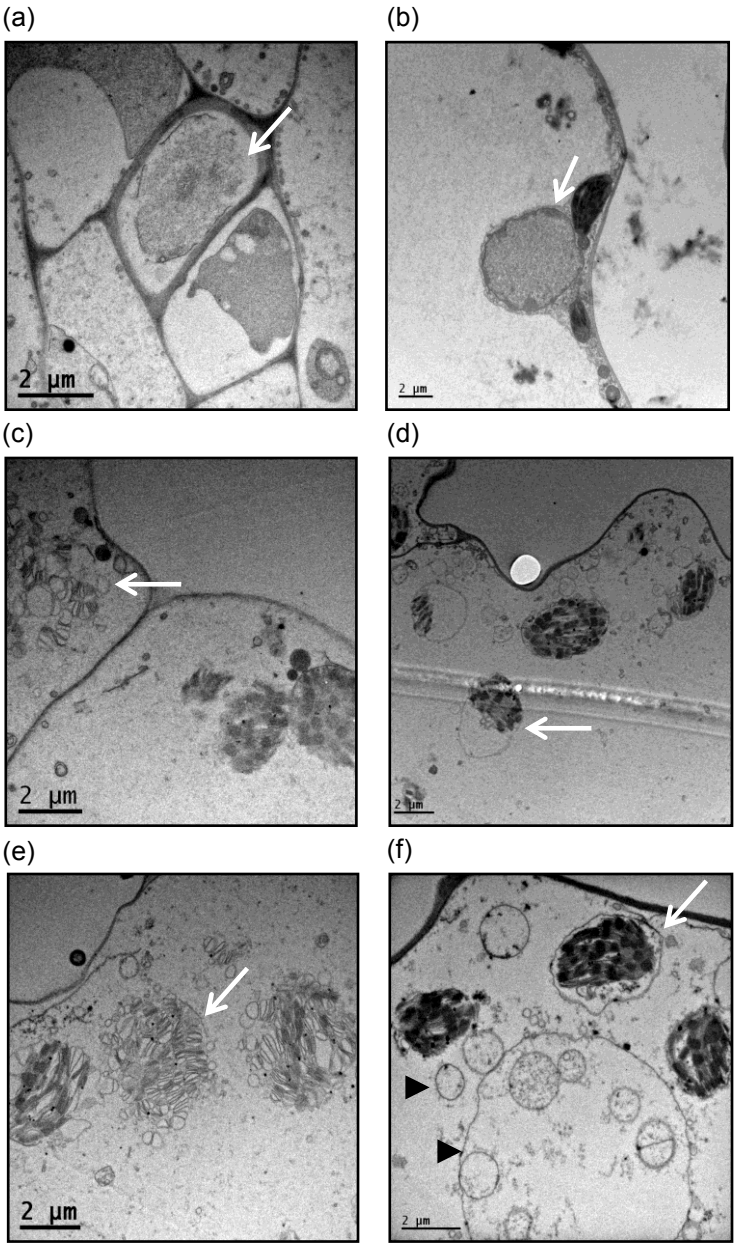

Figure 3.10. Transmission electron microscopy images representing ultrastructural changes in cells of the control and Phi-treated potato leaves at 5 dpi. (a) Disrupted nucleus membrane in control leaf cells (arrow). (b) Chromatin margination and condensation (arrow) shown in a cell of Phi-treated leaf. (c) Disrupted chloroplast in control leaf cell (arrow). (d) Chloroplasts in Phi-treated cell disrupted in an enveloped membrane (arrow). (e) Disrupted chloroplasts (arrow) in a cell of control leaf. (f) Chloroplast enveloped by a membrane (arrow) and vacuoles (arrowheads) shown in Phi-treated cell.

Callose deposition occurred around cells undergoing HR (Vorwerk *et al*., 2007). We identified areas exhibiting cell death in both infected control and infected Phi-treated leaves (Figure 3.11a and 3.11b). To identify the presence of callose, we examined both control and Phi-treated leaves stained with aniline blue. In the control leaves at 5 dpi, callose deposition was not observed (Figure 3.11c). As opposed to the control leaves, the Phi-treated leaves showed callose deposition in the cells surrounding the areas that underwent HR (Figure 3.11d).

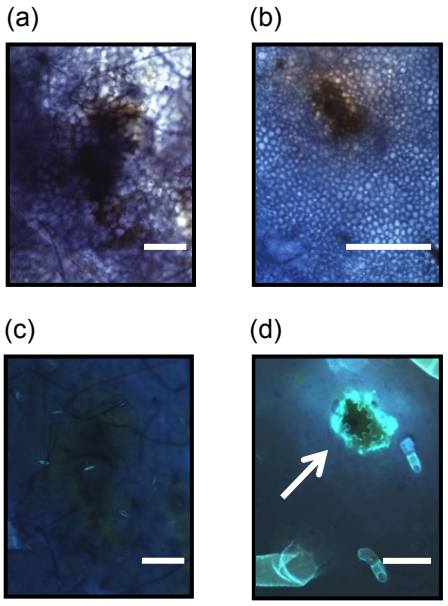

Figure 3.11. Observation of callose deposition in the control and Phi-treated potato leaves at 5 dpi. (a) Dark area indicates dead cells of the infected control leaf sample. (b) Dark area indicates dead cells of Phi-treated leaf sample. (c) Callose deposition was not observed in the infected control leaf sample. (d) Callose deposition (arrow) was shown around dead cells in the infected Phi-treated leaf sample,. Bar = 100 µm for all images.

3.3.6 Validation of the Differentially Regulated Proteins in Phi-Treated Sample by MRM

To perform technical validation of the differentially regulated proteins in the phi-treated leaves identified through this work, we employed a multiple reaction monitoring (MRM) approach with MRM Tags for Relative and Absolute Quantitation (mTRAQ). The method provides higher selectivity than shotgun proteomics (Wolf-Yadlin *et al*., 2007). High selectivity also allows use of 1-D LC, which is more rapid than the 2-D LC we used for profiling (Murphy and Pinto, 2010). By using 1-D LC, fifteen selected proteins within the 93 Phi-responsive proteins previously found by iTRAQ-based proteomics were successfully verified. The abundance of the peptides representing the 15 proteins showed the identical trend as by using iTRAQ-based proteomics (Figure 3.12). The consistent trend of the protein abundance between MRM and iTRAQ-based proteomics indicates the reliability of the iTRAQ-based proteomic analysis. This suggests that the 93 proteins identified from this study could be the differentially regulated proteins in Phi-treated leaves.

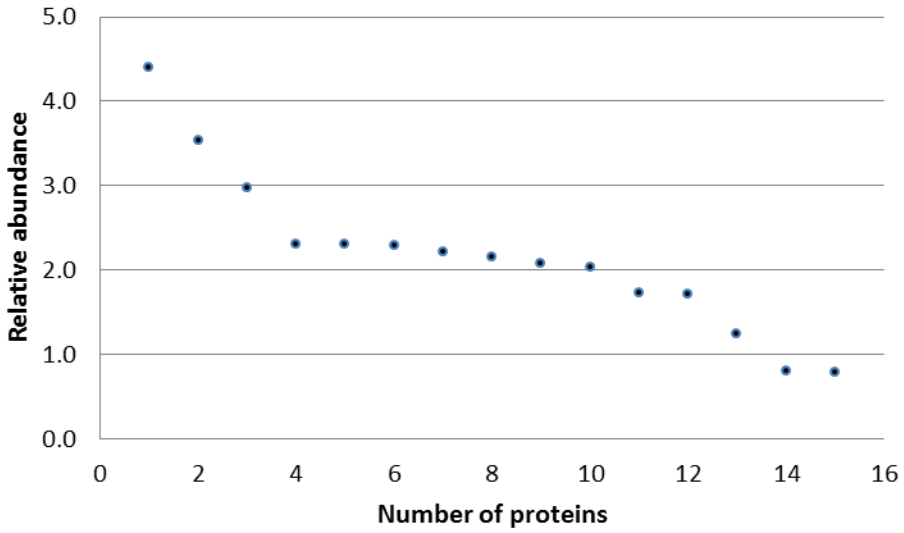

Figure 3.12. Validation of the 15 differentially regulated proteins by MRM analysis. The ratio of Phi-0/Con-0 for each protein corresponding to a peptide is shown. The integration of MRM chromatogram peak area generated by 3 or 4 MRM transition of a peptide is plotted. 1, beta-1,3-glucanase (TC163195); 2, PR-1 (TC168375); 3, PR protein P2 (TC172275); 4, peroxidase (TC172434); 5, endochitinase (TC163429); 6, calmodulin (TC168258); 7, beta-1,3-glucanase (TC173865); 8, cysteine protease inhibitor 1 (TC166762); 9, osmotin (TC165487); 10, endochitinase (TC163769); 11, cysteine protease (TC172593); 12, cysteine protease inhibitor 9 (TC181645); 13, serine hydroxymethyltransferase (TC163648); 14, fructose-bisphosphate aldolase (TC164121); 15, glycine dehydrogenase (TC163226)

3.3.7 The Identification of *P. infestans* Proteins

After infection with *P. infestans*, proteins of the pathogen would change in both infected control and Phi-treated samples. *P. infestans* proteins in Con-4 and Phi-4 were identified using *P. infestans* database (http://www.broadinstitute.org/annotation/genome/phytophthora_infestans). In total, 193 non-redundant iTRAQ-labeled proteins of *P. infestans*, 73 proteins from the potato cell wall fraction and 120 proteins from the cytoplasmic fraction of both Con-4 and Phi-4, were identified (Appendix E).

Metabolism-related proteins, such as transaldolase, trans-2-enol-CoA isomerase, enol-CoA hydrate, malate dehydrogenase, aldehyde dehydrogenase, isocitrate dehydrogenase, phosphoglycerate mutase, fatty acid synthase, succinyl-CoA ligase, bisphosphoglycerate-dependent phosphoglycerate mutase, triosephsphate isomerase, peroxisomal (S)-2-hydroxy acid oxidase, and S-adenosylmethionine synthetase were identified.

Defense-related proteins, such as glutathione S-transeferase, heat shock protein, lipase, superoxide dismutase, catalase, and proteins with the RXLR domain. Heat shock protein and ROS-related proteins represented the majorities of defense-related proteins. It is well documented that *P. infestans* secretes their proteins to inhibit host cellular processes and the secreted proteins have the RXLR domain (Hass *et al*., 2009). In this study, 4 RXLR proteins were identified. In addition to metabolism- and defense-related proteins, ribosomal proteins, histone subunit, 26S protease regulatory subunit, actin, tubulin, and unknown proteins were identified.

The infected Con-4 and Phi-4 samples showed significantly different disease development (Wang-Pruski *et al*, 2010). Therefore, the biomass of *P. infestans* on both infected samples at 4 dpi should be different, potentially with higher biomass in Con-4, and lower biomass in Phi-4. Since the iTRAQ-based proteome profiling cannot calculate the abundance based on biomass differences, the identification of changes in abundance of *P. infestans* proteins in both infected samples cannot be accurately presented. However, proteomics approach provides an advantage to identify host proteins as well as pathogen proteins simultaneously in plant-pathogen interactions.

3.4 Discussion

Phi has been reported to act through an indirect mode of action by inducing plant defense responses (Nemestothy and Guest, 1990; Jackson *et al*., 2000). However, the genome wide molecular mechanisms involved in this action have not been investigated (Daniel and Guest, 2006, Massound *et al*., 2012). Differentially regulated proteins in Phi-treated leaves identified from this study, therefore, provide key contributions to our understanding of Phi-induced resistance in host plants against oomycetes.

3.4.1 Up-Regulated Defense Proteins in Phi-Treated Sample

The major group of up-regulated proteins in Phi-treated sample had defense functions. These proteins play roles in the SA-dependent pathway, antimicrobial activities, the ROS pathway, the Ca^{2+}-dependent pathway, and the HR. Acidic PR gene expressions, including the SA-marker genes *PR-1* and *PR-9*, are induced via the SA-dependent pathway (Durrant and Dong, 2004). In this study, acidic PR proteins such as acidic PR-1 were identified. Since SA-dependent signaling pathway is involved in the activation of callose deposition and HR Halim *et al*., 2007), the responses elicited by Phi facilitate an increased level of resistance to infection by the hemibiotrophic pathogen *P. infestans*.

PR proteins play an important role in antimicrobial properties at local infection sites (Ahn *et al*., 2005). Some secretory proteins identified in this study, such as PR-2, PR-3, and lipase, act as hydrolytic enzymes. The secretory proteins contribute directly to the degradation of pathogen cell walls and to the disruption of pathogen membrane integrity (van Loon *et al*., 2006; Spoel *et al*., 2007). Levels of hydrolytic enzymes and PR

proteins at the transcription level were high in disease-resistant plants and low in susceptible plants (Shetty *et al*., 2009; Bariya *et al*., 2011). This suggests that the pre-activated proteins in Phi-treated sample before infection contribute to increased levels of disease resistance of the host to pathogens.

The alterations in ROS levels activate calmodulin (CaM), a Ca^{2+} binding protein that modulates CaM-binding protein, resulting in the activation of the Ca^{2+}-dependent signaling pathway. This pathway activates the expression of transcription factors (TF) that turn on stress-responsive genes, such as those for heat shock proteins (Mittler, 2002). Increases in ROS may cause increased abundance in levels of CaMs. Phi treatment may also trigger increases of Ca^{2+} and CaM. This work suggests that Phi influences Ca^{2+} homeostasis.

Finally, increases in levels of ROS and Ca^{2+} are associated with the induction of the HR in plants such as *Arabidopsis* and pepper upon infection (Mittler *et al*., 2004; Choi *et al*., 2009). Gilroy *et al*. (2007) reported that a cysteine protease, cathepsin B (TC137447), is involved in the activation of HR in potatoes upon infection with *P. infestans*. Interestingly, the up-regulated cathepsin B (TC176976) identified in this study showed a high degree of similarity (87% identity at the amino acid level) to cathepsin B (TC137447) studied by Gilroy *et al*. (2007) when comparing the peptidase unit (Figure 3.13). Alignment of 6 cathepsin B proteins, TC176976 from this study and five other proteins from two studies (Avrora *et al*., 2004; Gilroy *et al*., 2007), revealed four conserved protease active sites (Figure 3.13). It is, therefore, possible that the up-regulated cathepsin B in Phi-treated leaves has the same function as TC137447. The HR is preceded by a tightly regulated process through activation of proteases (Gilroy *et al*.,

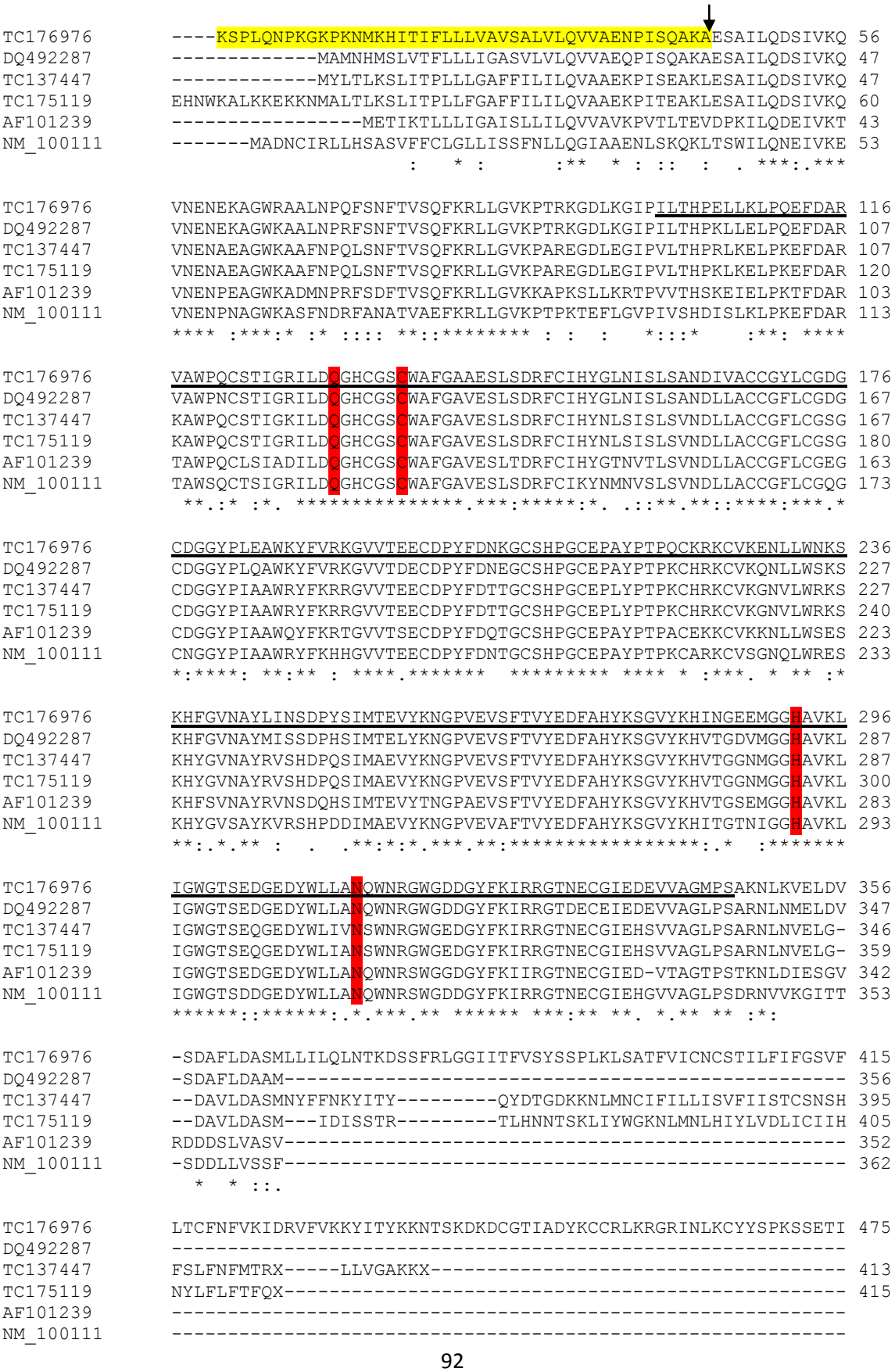
TC176976 ----KSPLQNPKGKPKNMKHITIFLLLVAVSALVLQVVAENPISQAKAESAILQDSIVKQ 56
DQ492287 -------------MAMNHMSLVTFLLLIGASVLVLQVVAEQPISQAKAESAILQDSIVKQ 47
TC137447 -------------MYLTLKSLITPLLLGAFFILILQVAAEKPISEAKLESAILQDSIVKQ 47
TC175119 EHNWKALKKEKKNMALTLKSLITPLLFGAFFILILQVAAEKPITEAKLESAILQDSIVKQ 60
AF101239 -----------------METIKTLLLIGAISLLILQVVAVKPVTLTEVDPKILQDEIVKT 43
NM_100111 -------MADNCIRLLHSASVFFCLGLLISSFNLLQGIAAENLSKQKLTSWILQNEIVKE 53
TC176976 VNENEKAGWRAALNPQFSNFTVSQFKRLLGVKPTRKGDLKGIPILTHPELLKLPQEFDAR 116
DQ492287 VNENEKAGWKAALNPRFSNFTVSQFKRLLGVKPTRKGDLKGIPILTHPKLLELPQEFDAR 107
TC137447 VNENAEAGWKAAFNPQLSNFTVSQFKRLLGVKPAREGDLEGIPVLTHPRLKELPKEFDAR 107
TC175119 VNENAEAGWKAAFNPQLSNFTVSQFKRLLGVKPAREGDLEGIPVLTHPKLKELPKEFDAR 120
AF101239 VNENPEAGWKADMNPRFSDFTVSQFKRLLGVKKAPKSLLKRTPVVTHSKEIELPKTFDAR 103
NM_100111 VNENPNAGWKASFNDRFANATVAEFKRLLGVKPTPKTEFLGVPIVSHDISLKLPKEFDAR 113
TC176976 VAWPQCSTIGRILDQGHCGSCWAFGAAESLSDRFCIHYGLNISLSANDIVACCGYLCGDG 176
DQ492287 VAWPNCSTIGRILDQGHCGSCWAFGAVESLSDRFCIHYGLNISLSANDLLACCGFLCGDG 167
TC137447 KAWPQCSTIGKILDQGHCGSCWAFGAVESLSDRFCIHYNLSISLSVNDLLACCGFLCGSG 167
TC175119 KAWPQCSTIGRILDQGHCGSCWAFGAVESLSDRFCIHYNLSISLSVNDLLACCGFLCGSG 180
AF101239 TAWPQCLSIADILDQGHCGSCWAFGAVESLTDRFCIHYGTNVTLSVNDLLACCGFLCGEG 163
NM_100111 TAWSQCTSIGRILDQGHCGSCWAFGAVESLSDRFCIKYNMNVSLSVNDLLACCGFLCGQG 173
TC176976 CDGGYPLEAWKYFVRKGVVTEECDPYFDNKGCSHPGCEPAYPTPQCKRKCVKENLLWNKS 236
DQ492287 CDGGYPLQAWKYFVRKGVVTDECDPYFDNEGCSHPGCEPAYPTPKCHRKCVKQNLLWSKS 227
TC137447 CDGGYPIAAWRYFKRRGVVTEECDPYFDTTGCSHPGCEPLYPTPKCHRKCVKGNVLWRKS 227
TC175119 CDGGYPIAAWRYFKRRGVVTEECDPYFDTTGCSHPGCEPLYPTPKCHRKCVKGNVLWRKS 240
AF101239 CDGGYPIAAWQYFKRTGVVTSECDPYFDQTGCSHPGCEPAYPTPACEKKCVKKNLLWSES 223
NM_100111 CNGGYPIAAWRYFKHHGVVTEECDPYFDNTGCSHPGCEPAYPTPKCARKCVSGNQLWRES 233
TC176976 KHFGVNAYLINSDPYSIMTEVYKNGPVEVSFTVYEDFAHYKSGVYKHINGEEMGGHAVKL 296
DQ492287 KHFGVNAYMISSDPHSIMTELYKNGPVEVSFTVYEDFAHYKSGVYKHVTGDVMGGHAVKL 287
TC137447 KHYGVNAYRVSHDPQSIMAEVYKNGPVEVSFTVYEDFAHYKSGVYKHVTGGNMGGHAVKL 287
TC175119 KHYGVNAYRVSHDPQSIMAEVYKNGPVEVSFTVYEDFAHYKSGVYKHVTGGNMGGHAVKL 300
AF101239 KHFSVNAYRVNSDQHSIMTEVYTNGPAEVSFTVYEDFAHYKSGVYKHVTGSEMGGHAVKL 283
NM_100111 KHYGVSAYKVRSHPDDIMAEVYKNGPVEVAFTVYEDFAHYKSGVYKHITGTNIGGHAVKL 293
TC176976 IGWGTSEDGEDYWLLANQWNRGWGDDGYFKIRRGTNECGIEDEVVAGMPSAKNLKVELDV 356
DQ492287 IGWGTSEDGEDYWLLANQWNRGWGDDGYFKIRRGTDECEIEDEVVAGLPSARNLNMELDV 347
TC137447 IGWGTSEQGEDYWLIVNSWNRGWGEDGYFKIRRGTNECGIEHSVVAGLPSARNLNVELG- 346
TC175119 IGWGTSEQGEDYWLIANSWNRGWGEDGYFKIRRGTNECGIEHSVVAGLPSARNLNVELG- 359
AF101239 IGWGTSEDGEDYWLLANQWNRSWGGDGYFKIIRGTNECGIED-VTAGTPSTKNLDIESGV 342
NM_100111 IGWGTSDDGEDYWLLANQWNRSWGDDGYFKIRRGTNECGIEHGVVAGLPSDRNVVKGITT 353
TC176976 -SDAFLDASMLLILQLNTKDSSFRLGGIITFVSYSSPLKLSATFVICNCSTILFIFGSVF 415
DQ492287 -SDAFLDAAM---------- 356
TC137447 --DAVLDASMNYFFNKYITY---------QYDTGDKKNLMNCIFILLISVFIISTCSNSH 395
TC175119 --DAVLDASM---IDISSTR---------TLHNNTSKLIYWGKNLMNLHIYLVDLICIIH 405
AF101239 RDDDSLVASV---------- 352
NM_100111 -SDDLLVSSF---------- 362
TC176976 LTCFNFVKIDRVFVKKYITYKKNTSKDKDCGTIADYKCCRLKRGRINLKCYYSPKSSETI 475
DQ492287 ----------
TC137447 FSLFNFMTRX-----LLVGAKKX---------- 413
TC175119 NYLFLFTFQX---------- 415
AF101239 ----------
NM_100111 ----------

Figure 3.13. Alignment of 6 cathepsin B proteins in different plant species using ClustalW. The TC176976 is a cathepsin B identified in this study. The aligned cathepsin B proteins were TC176976 and TC137447 from *Solanum tuberosum* (potato), DQ492287 from *Nicotiana benthamiana* (tobacco), TC175119 from *Solanum lycopersicum* (tomato), AF101239 from *Lpomoea batatas* (sweet potato), and NM_100111 from *Arabidopsis thaliana*. Four regions highlighted in red are the four protease active sites; the underlined amino acid sequence represents the cysteine protease domain (MEROPS-peptidase database, http://merops.sanger.ac.uk; Rawlings *et al*., 2008). Signal peptide cleavage site identified by SignalP is shown with an arrow. Amino acid sequences highlighted in yellow are the signal peptide. "*", same amino acid sequence of 6 cathepsin B proteins; ":", one amino acid difference of 6 cathepsin B proteins; ".", more than two amino acid sequence differences.

2007). Ectopic expression of a cysteine protease inhibitor blocks cysteine protease-induced HR (Solomon *et al*., 1999). Therefore, the up-regulated cysteine protease inhibitors in Phi-treated leaves may interact with cathepsin B to block the activation of HR in the absence of *P. infestans*.

3.4.2 Defense Responses in Phi-Treated Leaves After Infection

The tightly regulated process of the HR can be explained by the abundance of three cysteine protease inhibitors and cathepsin B identified in this study. Upon infection, down-regulated cysteine protease inhibitors allow the breakdown of the interaction with cathepsin B to activate the HR. To complement the proteomics approach, callose deposition and subcellular changes related to HR in the Phi-treated plants were analyzed by electron microscopy and a biochemical assay. Under SEM, collapsed epidermal cells in Phi-treated leaves were observed (Figure 3.9), suggesting that this observation of localized cell death could lead to an examination of morphological characteristics using TEM to identify the HR. Under TEM, typical programmed cell death symptoms, such as chloroplast disruption and vacuolization in cells (Mur *et al*., 2008; Coll *et al*., 2011) were

found in Phi-treated leaves (Figure 3.10). Callose deposition results in cell wall strengthening which therefore acts as a physical barrier against pathogen infections. Callose deposition in Phi-treated leaves appeared around areas comprising dead cells. This finding was in sharp contrast to the untreated samples where little or no callose deposition was observed (Figure 3.11). Callose deposition is significantly enhanced in tissues bordering cells experiencing HR (Lee and Hwang, 2005). Therefore, different pattern of callose deposition in Phi-treated vs. untreated control plants is indirect evidence that cells in Phi-treated plants undergo HR. Cellulose is one of the main cell wall components of *P. infestans* (Grenville-Briggs *et al*., 2008). The activity of beta-1,3-1,4-glucanase inhibits the infection process. Therefore, upon infection, beta-1,3-1,4-glucanase would likely be one of the first targets of proteins secreted by *P. infestans*, leading to decreased abundance of the protein.

3.4.3 Alterations of Carbohydrate Metabolism and Energy Production Before Infection

This work also identified that the majority of down-regulated proteins in Phi-treated leaves play roles in carbohydrate, energy, and amino acid metabolism, suggesting that Phi affects plant metabolism. Respiration is an essential process related to energy and carbon metabolism by glycolysis and TCA cycle (van Dongen *et al*., 2011). Proteins in the energy and metabolism categories found in this study are mainly involved in glycolysis and glycolysis-related metabolism. The abundance of glyceraldehyde-3-phosphate dehydrogenases (GAPDH) and triosephosphate isomerase suggests elevated levels of the second metabolic pool in glycolysis. This trend is supported by succinyl-

CoA ligase, an enzyme to convert succinyl-CoA to succinate in the TCA cycle, whose abundance was also increased in the Phi-treated leaves. Interestingly, down-regulation of two fructose-phosphate aldolases was identified, suggesting that the production of their substrate, fructose-1,6-bisphosphate, the third major component of the glycolytic metabolic pool, was reduced. The reason for this reduction may well be due to the limited ATP supply that is needed to convert fructose-6-bisphosphate to fructose-1,6-bisphosphate. It may suggest that Phi application influences energy balance and that ATP is less readily available than that in the untreated samples. This assumption is also supported by other down-regulated enzymes found in this study that are involved in glycolysis, namely glucose-6-phosphate isomerase for phosphorylated hexoses interconversion and pyruvate kinase for pyruvate conversion. This suggests reduced sources of the primary pool of glycolysis, glucose-6-phosphate, fructose-6-phosphate, and glucose-1-phosphate. This assumption is also supported by three down-regulated proteins found in this study, two α-glucan phosphorylases in the phosphorylating step of glucan and starch, and a sucrose synthase in the step of glucan and sucrose. Both are involved in starch and sucrose metabolism. Carbon fixation and the reductive pentose phosphate pathway were also down-regulated, which is shown by the presence of oxygen-evolving enhancer proteins and phosphoribulokinase. This result suggests the inactivation of carbon fixation in Phi-treated plants. Overall, data suggests that carbohydrate metabolism and energy production are influenced by Phi.

3.4.4 Alterations of Carbohydrate Metabolism and Energy Production After Infection

Metabolic changes occurred after infection with *P. infestans*. In Phi-treated samples upon infection, enzymes involved in starch and sucrose metabolism, such as α-glucan phosphorylases, α-glucan water dikinase, and sucrose synthase 2, were induced. Degradation of starch and sucrose supplies glucose-1-phosphate and glucose-6-phosphate, the source of the primary pool of glycolysis. It suggests that upon infection, Phi-treated plants produce more pyruvate and ATP by glycolysis. This assumption is supported by pyruvate kinase and phosphoenolpyruvate carboxylases that were more abundant in Phi-treated samples than in control samples following infection. Pyruvate metabolism and energy production through TCA seem to be induced in Phi-treated plants.

In the control plants after the pathogen infection, different expression trends were visible. In contrast to the challenged Phi-treated plants, the untreated plants showed down-regulation in starch mobilization and energy production through carbohydrate metabolism with the exception of sucrose synthase 2 and of one of the three GAPDHs. Succinyl-CoA ligase and 3-ketoacyl-CoA thiolase were strongly induced in the untreated samples after infection, suggesting that the energy source which can replenish TCA may be provided by fatty acid degradation rather than starch degradation. Overall, these trends suggest slightly more active metabolism in Phi-treated samples.

3.4.5 Differentially Expressed Proteins in Both Infected Phi-Treated and Infected Control Samples, and Pre-Activation of Proteins in Phi-Treated Sample may be Involved in Phi-IR

Proteins showing different levels of abundance in both infected Phi-treated and infected control plants may be the key components involved in Phi-IR against late blight of potatoes. Only four defense-related proteins, including heat shock protein, lipase, wound-induced proteinase inhibitor, and polygalacturonase inhibitor, were more abundant in infected Phi-treated plants than in infected untreated plants at 4 dpi (group 1, Figure 3.7). Heat shock protein and wound-induced proteinase inhibitor are universal stress-related proteins. Upon infection, lipase degrades pathogen membranes and polygalacturonase inhibitor reduces the activity of polygalacturonase to protect cell wall components. Their action underlying Phi-IR may be important to increase levels of resistance to *P. infestans*. In addition to these four proteins, two calmodulins were more abundant in Phi-treated plants than in untreated plants. Calcium signaling involving calmodulins is one of the essential early events in the activation of the HR. However, this suggests that a small number of proteins may be responsible for increased levels of disease resistance in the Phi-treated plants.

In contrast to this small number of proteins, the abundance of the rest of the proteins in Phi-treated plants was similar to that in control plants following infection (group 2, Figure 3.7). Nonetheless, at 4 dpi, Phi-treated plants showed increased resistance against *P. infestans*. It has been reported that resistance to pathogens is associated with a rapid accumulation of defense-related genes (Shetty *et al*., 2009). This suggests that pre-activation of proteins by Phi before infection facilitates the activation of

rapid defense responses, leading to increased levels of resistance to *P. infestans*. Defense responses, SA-dependent pathway and ROS burst, are partly associated with HR. Levels of defense proteins are similar in both treated and untreated plants. Nonetheless, callose deposition and subcellular changes related to HR were observed in the Phi-treated plants. Therefore, pre-activation of proteins by Phi is essential to increase levels of host resistance to pathogens.

3.4.6 The Effect of Senescence

By day 4, detached leaves would undergo senescence processes. For instance, degradation of Rubisco and chlorophyll proteins was identified during leaf senescence in *Arabidopsis* (Lim and Nam, 2005). Coupe *et al*. (2004) reported that senescence from detached Broccoli (*Brassica oleracea*) induced the expression of a series of genes such as lesion simulating disease (LSD1), Bax inhibitor (BI), and serine palmitoyltransferase (SPT). The expression of three homologues of these three genes (AtLDS1, AtBI-1, AtSPT1) in *Arabidopsis* was investigated by the authors. In the detached leaves of *Arabidopsis*, the expression levels of AtLSD1 and AtBI-1 did not change and expression of AtSPT1 was increased.

In this study, senescence in detached leaves after 4 days had occurred. Therefore, changes in protein composition had taken place in the infected Phi-treated and infected control samples at 4 dpi. However, most of the proteins in both samples showed similar abundance, meaning that the changes caused by senescence in both samples were similar. Therefore, the treatment of Phi suggests the changes in protein abundance when proteins in Phi-4 were compared with those in Con-4.

3.5 Conclusion

The quantitative comparison of proteomic profiles in this study suggests that Phi's indirect mode of action induces broader functional changes in plants than previously documented. This is the first broad molecular quantitative study to identify differentially regulated proteins in Phi-treated potato plants. From a total of 1172 iTRAQ-labeled reproducibly identified proteins, we identified 93 (8%) proteins whose abundance was changed in Phi-treated sample. The major functional category of up-regulated proteins fall into defense associated with the SA-dependent pathway, antimicrobial activity, the ROS pathway, the Ca^{2+}-dependent pathway and HR. The down-regulated proteins are involved in glycolysis, TCA cycle, starch metabolism, and amino acid metabolism. At 4 dpi, HR and callose deposition were observed in infected Phi-treated leaves, which contributed to increased levels of disease resistance. However, the expression trend of most of the differentially regulated proteins (except four defense proteins) in infected Phi-treated leaves was similar to the trend observed in infected control leaves at 4 dpi with *P. infestans*. It is probably that only a subset of the proteins differentially expressed in infected Phi-treated leaves are highly relevant in the process of induced disease resistance. Alternatively, pre-activation of proteins elicited by Phi before infection helps to induce faster and earlier defense responses, resulting in the increased levels of resistance.

Chapter 4. General Discussion

In plant-pathogen interactions, protein molecules in plants recognize the signals from pathogens to trigger resistance to the pathogen. When plant resistance systems fail, the plants become susceptible to the pathogen, causing death and/or economic losses when these are important food crops.

In compatible interactions, plants that are unable to activate appropriate and rapid defense responses for effective resistance against pathogens become susceptible to disease development. Pre-treatment of plants with inducing chemicals stimulates induced resistance that protects susceptible plants against a broad range of pathogens. The effects of the biopesticide Phi on oomycetes in various plant species have been reported, showing that Phi has two modes of action: indirect and direct. However, the indirect mode of action of Phi through induction of plant defense responses at the molecular level has not been well understood. The identification of molecular components involved in Phi-IR against *Phytophthora* species will provide data to understand Phi-IR in susceptible plants.

To investigate what functional changes are induced in Phi-treated potato leaf cells, iTRAQ-based quantitative proteomics was employed in this study. The molecular components associated with Phi-IR in potato plants before and after infection with *P. infestans* were investigated. A total of 93 differentially regulated proteins (62 up-regulated proteins and 31 down-regulated proteins) were identified in potato leaves after the Phi treatment and changes in abundance of these proteins upon infection were identified (Table 3.2, 3.3). The majority of these differentially regulated proteins have not been previously reported. The quantitative proteomics analysis carried out in this thesis

suggested that differentially regulated proteins changed the cellular activities in respect to defense, metabolism, and energy generation. For instance, Phi appears to stimulate the degradation of pathogen cell walls that can release PAMPs. Phi application triggers early events of defense response, such as ROS burst and calcium signaling, resulting in a rapid HR. These appropriate and rapid responses increased levels of disease resistance in Phi-treated potato plants. Proteins involved in glycolysis, TCA cycle, and amino acid metabolism were repressed, indicating that Phi triggers alterations of metabolism. This work provides key contributions to our understanding of the effects of Phi on oomycetes and their host plants.

4.1 Functions Associated with Phi-Induced Resistance in Potato Plants

These quantitative proteomics results suggested that diverse defense mechanisms, such as antimicrobial activity, ROS production, cell wall reinforcement, calcium signaling, and the SA-dependent pathway, have been triggered by Phi. These defense responses are partly associated with the activation of HR. Phi applications facilitate rapid recognition of *P. infestans* leading to, ultimately, a rapid HR, which is related to Phi-IR. Proposed models of functions related to Phi-IR before and after infection are depicted in Figures 4.1 and 4.2.

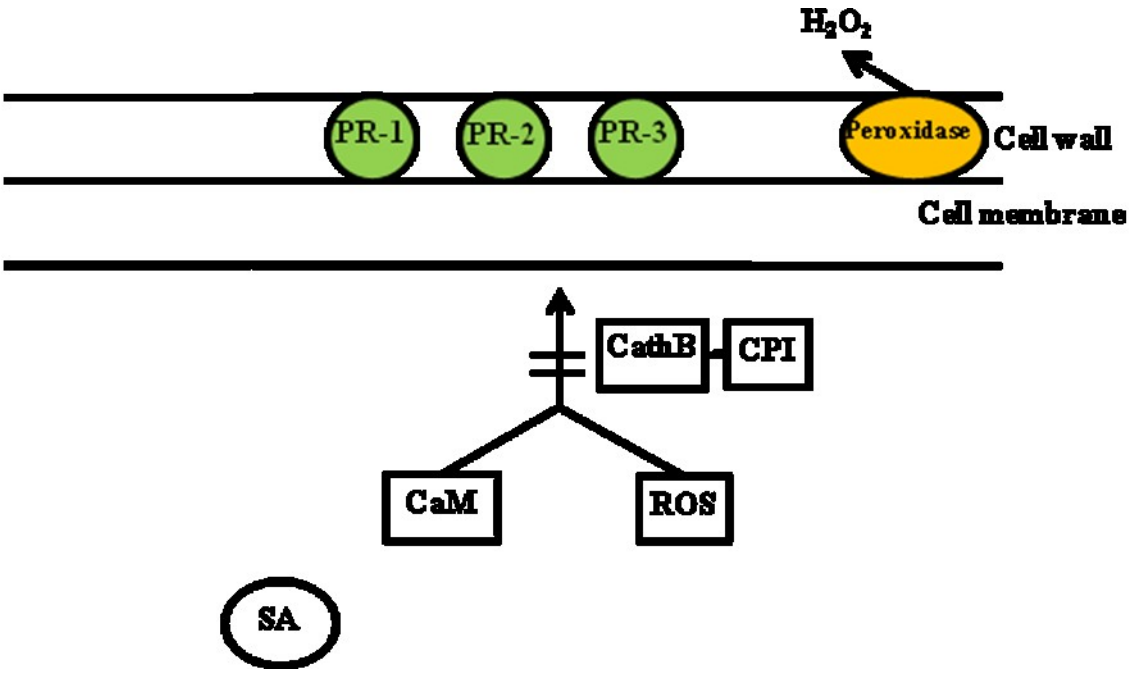

Figure 4.1. Proposed model of functions involved in defense-related proteins elicited by Phi before infection. Before infection, PR proteins with a secretory peptide, such as PR-1, PR-2, and PR-3, are located on the plant cell wall. Peroxidase plays a role in ROS production. Increased ROS and calmodulins (CaM) involved in Ca^{2+} signaling participate in triggering the HR. However, interactions of a cysteine protease cathepsin B (CathB) with cysteine protease inhibitors (CPI) block the activation of the HR before the infection. In addition, Phi triggers the SA-dependent signaling pathway in Phi-treated plants. All the proteins listed in the figure are found in this study.

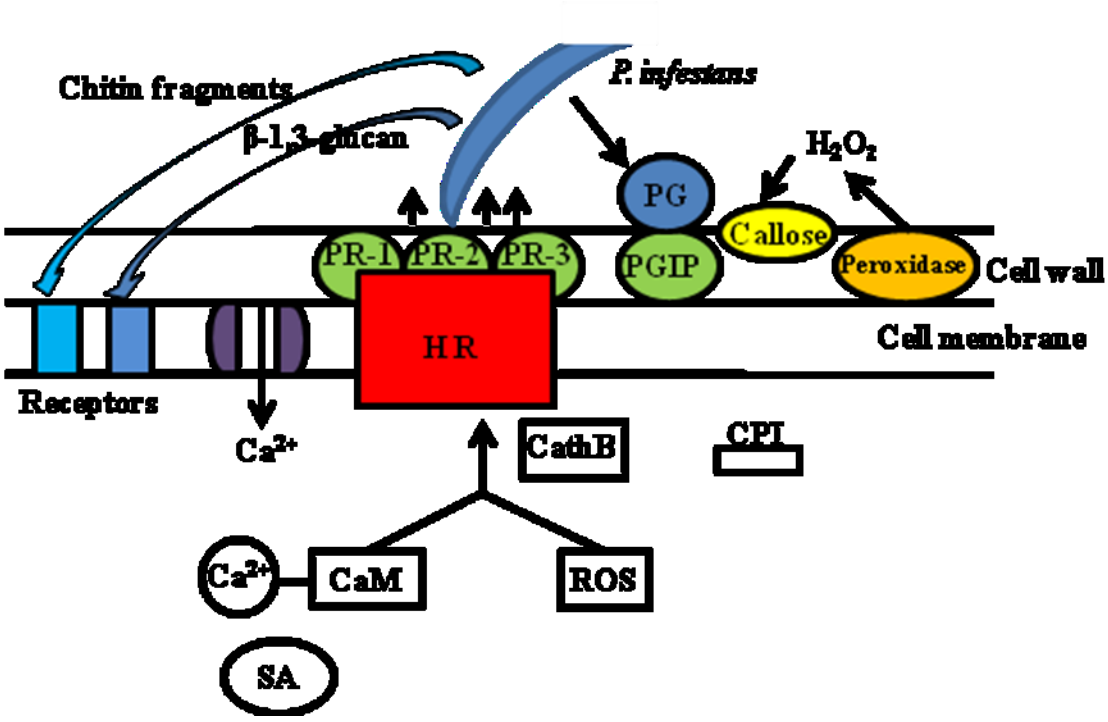

Figure 4.2. Proposed model of functions involved in defense-related proteins elicited by Phi after infection. After infection, antimicrobial PR proteins, such as PR-1 are activated. PR-2 and PR-3 proteins degrade the cell wall components of *P. infestans* that release PAMPs, such as beta-1,3-glucan and chitin fragment, respectively. The PAMPs are recognized by plant receptors, triggering an increase in Ca^{2+} in plant cells. Increased Ca^{2+} activates calmodulins (CaM). On the other hand, *P. infestans* secretes polygalacturonase (PG) to degrade components of the plant cell wall. As a counter-defense, plants secrete a polygalacturonase inhibitor (PGIP) to block the activity of PG. In addition, plants secrete PR proteins including PR-1 that has an antimicrobial activity. Levels of CPIs were decreased, resulting in breakdown of the interactions of the proteins with a cathepsin B (CathB). This activates the HR at local infection sites. H_2O_2-mediated callose accumulates around the HR. All the proteins, except receptors and calcium transporter, listed in the figure are found in this study.

4.1.1 Recognition of *P. infestans* is Facilitated in Phi-Treated Sample

In this study, 25 of the 35 up-regulated proteins in the defense group were found to be putative secretory proteins (Table 3.2). Among them, 20 proteins, including ten hydrolases, four PR-1 proteins, and six thaumatin/osmotin-like proteins (PR-5) have putative antimicrobial activities. Transgenic potato plants overexpressing the *PR-5* gene showed enhanced resistance to *P. infestans* due to antimicrobial activity of its product (Liu *et al*., 1994). The activity of PR proteins induced by Phi, therefore, may be an important factor in increasing levels of disease resistance.

Ten hydrolases, including two β-1,3-glucanases (PR-2), six chitinases (PR-3 and PR-4), a β-1,3-1,4-glucanase and a lipase were up-regulated in this study (Table 3.2). Plant hydrolases have antimicrobial activity that degrades the structure of cell walls and/or membranes of pathogens (van Loon *et al*., 2006; Spoel *et al*., 2007). Therefore, the up-regulated hydrolases contribute to disease resistance by direct inhibition of pathogen infection and releasing oligosaccharides and/or lipid-derived molecules. The released molecules, fragments from β-1,3-glucans and chitin, are considered as PAMPs. In potato - *P. infestans* interactions, the activity of PR-2 may have more contribution for resistance to *P. infestans* than that of PR-3 when it is considered that β-1,3-glucan, β-1,6-glucan, and cellulose are essential components of the oomycete cell wall, whereas the cell wall of most fungal pathogens consists of chitin (Grenville-Briggs *et al*., 2008). However, activation of PR-3 and PR-4 implies that Phi may be also effective at controlling fungal diseases.

Phi applications induce PAMP-triggered defense responses. It has been reported that higher expression of hydrolases was found in resistant wheat and pepper plants and

lower in susceptible wheat and pepper plants (Silvar *et al*., 2008; Shetty *et al*., 2009). The abundance of plant hydrolases induced by Phi facilitates the release of PAMPs leading to PAMP-triggered defense responses. Indeed, PAMP-triggered defense responses occurred in Phi-treated potato plants, because we found higher callose accumulation in the Phi-treated leaves, while this was absent or low in untreated leaves (Figure 3.11). Callose deposition is often used as a marker for PAMP-triggered defense response (Kim *et al*., 2005; Shetty *et al*., 2009). This result suggests that PAMP-triggered callose deposition for cell wall reinforcement is associated with Phi-IR.

In this study, interestingly, β-1,3-1,4-glucanase among the proteins that have antimicrobial activity was only down-regulated after infection with *P. infestans*. Grenville-Briggs *et al*. (2008) identified that cellulose synthesis of *P. infestans* is essential for successful infection of potato plants. *P. infestans* may secrete effectors to break β-1,3-1,4-glucanase in potato plants to maintain their cell wall in which cellulose is one of the main components. Therefore, β-1,3-1,4-glucanase induced by Phi before infection facilitates delay of infection of potato leaf tissues. The abundance of β-1,3-1,4-glucanase may be one of the key events in potato - *P. infestans* interactions.

On the other hand, pathogens secrete their hydrolases and plants increase counter-defense activity. An abundance of polygalacturonase inhibitor protein (PGIP) was repressed by Phi before infection (Table 3.3). PGIPs play a role in inhibiting the activity of pathogen polygalacturonase (PG), such as the *pipg1* gene from *P. infestans* (Torto *et al*., 2002), that acts to degrade the α-1,4-polygalaturonic acid of pectins, a component of plant cell walls (Howell and Davis, 2005). After *P. infestans* infection, the abundance of PGIP was up-regulated in Phi-treated plants (Figure 3.6b). Interestingly, PGIP was more

significantly abundant in the challenged Phi-treated plants than in the challenged untreated plants (Figure 3.7b). This result suggests that PGIP induced by Phi inhibits the effectiveness of penetration of potato cell walls by *P. infestans*, which contributes to increased levels of resistance to the pathogen.

4.1.2 Early Establishment of Defense Responses is Triggered in Phi-Treated Sample

Detection of pathogens triggers well-coordinated gene expression leading to early establishment of events involved in pathogen defense, such as ROS burst and calcium signaling. However, before infection, proteins related to ROS production and scavenging as well as calmodulins involved in calcium signaling were up-regulated. Therefore, the up-regulated proteins in Phi-treated sample facilitated rapid activation of the early defense from pathogen infection.

The abundance of three proteins that are involved in ROS scavenging, two glutathione-S-transferases (GST) and a monodehydroascorbate reductase (MDHAR), was up-regulated in Phi-treated sample in this study (Table 3.2). The up-regulation of these proteins that act as ROS scavengers indicates that Phi-treated plants produce higher levels of ROS than untreated plants. In addition, the abundance of four proteins, three peroxidases and a germin-like protein (GLP), involved in ROS production was enhanced in this study (Table 3.2). It was reported that GLP with oxalate oxidase activity contributed to the production of ROS by the oxidative degradation of oxalate (Patnaik and Khurana, 2001). Peroxidase is a key enzyme to produce ROS following successful pathogen recognition (Torres *et al*., 2006). O'Brien *et al*. (2012) found that the knockdown of two cell wall peroxidase genes, *PRX33* and *PRX34*, which are responsible

for half of the ROS production in *Arabidopsis*, blocks the induction of PAMP-triggered defense-related proteins. Therefore, up-regulated peroxidases in this study may be a key molecular component in the production of ROS, resulting in strengthening of plant cell walls. Two of the three peroxidases found in this study were classified into class III peroxidase that has a signal peptide (Table 3.2). Class III peroxidase-mediated cross linking of cell wall glycoprotein with H_2O_2 forms large papillae called callose at local infection sites (Figure 4.2). Indeed, large accumulations of callose in Phi-treated leaves were observed (Figure 3.11). In addition, peroxidase-mediated oxidative cross-linking with extensin and ferulic acid is involved in the formation process of physical barriers, such as lignification and suberization, which limit pathogen invasion (Jackson *et al*., 2000; Almagro *et al*., 2009). A previous study demonstrated that a Phi-treated Australian native tree accumulated lignin following infection with *Phytophthora* species (Suddaby *et al*., 2008). Hence, Phi contributed to cell wall reinforcement in potato leaves.

Increases in levels of Ca^{2+} are also one of the early events in the orchestration of defense responses triggered by recognition of a pathogen (O'Brien *et al*., 2012). In this study, two calmodulins, which are Ca^{2+} binding proteins were up-regulated (Table 3.2). Changes in Ca^{2+} concentrations in plant cytoplasm by Phi applications remain to be investigated. However, the up-regulated calmodulins facilitate binding of increased Ca^{2+} to calmodulins upon recognition of a pathogen. Active calmodulin triggers a cascade of signaling pathways leading ultimately to HR (Yang and Pooviah, 2003). Therefore, before pathogen attack, calmodulins pre-activated in Phi-treated sample facilitate a rapid HR upon infection. Notably, two calmodulins were more abundant in Phi-treated plants than in untreated plants after infection (group 1, Figure 3.7a). This result suggests that the

up-regulated calmodulins (TC168258 and TC166307) associated with calcium signaling contributes to increase in levels of pathogen resistance by, possibly, the involvement of HR.

4.1.3 Salicylic Acid-Dependent Signaling Pathway is Stimulated in Phi-Treated Sample

In this study, the abundance of a catalase and ascorbate peroxidase, key enzymes of ROS scavenging, was not changed or was slightly down-regulated in Phi-treated sample. The plant hormone SA binds to catalase and ascorbate peroxidase in order to inhibit their activity (Wendehenne *et al*., 1998). This result suggests that increases in levels of SA in Phi-treated potato plants leads to ROS production.

Since *PR* genes are expressed by the SA-dependent pathway (Durrant and Dong, 2004), we assume that Phi triggers the activation of SA signaling pathways. Indeed, up-regulation of PR-1 and PR-9 proteins that are SA-marker proteins indicates that the SA-dependent signaling pathway is induced. The activation of the SA signaling pathway has been found to contribute to the resistance of potato to *P. infestans*. Halim *et al*. (2007) demonstrated that callose deposition was an effective defense response activated via SA- and ROS-dependent pathway in potatoes against the biotrophic stage of *P. infestans*. SA-induced PR proteins play a role in defense response with antimicrobial property at local infection sites (Ahn *et al*., 2005). Levels of SA and PR proteins were found to be higher in disease-resistant than in susceptible potato cultivars (Bariya *et al*., 2011). Therefore, SA-dependent pathway contributes to increased levels of resistance to *P. infestans*.

Jasmonic acid is also plant hormones related to defense responses against pathogens. However, in this study, the abundance of 13-lipoxygenase and allene oxide cyclase, key enzymes involved in the JA biosynthetic pathway, was slightly repressed after Phi applications. This result suggests that Phi applications to potato plants led to stimulation of signaling pathways involved in SA rather than JA.

4.1.4 Rapid Hypersensitive Response is Induced in Phi-Treated Sample

Cysteine protease and cysteine protease inhibitor are related to the activation of HR. In this study, changes in abundance of 2 cysteine protease and 3 cysteine protease inhibitors were identified. Two cysteine proteases (TC176976 and TC172593) were found to be up-regulated in Phi-treated sample (Table 3.2). It is well known that the activation of caspases (cysteine-containing aspartate-specific proteases) family of cysteine proteases is essential to induce HR (Xu and Zhang, 2009). Interestingly, a cysteine protease cathepsin B (TC176976), identified in this study, is highly homologous at the amino acid level with a cathepsin B (TC137447) identified by Gilroy *et al*. (2007). The authors identified that cathepsin B plays a role in the activation of HR (Gilroy *et al*., 2007). The conserved four active sites and peptidase unit in the protein strongly suggests that the up-regulated cathepsin B has the same function for HR activation as TC137447.

The abundance of 3 different cysteine protease inhibitors was enhanced by Phi-treated sample (Table 3.2). HR is preceded by a tightly regulated cell death process at local infection sites. Cysteine protease-induced HR in tobacco plants was blocked by ectopic expression of a cysteine protease inhibitor, indicating that cysteine protease-cysteine protease inhibitor interactions modulate HR (Solomon *et al*., 1999). Therefore,

the up-regulated cysteine protease inhibitors may interact with cathepsin B to control cathepsin B-induced HR before pathogen infection. Four days post inoculation, only 4 of the 35 defense-related proteins in Phi-treated sample was repressed in Phi-treated plants (group 3, Figure 3.6a). The 4 proteins include all three cysteine protease inhibitors and β-1,3-1,4-glucanase that hydrolyzes a cell wall component. Upon infection with *P. infestans*, down-regulation of the cysteine protease inhibitors suggests breakdown of the interaction of cathepsin B with cysteine protease inhibitors, leading to the activation of HR.

Previous studies demonstrated a cell death-like response in tobacco against *Phytophthora nicotiana* using light microscopy (Guest, 1986), suggesting the needs for definitive evidence related to necrosis or HR, a localized PCD. Using a transmission electron microscope (TEM), indeed, morphological characteristics of HR, such as chromatin margination and condensation, vacuolization, and partial chloroplast disruption enclosed in a vesicle called an autophagosome, were observed in the cells of Phi-treated leaf samples at 5 dpi (Figure 3.10). HR leasions were observed in leaves of resistant potato cultivar from 2 dpi (Orlowska *et al*., 2012). A rapid HR response increases levels of resistance to *P. infestans* (Vleeshouwers *et al*., 2000). Increases in ROS and Ca^{2+} as early events of HR as well as the involvement of the SA pathway in Phi-treated potato plants are coordinated to activate, possibly, HR. In addition, essential molecular components, cysteine proteases and cysteine protease inhibitors to facilitate a rapid HR were up-regulated in Phi-treated sample.

4.2 Pre-Activation of Proteins Before Infection is Essential to Increase Levels of Resistance in Potato Plants to P. infestans

The proteomics data presented in this study has provided insight into how Phi confers enhanced resistance against *P. infestans* in treated potato plants. However, after infection, the abundance of most of the differentially regulated proteins in Phi-treated plants was similar to that in untreated plants (Figure 3.7). This result suggests that pre-activation of proteins in Phi-treated sample before pathogen infection is essential to increase levels of potato resistance to *P. infestans*. Levels of PR proteins and SA in resistant plants were higher than in susceptible plants, indicating that early accumulation of defense-related genes is associated with resistance to pathogens (Shetty *et al*., 2009). The expression level of *PR* genes, such as PR-1, chitinase, osmotin, and peroxidase, was rapidly accumulated in detached leaves of a resistant cultivar at 1 and 17 hours post infection (Orlowska *et al*., 2012). Wild *Solanum* species resistant to *P. infestans* triggered the orchestration of Ca^{2+} signaling pathway, ROS production, and the expression of caspase-like protease, resulting in a rapid HR. In contrast to resistant wild species, the delay of effective defense responses in cultivated potatoes renders them susceptible to the pathogen (Vleeshouwers *et al*., 2000). Therefore, pre-activation of proteins in Phi-treated sample facilitates the rapid activation of defense responses, resulting in enhanced resistance in potato plants to *P. infestans*.

In contrast to most of the differentially regulated proteins, several proteins, including lipase, polygalacturonase inhibitor protein, two calmodulins, cysteine protease inhibitor 7, heat shock protein, and wound-induced protease inhibitor, were more abundant in Phi-treated plants than in untreated plants after infection (group 1, Figure

3.7a, b). These proteins showing different abundance in Phi-treated and untreated plants may also be important in increasing levels of resistance. Lipase plays a role in degrading membranes of pathogens. Polygalacturonase inhibitor protein delays pathogen progress by protecting plant cell wall components. The transient expression of calmodulin in pepper leaves showed the activation of ROS burst and HR (Choi *et al*., 2009). Cysteine protease inhibitor is also related to the HR. Heat shock protein and wound-induced protease inhibitor are universal stress-related proteins. Therefore, they may be core proteins involved in Phi-IR and direct evidence for their involvement in Phi-IR remains to be investigated.

4.3 Differential Centrifugation Approach

To understand broad functional changes differentially regulated in Phi-treated potato leaves, improvements were needed to isolate more proteins from the plant cell wall and cytoplasm (Figure 2.1; Lim *et al*., 2012). The use of differential centrifugation was an effective approach to deal with the immense complexity of the plant leaf, and the highly abundant RuBisCO proteins that interfere with the quality of the leaf protein profile. By using this approach, 1172 proteins in the two fractions were reproducibly identified. Reproducibly identified proteins corresponded to over 70% of proteins identified in each replicate. This is a very high success rate, especially since the samples were produced under field conditions.

Unexpectedly, this approach to separate fractions provided another benefit for the study of protein localization. In this study, 10 proteins were identified in both cell wall and cytoplasmic fractions (Table 3.2). The abundance in levels of each protein was

similar in both fractions of Phi-treated leaves (Table 3.2). However, in *P. infestans* challenged Phi-treated leaves, the abundance of all 10 proteins identified from the cytoplasmic fraction was higher than their abundance in the cell wall fraction (Figure 3.6a). It is known that cathepsin B is relocalized from the lysosome to the cytosol during PCD (Gilroy *et al*., 2007). This suggests that the trend in abundance of the 10 proteins indicates their relocalization during Phi-IR. The use of differential centrifugation to identify relocalization of proteins deserves further investigation.

Differential centrifugation approach would also allow identification of many PR and secretory proteins from the cell wall fraction and proteins involved in metabolism and energy production from the cytoplasmic fraction. This approach could be applied to isolate interesting organelles and identify proteins in samples taken at earlier time points, such as 1 or 2 dpi. Identification of differentially regulated proteins at these earlier sampling points would further facilitate understanding of the molecular mechanisms involved in Phi-IR in potato against *P. infestans*.

4.4 Further Studies

The identification of differentially regulated proteins in potato leaves has improved our understanding of Phi-induced resistance against *P. infestans*. Rapid recognition of PAMPs is facilitated in Phi-treated sample by increasing PR proteins including hydrolases. The recognition triggers early events, the activation of Ca^{2+} signaling and ROS production, resulting in HR. SA-dependent pathway is involved in Phi-IR. Overall, pre-activation of proteins up-regulated in Phi-treated sample and a small set of proteins increase levels of host resistance to *P. infestans*. This knowledge can be

used for suppressing late blight through modulation of prominent defense responses, such as a rapid induction of the HR and secretory proteins to target pathogen components. However, many unanswered questions remain. For example, involvements of some components involved in the activation of HR, such as up-regulated cathepsin B, interactions of cathepsin B with cysteine protease inhibitor, calmodulins, remain to be investigated using molecular genetics. Overexpression of up-regulated proteins in Phi-treated sample, such as hydrolases, may increase host resistance to the pathogen. If the HR occurs in Phi-treated plants, can *P. infestans* delimited by the HR in Phi-treated sample change from a biotroph to a necrotroph? If so, proteins secreted by the pathogen may target plant proteins involved in the HR and/or early events of defense responses. The identification of plant proteins targeted by effector proteins of *P. infestans* remains to be investigated. Further studies to answer these intriguing questions will provide knowledge to assist with late blight management in agricultural crop production systems.

References

Aghaei K, Ehsanpour AA, Komatsu S (2008) Proteome analysis of potato under salt stress. J. Proteome Res. 7: 4858 – 4868

Agrawal L, Chakraborty S, Jaiswal DK, Gupta S, Datta A, Chakraborty N (2008) Comparative proteomics of tuber induction, development and maturation reveal the complexity of tuberization process in potato (*Solanum tuberosum* L.). J. Proteome Res. 7: 3803 – 3817

Ahn I-P, Kim S, Lee Y-H (2005) Vitamin B1 functions as an activator of plant disease resistance. Plant Physiol. 138: 1505 – 1515

Almagro L, Ros LVG, Belchi-Navarro S, Bru R, Barcelo AR, Pedreno MA (2009) Class III peroxidases in plant defence reactions. J. Exp. Bot. 60: 377 – 390

Andreu A, Guevara M, Wolski E, Daleo G, Caldiz D (2006) Enhancement of natural disease resistance in potatoes by chemicals. Pest Manag. Sci. 62: 162 – 170

Arbogast M, Powelson ML, Cappaert MR, Watrud LS (1999) Response of six potato cultivars to amount of applied water and *verticillium dahlia*. Phytopathol. 89: 782 – 788

Avrova AO, Stewart HE, De Jong WD, Heilbronn J, Lyon GD, Birch PR (1999) A cysteine protease gene is expressed early in resistant potato interactions with *Phytophthora infestans*. Mol. Plant-Microbe Interact. 12: 1114 – 1119

Avrova AO, Taleb N, Rokka V, Heilbronn J, Campbell E, Hein I, Gilroy EM, Cardle L, Bradshaw JE, Stewart HE, Fakim YJ, Loake G, Birch PR (2004) Potato oxysterol binding protein and cathepsin B are rapidly up-regulated in independent defense pathways that distinguish *R* gene-mediated and field resistances *to Phytophthoa infestans*. Mol. Plant Pathol. 5: 45 – 56

Balci Y, Balci S, Eggers J, MacDonal WL, Juzwik J, Long RP, Gottschalk KW (2007) *Phytophthora* spp. associated with forest soils in eastern and north-central US oak ecosystems. Plant Dis. 91: 705 – 710

Barel G, Ginzberg I (2008) Potato skin proteome is enriched with plant defence components. J. Exp. Bot. 59: 3347 – 3357

Bariya HS, Thakkar VR, Thakkar AN, Subramanian RB (2011) Induction of systemic resistance in different varieties of *Solanum tuberosum* by pure and crude elicitor treatment. Indian J. Exp. Biol. 49: 151 – 162

Bendtsen JD, Nielsen H, von Heijne G, Brunak S (2004) Improved prediction of signal peptides: SignalP 3.0. J. Mol. Biol. 340: 783 – 795

Berg M, Parbel A, Pettersen H, Fenyo D, Bjorkesten L (2006) Reproducibility of LC-MS-based protein identification. J. Exp. Bot. 57: 1509 – 1514

Bevan M, Bancroft I, Bent E, Love K, Goodman H, Dean C, Bergkamp R, Dirkse W (1998) Analysis of 1.9 Mb of contiguous sequence from chromosome 4 of *Arabidopsis thaliana*. Nature 391: 485 – 488

Bhadauria V, Miraz P, Kennedy R, Banniza S, Wei Y (2010) Dual trypan-aniline blue fluorescence staining methods for studying fungus-plant ingteractions. Biotech. Histochem. 85: 99 – 105

Bozkurt TO, Schornack S, Win J, Shindo T, Ilyas M, Oliva R, Cano LM, Jones AME, Huitema E, van der Hoorn RAL, Kamoun S (2011) *Phytophthora infestans* effector AVRblb2 prevents secretion of a plant immune protease at the haustorial interface. Proc. Natl. Acad. Sci. USA 108: 20832 – 20837

Bradford MM (1976) A rapid and sensitive method for the quantitation of microgram quantities of protein utilizing the principle of protein-dye binding. Anal. Biochem. 72: 248 – 254

Brunner F, Rosahl S, Lee J, Rudd JJ, Geiler C, Kauppinen S, Rasmussen G, Scheel D, Nurnberger (2002) Pep-13, a plant defense-inducing pathogen-associated pattern from *Phytophthora* transglutaminasa. EMBO J. 21: 6681 – 6688

Cahill DM, Rookes JE, Wilson BA, Gibson L, McDougall KL (2008) *Phytophthora cinnamomi* and Australia's biodiversity: impacts, predictions and progress towards control. Aus. J. Bot. 56: 279 – 310

Camire ME, Kubow S, Donnelly DJ (2009) Potatoes and human health. Crit. Rev. Food Sci. Nutri. 49: 823 – 840

Candela ME, Alcazar MD, Espin A, Egea C, Almela L (1995) Soluble phenolic acids in *Capsicum annuum* stems infected with *Phytophthora capsici*. Plant Pathol. 44: 116 – 123

Cao H, Glazebrook J, Clarke JD, Volko S, Dong X (1997) The Arabidopsis *NPR1* gene that controls systemic acquired resistance encodes a novel protein containing ankyrin repeats. Cell 88: 57 – 63

Carter C, Pan S, Zouhar J, Avila EL, Girke T, Raikhel NV (2004) The vegetative vacuole proteome of *Arabidopsis thaliana* reveals predicted and unexpected proteins. Plant Cell 16: 3285 – 3303

Caux P-Y, Kent R, Fan G, Stephenson G (1996) Environmental fate and effects of chlorothalonil: A canadian perspective. Crit. Rev. Environ. Sci. Technol. 26: 45 – 93

Chakravarthy S, Tuori RP, D'Ascenzo MD, Fobert PR, Despres C, Martin GB (2003) The tomato transcription factor Pti4 regulates defense-related gene expression via GCC box and non-GCC box cis elements. Plant Cell 15: 3033 – 3050

Chaves I, Pinheiro C, Paiva JAP, Planchon S, Sergeant K, Renaut J, Graca JA, Costa G, Coelho AV, Ricardo CPP (2009) Proteomic evaluation of wound-healing processes in potato (*Solanum tuberosum* L.) tuber tissue. Proteomics 9: 4154 – 4175

Chen J, Zhang Y, Wang C, Lu W, Jin JB, Hua X (2010) Proline induces calcium-mediated oxidative burst and salicylic acid signaling. Amino acids 40: 1473 – 1484

Chester K (1933) The problem of acquired physiological immunity in plants. Quar. Rev. Biol. 8: 129 – 154

Chisholm ST, Coaker G, Day B, Staskawicz BJ (2006) Host-microbe interactions: shaping the evolution of the plant immune response. Cell 124: 803 – 814

Chivasa S, Ndimba B, Simon W, Robertson D, Yu X-L, Knox J, Bolwell P, Slabas A (2002) Proteomic analysis of the *Arabidopsis thaliana* cell wall. Electrophoresis 23: 1754 – 1765

Choi HW, Lee DH, Hwang BK (2009) The pepper calmodulin gene *CaCaM1* is involved in reactive oxygen species and nitric oxide generation required for cell death and the defense response. Mol. Plant-Microbe Interact. 22: 1389 – 1400

Cline M, Smoot M, Cerami E, Kuchinsky A, Landys N, Workman C, Chrismas R, Avila-Campilo I, Creech M, Gross B, Hanspers K, Isserlin R, Kelley R, Killcoyne S, Lotia S, Maere S, Morris J, Ono K, Pavlovic V, Pico A, Vailaya A, Wang P-L, Adler A, Conklin B, Hood L, Kuiper M, Sander C, Schmulevich I, Warner G, Ideker T, Bader G (2007) Integration of biological networks and gene expression data using Cytoscape. Nature Protocols 2: 2366 – 2382

Cohen Y, Coffey MD (1986) Systemic fungicides and the control of oomycetes. Ann. Rev. Phytopathol. 24: 311 – 338

Coffey MD, Joseph MC (1985) Effects of phosphorous acid and fosetyl-Al on the life cycle of *Phytophthora cinnamomi* and *Phytophthora citricola*. Phytopathol. 75: 1042 – 1046

Coll NS, Epple P, Dangl JL (2011) Programmed cell death in the plant immune system. Cell Death Differ. 18: 1247 – 1256

Conrath U, Linke C, Jeblick W, Geigenberger P, Quick WP, Neuhaus HE (2003) Enhanced resistance to *Phytophthora infestans* and *Alternaria solani* in leaves and tubers, respectively, of potato plants with decreased activity of the plastidic ATP/ADP transporter. Planta 217: 75 – 83

Coupe SA, Watson LM, Ryan DJ, Pinkney TT, Eason JR (2004) Molecular analysis of programmed cell death during senescence in *Arabidopsis thaliana* and *Brassica oleracea*: cloning broccoli LSD1, Bax inhibitor and serine palmitoyltransferase homologues. J. Exp. Bot. 55: 59 – 68

Daniel R, Guest D (2006) Defence responses induced by potassium phosphonate in *Phytophthora palmivora*-challenged *Arabidopsis thaliana*. Physiol. Mol. Plant Pathol. 67: 194 – 201

Dastoor Z, Dreyer J-C (2001) Potential role of nuclear translocation of glyceraldehydes-3-phosphate dehydrogenase in apotosis and oxidative stress. J. Cell Sci. 114: 1643 – 1653

De Godoy L, Olsen J, de Souza Lee G, Li G, Mortensen P, Mann M (2006) Status of complete proteome analysis by mass spectrometry: SILAC labeled yeast as a model system. Genome Biol. 7: R50

De Jong CF, Laxalt AM, Bargmann BO, de Wilt PJ, Joosten MH, Munnik T (2004) Phosphatidic acid accumulation is an early response in the Cf-4/Avr4 interaction. Plant J. 39: 1 – 12

Debroy S, Thilmony R, Kwack YB, Nomura K, He SY (2004) A family of conserved bacterial effectors inhibits salicylic acid-mediated basal immunity and promotes disease necrosis in plants. Proc. Natl. Acad. Sca. USA 101: 9927 – 9932

Delaney T, Uknes S, Vernooij B, Friedrich L, Weymann K (1994) A central role of salicylic acid in plant disease resistance. Science 266: 1247 – 1250

Dempsey JJ, Arnold DL, Wilson I, Spencer-Phillips PTN (2011) The role of phosphite in suppressing *Microdochium nivale* in amenity turfgrass. Forum poster presentation

Desveaux D, Subramaniam R, Despres C, Mess J, Levesque C, Fobert P, Dangle J, Brisson N (2004) A 'whirly' transcription factor is required for salicylic acid-dependent disease resistance in *Arabidopsis*. Dev. Cell 6: 229 – 240

Diallo S, Crepin A, Barbey C, Orange N, Burini JF, Latour X (2011) Mechanisms and recent advances in biological control mediated through the potato rhizosphere. FEMS Microbiol. Ecol. 75: 351 – 364

Dowley LJ, O'Sullivan E (1981) Metalaxyl-resistance in populations of *Phytophthora infestans* (Mont.) de Bary in Ireland. Potato Res. 24: 417 – 421

Durrant W, Dong X (2004) Systemic acquired resistance. Annu. Rev. Phytopathol. 42: 185 – 209

Eschen-Lippold L, Altmann S, Rosahl S (2010) DL-β-aminobutyric acid-induced resistance of potato against *Phytphthora infestans* requires salicylic acid but not oxylipins. Mol. Plant-Microbe Interact. 23: 585 – 592

Eshraghi L, Anderson J, Aryamanesh N, Shearer B, McComb J, Hardy GES, O'Brien PA (2011) Phosphite primed defence responses and enhanced expression of defence genes in *Arabidopsis thaliana* infected with *Phytophthora cinnamomi*. Plant Pathology 60: 1086 – 1095

Eulgem T, Somssich IE (2007) Networks of WRKY transcription factors in defense signaling. Curr. Opin. Plant Biol. 10: 366 – 371

FAOSTAT (2008) Food and agricultural organization of the United Nations retrieved from http://www.potato2008.org/en/world/index.html

FAOSTAT (2011) Food and agricultural organization of the United Nations retrieved from http://faostat.fao.org/default.aspx

Feiz L, Irshad M, Pont-Lezica R, Canut H, Jamet E (2006) Evaluation of cell wall preparations for proteomics: a new procedure for purifying cell walls from Arabidopsis hypocotyls. Plant Methods 2: 10

Fenn ME, Coffey MD (1984) Studies on the in vitro and in vivo antifungal activity of fosetyl-Al and phosphorous acid. Phytopathol. 74: 606 – 611

Ferro M, Salvi D, Brugiere S, Miras S, Kowalski S, Louwagie M, Garin J, Joyard J, Rolland N (2003) Proteomics of the chloroplast envelope membranes from *Arabidopsis thaliana*. Mol. Cell. Proteomics 2: 325 – 345

Fry W (2008) *Phytophthora infestans*: the plant (and *R* gene) destroyer. Mol. Plant Pathol. 9: 385 – 402

Garcia-Brugger A, Lamotte O, Vandelle E, Bourque S, Lecourieux, Penoit B, Wendehenne D, Pugin A (2006) Early signaling events induced by elicitors of plant defenses. Mol. Plant-Microbe Interact. 7: 711 – 724

Garron C, Knopper LD, Ernst WR, Mineau P (2012) Assessing the genotoxic potential of chlorothalonil drift from potato fields in Prince Edward Island, Canada. Arch. Environ. Contam. Toxicol. 62: 222 – 232

Gilroy EM, Hein I, van der Hoon R, Boevink PC, Venter E, McLellan H, Kaffarnik F, Hrubikova K, Shaw J, Holeva M, Lopez EC, Borras-Hidago O, Pritchard L, Loake GJ, Lacomme C, Birch PR (2007) Involvement of cathepsin B in the plant disease resistance hypersensitive response. Plant J. 52: 1 – 13

Glazebrook J (2005) Contrasting mechanisms of defense against biotrophic and necrotrophic pathogens. Annu. Rev. Phytopathol. 43: 205 – 227

Goellner K, Conrath U (2008) Priming: it's all the world to induced disease resistance. Eur. J. Plant Pathol. 121: 233 – 242

Goodwin S, Cohen B, Deahl K, Fry W (1994) Migration from northern Mexico was the probable cause of recent genetic changes in populations of *Phytophthora infestans* in the United States and Canada. Phytopathol. 84: 553 – 558

Goulet C, Goulet C, Goulet M-C, Michaud D (2010) 2-DE proteome maps for the leaf apoplast of *Nicotiana benthamiana*. Proteomics 10: 2536 – 2544

Govrin EM, Levine A (2000) The hypersensitive response facilitates plant infection by the necrotrophic pathogen *Botrytis cinerea*. Curr. Biol. 10: 751 – 757

Grennan AK (2006) Plant response to bacterial pathogens. Overlap between innate and gene-for-gene defense response. Plant Physiol. 142: 809 – 811

Grenville-Briggs LJ, Anderson LV, Fugelstad J, Avrova AO, Bouzenzana J, Williams A, Wawra S, Whisson SC, Birch PRJ, Bulone V, van West P (2008) Cellulose synthesis in *Phytophthora infestans* is required for normal appressorium formation and successful infection of potato. Plant Cell 20: 720 – 738

Guest D (1986) Evidence from light microscopy of living tissues that Fosetyl-Al modifies the defense in tobacco seedlings following inoculation by *Phytophthora nicotiana* var *nicotianae*. Physiol. Mol. Plant Pathol. 29: 251 – 261

Guest D, Bompeix G (1990) The complex mode of action of phosphonates. Australas. Plant Pathol. 19: 113 – 115

Guest D, Grant B (1991) The complex action of phosphonates as antifungal agents. Bio. Rev. 66: 159 – 187

Guevara MG, Oliva CR, Huarte M, Daleo GR (2002) An aspartic protease with antimicrobial activity is induced after infection and wounding in intercellular fluids of potato tubers. Eur. J. Plant Pathol. 108: 131 – 137

Halim VA, Hunger A, Macioszek V, Landgraf P, Nurnberger T, Scheel D, Rosahl S (2004) The oligopeptide elicitor Pep-13 induces salicylic acid-dependent and-independent defense reactions in potato. Physiol. Mol. Plant Pathol. 64: 311 – 318

Halim VA, Eschen-Lippold L, Altmann S, Birschwilks M, Scheel D, Rosahl S (2007) Salicylic acid is important for basal defense of *Solanum tuberosum* against *Phytophthora infestans*. Mol. Plant-Microbe Interact. 20: 1346 – 1352

Halim VA, Altmann S, Ellinger D, Eschen-Lippold L, Miersch O, Scheel D, Rosahl S (2009) PAMP-induced defense responses in potato require both salicylic and jasmonic acid. Plant J. 57: 230 – 242

Hammerschmidt R, Metraux J-P, van Loon LC (2001) "Inducing resistance" a summary of papers presented at the first international symposium on induced resistance to plant diseases, Corfu, May 2000. Eur. J. Plant Pathol. 107: 1 – 6

Hass BJ, Komuon S, Zody MC, Jiang RHY, *et al*. (2009) Genome sequence and analysis of the Irish potato famine pathogen Phytophthora infestans. Nature. 461: 393 – 398

Hein I, Gilroy EM, Armstrong MR, Birch PRJ (2009) The zig-zag-zig in oomycete-plant interactions. Mol. Plant Pathol. 10: 547 – 562

Howell JT, Davis MR (2005) Plant defense mechanisms against fungal pathogens: polygalacturonase inhibitor proteins. Can. J. Plant Pathol. 27: 5 – 15

Hutchings D, Rawsthorne S, Emes MJ (2005) Fatty acid synthesis and the oxidative pentose phosphate pathway in developing embryos of oilseed rape (*Brassica napus* L.). J. Exp. Bot. 56: 577 – 585

Iriti M, Faoro F (2009) Chitosan as a MAMP, searching for a PRR. Plant Signal. Behav. 4: 66 – 68

Jabs T (1999) Reactive oxygen intermediates as mediators of programmed cell death in plants and animals. Biochem. Phamacol. 57: 231 – 245

Jackson T, Burgess T, Colquhoun I, Hardy G (2000) Action of the fungicide phosphite on *Eucalyptus marginata* inoculated with *Phytophthora cinnamomi*. Plant Pathol. 49: 147 – 154

James WC (1971) A manual of assessment keys for plant disease, APS Press, UK, Key No. 3.1.1

Jamet E, Canut H, Boudart G, Pont-Lezica RF (2006) Cell wall proteins: a new insight through proteomics. Trends Plant Sci. 11: 33 – 39

Jiang T, Zhang XF, Wang XF, Zhang DP (2011) *Arabidopsis* 3-ketoacyl-CoA thiolase-2 (KAT2), an enzyme of fatty acid β-oxidation, is involved in ABA signal transduction. Plant Cell Physiol. 52: 528 – 538

Johnson DA, Inglis DA, Miller JS (2004) Control of potato tuber rots caused by oomycetes with foliar applications of phosphorous acid. Plant Disease 88: 1153 – 1159

Jones JDG, Dangl JL (2006) The plant immune system. Nature 444: 323 – 329

Judelson HS (1997) The genetics and biology of *Phytophthora infestans*: modern approaches to a historical challenge. Fungal Gene. Biol. 22: 65 – 76

Kaschani F, Shabab M, Bozkurt T, Shindo T, Schornack S, Gu C, Ilyas M, Win J, Kamoun S, van der Hoorn RAL (2010) An effector-targeted protease contributes to defense against *Phytophthora infestans* and is under diversifying selection in natural hosts. Plant Physiol. 154: 1794 – 1804

Kawchuk LM, Kalischuk M, Al-Mughrabi KI, Peters RD, Howard RJ, Platt HW (2012) Genetic composition of *Phytophthora infestans* in Canada reveals migration and increased diversity. Plant Dis. Accepted

Kikuchi S, Hirohashi T, Nakai M (2006) Charaterization of the preprotein translocation at the outer envelope membrane of chloroplasts by blue native PAGE. Plant Cell Physiol. 47: 363 – 371

Kim MG, da Cunha L, McFall AJ, Belkhadir Y, DebRoy S, Dangl JL, Mackey D (2005) Two *Pseudomonas synringae* type III effectors inhibit RIN4-regulated basal defense in *Arabidopsis*. Cell 121: 749 – 759

King M, Reeve W, van der Hoek MB, Williams N, McComb J, O'Brien PA, Hardy GES (2010) Defining the phosphite-regulated transcriptome of the plant pathogen *Phytopthora cinnamomi*. Mol. Genet. Genomics 284: 425 – 435

Kobayashi M, Yoshioka M, Asai S, Nomura H, Kuchimura K, Mori H, Doke N, Yoshioka H (2012) StCDPK5 confers resistance to late blight pathogen but increases susceptibility to early blight pathogen in potato via reactive oxygen species burst. New Phytol. 196: 223 – 237

Kuc J (1982) Induced immunity to plant disease. Biosci. 32: 854 – 860

Kuc J (1987) Translocated signals for plant immunization. Annals New York Acad. Sci. 494: 221 – 223

Kwon C, Bednarek P, Schulze-Lefert P (2008) Secretory pathways in plant immune responses. Plant Physiol. 147: 1575 – 1583

Lagaert S, Belien T, Volckaert G (2009) Plant cell walls: protecting the barrier from degradation by microbial enzymes. Semin. Cell Dev. Biol. 20: 1064 – 1073

Lee J, Cooper B (2006) Alternative workflows for plant proteomic analysis. Mol. Biosyst. 12: 621 – 626

Lee J, Garrett WM, Cooper B (2007) Shotgun proteomic analysis of *Arabidopsis thaliana* leaves. J. Sep. Sci. 30: 2225 – 2230

Lee SC, Hwang BK (2005) Induction of some defense-related genes and oxidative burst is required for the establishment of systemic acquired resistance in *Capsicum annuum*. Planta 221: 790 – 800

Lehesranta SJ, Davies HV, Shepherd LV, Koistinen KM, Massat N, Nunan N, McNicol JW, Karenlampi SO (2006) Proteomic analysis of the potato tuber life cycle. Proteomics 6: 6042 – 6052

Lehesranta SJ, Koistinen KM, Massat N, Davies HV, Shepherd LV, McNicol JW, Cakmak I, Cooper J, Luck L, Karenlampi SO, Leifert C (2007) Effects of agricultural production systems and their components on protein profiles of potato tubers. Proteomics 7: 597 – 604

Li X, Zhang Y, Clarke J, Li Y, Dong X (1999) Identification and cloning of a negative regulator of systemic acquired resistance, SNI1, through a screen for suppressors of *npr1-1*. Cell 98: 329 – 339

Lim PO, Nam HG (2005) The molecular and genetic control of leaf senescence and longevity in Arabidopsis. Curr. Top. Dev. Biol. 67: 49 – 83

Lim S, Chisholm K, Coffin RH, Peters RD, Al-Mughrabi KI, Wang-Pruski G, Pinto DM (2012) Protein profiling in potato (*Solanum tuberosum* L.) leaf tissues by differential centrifugation. J. Proteome Res. 11: 2594 – 2601

Liu D, Raqhothama KG, Hasegawa PM, Bressan RA (1994) Osmotin overexpression in potato delays development of disease symptoms. Proc. Natl. Acad. Sci. USA 91: 1888 – 1892

Liu Y, Schiff M, Czymmek K, Talloczy Z, Levine B, Dinesh-Kumar SP (2005) Autophagy regulates programmed cell death during the plant innate immune response. Cell 121: 567 – 577

Liu Z, Halterman D (2009) Analysis of proteins differentially accumulated during potato late blight resistance mediated by the *RB* resistance gene. Physiol. Mol. Plant Pathol. 74: 151 – 160

Lobato M, Olivieri F, Altamiranda E, Wolski E, Daleo G, Caldiz, Andreu A (2008) Phosphite compounds reduce disease severity in potato seed tubers and foliage. Eur. J. Plant Pathol. 122: 349 – 358

Lucker J, Laszczak M, Smith D, Lund S (2009) Generation of a predicted protein database from EST data and application to iTRAQ analyses in grape (*Vitis vinifera* cv. *Cabernet* Sauvignon) berries at ripening initiation. BMC Genomics 10: 50

Maere S, Heymans K, Kuiper M (2005) BiNGO: a Cytoscape plugin to assess overrepresentation of gene ontology categories in biological networks. Bioinformatics 21: 3448 – 3449

Machinandiarena MF, Olivieri FP, Daleo GR, Oliva CR (2001) Isolation and characterization of a polygalacturonase-inhibiting protein from potato leaves. Accumulation in response to salicylic acid, wounding and infection. Plant Physiol. and Biochem. 39: 129 – 136

Massoud K, Barchietto T, Le Rudulier T, Pallandre L, Didierlaurent L, Garmier M, Ambard-Bretteville F, Seng JM, Saindrenan P (2012) Dissecting the phosphite-induced priming in Arabidopsis infected with *Hyaloperonospora arabidopsis*. Plant Physiol. 159: 286 – 298

Matheron M, Porchas M (2000) Impact of azoxystrobin, dimethomorph, fluazinam, fosetyl-Al and metalaxyl on growth, sporulation, and zoospore cyst germination of three *Phytophthora* spp. Plant Dis. 84: 454 – 458

Mayton H, Myers K, Fry WE (2008) Potato late blight in tubers-The role of foliar phophonate applications in suppressing pre-harvest tuber infections. Crop Protection 27: 943 – 950

McMahon PJ, Purwantara A, Wahab A, Imron M, Lambert S, Keane PJ, Guest D (2010) Phosphonate applied by truck injection controls stem canker and decreases *Phytophthora* pod rot (black pod) incidence in cocoa in Sulawesi. Australas. Plant Pathol. 29: 170 – 175

Medzhitov R (2001) Toll-like receptors and innate immunity. Nat. Rev. Immunol. 1: 135 – 145

Miflin B, Habash DZ (2002) The role of glutamine synthetase and glutamate dehydrogenase in nitrogen assimilation and possibilities for improvement in the nitrogen utilization of crops. J. Exp. Bot. 53: 979 – 987

Miller J, Miller T (2011) Fungicide for managing late blight in potato retrieved from http://www.millerresearch.com/reports/LateBlight/Overview_of_Fungicides_for_Late_Blight.pdf

Mittler R (2002) Oxidative stress, antioxidants and stress tolerance. Trends Plant Sci. 7: 405 – 410

Mittler R, Vanderauwera S, Gollery M, Van Breusegem F (2004) Reactive oxygen gene network of plants. Trends Plant Sci. 9: 490 – 498

Moreno JI, Martin R, Castresana C (2005) Arabidopsis SHMT1, a serine hydroxymethyl transferase that functions in the photorespiratory pathway influences resistance to biotic and abiotic stress. Plant J. 41: 451 – 463

Muetzelburg M, Hofmann F, Just I, Pich A (2009) Identification of biomarkers indicating cellular changes after treatment of neuronal cells with the C3 exoenzyme from *Clostridium botulinum* using the iTRAQ protocol and LC-MS/MS analysis. J. Chromatogr. B 877: 1344 – 1351

Mullins E, Milbourne D, Petti C, Doyle-Prestwich BM, Meade C (2006) Potato in the age of biotechnology. Trends Plant Sci. 11: 254 – 260

Mur LAJ, Kenton P, Lloyd AJ, Ougham H, Prats E (2008) The hypersensitive response; the centenary is upon us but how much do we know? J. Exp. Bot. 59: 501 – 520

Murphy JP, Kong F, Pinto DM, Wang-Priski G (2010) Relative quantitative proteomics analysis reveals wound response proteins correlated with after-cooking darkening. Proteomics 10: 4258 – 4269

Murphy JP, Pinto DM (2010) Temporal proteomic analysis of IGF-1R signaling in MCF-7 breast adenocarcinoma cells. Proteomics 10: 1847 – 1860

Navarre DA, Mayo D (2004) Differential charteristics of salicylic acid-mediated signaling in potato. Physiol. Mol. Plant Pathol. 64: 179 – 188

Nemestothy G, Guest D (1990) Phytoalexin accumulation, phenylalanine ammonia lyase activity and ethylene biosynthesis in fosetyl-Al treated resistant and susceptible tobacco cultivars infected with *Phytophthora nicotiana* var. *nicotianae*. Physiol. Mol. Plant Pathol. 37: 207 – 219

Nurnberger T, Kemmerling B (2006) Receptor protein kinases – pattern recognition receptors in plant immunity. Trends Plant Sci. 11: 519 – 522

O'Brien JA, Daudi A, Finch P, Butt VS, Whitelegge JP, Souda P, Ausubel FM, Bolwell GP (2012) A peroxidase-dependent apoplastic oxidative burst in cultured *Arabidopsis* cells functions in MAMP-elicited defense. Plant Physiol. 158: 2013 – 2027

Olivieri FP, Feldman ML, Machinandiarena MF, Lobato MC, Caldiz DO, Daleo GR, Andreu AB (2012) Phosphite applications induce molecular modifications in potato tuber periderm and cortex that enhance resistance to pathogens. Crop Protection 32: 1 – 6

Oostendorp M, Kunz W, Dietrich B, Staub T (2001) Induced disease resistance in plants by chemical. Eur. J. Plant Pathol. 107: 19 – 28

Orlowska E, Basile A, Kandzia I, Llorenta B, Kirk HG, Cvitanich C (2012) Revealing the importance of meristems and roots for the development of hypersensitive responses and full foliar resistance to *Phytophthora infestans* in the resistant potato cultivar Sarpo Mira. J. Exp. Bot. 63: 4765 – 4779

Pasqualini S, Piccioni C, Reale L, Ederli L, Torre GD, Ferranti F (2003) Ozone-induced cell death in tobacco cultivar Bel W3 plants. The role of programmed cell death in lesion formation. Plant Physiol. 133: 1122 – 1134

Patnaik D, Khurana P (2001) Germin and germin-like proteins: an overview. Indian J. Exp. Biol. 39: 191 – 200

Percival GC, Noviss K (2010) Evaluation of potassium phosphite and myclobutanil combinations for pear scab (*Venturia pirina*) suppression. Arboricul. Urban Forestry 36: 86 – 92

Peters RD, Forster H, Platt HW, Hall R, Coffey MD (2001) Novel genotypes of *Phytophthora infestans* in Canada during 1994 and 1995. Am. J. Pot. Res. 78: 39 – 45

Peters RD, Platt HW, Hall R (1999) Use of allozyme markers to determine genotypes of *Phytophthora infestans* in Canada. Can. J. Plant Pathol. 21: 144 – 153

Petersen M, Brodersen P, Naested H, Andreasson E, Lindhardt U, Johansen B, Nielsen HB, Lacy M, Austin MJ, Parker JE, *et al*. (2000) *Arabidopsis* MAP kinase 4 negatively regulates systemic acquired resistance. Cell 103: 1111 – 1120

Pieterse CMJ, Leon-Reyes A, van der Ent S, van Wees SCM (2009) Networking by small-molecule hormones in plant immunity. Nature Chem. Biol. 5: 308 – 316

Pieterse CMJ, van Loon L (2004) NPR1: the spider in the web of induced resistance signaling pathways. Curr. Opin. Plant Biol. 7: 456 – 464

Polkowska-Kowalczyk L, Wielgat B, Maciejewska U (2007) Changes in the antioxidant status in leaves of *Solanum* species in response to elicitor from *Phytophthora infestans*. J. Plant Physiol. 164: 1268 – 1277

Rasmussen MW, Roux M, Petersen M, Mundy J (2012) MAP kinase cascades in Arabidopsis innate immunity. Frontiers in Plant Sci. 3: 169

Rawlings ND, Morton FR, Kok CY, Kong J, Barrett AJ (2008) MEROPS: The peptidase database. Nucleic Acids Res. 36: 320 – 325

Relyea HA, van der Donk WA (2005) Mechanism and applications of phosphite dehydrogenase. Bioorganic Chem. 33: 171 – 189

Riviere M-P, Marais A, Ponchet M, Willats W, Galiana E (2008) Silencing of acidic pathogenesis-related PR-1 genes increases extracellular β-(1→3)-glucanase activity at the onset of tobacco defence reactions. J. Exp. Bot. 59: 1225 – 1239

Rocha M, Licausi F, Araujo WL, Nunes-Nesi A, Sodek L, Fernie AR, van Dongen JT (2010) Glycolysis and the tricarboxylic acid cycle are linked by alanine aminotransferase during hypoxia induced by waterlogging of *Lotus japonicas*. Plant Physiol. 152: 1501 – 1513

Rooney H, Klooster J, van der Hoorn R, Joosten M, Jones J, Wit P (2005) *Cladosporium* Avr2 inhibits tomato Rcr3 protease required for Cf-2 dependent disease resistance. Science 308: 1783 – 1786

Ross AF (1961) Systemic acquired resistance induced by localized virus infections in plants. Virology 14: 340 – 358

Ryals J, Uknes S, Ward E (1994) Systemic acquired resistance. Plant Physiol. 104: 1109 – 1112

Ryan CA, Huffker A, Yamaguchi Y (2007) New insights into innate immunity in *Arabidopsis*. Cell Microbiol. 9: 1902 – 1908

Sachs AN, Pisitkun T, Hoffert JD, Yu M-J, Knepper MA (2008) LC-MS/MS analysis of differential centrifugation fractions from native inner medullary collecting duct of rat. Am. J. Physiol. Renal. Physiol. 295: 1799 – 1806

Shah S, Lee Y-J, Hannapel DJ, Rao AG (2011) Protein profiling of the potato petiole under short day and long day photoperiods. J. Proteomics 74: 212 – 230

Shetty N, Jensen JD, Kundsen A, Finnie C, Geshi N, Blennow A, Collinge DB, Jorgensen HJL (2009) Effects of β-1,3-glucan from *Septoria tritici* on structural defence responses in wheat. J. Exp. Bot. 60: 4287 – 4300

Shimono M, Sugano S, Nakayama A, Jiang C-J, Ono K, Toko S, Takatsuji H (2007) Rice WRKY45 plays a crucial role in benzothiazole-inducible blast resistance. Plant cell 19: 2064 – 2076

Shindo T, van der Hoorn RAL (2008) Papain-like cysteine proteases: key players at molecular battlefields employed by both plants and their invaders. Mol. Plant Pathol. 9: 119 – 125

Si-Ammour A, Mauch-mani B, Mauch F (2003) Quantification of induced resistance against *Phytophthora* species expressing GFP as a vital marker: β-aminobutyric acid but not BTH protects potato and *Arabidopsis* from infection. Mol. Plant Pathol. 4: 237 – 248

Silvar C, Merino F, Diaz J (2008) Differential activation of defense-related genes in susceptible and resistant pepper cultivars infected with *Phytophthora capsici*. J. Plant Physiol. 165: 1120 – 1124

Solomon M, Belenghi B, Delledonne M, Menachem E, Levine A (1999) The involvement of cystein proteases and protease inhibitor genes in the regulation of programmed cell death in plants. Plant Cell 11: 431 – 443

Spoel SH, Johnson JS, Dong X (2007) Regulation of tradeoffs between plant defenses against pathogens with different lifestyles. Proc. Natl. Acad. Sci. USA 104: 18842 – 18847

Spooner D, Mclean K, Ramsay G, Waugh R, and Bryan G (2005) A single domestication for potato based on multilocus amplified fragment length polymorphism genotyping. Proc. Natl. Acad. Sci. USA 102: 14694 – 14699

Spreitzer RJ, Salvucci ME (2002) Rubisco: structure, regulatory interactions and possibilities for a better enzyme. Annu. Rev. Plant Biol. 53: 449 – 475

Sticher L, Mauch-Mani B, Metraux J-P (1997) Systemic acquired resistance. Annu. Rev. Phytopathol. 35: 235 – 270

Suddaby T, Alhussaen K, Daniel R, Guest D (2008) Phosphonate alters the defense responses of *Lambertia* species challenged by *Phytophthora cinnamomi*. Aust. J. Bot. 56: 550 – 556

Tabuchi M, Abiko T, Ymaya T (2007) Assimilation of ammonium ions and reutilization of nitrogen in rice (*Oryza sativa* L.). J. Exp. Bot. 58: 2319 – 2327

Tanaka N, Fujita M, Handa H, Murayama S, Uemura M, Kawamura Y, Mitsui T, Mikami S, Tozawa Y, Yoshinaga T, Komatsu S (2004) Proteomics of the rice cell: systemic identification of the protein populations in subcelluar compartments. Mol. Genet. Genomics 271: 566 – 576

The potato genome sequencing consortium (2011) Genome sequence and analysis of the tuber crop potato. Nature 475: 189 – 195

Tian M, Win J, Song J, van der Hoon R, van der Knaap E, Kamoun S (2007) A *phytophthora infestans* cystatin-like protein targets a novel tomato papain-like apoplastic protease. Plant Physiol. 143: 364 – 377

Ton J, Jakab G, Toquin V, Flors V, Iavicoli A, Maeder MN, Metraux J-P, Mauch-Mani B (2005) Dissecting the β-aminobutyric acid-induced prming phenomenon in *Arabidopsis*. 17: 987 – 999

Ton J, Mauch-Mani B (2004) β-aminobutyric acid induced resistance against necrotrophic pathogens is based on ABA-dependent priming for callose. Plant J. 38: 119 – 130

Tonon CV, Oliva CR, Guevara MR, Daleo GR (2002) Isolation of a potato acidic 39 kDa β-1,3-glucanase with antifungal activity against *Phytophthora infestans* and analysis of its expression in potato cultivars differeing in their degrees of field resistance. J. Phytopathol. 150: 189 – 195

Torres MA, Jones JD, Dangl JL (2006) Reactive oxygen species signaling in response to pathogens. Plant Physiol. 141: 373 – 378

Torto TA, Rauser L, Kamoun S (2002) The pipg 1 gene of the oomycete *Phytophthora infestans* encodes a fungal-like endopolygalacturonase. Curr. Genet. 40: 385 – 390

Turner JG, Ellis C, Devoto A (2002) The jasmonate signal pathway. Plant Cell 14: 5153 – 5164

Uknes S, Mauch-Mani B, Moyer M, Potter S, Williams S, Dincher S, Chandler D, Slusarenko A, Ward E, Ryals J (1992) Acquired resistance in Arabidopsis. Plant Cell 4: 645 – 656

van der Ent S, van Hulten M, Pozo MJ, Czechowski T, Udvardi MK, Pieterse CMJ, Ton J (2009) Priming of plant innate immunity by rhizobacteria and β-aminobutyric acid: differences and similarities in regulation. New Phytol. 183: 419 – 431

van Dongen JT, Gupta KJ, Ramirez-Aguilar SJR, Araujo WL, Nunes-Nesi A, Fernie AR (2011) Regulation of respiration in plants: A role for alternative metabolic pathways. J. Plant Physiol. 168: 1434 – 1443

van Loon LC, Bakker P, Pieterse C (1998) Systemic resistance induced by *rhizospere* bacteria. Annu. Rev. Phytopathol. 36: 453 – 483

van Loon LC, Rep M, Pieterse CMJ (2006) Significance of inducible defense-related proteins in infected plants. Annu. Rev. Phytopathol. 44: 135 – 162

van Loon LC, van Strien EA (1999) The families of pathogenesis-related proteins, their activities, and comparative analysis of PR-1 type proteins. Physiol. Mol. Plant Pathol. 55: 85 – 97

Verhage A, van Wees SCM, Pieterse CMJ (2010) Plant immunity: It's the hormones talking, but what do they say? Plant Physiol. 154: 536 – 540

Verhagen BWM, Glazebrook J, Zhu T, Chang H-S, van Loon LC, Pieterse CMJ (2004) The transcriptome of rhizobacteria-induced systemic resistance in *Arabidopsis*. Mol. Plant-Microbe Interact. 17: 895 – 908

Vleeshouwers VGAA, van Dooijeweert W, Govers F, Kamoun S, Colon LT (2000) The hypersensitive response is associate with host and nonhost resistance to *Phytophthora infestans*. Planta 210: 853 – 864

Vorwerk S, Schiff C, Santamaria M, Koh S, Nishimura M, Vogel J, Somerville C, Somerveiile S. (2007) *EDR2* negatively regulates salicylic acid-based defenses and cell death during powdery mildew infections of *Arabidopsis thaliana*. BMC Plant Biol. 7:35

Wang H, Alvarez S, Hicks LM (2012) Comprehensive comparison of iTRAQ and label-free LC-based quantitative proteomics approaches using two *Chlamydomonas reinhardtii* strains of interest for biofuels engineering. J. Proteome Res. 11: 487 – 501

Wang W, Vignani R, Scali M, Cresti M (2006) A universal and rapid protocol for protein extraction from recalcitrant plant tissues for proteomics analysis. Electrophoresis 27: 2782 – 2786

Wang-Pruski G, Coffin RH, Peters RD, Al-Mughrabi KI, Platt AW, Pinto D, Veenhuis-MacNeill S, Hardy W, Lim S, Astatkie T (2010) Phosphorous acid for late blight suppression in potato leaves. Americas J. Plant Sci. Biotech. 4: 25 – 29

Watson B, Lei Z, Dixon RA, Sumner LW (2004) Proteomics of *Medicago sativa* cell walls. Phytochem. 65: 1709 – 1720

Wendehenne D, Durner J, Chen Z, Klessig D (1998) Benzothiadiazole, an inducer of plant defences, inhibits catalase and ascorbate peroxidase. Phytochem. 47: 651 – 657

Wiermer M, Feys BJ, Parker JE (2005) Plant immunity: The EDS1 regulatory node. Curr. Opin. Plant Biol. 8: 383 – 389

Wildermuth MC, Dewdney J, Wu G, Ausubel FM (2001) Isochorismate synthase is required to synthesize salicylic acid for plant defense. Nature 414: 562 – 565

Wilkinson CJ, Holmes JM, Dell B, Tynan KM, McComb JA, Shearer BL, Colquhoun IJ, Hardy GES (2001) Effect of phosphite on *in planta* zoospore production of *Phytophthora cinnamomi*. Plant Pathol. 50: 587 – 593

Wojtaszek P (1997) Oxidative burst: an early plant response to pathogen infection. Biochem. J. 322: 681 – 692

Wolf-Yadlin A, Hautaniemi S, Lauffenburger DA, White FM (2007) Multiple reaction monitoring for robust quantitative proteomic analysis of cellular signaling networks. Proc. Natl. Acad. USA 104: 5860 – 5865

Wong M, McComb JA, Hardy GES, O'Brien PA (2009) Phosphite induces expression of a putative proteophosphoglycan gene in *Phytophthora cinnamomi*. Australas. Plant Pathol. 38: 235 – 241

Woodell L, Miller J, Olsen N (2005) Phosphorous acid efficacy on storage disease control. Presentation at Idaho Potato Conference retrieved from http://www.kimberly.uidaho.edu/potatoes/phostrol05.pdf

Wright JC, Sugden D, Francis-McIntyre S, Riba-Garcia I, Gaskell S, Grigoriev I, Baker S, Beynon R, Hubbard S (2009) Exploiting proteomic data for genome annotation and gene model validation in *Aspergillus niger*. BMC Genomics 10: 61

Xie Z, Klionsky DJ (2007) Autophagosome formation: core machinery and adaptations. Nature Cell Biol. 9: 1102 – 1109

Xu Q, Zhang L (2009) Plant caspase-like proteases in plant programmed cell death. Plant Signal. Behav. 4: 920–904.

Yan Z, Reddy MS, Ryu C-M, McInroy JA, Wilson M, Kloepper JW (2002) Induced systemic protection against tomato late blight elicited by plant growth-promoting rhizobacteria. Phytopathol. 92: 1329 – 1333

Yang T, Poovaiah BW (2003) Calcium/calmodulin-mediated signal network in plants. Trends Plant Sci. 8: 505 – 512

Yoshioka H, Numata N, Nakajima K, Katou S, Kawakita K, Rowland O, Jones JDG, Doke N (2003) *Nicotiana benthamiana* gp91^{phox} homologs *NbrbohA* and *NbrbohB* participate in H_2O_2 accumulation and resistance to *Phytophthora infestans*. Plant Cell 15: 706 – 718

Zhu M, Dai S, McClung S, Yan X, Chen S (2009) Functional differentiation of *Brassica napus* guard cells and mesophyll cells revealed by comparative proteomics. Mol. Cell. Proteomics 8: 752 – 766

Zimmerli L, Metraux JP, Mauch-Mani B (2001) beta-Aminobutyric acid-induced protection of *Arabidopsis* against the necrotrophic fungus *Botrytis cinerea*. Plant Physiol. 126: 517 – 523

Zipfel C, Kunze G, Chinchilla D, Caniard A, Jones JDG, Boller T, Felix G (2006) Perception of the bacterial PAMP EF-Tu by the receptor EFR restricts *Agrobacterium*-mediated transformation. Cell 125: 749 – 760

Appendix A. The 364 Reproducible Proteins Identified in the Wall Fractions

TC number	UniRef100	Protein description	Mascot score	Protein mass	Protein coverage	pI	Peptide numbers	Secretory Signal peptide
TC178504	O04678	Subtilisin-like protease	732	53776	32.1	9.41	12	no
TC170624	O82777	Subtilisin-like protease	66	30604	3.7	8.92	1	yes
TC185687	O82777	Subtilisin-like protease	56	31917	4.1	9	1	yes
TC169727	Q0WVJ9	Subtilisin-like protease	96	44071	10.6	9.27	3	yes
TC165394	A7P6H1	Subtilisin-like serine proteinase	154	44103	7.4	6.84	2	yes
TC181547	O82777	Subtilisin-like protease	49	22924	10.4	8.69	3	no
TC176030	O04678	Subtilisin-like protease	119	38003	11.6	8.84	4	no
TC186795	Q9FK76	Subtilisin-like protease	134	27168	4.9	8.87	1	no
TC186268	Q0WWH7	Subtilisin-like serine proteinase	58	94545	3.1	8.85	4	no
TC179155	O82007	Serine protease	47	31953	6	5.64	1	no
TC165366	Q5NT86	Nucellin-like protein	263	58276	8.8		5	yes
TC175223	Q9C6Y5	Putative nucellin	66	44725	4.7	8.45	2	yes
CK262983	Q2VCI9	Aspartic protease	122	35849	10.5		3	no
CX161954	Q03197	Aspartic protease inhibitor 10	129	41065	14.4	8.74	5	yes
TC167837	Q6ST24	Cathepsin B-like cysteine proteinase	139	46852	6.7	8.24	7	yes
TC176976	Q1HER6	Cathepsin B	147	71563	6.6	8.53	8	yes
TC172593	Q40143	Cysteine proteinase 3	176	48950	9.6	8.76	3	yes
TC186926	Q9ST61	Cysteine protease	88	72408	2.5	8.49	2	yes
TC174835	Q93XC2	Papain-like cystein peptidase	61	31288	11.1	8.09	2	yes
TC164333	Q07491	Pre-pro-cysteine proteinase	52	45828	6.1	6.36	5	yes
TC186362	Q41489	Proteinase inhibitor type-2	60	24118	8.5	8.43	3	yes
TC166762	P20347	Cysteine protease inhibitor 1	64	32806	4	5.74	3	yes
TC183181	Q9SE08	Cystatin	62	35464	5.1	9.32	1	yes
TC189437	Q58I46	Kunitz-type proteinase inhibitor	56	24517	4.1	9.92	2	yes
TC176398	Q42890	Glucan endo-1,3-beta-D-glucosidase	322	45495	13.3	8.93	6	yes
TC163195	Q70C53	1,3-beta-D-glucan glucanohydrolase	192	46693	15.4	9	8	yes
TC190098	Q9M4A9	beta-1,3-glucanase	65	57086	1.8	9.01	4	yes
TC169673	Q8GUR3	Acidic class II 1,3-beta-glucanase	169	42767	10.3	7.82	4	yes
TC163179	P52401	Glucan endo-1,3-beta-glucosidase	216	48060	10	6.78	5	yes
TC176971	Q8H6W9	Leucine-rich repeat protein	52	31430	4.5	9.49	1	no
TC165481	Q2HTP6	Leucine-rich repeat protein	91	54994	9.3		6	yes
TC177341	Q9S8M0	Chitin-binding lectin 1	55	60523	3.4	9.57	2	yes
TC172275	P32045	Pathogenesis-related protein P2	109	25590	10.2	9.35	2	no
TC170396	Q8L688	Pathogenesis related protein isoform b1	459	28345	16.4	8.62	2	yes
TC169479	O65157	Basic PR-1 protein	137	28506	20.1	8.48	6	yes
TC176356	O65157	Basic PR-1 protein	291	28301	25.2	9.35	5	yes
TC180137	Q84N00	Putative class 5 chitinase	44	50900	2.2	9.06	2	yes
TC168318	Q43834	Class II chitinase	156	35852	9.9	6.05	4	yes
CV475452	P52404	Endochitinase 2	225	30440	19.7	9.12	3	yes
TC185914	Q05538	Basic 30 kDa endochitinase	198	44945	12.9	8.24	3	yes
TC163429	Q43184	Endochitinase	138	35589	8.3	8.98	3	yes
TC164936	P52404	Endochitinase 2	224	42653	9.5	5.88	5	yes
TC164671	P52406	Endochitinase 4	214	41179	13.3	8.74	5	yes
TC190989	Q5ND92	Thaumatin-like protein	134	28622	11.6	8.75	3	no
TC165908	O65358	Germin-like protein	96	32438	7	9.33	4	no
TC173874	Q0PWM4	Germin-like protein	267	27101	19	8.63	3	yes
TC164825	Q7XZV3	Germin-like protein	238	30391	5.7	8.53	2	yes
TC166752	Q0PWM4	Germin-like protein	56	29087	5.4	8.59	2	yes
TC166199	Q38JH9	Glycine rich protein	68	42613	3.5	10.09	1	yes

CX161931	Q9SVG4	Reticuline oxidase-like proteine	76	30491	4.3	8.23	1	yes
TC183764	Q9FR61	Phospholipase D	87	85775	2	8.99	3	no
TC166895	Q9LZB2	Lipase-like protein	217	50600	11.7	9.04	6	yes
TC172455	Q75LC6	GDSL-like lipase	66	35208	3.8	9.16	1	yes
TC190922	Q0R4F7	GDSL-like lipase	92	47636	2.6	8.95	2	no
TC173720	Q9FZ08	Patatin-like protein	95	29287	6.2	8.88	1	no
TC173018	Q5XUH0	Osmotin-like protein	496	32905	16.9	8.17	4	yes
TC171679	Q5XUH3	Osmotin-like protein	277	35244	6.5	9.17	3	yes
AM907859	Q9ARG0	Osmotin-like protein	78	8949	22.5	11.06	1	yes
TC165487	Q5XUH6	Osmotin-like protein	369	42130	10.3	8.99	4	yes
TC178677	Q9SDS4	Non-specific lipid-transfer protein	243	25672	15	9.79	3	yes
TC163642	Q94IQ1	Peroxidase	203	50424	7.6	8.54	7	no
TC167619	A0S5Z4	Peroxidase	94	48066	6.9	9.63	6	yes
TC173498	P11965	Lignin-forming anionic peroxidase	282	31892	11	9.12	4	no
BQ046158	Q4A3Y6	Peroxidase	96	22906	32.2	7.79	5	yes
TC167434	Q9XIV9	Peroxidase	171	46537	8.3	9.33	4	yes
TC187382	Q9THX6	Putative L-ascorbate peroxidase	59	28972	7.3	7.72	1	no
TC166840	A7LNX7	Thioredoxin	105	33882	6.7	8.93	3	yes
TC163544	Q8RVF8	Thioredoxin peroxidase	152	46528	3.9	7.28	1	no
TC170244	Q76KW1	Glutathione S-transferase	55	41993	2.9	8.45	2	no
TC181216	P80461	Glutathione reductase	105	23306	4.7	9.35	1	no
TC168896	P22302	Superoxide dismutase	93	30896	9.8	6.01	4	no
TC190224	A7PBM5	Superoxide dismutase	95	23299	10.2	5.3	2	no
TC178042	Q7YK44	Superoxide dismutase	114	33581	13.6	5.61	4	yes
TC174920	Q6BDJ3	Polygalacturonase inhibitor protein	59	38486	6.7	9.64	3	yes
TC183017	Q8S989	Polygalacturonase-inhibiting protein	168	42928	10.9	8.82	7	yes
TC165802	Q8LGC3	Putative disease resistance protein	88	54114	4.1		5	yes
BG597038	Q8LGC3	Putative disease resistance protein	107	24546	5.3	9.8	3	yes
TC170882	Q27JA2	Dirigent-like protein	41	25544	3.4	9	2	yes
DR037720	A7P031	Dirigent-like protein	42	35823	4.1	9.51	1	yes
TC175527	A3SC86	Xylogucan-specific fungal endoglucanase inhibitor protein	100	30775	4.4	9.59	2	yes
TC163900	Q6RHX9	Xyloglucan endotransglucosylase	73	50446	2.5	9.45	1	yes
TC169457	Q9FZ05	Xyloglucan endotransglucosylase	44	39141	3.5	8.84	2	yes
BQ047373	Q6RHY0	Xyloglucan endotransglucosylase	60	15512	10.1	4.62	1	yes
BG097865	Q6Z8I7	Putative bate-D-xyloxidase	98	20670	12.4	9.25	2	yes
TC187803	Q2MCJ4	Xylan 1,4-beta-xyloxidase	89	26718	10	9.19	2	yes
TC172381	Q2MCJ5	Xylan 1,4-beta-xyloxidase	81	44974	2.7	8.46	2	yes
CK275480	Q2MCJ4	Xylan 1,4-beta-xyloxidase	98	28184	10.8	9.3	2	yes
CK863115	A1X8W3	Expansin-like protein	57	19993	4.9	8.27	1	no
TC172539	O82625	Expansin	33	33583	3.9	8.61	1	yes
TC166088	Q153F8	Pectin acetylesterase	130	51771	7.3	8.33	3	no
TC164005	Q9SEE6	Pectin methyl esterase	161	74162	6.1	8.91	5	no
TC166701	A1IIA8	Pectate lyase	57	36366	3.1	5.88	1	yes
TC172945	Q9SEE7	Pectin methyl esterase	72	66844	4.3	8.71	5	yes
TC168435	Q43143	Pectinesterase	68	33957	8.4	9.94	3	yes
TC191540	O04870	Pectinesterase	63	69062	3.7	8.92	3	yes
TC168310	P85076	Pectinesterase	49	53941	2	9.83	1	yes
TC166362	A1KXE1	pectin acetylesterase	267	56301	16.7	9.17	12	yes
TC166103	Q41695	pectin acetylesterase	154	35197	18.5	8.97	6	yes
TC165690	P04045	alpha-glucan phosphorylase	56	187372	0.8	8.61	1	yes

TC163242	Q8RU27	Alpha-1,4-glucan-protein synthase	249	52011	15.7	6.78	7	no
TC176370	Q9LEC9	Alpha-glucosidase	65	115197	1.7	8.56	1	yes
TC171128	A8Y5V3	Alpha galactosidase	45	57797	2.3	9.54	1	yes
TC163932	Q2MK92	Alpha galactosidase	74	61775	2.8	8.46	2	no
TC168294	P48980	Beta-galactosidase	61	54700	2.5	9	1	no
TC176788	A2JGW9	Beta-galactosidase	66	26119	6.4	8.86	1	yes
TC173565	Q42875	Endo-1,4-beta-glucanase	55	33490	6.3	9.24	2	no
TC186617	Q9LYL2	Alpha galactosidase	51	36920	4.5	5.91	2	yes
TC183478	O82151	Beta-D-glucan exohydrolase	61	40910	2.9	9.31	3	yes
TC178060	O82151	Beta-D-glucan exohydrolase	62	32176	8.6	9.51	3	yes
TC181714	Q41441	Alpha-amylase	125	49422	7.3	8.46	3	no
TC163068	Q1KL65	Acid invertase	46	86836	1.3	6	2	yes
TC168055	Q8VWL8	Beta-mannosidase	97	68795	8.6	8.93	8	yes
TC172847	Q43171	Beta-fructofuranosidase	76	73694	3.4		5	yes
TC181581	A7WM73	Beta-N-acetylhexosaminidase	46	30302	4.5	5.75	1	yes
TC163554	Q08276	Heat shock 70 kDa protein	104	83189	5.4	8.78	6	
TC185190	Q0WM51	HSP like protein	43	34032	5.9	8.61	3	
TC164265	Q5QHT4	Heat shock 70 kDa protein	59	35861	3.4	4.84	2	
CN215855	Q45NN0	Heat shock 70 kDa protein	83	28875	8.7	9.96	2	
TC169185	Q9M4H8	Putative ripening-related protein	140	36294	9.5	9.7	2	
TC165450	Q308A7	Ripening regulated protein DDTFR10-like	47	34790	2.8	4.62	1	
TC166980	Q308A7	Ripening regulated protein DDTFR10-like	50	34817	2.8	4.5	1	
TC163680	Q41300	Abscisic stress ripening protein	55	40394	6.5	5.24	1	
TC169493	Q6H660	Putative stress-induced protein	95	33831	16.2	6.48	6	
TC164075	O04002	Drought stress-induced protein	47	47142	2.1	8.29	4	
TC163533	Q9FG81	Aluminum-induced protein	113	39969	8.1	6.4	2	
CX161485	Q7Y1A0	25 kDa protein dehydrin	148	35490	7.8	8.84	2	
TC165596	Q38JD8	Temperature-induced lipocalin	66	30693	5.5	8.77	1	
TC164981	P80471	Light-induced protein	51	45550	3.2	9.07	2	
TC163587	O82161	Phi-1 protein	87	45885	8.8	9.51	4	
TC164219	Q7Y0S8	Phi-1 protein	160	34933	11	9.14	4	
TC170121	Q6RYA0	Salicylic acid-binding protein	149	43181	9.4	6.84	6	
TC181052	Q6DN46	Rapid alkalinization factor 5	49	22734	6	8.49	2	
TC165523	A0FH76	EBP1	125	53826	11.1	7.63	6	
TC163991	Q2VCI6	Putative glycine-rich RNA binding protein	138	38726	10.5	5.71	4	
TC170792	Q9SMV2	Light inducible protein	80	31693	4.2	8.91	1	
TC166245	A9XTL7	Fasciclin-like arabinogalactan protein	80	39512	4.8	8.62	1	
TC191536	O04070	SGRP-1 protein	60	52589	10.8		6	
TC177800	Q947H4	Non-cell-autonomous protein	147	41800	14.1	9.5	6	
TC164705	Q9M4D6	Putative acid phosphatase	1054	31897	26.9	9.27	6	
TC168083	Q9M4D6	Putative acid phosphatase	913	34780	38.1	8.87	10	
TC173101	Q9M4D6	Putative acid phosphatase	976	26590	34.6	8.76	7	
TC190056	Q9M4D6	Putative acid phosphatase	283	35088	23.1		6	
TC163111	Q6J5M9	Purple acid phosphatase 2	48	60000	2.7	8.66	3	
TC172225	Q9SU83	Nucleotide pyrophosphatase	86	34358	5.4	9.46	1	
TC170962	Q008R7	Calcineurin B-like protein	251	49950	21.4	4.92	8	
TC179354	Q8LJ85	Putative calreticulin	263	58440	17	7.23	9	
TC168258	P27161	Calmodulin	112	33715	9.6	4.85	4	
TC165630	UPI00005DB	Ran GTPase binding	46	35833	2.7	8.16	1	
TC187760	A2Q5A3	H+-transporting two-sector ATPase	2081	72266	41.6	9.34	19	

TC192386	O04977	Ferredoxin--NADP reductase	2321	53829	46.2	8.86	16	
TC163337	P93566	Oxygen-evolving enhancer protein 2	1536	41414	27.4	8.84	8	
AM908651	Q41413	Epoxide hydrolase	49	23529	4.1	8.72	1	
TC178551	A8VYL5	Thioredoxin	62	27477	8.4		4	
TC189862	Q6QPJ6	Peroxiredoxin	777	33182	22		5	
TC177228	Q5JBR7	Peroxiredoxin	60	29408	4.1	9.21	2	
BM112490	P12372	Photosystem I reaction center subunit II	837	23156	26.7	9.49	8	
TC163226	O49954	Glycine dehydrogenase	729	133318	14.9	7.76	16	
TC166043	Q43797	Inorganic pyrophosphatase	136	89327	8	8.82	10	
TC167578	P26574	Ribulose bisphosphate carboxylase small chain 1	191	30049	31.8	8.82	8	
TC171271	Q2QU06	RuBisCO subunit binding-protein alpha subunit	55	61158	1.6	8.45	2	
TC163152	P25079	Ribulose bisphosphate carboxylase large chain	309	57421	9.7	6.76	10	
TC163877	Q9LRR9	Probable peroxisomal (S)-2-hydroxy-acid oxidase 2	205	53365	15.4	9.09	8	
TC163250	O78327	Transketolase 1	220	89235	7.4	5.98	9	
TC181436	A7UH66	Phosphoenolpyruvate carboxylase	470	92030	14.7		14	
TC163367	Q6V1W4	Aminotransferase 2	190	52624	16.1	8.84	11	
TC167569	Q93XV7	Hydroxypyruvate reductase	394	48020	24.5	5.98	11	
TC191209	Q645M9	Glyoxisomal malate dehydrogenase	241	46647	16.3	9.08	8	
TC165002	Q5F306	Copper-containing amine oxidase	174	43180	9.1	6.1	4	
TC166413	P26520	Glyceraldehyde-3-phosphate dehydrogenase	385	47357	18.4	8.91	8	
TC164316	P26300	Enolase	137	61546	4.2	7.05	8	
TC164121	Q9SXX5	Fructose-bisphosphate aldolase	981	57596	22.3	8.95	11	
TC163042	P29196	Phosphoenolpyruvate carboxylase	239	119447	7.6	5.35	10	
TC177431	Q6RUF6	Fructose-bisphosphate aldolase	276	47647	10.3	9.04	4	
TC163169	Q8L5C9	Malate dehydrogenase	235	50673	17.7	8.77	6	
TC179073	Q6Q8B8	ferredoxin I	92	22917	6.3	4.66	2	
TC169318	Q7M242	Glutamate synthase	134	100217	3.2	9.4	4	
TC165699	Q8GT30	Dihydrolipoyl dehydrogenase	154	67865	8.2	8.72	7	
TC163459	Q9LM03	Methionine synthase	146	97984	6.8	7.06	9	
TC163648	P50433	Serine hydroxymethyltransferase	119	67475	6.7	9.15	3	
TC171593	O82802	Sulfite reductase	93	90065	4.9		6	
TC163524	P54260	Aminomethyltransferase	95	53021	8.5	9.2	6	
TC168267	Q9SXX4	Fructose-bisphosphate aldolase	440	51663	23.4	8.69	8	
TC165914	Q9XF82	Fructose-bisphosphate aldolase	251	53245	15.9	7.05	7	
TC165512	P93541	Glutamate dehydrogenase	168	59464	13.4	6.78	8	
TC163604	Q2HUF7	Enoyl-CoA hydratase/isomerase	108	35114	10.2	8.9	3	
TC165660	Q672Q6	Photosystem II oxygen-evolving complex protein 3	177	33386	18.6	9.47	6	
TC167109	Q8L5C8	Malate dehydrogenase	167	45618	16.4	8.8	6	
TC165902	Q940A4	Putative lactoylglutathione lyase	77	42579	6.1	6.04	3	
TC170003	A7R1S3	Peptidyl-prolyl cis-trans isomerase	133	29021	9.1	8.6	3	
TC192060	P62090	Photosystem I iron-sulfur center	99	35516	6.9	9.38	4	
TC175869	P00061	Cytochrome c	82	25933	4.7	9.84	2	
DN906411	Q9XF82	Fructose-1,6-bisphosphatase	60	25034	5.4	10.26	1	
TC173338	Q6UJ35	Glycine decarboxylase complex H-protein	90	29508	5.8	6.32	1	
TC163512	Q2V9B3	Phosphoglycerate kinase	47	71212	1.7	9.49	3	
TC176495	P93338	NADP-dependent glyceraldehyde-3-phosphate dehydrogenase	43	32956	8.4	9.42	3	
CN215773	O04397	Ferredoxin--NADP reductase	49	15472	7.6	8.3	1	
TC164104	Q9SXX4	Fructose-bisphosphate aldolase	242	55193	24.1		10	
TC163439	Q6T379	Triosephosphate isomerase	66	39252	2.5	7.66	4	
TC180549	P23509	Glucose-1-phosphate adenylyltransferase	80	33416	4	6.35	2	

TC172223	Q8S915	Phosphoenolpyruvate carboxylase	72	64547	6.1	8.54	5	
TC174142	P29790	ATP synthase gamma chain	117	31051	9.7	7.85	3	
TC163473	A8DUA7	Sedoheptulose-1 7-bisphosphatase	87	52496	16.7	8.96	7	
TC163404	A5BVN4	Nucleoside diphosphate kinase	63	35606	2.7	8.7	2	
TC190060	P54928	Inositol monophosphatase	85	44816	5.5	6.1	1	
TC163860	Q43840	NADH dehydrogenase	47	65820	6.2	8.48	4	
TC190122	P23322	Oxygen-evolving enhancer protein	205	34684	18.3		7	
CK863886	P93566	Oxygen-evolving enhancer protein	290	34487	19.5		5	
TC163384	P26320	Oxygen-evolving enhancer protein	532	40745	28.4	8.03	10	
TC164001	P23322	Oxygen-evolving enhancer protein	501	40560	37.1	7.04	10	
TC166263	Q9XF12	Peptidyl-prolyl cis-trans isomerase	80	28466	4.4	9.02	2	
TC172190	Q2V9A5	Glutamine cyclotransferase	123	35907	14.1	8.78	3	
DN588905	Q84VQ6	Gamma-glutamyl transferase	120	29735	14.8	9.11	4	
TC170266	Q8H9C1	Citrate binding protein	55	32471	6.5	9.17	2	
TC164605	A5BE19	Phosphoribulokinase	84	44069	3.1	7.18	3	
TC171908	Q07346	Glutamate decarboxylase	238	69934	10	6.08	6	
TC169382	O04397	Ferredoxin--NADP reductase	67	57864	2.3	8.78	3	
TC176032	A7Q1K3	Photosystem II reaction center psb28 protein	53	29144	4.2	9.28	1	
TC163128	Q2PYW7	Succinyl CoA ligase	87	55394	2.5	6.01	1	
DR034357	Q93ZN9	LL-diaminopimelate aminotransferase	77	26394	8.5	8.75	2	
TC168993	O24258	Enoyl-ACP reductase	57	36816	3.6	9.15	2	
TC178085	Q8LK04	Glyceraldehyde 3-phosphate dehydrogenase	604	53152	23.9	7.96	9	
TC188355	Q41229	Photosystem I reaction center subunit IV	426	50985	16.3	9.92	6	
TC164307	Q9SXX4	Fructose-bisphosphate aldolase	954	52176	32.7	8.85	13	
TC165960	A7QZG8	Malate dehydrogenase	224	57157	11.5	9.18	3	
TC185934	Q2PYY8	Malate dehydrogenase	196	66873	9.4	8.78	4	
TC164340	P09043	Glyceraldehyde 3-phosphate dehydrogenase A	139	56514	12.5	9	6	
TC176570	Q9XG67	Glyceraldehyde 3-phosphate dehydrogenase	258	48718	19	8.42	7	
TC163804	P09044	Glyceraldehyde 3-phosphate dehydrogenase B	163	52568	13.6	7.92	6	
TC186718	Q9FJL3	Peptidylprolyl isomerase	70	73567	2.2	5.77	1	
TC172601	Q94IK1	Ferredoxin-thioredoxin-reductase	77	31694	14.2	9.82	3	
TC181183	P93338	NADP-dependent glyceraldehyde-3-phosphate dehydrogenase	63	50745	8.2		5	
TC173181	Q9XF14	Bundle sheath defective protein	74	40778	2.4	8.59	1	
TC164832	Q94B07	Gamma hydroxybutyrate dehydrogenase	62	41970	11.1	9.21	3	
TC163833	Q8L742	Copper amine oxidase	65	35815	3.2	8.78	1	
TC167892	Q84NI5	Aconitase	78	46421	8.3	9.01	3	
TC170307	Q852S5	Nucleoside diphosphate kinase	84	30459	9.9	9.58	3	
TC184705	Q8LFE2	Photosystem II	81	20902	6.2	9.47	1	
TC178467	Q69B32	Glutamine synthetase	49	59998	2.6	6.01	1	
TC166882	P17340	Plastocyanin	164	55371	8.1	8.64	2	
TC163835	Q3S832	Delta-1-pyrroline-5-carboxylate dehydrogenase	88	71967	4.6	9.38	3	
TC169017	Q940M2	Alanine--glyoxylate aminotransferase	46	44940	2.8	8.69	2	
TC164093	Q84NI5	Aconitase	114	84139	6.5	7.62	5	
TC189109	Q2HU25	Dihydrolipoyl dehydrogenase	73	30301	4.6	7.22	1	
TC164228	Q9FS87	Isovaleryl-CoA dehydrogenase	74	62145	4.5	9.12	1	
TC171302	Q2WGN6	Putative glycerophosphoryl diester phosphodiesterase	80	63781	3	5.17	2	
TC169267	Q7XBT1	NADH:ubiquinone oxidoreductase	99	29914	8.5	9.19	3	
TC163382	O22769	NADH:ubiquinone oxidoreductase	218	47881	9.4	8.93	3	
TC169365	Q9LLH9	Acyl-coenzyme A oxidase	38	55069	1.6	8.79	1	
TC175349	A8CWX0	Apyrase	50	50968	4.8	8.99	3	

TC173813	Q2LFC4	AGO1-1	49	118822	1.9	9.48	2	
TC169737	A0AQW5	T2-type Rnase	51	53847	2.3	8.36	2	
TC184248	Q5NE20	Carbonic anhydrase	111	40886	9.9	6.69	5	
TC166985	A2PYH3	nascent polypeptide associated complex	45	30535	4.6	4.7	2	
TC165993	Q8GZD8	Neutral leucine aminopeptidase preprotein	83	35071	4.5	9.06	2	
TC164848	Q8LEY7	Putative glyoxalase	85	60018	6	9.3	4	
TC169232	P83291	NADH-cytochrome b5 reductase-like protein	63	47579	5.3	8.86	4	
TC165996	Q9SXV0	Cytochrome c oxidase	90	34942	6.6	4.8	3	
BG887419	Q8LCP1	Cytochrome c oxidase	34	24343	4.5	4.27	1	
TC176693	Q9ZUC1	Quinone oxidoreductase	113	42853	10.6	8.62	4	
TC166057	Q5Z5A8	Photosystem II assembly factor	213	53685	12.8	6.79	8	
TC173809	P49107	Photosystem I reaction center	522	25072	10.2	9.06	3	
TC164369	Q9S7E9	Alanine aminotransferase	148	60331	18.3	8.8	9	
TC163136	P56757	ATP synthase CF0 subunit I	203	58636	12.4	5.72	10	
TC179723	O24136	CP12	53	24006	5	5.76	1	
TC182040	O24136	CP12	158	22095	23.2	8.46	5	
TC163961	A7PFP1	Translation initiation factor	150	37987	12.6	9.3	5	
TC177316	O22636	Poly(A) polymerase	74	24008	7	5.48	2	
TC163292	Q2V985	Elongation factor 1	49	61941	3.5	8.86	3	
TC186583	P82231	Ribosome recycling factor	245	41266	11.1	7.67	3	
TC183535	Q94KR9	Translation initiation factor IF-1	101	36632	10.1	10.16	2	
TC185814	Q6K853	40S ribosomal protein S30	71	18659	6.6	10.69	1	
TC163988	Q40450	Elongation factor TuA	184	63855	5.2		3	
TC171845	P42798	40S ribosomal protein S15a	46	26827	5.8	9.92	1	
TC163589	Q43364	Elongation factor TuB	95	63208	5.2	7.78	3	
TC167919	A5BH65	40S ribosomal protein S24	79	30543	4.6	10.17	1	
TC171540	Q3HRX4	40S ribosomal protein S17	116	27341	5	8.6	2	
TC181039	O23049	50S ribosomal protein L6	76	32333	7.2	9.88	2	
BG097709	Q6RJY9	Putative ribosomal protein	55	14734	6.3	9.64	1	
TC163269	Q3HVK4	Ribosomal protein S6	97	37163	9.5	10.55	3	
TC172172	P37218	Histone H1	88	39854	10.4	10.51	4	
TC191924	P80196	Intracellular ribonuclease	59	17772	7	6.39	1	
TC168123	Q8H7Y8	Probable histone H2A	158	26540	9.2	9.52	2	
TC164420	Q9FI15	Small nuclear ribonucleoprotein	66	34537	4.3	11.18	1	
TC178423	Q6YU78	Putative small nuclear ribonucleoprotein polypeptide D3	83	31403	3.6	10.49	2	
TC165716	Q9SHY8	Pre-mRNA-slicing factor	213	74727	7	9.15	4	
TC163314	P19682	28 kDa ribonucleoprotein	36	48870	7.5	5.21	3	
TC170822	O49948	High mobility group protein	111	30676	5.5	9.32	1	
TC170128	O04692	DNA-binding protein	61	30122	10.2	8.72	2	
TC168117	Q8H9F4	41 kD chloroplast nucleoid DNA binding protein	181	28733	20.4	8.73	5	
TC164698	Q40451	DNA-binding protein	58	70452	6.5	9.84	4	
TC165047	Q8W214	Single-stranded DNA binding protein	86	43518	6	5.21	4	
TC163566	Q8L934	Nucleoid DNA-binding-like protein	1168	62091	18.4	9.18	11	
TC164401	O23792	Chloroplast nucleoid DNA binding protein precursor	196	46482	13.5	9.51	4	
TC165454	Q3HVN0	Ubiquitin-conjugating enzyme family protein	46	32862	8.8	8.09	5	
TC175288	Q9XG77	Proteasome subunit alpha type-6	78	31277	8.9	9.51	3	
TC179524	P55852	Ubiquitin-like protein	81	24161	4.6	6.12	1	
TC166220	Q852T2	Vacuolar processing enzyme	57	40699	3.5	5.18	1	
TC188425	Q9SFB5	Serine carboxypeptidase	74	47954	7.2	9.23	3	
TC182746	Q9FEU4	Putative serine carboxypeptidase	191	66653	9		9	

TC166625	Q8S8L0	Putative prolylcarboxypeptidase	40	37811	3	9.14	3	
DN923050	Q67WZ5	Putative prolylcarboxypeptidase	73	30638	3.7	5.76	1	
TC168900	Q67X97	Putative prolylcarboxypeptidase	97	61658	5.8		5	
TC180911	Q8S3I6	D1 protease	54	29531	3.6	9.93	1	
TC173147	A7Y7E9	Dynein light chain	42	29292	4.5	8.95	1	
TC164361	P93570	Chaperonin-60 beta subunit	76	59193	2.2	7	1	
TC184361	P49118	Luminal-binding protein	47	45660	3.2	8.51	3	
TC164360	Q9M5A8	Chaperonin 21	107	36912	7.2	9.32	3	
TC167003	A7R3H4	Putative uncharacterized protein	179	32069	12.3	8.66	4	
TC194485	A4F354	Coat protein	126	45924	8.5	6.08	3	
TC170111	U02970	Putative uncharacterized protein	104	68159	3.4	8.37	2	
TC163703	Q4KR14	CT099	77	53606	6.6	8.76	3	
TC178181	A9P9T4	Putative uncharacterized protein	162	23733	16.9	7.05	4	
TC164815	A7R397	Putative uncharacterized protein	103	43050	12.3	7.16	6	
TC165572	A7Q9K7	Putative uncharacterized protein	71	31458	9.3	8.84	5	
TC175639	A7R8H8	Putative uncharacterized protein	89	29055	26.1	9.35	9	
TC176079	A7Q4T6	Putative uncharacterized protein	203	69035	7.1		6	
TC190640	A7QXG6	Putative uncharacterized protein	256	35551	17.5	9.36	8	
TC167164	A7Q2C0	Putative uncharacterized protein	61	33887	3.3	8.22	2	
TC184612	A7PU90	Putative uncharacterized protein	62	31228	9.6	8.62	3	
TC182237	A7QTL4	Putative uncharacterized protein	105	49539	5	6.88	2	
TC185943	A7PMB3	Putative uncharacterized protein	60	35839	4.2	8.73	1	
TC177199	A7PGY3	Putative uncharacterized protein	132	40869	7.4		2	
TC174493	A7PW57	Putative uncharacterized protein	120	23831	17	9.24	3	
TC169142	A7P8N6	Putative uncharacterized protein	44	34072	3.7	9.56	1	
TC184290	A7P0A9	Putative uncharacterized protein	113	44816	4.8	8.25	3	
TC166113	A7Q0B9	Putative uncharacterized protein	57	33245	6.7	10.44	4	
TC193683	A7QEV7	Putative uncharacterized protein	75	39335	4.6	6.71	2	
TC191321	A7NVH3	Putative uncharacterized protein	308	61681	17	8.95	7	
TC179738	A7P6C6	Putative uncharacterized protein	37	46261	1.9	9.28	2	
TC166760	A7PVI8	Putative uncharacterized protein	59	40470	6.3	8.73	3	
TC179248	A7R523	Putative uncharacterized protein	97	49204	6.3	8.98	6	
TC163569	A7P5N4	Putative uncharacterized protein	117	52856	4.9	7.05	5	
TC186660	A7PXD5	Putative uncharacterized protein	71	22245	5	9.72	2	
TC181663	A7QQE7	Putative uncharacterized protein	45	27921	3.3	9.77	1	
EG012248	A7QPP7	Putative uncharacterized protein	58	22637	8.5	9.37	2	
DR037760	A7Q1G5	Putative uncharacterized protein	139	33593	13.1	9.94	4	
TC164409	A7P597	Putative uncharacterized protein	236	45688	13.9	8.13	4	
CV430199	A7Q077	Putative uncharacterized protein	109	26153	11.2		4	
TC185331	A7PU90	Putative uncharacterized protein	74	27644	16.9	9.62	5	
TC172502	A7P9G6	Putative uncharacterized protein	140	40087	2.6	9.31	2	
TC165011	A7NYA2	Putative uncharacterized protein	53	55663	3.9	8.63	3	
TC164168	A7Q261	Putative uncharacterized protein	101	54130	7.8	9.22	4	
TC163885	A7R2Z4	Putative uncharacterized protein	51	45537	2.4	6.67	1	
CV504223	A7PY94	Putative uncharacterized protein	61	27127	3.6	10.12	1	
TC164491	A7P4I3	Putative uncharacterized protein	75	60655	5.1	5.86	2	
DR036301	A7PEC9	Putative uncharacterized protein	52	28161	3.9	6.48	1	
CN516805	A7P5N4	Putative uncharacterized protein	96	24780	9.6		2	
TC170328	A7QI69	Putative uncharacterized protein	55	28025	3.6	6.66	1	
TC170549	A7Q977	Putative uncharacterized protein	47	34211	9.1	8.77	2	

TC165869	A7QL60	Putative uncharacterized protein	75	50998	5.5	8.87	3	
TC172041	A7QY53	Putative uncharacterized protein	90	39368	4	9.13	1	
TC181676	A7QH87	Putative uncharacterized protein	103	83587	1.7	8.89	1	
TC183334	A7QIN6	Putative uncharacterized protein	51	55544	4.6	5.05	2	
TC164902	A7PLE6	Putative uncharacterized protein	68	35331	7.6		2	
TC188798	O80934	Putative uncharacterized protein	89	47676	7.4	8.55	2	
TC180396	A2X6K5	Putative uncharacterized protein	60	22064	10.8	10.44	1	
TC169704	A7Q8P6	Putative uncharacterized protein	60	31451	10.2	7.64	2	
CX162488	A7S2F0	Putative uncharacterized protein	62	12052	14.9	8.05	1	
TC180111	A7R3R4	Putative uncharacterized protein	61	34800	6.8	8.72	2	
TC173996	A7PMA7	Putative uncharacterized protein	64	30530	4.2	9.04	1	
TC167526	A7QDV5	Putative uncharacterized protein	57	30854	3.3	9.57	1	
AM906908	Q9LMQ6	Putative uncharacterized protein	52	19298	11.9	10.45	1	
TC168658	A7QF07	Putative uncharacterized protein	50	34053	3.5	8.48	2	
TC168643	Q3HRY8	Putative uncharacterized protein	63	27336	11.7	10.16	3	

Appendix B. The 447 Reproducible Proteins Identified in the Cytoplasmic Fractions

TC number	UniRef100	Protein description	Mascot score	Protein mass	Protein coverage	p/	Peptide numbers
TC178504	O04678	Subtilisin-like protease	732	53776	32.1	9.41	12
TC165394	A7P6H1	Subtilisin-like serine proteinase	154	44103	7.4	6.84	2
TC176030	O04678	Subtilisin-like protease	119	38003	11.6	8.84	4
TC169727	Q0WVJ9	Subtilisin-like protease	96	44071	10.6	9.27	3
TC176976	Q1HER6	Cathepsin B	147	71563	6.6	8.53	8
TC186926	Q9ST61	Cysteine protease	88	72408	2.5	8.49	2
TC172593	Q40143	Cysteine proteinase 3	176	48950	9.6	8.76	3
TC165366	Q5NT86	Nucellin-like protein	263	58276	8.8		5
CX161954	Q03197	Aspartic protease inhibitor 10	129	41065	14.4	8.74	5
TC163098	Q6B9W9	Aspartic protease	63	60927	2	5.51	2
TC174835	Q93XC2	Papain-like cystein peptidase	61	31288	11.1	8.09	2
TC166762	P20347	Cysteine protease inhibitor 1	64	32806	4	5.74	3
TC169550	P58602	Cysteine protease inhibitor 4	33	29003	6.6	5.72	3
TC164333	Q07491	Pre-pro-cysteine proteinase	52	45828	6.1	6.36	5
TC186362	Q41489	Proteinase inhibitor type-2	60	24118	8.5	8.43	3
TC180217	Q43710	Proteinase inhibitor type-2	49	28354	4.4	8.72	1
CN516536	Q43710	Proteinase inhibitor type-2	56	19842	5.7	10	1
TC172275	P32045	Pathogenesis-related protein P2	109	25590	10.2	9.35	2
TC170396	Q8L688	Pathogenesis related protein isoform b1	459	28345	16.4	8.62	2
TC166558	P16273	Pathogen-related protein	66	31849	7.5	7.72	3
TC169479	O65157	Basic PR-1 protein	137	28506	20.1	8.48	6
TC166761	Q4KYL1	Pathogenesis related protein 10	1151	30695	27.8	7.9	6
TC189821	P13046	Pathogenesis-related protein R major form	195	29798	18.9	8.09	3
TC163234	O81145	Class I chitinase	540	42200	11.6	6.43	4
TC168318	Q43834	Class II chitinase	156	35852	9.9	6.05	4
CV497183	P29060	Acidic endochitinase	145	28786	5	6.32	1
TC163209	P52403	Endochitinase 1	275	41093	11.9	8.03	2
TC164936	P52404	Endochitinase 2	224	42653	9.5	5.88	5
TC164671	P52406	Endochitinase 4	214	41179	13.3	8.74	5
TC185914	Q05538	Basic 30 kDa endochitinase	198	44945	12.9	8.24	3
TC165908	O65358	Germin-like protein	96	32438	7	9.33	4
TC173018	Q5XUH0	Osmotin-like protein	496	32905	16.9	8.17	4
TC163801	Q5XUH7	Osmotin-like protein	66	34125	3.2	8.53	2
TC169893	Q5XUH9	Osmotin-like protein	149	34510	10.5	8.73	4
TC163195	Q70C53	1,3-beta-D-glucan glucanohydrolase	192	46693	15.4	9	8
TC176398	Q42890	Glucan endo-1,3-beta-D-glucosidase	322	45495	13.3	8.93	6
TC169673	Q8GUR3	Acidic class II 1,3-beta-glucanase	169	42767	10.3	7.82	4
TC163179	P52401	Glucan endo-1,3-beta-glucosidase	216	48060	10	6.78	5
TC167839	Q5GMM5	Glutathione S-transferase/peroxidase	111	29648	11.7	8.71	4
TC170096	P32111	Probable glutathione S-transferase	179	29949	21	6.53	5
TC167597	Q2VT56	Probable glutathione S-transferase	107	33183	6.8	5.46	2
TC188176	Q8GVD1	Glutathione S-transferase	70	36725	6.2	8.95	2
TC174803	Q9M558	Glutathione S-transferase	41	37930	4.7	6.89	1
TC170244	Q76KW1	Glutathione S-transferase	55	41993	2.9	8.45	2
CV475703	Q8H8E0	Probable glutathione S-transferase	119	31906	13.7		4
TC181216	P80461	Glutathione reductase	105	23306	4.7	9.35	1
TC178648	Q9ZR41	Glutaredoxin	73	22225	7.4	9.49	2
TC165626	A7XTY1	Cytosolic glutathione reductase	76	61304	3.6	6.44	3
TC174916	A7LNX7	Thioredoxin	44	27144	6.5	9.14	3

TC168437	Q8RVF8	Thioredoxin peroxidase	129	45311	7.5	6.22	5
TC166840	A7LNX7	Thioredoxin	105	33882	6.7	8.93	3
TC176132	Q9SRD7	Thioredoxin	49	31308	4.7	9.03	1
TC178551	A8VYL5	Thioredoxin	62	27477	8.4		4
TC171996	Q95AH9	Thioredoxin	47	28435	6.2	9.49	2
TC172430	Q8LD49	Thioredoxin	60	26974	4.1	9.46	2
TC166527	A5BR41	Superoxide dismutase	154	34719	4.8	8.24	2
TC168896	P22302	Superoxide dismutase	93	30896	9.8	6.01	4
TC178042	Q7YK44	Superoxide dismutase	114	33581	13.6	5.61	4
TC190224	A7PBM5	Superoxide dismutase	95	23299	10.2	5.3	2
TC163092	Q2PYW5	Catalase	90	68512	12.1	6.91	13
CV431728	P30264	Catalase	71	40215	24.4	8.7	6
TC164094	Q9XHH3	Catalase	277	67852	20.1	6.11	15
TC172434	Q9LWA2	Peroxidase	41	32825	2.6	8.48	2
TC169870	Q43774	Peroxidase	116	31125	5.3	4.74	2
TC173498	Q42964	Peroxidase	282	31892	11	9.12	4
BQ046158	Q4A3Y6	Peroxidase	96	22906	32.2	7.79	5
TC177228	Q5JBR7	Peroxiredoxin	60	29408	4.1	9.21	2
TC172263	Q69TY4	Peroxiredoxin	126	28109	11.2	8.88	3
TC172024	Q69TY4	Peroxiredoxin	77	29867	4	8.76	2
TC163970	Q8H9F0	Ascorbate peroxidase	242	40061	18.3	6.2	10
TC163449	Q3I5C4	Ascorbate peroxidase	151	42856	13.9	6.33	11
TC183511	Q9THX6	Ascorbate peroxidase	96	22058	16.3	5.63	2
TC164467	Q3SC88	Thylakoid-bound ascorbate peroxidase	106	48710	6.9	8.44	4
TC174571	Q43497	Monodehydroascorbate reductase	179	25229	31.2		8
TC176436	Q43497	Monodehydroascorbate reductase	201	57558	14.5		8
TC167795	Q3HVN5	Dehydroascorbate reductase	79	37138	11.9		4
TC165600	A2ICR9	Dehydroascorbate reductase	56	37196	2.7	8.48	4
TC163554	Q08276	Heat shock 70 kDa protein	104	83189	5.4	8.78	6
TC164767	Q67BD0	Heat shock 70 kDa protein	399	82435	25.1	5.3	15
TC166185	P27322	Heat shock 70 kDa protein	396	81128	20.1	5.56	14
TC164532	P36181	Heat shock cognate protein 80	319	74774	8.5	5.11	12
TC167319	P27322	Heat shock 70 kDa protein	373	71734	24.5	5.44	15
TC164053	A2TJV6	Heat shock 70 kDa protein	52	34495	4.4	9.58	6
TC165994	Q4LDR0	Heat shock protein	57	65840	1.9	5.18	1
TC179551	Q96269	Heat shock protein	51	46253	6.8	5.62	1
TC163282	P36181	Heat shock cognate protein 80	364	48301	23	5.2	10
TC166332	A2TJV6	Heat shock 70 kDa protein	133	53876	13.7	5.67	10
TC165523	A0FH76	EBP1	125	53826	11.1	7.63	6
TC163533	Q9FG81	Aluminum-induced protein	113	39969	8.1	6.4	2
TC172032	P09762	Wound-induced protein WIN2	87	31364	4.6	8.84	1
TC165883	Q9XHD7	UVB-resistance protein UVR8	51	60491	3.5	7.09	3
CX161485	Q7Y1A0	25 kDa protein dehydrin	148	35490	7.8	8.84	2
TC164075	O04002	Drought stress-induced protein	47	47142	2.1	8.29	4
TC165450	Q308A7	Ripening regulated protein DDTFR10-like	47	34790	2.8	4.62	1
TC166980	Q308A7	Ripening regulated protein DDTFR10-like	50	34817	2.8	4.5	1
TC163668	Q38M75	Ripening regulated protein	45	46112	2.3	8.75	1
BG597038	Q8LGC3	Putative disease resistance protein	107	24546	5.3	9.8	3
TC186005	Q9SJI7	Putative lipase	101	30843	5.1	5.1	1
TC180261	Q9AWC0	Phospholipase	69	76629	3.9	5.21	2

TC164393	Q41453	Putative glycine rich RNA binding protein	278	39631	9.6	9.6	5
TC170121	Q6RYA0	Salicylic acid-binding protein	149	43181	9.4	6.84	6
TC164644	Q67RG9	Multidrug efflux protein	52	34562	3.1	9.77	1
TC165550	A9XTM4	Fasciclin-like arabinogalactan protein	74	58515	3	6.05	1
TC183017	Q8S989	Polygalacturonase-inhibiting protein	168	42928	10.9	8.82	7
TC163174	P12437	Suberization-associated anionic peroxidase	158	46619	5.6	5.02	4
TC163746	Q338B1	Auxin-induced protein	69	50495	13.3	6.46	5
TC184337	Q21IA8	Pectin/pectate lyase	42	29431	3.9	9.13	1
TC168435	Q43143	Pectinesterase	68	33957	8.4	9.94	3
TC169486	Q9SEE7	Pectin methyl esterase	348	26803	13.1	8.85	2
TC166122	P53535	Starch phosphorylase	125	119793	4.8	5.68	8
TC163054	Q84UC3	Sucrose synthase 2	96	103706	2.9	6.3	3
TC163255	A7LH87	Sucrose-phosphatase	70	60145	4.8	6.52	3
TC163052	Q9XGA6	Starch branching enzyme	151	114057	6.2	5.36	7
TC163166	Q43163	Chalcone synthase	60	51357	6.2	8.17	3
TC179676	Q43847	Granule-bound starch synthase 2	50	103125	0.8	9.57	1
TC163112	P19595	UTP--glucose-1-phosphate uridylyltransferase	250	64000	15	6.06	12
TC165690	P04045	Alpha-glucan phosphorylase	56	187372	0.8	8.61	1
TC165919	P32811	Alpha-glucan phosphorylase	124	106515	6.5	6.49	8
TC163028	Q9AWA5	Alpha-glucan water dikinase	119	181222	2.5	6.25	7
TC177982	Q06801	4-alpha-glucanotransferase	46	86856	1.2	8.63	4
TC179460	Q42678	Alpha amylase	153	53155	2.1	6.24	1
TC174114	Q5BLY3	Alpha amylase	46	34499	5.9	8.83	1
TC181618	Q5XTZ3	Glycosyl hydrolase family-like protein	61	29555	8.8	6.13	2
TC163051	P30924	1,4-alpha-glucan-branching enzyme	47	118291	0.9	5.38	1
TC163242	Q8RU27	Alpha-1,4-glucan-protein synthase	249	52011	15.7	6.78	7
TC163068	Q1KL65	Acid invertase	46	86836	1.3	6	2
TC165754	A5JPK5	GDP-mannose-3' 5'-epimerase	49	57946	5.7	8.36	6
TC168055	Q8VWL8	Beta-mannosidase	97	68795	8.6	8.93	8
TC176788	A2JGW9	Beta-galactosidase	66	26119	6.4	8.86	1
TC193512	Q6VAA5	UDP-glycosyltransferase	51	58032	2.1	6.6	1
TC167578	P26574	Ribulose bisphosphate carboxylase small chain 1	191	30049	31.8	8.82	8
TC163152	P25079	Ribulose bisphosphate carboxylase large chain	309	57421	9.7	6.76	10
TC167516	P26575	Ribulose bisphosphate carboxylase small chain 2A	2488	28811	40.3	8.73	11
TC168353	P26574	Ribulose bisphosphate carboxylase small chain 1	2141	31182	37	8.93	9
TC169850	O49074	Ribulose bisphosphate carboxylase/oxygenase activase	1650	65615	32.1	8.76	23
TC187943	Q40565	Ribulose bisphosphate carboxylase/oxygenase activase 2	1560	61521	27.3	8.71	14
BM111091	P26575	Ribulose bisphosphate carboxylase small chain 2A	2587	25991	45.1	8.38	10
TC169687	P10647	Ribulose bisphosphate carboxylase large chain C	2269	28110	42.4	8.46	8
TC190038	P08926	RuBisCO large subunit-binding protein	163	51419	20.3	5.43	5
TC171271	Q2QU06	RuBisCO subunit binding-protein alpha subunit	55	61158	1.6	8.45	2
TC163967	O81394	Phosphoglycerate kinase	566	67417	35.4	8.93	16
TC164589	Q8LK04	Glyceraldehyde 3-phosphate dehydrogenase	251	45054	12.8	6.23	4
TC164340	P09043	Glyceraldehyde 3-phosphate dehydrogenase A	139	56514	12.5	9	6
TC163804	P09044	Glyceraldehyde 3-phosphate dehydrogenase B	163	52568	13.6	7.92	6
TC166486	P09044	Glyceraldehyde 3-phosphate dehydrogenase B	784	57796	22.7	7.63	7
TC164986	P48496	Triosephosphate isomerase	212	46958	22	9.12	7
TC163439	Q6T379	Triosephosphate isomerase	66	39252	2.5	7.66	4
TC167721	P48496	Triosephosphate isomerase	88	40812	14.2	8.32	5
TC164104	Q9SXX4	Fructose-bisphosphate aldolase	242	55193	24.1		10

TC164121	Q9SXX5	Fructose-bisphosphate aldolase	981	57596	22.3	8.95	11
TC168267	Q9SXX4	Fructose-bisphosphate aldolase	440	51663	23.4	8.69	8
TC177431	Q6RUF6	Fructose-bisphosphate aldolase	276	47647	10.3	9.04	4
TC175736	Q9SXX4	Fructose-bisphosphate aldolase	174	29501	14.9	5.79	3
TC164309	Q38HV4	Fructose-bisphosphate aldolase	104	36048	7.8	8.67	4
TC165914	Q9XF82	Fructose-bisphosphate aldolase	251	53245	15.9	7.05	7
TC169768	O78327	Transketolase 1	673	89615	11.5	5.9	7
TC163250	O78327	Transketolase 1	220	89235	7.4	5.98	9
TC163473	A8DUA7	Sedoheptulose-1 7-bisphosphatase	87	52496	16.7	8.96	7
TC191617	A5BE19	Phosphoribulokinase	1606	56719	20.5	6.33	9
TC163395	P46276	Fructose-1,6-bisphosphatase	200	54837	5.4	6.29	4
TC166413	P26520	Glyceraldehyde-3-phosphate dehydrogenase	385	47357	18.4	8.91	8
TC181183	P93338	NADP-dependent glyceraldehyde-3-phosphate dehydrogenase	63	50745	8.2		5
TC164316	P26300	Enolase	137	61546	4.2	7.05	8
TC171649	Q1SN32	Pyruvate kinase	70	76230	2.7	8.5	3
TC192433	A7PPM9	Pyruvate kinase	156	47393	9.8		4
TC172223	Q8S915	Phosphoenolpyruvate carboxylase	72	64547	6.1	8.54	5
TC181436	A7UH66	Phosphoenolpyruvate carboxylase	470	92030	14.7		14
TC163042	P29196	Phosphoenolpyruvate carboxylase	239	119447	7.6	5.35	10
TC165805	Q2Z1Y6	Alcohol dehydrogenase	94	41375	7.1	8.89	5
TC168675	Q9SLN8	Alcohol dehydrogenase	138	41078	9	9.11	3
TC182591	P37830	Glucose-6-phosphate 1-dehydrogenase	49	74217	2.9	6.44	4
TC167284	Q8LG34	6-phosphogluconate dehydrogenase	104	59368	6.2	5.77	5
TC163260	P37225	NAD-dependent malic enzyme	104	82905	2.3	7.07	2
TC163763	O24135	Citrate synthase	197	70623	5.4		5
TC164093	Q84NI5	Aconitase	114	84139	6.5	7.62	5
TC167892	Q84NI5	Aconitase	78	46421	8.3	9.01	3
TC164754	Q9ZNX1	NAD-dependent isocitrate dehydrogenase	96	56763	5	8.56	4
TC165027	Q8GTQ9	Succinyl-CoA ligase	59	50552	3.4	8.96	3
TC163128	Q2PYW7	Succinyl CoA ligase	87	55394	2.5	6.01	1
TC192340	O82663	Succinate dehydrogenase	53	91925	1.2	6.42	2
TC187255	Q5NE17	Malate dehydrogenase	61	33147	4.8	8.9	1
TC185934	Q2PYY8	Malate dehydrogenase	196	66873	9.4	8.78	4
TC163169	Q8L5C9	Malate dehydrogenase	235	50673	17.7	8.77	6
TC165960	A7QZG8	Malate dehydrogenase	224	57157	11.5	9.18	3
TC167109	Q8L5C8	Malate dehydrogenase	167	45618	16.4	8.8	6
DN849126	Q3S2I1	Serine-glyoxylate aminotransferase	152	34567	11.7	9.6	5
EG010294	A9PL04	Serine hydroxymethyltransferase	64	21556	8.5	8.95	2
CV499691	A7P4I0	Serine hydroxymethyltransferase	37	23421	6.6	7.83	1
TC163648	P50433	Serine hydroxymethyltransferase	119	67475	6.7	9.15	3
TC167569	Q93XV7	Hydroxypyruvate reductase	394	48020	24.5	5.98	11
TC180484	P12424	Glutamine synthetase	124	31470	4.9	6.76	1
TC178467	Q69B32	Glutamine synthetase	49	59998	2.6	6.01	1
TC169318	Q7M242	Glutamate synthase	134	100217	3.2	9.4	4
TC164391	A7PEM9	Aspartate aminotransferase	53	52142	2.7	6.86	1
TC164402	Q2XTE6	Aspartate aminotransferase	95	37587	6.8	7.79	3
TC164443	Q39108	Geranylgeranyl pyrophosphate synthase	80	46804	3.2	10.03	1
TC163245	Q9XE59	Phosphoglycerate mutase	101	70303	5.6	5.99	4
TC170770	Q9M4G4	Phosphoglucomutase	118	74640	4.3	7.32	9
TC164886	Q9M4G5	Phosphoglucomutase	330	95347	7.6		10

TC184731	Q42910	Pyruvate phosphate dikinase	63	58203	2.8	8.37	4
CV503056	Q68HC8	Glucose-6-phosphate isomerase	62	22103	5	7.94	1
TC163877	Q9LRR9	Probable peroxisomal (S)-2-hydroxy-acid oxidase	205	53365	15.4	9.09	8
TC191209	Q645M9	Glyoxisomal malate dehydrogenase	241	46647	16.3	9.08	8
TC163226	O49954	Glycine dehydrogenase	729	133318	14.9	7.76	16
TC163337	P93566	Oxygen-evolving enhancer protein	1536	41414	27.4	8.84	8
TC190122	P23322	Oxygen-evolving enhancer protein	205	34684	18.3		7
TC163384	P26320	Oxygen-evolving enhancer protein	532	40745	28.4	8.03	10
TC164001	P23322	Oxygen-evolving enhancer protein	501	40560	37.1	7.04	10
TC192386	O04977	Ferredoxin--NADP reductase	2321	53829	46.2	8.86	16
TC176032	A7Q1K3	Photosystem II reaction center psb28 protein	53	29144	4.2	9.28	1
TC165660	Q672Q6	Photosystem II oxygen-evolving complex protein	177	33386	18.6	9.47	6
BM112490	P12372	Photosystem I reaction center subunit II	837	23156	26.7	9.49	8
TC165699	Q8GT30	Dihydrolipoyl dehydrogenase	154	67865	8.2	8.72	7
TC191208	Q1AFF6	Aldehyde dehydrogenase	144	72133	8	8.81	8
TC163615	Q5DKU8	Adenosine kinase	129	49625	6.2	5.72	2
TC165002	Q5F306	Copper-containing amine oxidase	174	43180	9.1	6.1	4
TC190060	P54928	Inositol monophosphatase	85	44816	5.5	6.1	1
DR034357	Q93ZN9	LL-diaminopimelate aminotransferase	77	26394	8.5	8.75	2
TC179073	Q6Q8B8	ferredoxin I	92	22917	6.3	4.66	2
TC175869	P00061	Cytochrome c	82	25933	4.7	9.84	2
TC163459	Q9LM03	Methionine synthase	146	97984	6.8	7.06	9
TC187308	P93230	Glucose-1-phosphate adenylyltransferase	78	62417	4.3	9.5	5
TC193346	P23509	Glucose-1-phosphate adenylyltransferase	82	68765	6.8	8.45	6
TC171908	Q07346	Glutamate decarboxylase	238	69934	10	6.08	6
TC179171	Q40147	Glutamate-1-semialdehyde 2,1-aminomutase	66	34976	5	6.09	3
TC165743	Q40147	Glutamate-1-semialdehyde 2,1-aminomutase	96	30886	4.6	8.39	1
TC164387	Q45FF1	Pyridoxine biosynthesis protein	65	46414	5.2	5.75	4
TC186491	Q04032	Ferredoxin--nitrite reductase	43	16731	7.9	5.52	1
TC194240	O04936	NADP-malic enzyme	164	99046	7.9	9.3	10
TC164410	P50217	Isocitrate dehydrogenase	300	59519	19.1	7.86	8
TC176696	Q09IV6	Solanesyl diphosphate synthase	62	32599	7.9	9.17	2
TC163586	Q9SEC2	Peptide methionine sulfoxide reductase	77	39308	4	8.53	1
TC164369	Q9S7E9	Alanine aminotransferase	148	60331	18.3	8.8	9
TC172926	Q3HVL5	NADPH quinone oxidoreductase	54	52879	3.5	8.76	1
TC167215	O04974	2-isopropylmalate synthase B	50	35467	2.6	8.97	2
TC181308	Q9AXR6	ATP:citrate lyase	49	89801	1.8	8.87	1
TC163367	Q6V1W4	Aminotransferase 2	190	52624	16.1	8.84	11
TC165895	Q9XG54	12-oxophytodienoate reductase	55	32200	3.5	4.93	1
TC166803	Q05758	Ketol-acid reductoisomerase	84	74982	1.9	6.79	3
TC170738	Q6Z6H0	S-adenosylmethionine:2-demethylmenaquinone methyltransferase	81	27884	3.6	7.7	4
TC182973	Q2XPW6	NAD-dependent epimerase/dehydratase family protein	77	44372	10.5	5.98	5
TC173103	Q8LBT0	Hydroxymethylbilane synthase	73	35710	6.7	7.05	3
TC167001	Q43170	Sulfate adenylyltransferase	64	60808	3.3	6.45	2
TC180488	O22493	Glutamate--cysteine ligase	80	60872	1.8	9.21	1
BM111283	A7P2K0	Peptidyl-prolyl cis-trans isomerase	54	27921	3.9	8.76	2
TC166263	Q9XF12	Peptidyl-prolyl cis-trans isomerase	80	28466	4.4	9.02	2
AM908242	A7QT90	Peptidyl-prolyl cis-trans isomerase	54	26954	5.4	9.63	3
TC186718	Q9FJL3	Peptidylprolyl isomerase	70	73567	2.2	5.77	1
TC184394	Q96556	Spermidine synthase	87	43072	3.6	5.62	2

TC189636	Q9FYW9	Adenylosuccinate synthetase	64	63462	2.6	8.73	2
TC176539	P54260	Aminomethyltransferase	310	52851	22.6	8.39	12
TC163835	Q3S832	Delta-1-pyrroline-5-carboxylate dehydrogenase	88	71967	4.6	9.38	3
TC163500	Q94A94	Diaminopimelate decarboxylase	82	60907	5.6	7.08	3
TC169096	A7U629	Methionine sulfoxide reductase B2	82	29415	7.4	8.37	1
TC183342	Q6W6X6	Acetoacetyl CoA thiolase	59	61922	1.9	8.96	2
TC169365	Q9LLH9	Acyl-coenzyme A oxidase	38	55069	1.6	8.79	1
TC163431	P28643	3-oxoacyl-[acyl-carrier-protein] reductase	74	53696	2.6	9.35	1
TC173556	Q9S7E9	Putative alanine aminotransferase	130	36593	9.7	9.18	4
TC168961	O48917	UDP-sulfoquinovose synthase	65	64382	3.5	8.05	1
TC169267	Q7XBT1	NADH:ubiquinone oxidoreductase	99	29914	8.5	9.19	3
TC168854	Q6Z702	Putative 3-isopropylmalate dehydratase large subunit	108	66578	5.8	9.29	3
TC179276	Q68HC8	Glucose-6-phosphate isomerase	36	36859	3.3	6.08	4
TC183574	Q8LDM4	Putative acetylornithine transaminase	216	38435	4.6	9.67	2
TC169619	A7PYV3	3-isopropylmalate dehydrogenase	48	50457	2.3	5.66	2
TC163136	P56757	ATP synthase CF0 subunit I	203	58636	12.4	5.72	10
TC163344	O82722	ATP synthase subunit beta	112	78853	3.3	7.27	3
TC187760	A2Q5A3	H+-transporting two-sector ATPase	2081	72266	41.6	9.34	19
TC167521	Q84UZ8	Vacuolar H(+)-ATPase subunit B	87	40197	4	7.75	1
TC189862	Q6QPJ6	Peroxiredoxin	777	33182	22		5
TC166882	P17340	Plastocyanin	164	55371	8.1	8.64	2
TC163076	P31427	Leucine aminopeptidase	103	67911	3.7	6.81	6
TC186793	Q5NE20	Carbonic anhydrase	691	49990	21.7	8.66	8
TC183389	Q0WM29	Methylmalonate-semialdehyde dehydrogenase	155	61859	3	9.38	2
TC163383	Q2XTD0	Adenosylhomocysteinase	90	54507	2.6	6.11	2
TC178939	P31212	Threonine dehydratase	56	47407	4.6	5.56	3
TC165870	P29696	3-isopropylmalate dehydrogenase	48	56278	2.8	8.53	1
TC164905	Q8RU74	Dehydroquinate synthase	164	67997	5.1	8.89	2
TC164764	Q5NE21	Carbonic anhydrase	143	39731	7.6	6.07	2
TC171415	P28723	Formate--tetrahydrofolate ligase	55	59832	2.4	8.67	2
TC173489	Q3Y5A4	Cytosolic nucleoside diphosphate kinase	52	38491	5.1	9.53	2
TC166813	Q9M1R2	Multifunctional aminoacyl-tRNA ligase	95	57905	4.9	8.75	2
TC184476	Q93WX6	Cysteine desulfurase	45	59812	3.3	6.64	1
TC178094	Q6ZEZ1	Putative ribose-5-phosphate isomerase	109	45484	10.5	7.82	3
TC167156	A3F7Q3	Benzoquinone reductase	56	37296	3.3	7.89	1
TC163172	Q9FS26	Cysteine synthase	86	51100	9.2		5
TC163239	Q9FS27	Cysteine synthase	133	46478	7.1	8	4
TC188237	Q10GW4	Oxidoreductase aldo/keto reductase	51	34081	4.1	8.26	2
TC173616	Q8H6B5	Putative dehydrogenase	53	31425	3.9	7.67	1
TC164848	Q8LEY7	Putative glyoxalase	85	60018	6	9.3	4
TC178938	Q45RS3	AlaT1	141	37502	16.7	n/a	6
TC173181	Q9XF14	Bundle sheath defective protein 2	74	40778	2.4	8.59	1
TC170266	Q8H9C1	Citrate binding protein	55	32471	6.5	9.17	2
BG594905	Q0W626	Anthranilate synthase	71	24691	7.5	4.16	1
TC163215	Q3LHL1	Short chain dehydrogenase	54	40877	3.1	9.08	1
TC163237	Q6IVI7	Protein disulfide isomerase	54	64737	2.7	4.89	4
TC172552	P31542	ATP-dependent Clp protease ATP-binding subunit	209	71945	13.5	5.6	7
TC182603	A7PJQ1	ATP-dependent Clp protease ATP-binding subunit	87	42445	8	5.59	2
TC177357	P31542	ATP-dependent Clp protease ATP-binding subunit	164	67649	9.4	8.96	4
TC172917	Q8S9M1	Probable plastid-lipid-associated protein	53	28244	6.7	9.51	3

TC165274	Q7XAB8	Protein THYLAKOID FORMATION1	166	47645	12	9.12	4
BM405677	Q43082	Porphobilinogen deaminase	70	23055	9.3	5.8	2
TC172901	Q94FW7	Heme oxygenase	100	45851	3.2	8.33	2
TC174912	Q07511	Formate dehydrogenase	59	51087	11.2	8.42	4
TC173383	Q42891	Lactoylglutathione lyase	57	37724	2.9	8.43	3
TC178822	A9YWR9	Oligopeptidase A	41	51901	2.6	9.25	3
TC188161	Q39751	H-Protein	145	21912	22.2		3
TC177289	Q8GZD8	Leucine aminopeptidase preprotein	141	47085	7.8	8.92	4
TC165258	Q8GZD8	Leucine aminopeptidase preprotein	140	38014	10.6	7.07	3
TC165323	Q9LM08	Esterase	42	46795	3.2	7.94	3
TC167446	A5ADV7	ATP-dependent Clp protease proteolytic subunit	80	34766	3.1	9.44	1
TC165200	Q94IK0	Ferredoxin-thioredoxin-reductase catalytic subunit B	48	33295	3.8	7.07	2
TC164828	Q9T0K7	3-hydroxyisobutyryl-coenzyme A hydrolase	54	53483	3.5	8.48	3
TC163550	Q84YG5	Isoamylase	49	95664	1.4	6.32	2
TC182040	O24136	CP12	158	22095	23.2	8.46	5
TC179723	O24136	CP12	53	24006	5	5.76	1
TC168543	Q8GZR6	GcpE	143	50247	7.4	5.58	3
TC173418	Q8GZR6	GcpE	55	38301	3.1	5.29	1
TC166407	P33191	Induced stolen tip protein	48	29933	3.4	4.05	1
EG014373	Q944I4	Glycerate 3-kinase	48	22768	5.5	8.08	3
TC163526	Q308A0	P40-like protein	181	37001	8.5	4.96	2
TC163372	P41379	Eukaryotic initiation factor 4A	109	61746	5.3	6.31	5
BG098152	P56336	Eukaryotic translation initiation factor 5A	79	20742	9.6	8.77	2
TC163988	Q40450	Elongation factor TuA	184	63855	5.2		3
TC163589	Q43364	Elongation factor TuB	95	63208	5.2	7.78	3
TC163292	Q2V985	Elongation factor 1	49	61941	3.5	8.86	3
TC164183	Q3HVL1	Elongation factor	158	36886	5.7	5.1	3
TC181534	Q9SGT4	Elongation factor EF-2	242	77568	13	8.59	7
TC165559	Q2VCK4	Putative elongation factor 1	131	62132	8.8	6.48	7
TC164666	Q9SGT4	Elongation factor EF-2	117	75116	8.7	7.81	5
TC163961	A7PFP1	Translation initiation factor	150	37987	12.6	9.3	5
TC186583	P82231	Ribosome recycling factor	245	41266	11.1	7.67	3
TC176792	P42732	30S ribosomal protein S13	67	26797	5.5	10.19	2
TC168866	Q9FVT2	Probable elongation factor 1	55	34755	9.4	5.39	5
TC173813	Q2LFC4	AGO1	98	118822	2.2	9.48	3
TC164360	Q9M5A8	Chaperonin 21	107	36912	7.2	9.32	3
TC165880	Q9M5A8	Chaperonin 21	119	38721	9.3	8.53	5
TC164361	P93570	Chaperonin-60	76	59193	2.2	7	1
TC183174	P33570	Chaperonin-60	342	80784	16.9	6.11	9
TC165209	Q1SKX2	Chaperone DnaK	268	33976	13.6	5.2	5
TC180568	P34893	10 kDa chaperonin	99	20078	14.4	8.46	2
TC163968	Q5K4L4	Villin 2	48	43499	8	7.77	2
TC165273	Q7XZJ2	Actin	78	58816	6.9		4
TC165526	Q9XQC7	GrpE protein	113	52708	4.4	4.73	2
TC166795	Q3HVK2	P23-like protein	101	33415	7.9	5.08	3
TC165047	Q8W214	Single-stranded DNA binding protein	86	43518	6	5.21	4
TC163566	Q8L934	Nucleoid DNA-binding-like protein	1168	62091	18.4	9.18	11
TC168117	Q8H9F4	41 kD chloroplast nucleoid DNA binding protein	181	28733	20.4	8.73	5
TC163314	P19682	28 kDa ribonucleoprotein	36	48870	7.5	5.21	3
TC191924	P80196	Intracellular ribonuclease	59	17772	7	6.39	1

TC164185	O65820	Histone H1	65	37284	3.7	10.49	2
TC165716	Q9SHY8	Pre-mRNA-slicing factor	213	74727	7	9.15	4
TC178423	Q6YU78	Putative small nuclear ribonucleoprotein polypeptide D3	83	31403	3.6	10.49	2
TC163647	Q9LEB4	RNA Binding Protein	49	63556	1.9	6.12	1
TC165127	Q2QKB0	Alternative splicing regulator	88	33324	6	11.26	2
BF053387	Q1MSH0	ALY protein	156	19888	12.6	5.86	2
TC176180	Q9XEJ6	MRNA binding protein	164	46185	11.6	9.15	6
TC174511	Q96372	Cell division cycle protein	67	30659	5.2	9.28	2
TC166963	Q2Q0V7	Patellin 1	48	35712	8.7	8.49	3
TC164625	Q2Q0V7	Patellin 1	106	32827	5.5	4.38	2
TC178515	Q9SCN8	Cell division control protein	112	24721	20.7	8.82	3
TC171983	A7P6B1	Proteasome subunit alpha type	147	40136	5.2	7.78	3
TC170699	Q9LFN6	DEAD-box ATP-dependent RNA helicase	57	59872	1.7	6.5	4
TC166636	Q45W77	Ubiquitin carrier protein	45	32809	6.5	7.16	1
TC184097	A6XIA1	Ubiquitin	444	47596	3.8	10.63	2
TC164171	Q93YH0	Clp protease 2 proteolytic subunit	73	48151	2.8	9.23	1
TC166117	Q40475	Biotin carboxylase	56	41806	4	5.28	2
TC171049	Q9CAE1	Aminopeptidase	100	65589	5.5	8.87	7
TC174407	Q6ZBX8	Putative aminopeptidase	65	69789	3.1	9.41	8
TC179682	Q9LJL3	Presequence protease	161	44186	11.6	4.94	4
TC182746	Q9FEU4	Putative serine carboxypeptidase	191	66653	9		9
TC166220	Q852T2	Vacuolar processing enzyme	57	40699	3.5	5.18	1
TC166307	Q7DMN9	Calmodulin-5/6/7/8	98	31833	10.2	4.67	3
TC173655	Q9CB00	Ara4-interacting protein	61	31695	7	4.88	1
TC167392	Q67YE7	Protein-tyrosine-phosphatase	64	34647	6.5	9.02	3
TC168202	A7Q204	WD-40 repeat family protein	50	62120	2	9.9	1
TC172225	Q9SU83	Nucleotide pyrophosphatase	86	34358	5.4	9.46	1
TC165352	Q8LJ85	Putative calreticulin	99	64530	5.9	7.7	3
TC179354	Q8LJ85	Putative calreticulin	263	58440	17	7.23	9
TC166013	P38547	GTP-binding nuclear protein Ran2	87	37039	10.3	8.05	4
TC170307	Q852S5	Nucleoside diphosphate kinase	84	30459	9.9	9.58	3
TC165578	P42652	14-3-3 protein	103	39858	8.1	5.18	3
TC173570	Q948K3	14-3-3 protein	158	26803	12.6	5.42	2
TC163416	P93212	14-3-3 protein	130	40003	8.6	6.16	2
TC163381	P93786	14-3-3 protein	235	48713	11.4	8.29	4
TC164695	P93785	14-3-3 protein	162	41710	9.6	4.95	4
TC163212	Q6PWL7	14-3-3 protein	131	39410	9.9	4.78	4
TC163559	P93207	14-3-3 protein	103	40776	9.5	5.17	3
TC171013	P93784	14-3-3 protein	180	43513	13	5.13	4
TC176693	Q9ZUC1	Quinone oxidoreductase	113	42853	10.6	8.62	4
TC194329	Q945M8	UPF0497 membrane protein	54	32397	2.7	9.55	1
TC171797	Q9AR56	Putative membrane protein	47	60139	1.3	9.82	1
BQ046932	Q4KR14	CT099	131	23570	9.5	6.4	2
TC175211	Q0JR13	TUDOR protein with multiple SNc domains	75	28581	4.6	8.84	2
TC178181	A9P9T4	Putative uncharacterized protein	162	23733	16.9	7.05	4
TC179955	A9P8J5	Putative uncharacterized protein	584	23162	40.6	4.62	7
TC192329	A5BA15	Putative uncharacterized protein	137	21005	16.1	n/a	2
TC164815	A7R397	Putative uncharacterized protein	103	43050	12.3	7.16	6
TC190640	A7QXG6	Putative uncharacterized protein	256	35551	17.5	9.36	8
TC175639	A7R8H8	Putative uncharacterized protein	89	29055	26.1	9.35	9

TC188798	O80934	Putative uncharacterized protein	89	47676	7.4	8.55	2
TC166760	A7PVI8	Putative uncharacterized protein	59	40470	6.3	8.73	3
TC191321	A7NVH3	Putative uncharacterized protein	308	61681	17	8.95	7
TC177199	A7PGY3	Putative uncharacterized protein	132	40869	7.4		2
TC179248	A7R523	Putative uncharacterized protein	97	49204	6.3	8.98	6
TC167164	A7Q2C0	Putative uncharacterized protein	61	33887	3.3	8.22	2
TC172502	A7P9G6	Putative uncharacterized protein	140	40087	2.6	9.31	2
TC164409	A7P597	Putative uncharacterized protein	236	45688	13.9	8.13	4
TC165011	A7NYA2	Putative uncharacterized protein	53	55663	3.9	8.63	3
TC163569	A7P5N4	Putative uncharacterized protein	117	52856	4.9	7.05	5
TC174493	A7PW57	Putative uncharacterized protein	120	23831	17	9.24	3
TC184290	A7P0A9	Putative uncharacterized protein	113	44816	4.8	8.25	3
TC168658	A7QF07	Putative uncharacterized protein	50	34053	3.5	8.48	2
TC164491	A7P4I3	Putative uncharacterized protein	75	60655	5.1	5.86	2
TC167003	A7R3H4	Putative uncharacterized protein	179	32069	12.3	8.66	4
TC178532	Q84VZ7	Putative uncharacterized protein	438	24692	22.7	6.96	8
TC179961	A7QVC7	Putative uncharacterized protein	201	67850	10.9		8
TC191129	A7P9H4	Putative uncharacterized protein	329	63279	9.6	8.87	10
TC179884	Q9SA52	Putative uncharacterized protein	285	50485	18.6	8.59	10
TC176045	A7PVK1	Putative uncharacterized protein	180	46167	15.2	6.08	7
TC180524	A7P4R6	Putative uncharacterized protein	120	62814	3.5	8	3
TC170604	A7PCK8	Putative uncharacterized protein	104	42103	8.3	6.29	6
TC173471	A7P8S3	Putative uncharacterized protein	80	47827	3.3	4.98	2
TC163499	A7P3H1	Putative uncharacterized protein	76	35889	4.8	7.85	4
BG095905	A7P713	Putative uncharacterized protein	555	15329	22.1		3
TC165383	A7PHS0	Putative uncharacterized protein	61	40891	2.2	6.06	1
TC173095	A7NVM4	Putative uncharacterized protein	67	31672	3.9	9.53	1
TC184297	A7NU08	Putative uncharacterized protein	91	41372	3.4	9.12	1
TC181617	A7P9H4	Putative uncharacterized protein	166	57347	7.1		9
TC163956	A7PTT3	Putative uncharacterized protein	47	48989	2.2	5.53	2
TC177711	A7NZZ2	Putative uncharacterized protein	49	41442	2.2	9.21	1
TC174843	A7P043	Putative uncharacterized protein	56	29569	5.8	9.33	1
BQ113165	A7PS00	Putative uncharacterized protein	55	21441	5.3	7.52	1
TC185171	Q9LK42	Putative uncharacterized protein	52	30152	4.2	5.31	1
TC171061	A7PNA3	Putative uncharacterized protein	53	61233	6.6	4.99	3
TC163488	A7Q9L0	Putative uncharacterized protein	79	57406	3	8.74	2
TC189081	A7NWU2	Putative uncharacterized protein	84	30079	16.1	6.1	4
TC163316	A7PQF2	Putative uncharacterized protein	42	52820	2.4	9.33	2
TC163536	A7QSN3	Putative uncharacterized protein	54	48491	3.9	8.99	2
CK860657	A7PNA3	Putative uncharacterized protein	54	24853	11.9	5.46	2
TC184906	A7QLW5	Putative uncharacterized protein	56	30786	4	5.02	1
TC167723	A7R2Z4	Putative uncharacterized protein	46	31985	2.8	9.46	1
BG889721	A7PIX9	Putative uncharacterized protein	43	28076	9.6	8.75	2
TC181920	A7QCI7	Putative uncharacterized protein	58	39864	3.5	8.16	1
TC166314	A7QMS5	Putative uncharacterized protein	50	40710	4.4	5.39	1
CV498800	Q8L7U1	Putative uncharacterized protein	88	29648	14.6	7.46	4
TC174158	A7NVB7	Putative uncharacterized protein	42	45182	2.9	9.03	2
CN463732	O04428	Putative uncharacterized protein	44	31229	2.9	10.63	1

Appendix C. The 577 iTRAQ-Labeled Reproducible Proteins Identified in the Wall Fractions

TC number	115/114	117/115	116/114	117/116	Annotation
TC194485	1.19	0.96	0.25	4.80	Coat protein - Potato virus S
TC194216	1.40	0.73	0.59	1.33	Glyceraldehyde-3-phosphate dehydrogenase
TC194204	1.14	0.63	0.37	1.91	Aspartic protease inhibitor 1 precursor
TC193683	1.12	1.10	1.55	0.83	Cucumisin
TC193350	1.21	0.69	0.95	0.89	Histone H1
TC193019	1.25	0.67	0.97	0.90	SGRP-1 protein
TC192743	0.95	0.99	0.89	1.68	Leucine-rich repeat protein
TC192606	1.39	0.49	0.57	1.17	Heparanase-like protein 1
TC192386	1.02	0.43	0.32	1.38	Ferredoxin--NADP reductase
TC191924	1.15	1.65	2.53	0.75	Intracellular ribonuclease LX
TC191654	1.05	0.94	1.14	0.89	2-hydroxyphytanoyl-CoA lyase-like protein
TC191617	0.71	1.22	0.86	1.16	Phosphoribulokinase
TC191540	0.96	1.01	1.08	0.92	Pectinesterase
TC191536	0.87	0.67	0.50	1.17	SGRP-1 protein
TC191529	0.88	1.08	0.73	1.31	Peptidyl-prolyl cis-trans isomerase
TC191443	1.02	3.10	6.05	0.54	Aspartate aminotransferase
TC191403	0.95	0.93	0.78	1.12	Thylakoid lumenal 16.5 kDa protein
TC191321	0.92	0.71	0.77	0.87	undetermined protein
TC191284	0.89	0.70	0.25	2.59	Transcription factor BTF3
TC191209	0.98	0.38	0.51	0.72	Glyoxisomal malate dehydrogenase
TC191142	1.21	2.66	5.21	0.65	Class I chitinase
TC191103	0.97	0.50	0.43	1.14	Apyrase GS50
TC191045	1.16	0.63	0.96	0.78	Peptidyl-prolyl cis-trans isomerase
TC190989	1.33	2.12	1.89	1.18	Thaumatin-like protein
TC190922	1.16	0.96	1.26	0.87	GDSL-lipase 1
TC190887	0.97	0.52	0.54	0.95	Ribulose bisphosphate carboxylase
TC190827	1.17	1.30	0.74	2.02	Wound-induced proteinase inhibitor 1
TC190640	0.98	0.73	0.92	0.79	Ubiquitin-specific protease 15
TC190622	1.22	1.56	1.92	1.01	Cyanate lyase
TC190413	0.79	0.89	0.48	1.45	dehydrogenase E1 component subunit
TC190122	0.91	0.42	0.57	0.70	Oxygen-evolving enhancer protein 1
TC190098	0.96	0.76	0.69	1.06	Beta-1 3 glucanase precursor
TC190056	1.16	0.54	0.46	1.39	Putative acid phosphatase
TC189862	0.89	1.49	1.10	1.20	Peroxiredoxin Q, chloroplast precursor
TC189821	1.82	1.00	2.12	0.83	Thaumatin-like protein
TC189750	1.49	9.21	13.17	1.14	Wound-induced protein WIN1
TC189109	1.00	0.46	0.46	0.98	Dihydrolipoyl dehydrogenase
TC188866	0.76	0.98	0.41	2.03	Xylem serine proteinase 1
TC188798	1.08	0.57	0.83	0.75	NAD-dependent epimerase/dehydratase
TC188524	0.98	0.94	0.59	1.62	Aldehyde dehydrogenase
TC188516	1.16	0.48	0.43	1.29	Kunitz-type protease inhibitor
TC188425	0.97	0.81	0.77	1.08	Serine carboxypeptidase-like 27
TC188237	1.20	0.62	0.87	0.86	Oxidoreductase aldo/keto reductase
TC188229	0.94	0.86	0.68	1.18	thylakoid lumenal 29.8 kDa protein
TC188161	1.19	0.80	1.55	0.65	H-Protein
TC188093	1.14	9.35	9.70	1.09	Ethylene-responsive proteinase inhibitor 1
TC188087	0.95	0.86	0.51	1.61	U2 small nuclear ribonucleoprotein A
TC187937	1.16	0.41	0.36	1.41	undetermined protein
TC187803	0.97	0.83	0.82	0.97	Xylan 1 4-beta-xylosidase

TC187803	0.83	0.99	0.58	1.41	Periplasmic beta-glucosidase
TC187760	1.13	0.67	0.59	1.23	H+-transporting two-sector ATPase
TC187647	0.99	13.04	10.00	1.40	purple acid phosphatase
TC187570	0.98	0.88	0.56	1.58	EBP1
TC187440	0.94	0.93	0.72	1.48	Aminotransferase
TC187382	0.93	1.07	1.05	0.94	Putative L-ascorbate peroxidase
TC187295	1.04	1.00	0.76	1.35	Luminal-binding protein 5
TC187074	1.29	3.86	3.85	1.32	Aspartyl-tRNA synthetase
TC186926	1.02	1.18	1.02	1.18	Cysteine protease
TC186921	1.46	0.92	2.02	0.63	Glutathione S-transferase
TC186921	0.94	0.83	1.32	0.65	Glutathione S-transferase
TC186830	1.17	0.32	0.30	1.21	50S ribosomal protein L31
TC186795	0.99	0.85	0.63	1.33	Subtilisin-like protease
TC186793	0.83	0.45	n/a	n/a	Carbonic anhydrase
TC186718	0.84	0.82	0.28	2.45	Peptidylprolyl isomerase
TC186668	1.15	0.90	0.78	1.33	Leucine-rich repeat/extensin
TC186660	1.08	3.14	1.15	2.72	Photosystem II 11 kDa protein
TC186617	1.00	0.90	1.30	0.70	Glycosyl hydrolase family-like protein
TC186583	0.99	0.65	0.57	1.22	Ribosome recycling factor
TC186567	1.30	5.03	5.96	1.59	Hydrolase
TC186294	0.97	0.62	0.47	1.28	Methionine synthase
TC186221	1.63	1.47	1.02	2.35	Putative heat shock protein
TC186177	0.92	1.48	1.71	0.90	Papain-like cysteine peptidase
TC186148	0.99	0.40	0.31	1.21	50S ribosomal protein L11
TC185943	0.95	0.84	0.91	0.91	Peptidyl-prolyl cis-trans isomerase
TC185934	1.03	0.78	1.01	0.80	Malate dehydrogenase
TC185914	1.06	0.97	1.38	0.74	endochitinase precursor
TC185687	0.97	0.88	1.24	0.69	Subtilase
TC185610	1.24	0.78	1.10	0.84	1,3-beta-glucan glucanohydrolase
TC185332	1.02	0.73	0.56	1.34	Dihydrolipoamide dehydrogenase
TC185331	0.97	0.92	0.86	1.04	Basic 7S globulin 2 small subunit
TC185280	0.91	0.82	0.56	1.33	Glycylpeptide N-tetradecanoyltransferase
TC185196	1.08	1.00	0.75	1.42	Luminal-binding protein precursor
TC185177	0.89	1.22	0.75	1.68	Glycylpeptide N-tetradecanoyltransferase
TC185153	1.11	2.54	1.51	2.29	60S acidic ribosomal protein P0
TC185027	1.00	0.40	0.51	0.84	Thylakoid soluble phosphoprotein
TC184745	1.03	1.00	0.82	1.29	Hydroxyproline-rich glycoprotein-like
TC184705	1.20	0.64	0.66	1.14	Photosystem II
TC184612	0.99	0.82	0.78	1.07	Basic 7S globulin 2 small subunit
TC184486	0.93	0.78	0.31	2.32	50S ribosomal protein L12
TC184466	0.98	0.58	0.15	4.82	polypeptide associated complex alpha
TC184361	1.00	0.97	0.79	1.23	Luminal-binding protein precursor
TC184290	0.95	0.65	0.46	1.39	Binding protein
TC184173	1.00	0.82	0.74	1.13	Histone H1
TC183932	1.09	0.95	0.62	1.66	Patellin 1
TC183705	0.79	0.47	0.28	1.17	Osmotin-like protein
TC183564	1.03	1.21	1.31	0.96	Subtilisin-like protease
TC183535	0.96	0.49	0.29	1.63	Translation initiation factor IF-1
TC183511	0.86	0.94	0.90	0.91	Putative L-ascorbate peroxidase
TC183478	1.09	1.22	0.96	1.35	Beta-D-glucan exohydrolase
TC183342	1.07	2.28	3.38	0.85	3-ketoacyl-CoA thiolase 2
TC183334	1.05	0.67	0.55	1.28	Nucleosome-binding protein

TC183181	1.03	n/a	0.69	n/a	Cystatin
TC183147	0.87	0.73	0.62	1.09	Epoxide hydrolase
TC183017	1.05	0.83	0.86	1.02	Polygalacturonase-inhibiting protein
TC182944	0.79	0.94	0.70	1.06	Basic blue copper protein
TC182930	0.92	1.48	2.31	0.58	Aspartate aminotransferase
TC182850	0.99	16.73	22.17	0.80	Citrate binding protein
TC182746	1.10	0.97	0.99	1.09	Putative serine carboxypeptidase
TC182555	0.82	0.82	0.37	2.13	50S ribosomal protein L12
TC182443	1.14	0.54	0.83	0.74	Lactoylglutathione lyase
TC182291	1.72	6.77	15.27	0.75	Osmotin-like protein
TC182140	1.20	0.56	0.70	0.93	MRNA binding protein precursor
TC182040	1.08	0.74	0.84	0.97	CP12 precursor
TC182026	1.07	1.30	0.83	1.72	Proteasome subunit beta type
TC181714	1.09	0.70	0.66	1.13	Alpha amylase
TC181645	1.79	0.38	0.55	1.16	Cysteine protease inhibitor 1
TC181547	0.99	0.84	1.20	0.69	Subtilase
TC181436	1.07	0.75	0.66	1.25	Phosphoenolpyruvate carboxylase
TC181410	1.11	0.65	0.87	0.81	Putative glutathione S-transferase
TC181286	0.96	1.23	1.03	1.15	Peptidyl-prolyl cis-trans isomerase
TC181183	1.47	0.86	1.36	0.93	glyceraldehyde-3-phosphate dehydrogenase
TC181167	0.96	0.81	0.39	2.43	Multicopper oxidase
TC180977	0.91	0.81	0.93	0.79	Heme-binding protein
TC180805	2.20	0.44	1.68	0.41	Threonine endopeptidase
TC180730	0.98	1.11	0.87	1.24	60s acidic ribosomal protein-like protein
TC180616	1.17	1.00	0.96	1.22	Leucine aminopeptidase 2
TC180320	1.23	0.77	0.79	1.26	Xylan 1 4-beta-xylosidase
TC180258	0.82	1.26	0.71	1.44	Peptidyl-prolyl cis-trans isomerase
TC180217	0.87	0.54	0.56	0.84	Proteinase inhibitor type-2 TR8 precursor
TC180137	1.01	1.07	1.25	0.86	Putative class 5 chitinase
TC179956	1.28	0.34	0.52	0.85	Enzyme of the cupin superfamily
TC179884	1.00	0.75	0.83	0.82	RNA binding protein putative
TC179738	1.40	0.78	0.42	2.41	GDSL-motif lipase
TC179723	1.04	0.53	0.56	0.97	CP12 precursor
TC179561	1.18	1.49	1.55	1.12	Subtilisin-like protease
TC179525	1.21	1.44	1.29	1.35	Lignin-forming anionic peroxidase precursor
TC179354	0.92	0.42	0.29	1.38	Putative calreticulin
TC179323	0.98	0.86	0.96	0.89	Beta-hexosaminidase 1
TC179248	1.25	0.34	0.52	0.76	4-nitrophenylphosphatase
TC179073	0.63	0.67	0.64	0.61	ferredoxin I
TC179026	0.97	0.69	n/a	n/a	4-methyl-5-thiazole monophosphate
TC178903	0.78	2.50	2.22	0.91	Gulonolactone oxidase
TC178861	1.04	0.53	0.73	0.81	Fasciclin-like arabinogalactan protein 14
TC178648	1.13	0.74	0.88	0.94	Glutaredoxin
TC178639	1.23	0.74	0.92	1.00	Thioredoxin H-type 2
TC178551	1.09	0.29	0.41	0.85	Chloroplast thioredoxin f
TC178532	0.96	0.58	0.86	0.67	undetermined protein
TC178504	1.10	1.56	1.68	1.00	Subtilisin-like protease
TC178423	0.95	0.81	0.32	2.54	Small nuclear ribonucleoprotein
TC178318	1.22	0.67	0.38	2.16	26S proteasome subunit RPN2a
TC178181	1.03	0.50	0.48	1.13	Globulin
TC178094	1.15	0.55	0.88	0.73	Ribose-5-phosphate isomerase
TC178060	1.08	1.14	1.00	1.21	Beta-D-glucan exohydrolase

TC178042	1.06	0.80	1.28	0.67	Superoxide dismutase
TC177843	1.17	0.56	0.69	1.61	Pectin methylesterase inhibitor isoform
TC177800	1.01	1.04	0.75	1.41	Non-cell-autonomous protein pathway2
TC177643	0.87	0.58	0.58	0.85	Enoyl-ACP reductase precursor
TC177500	0.93	0.86	0.87	0.93	Histone H1
TC177499	0.98	0.61	0.64	0.96	Glutathione S-transferase
TC177431	0.92	0.71	0.55	1.14	Fructose-bisphosphate aldolase
TC177389	1.22	0.70	1.36	0.62	undetermined protein
TC177316	1.01	0.77	0.88	0.89	Poly(A) polymerase
TC177289	1.00	1.02	0.95	1.07	Neutral leucine aminopeptidase
TC177270	1.08	1.90	2.33	0.89	Subtilisin-like protease
TC177202	1.13	0.98	1.53	0.73	Protein CREG1
TC177199	1.12	0.90	1.24	0.80	Inducer of CBF expression 2 protein
TC176976	1.11	1.21	1.27	1.06	Cathepsin B
TC176971	0.99	0.89	0.98	0.87	Leucine-rich repeat protein
TC176693	1.12	0.46	0.63	0.81	Quinone oxidoreductase-like protein
TC176583	0.94	0.91	0.71	1.21	Putative serine carboxypeptidase
TC176570	0.97	0.74	0.65	1.11	Glyceraldehyde-3-phosphate dehydrogenase
TC176539	1.02	0.54	0.73	0.71	Aminomethyltransferase
TC176507	1.15	1.35	2.08	0.79	Plastid enolase
TC176501	1.07	1.16	1.38	0.92	Coatomer subunit delta-2
TC176436	1.41	0.87	1.45	0.87	Monodehydroascorbate reductase
TC176431	0.93	0.98	1.16	0.79	Cytosolic aconitase
TC176419	1.11	0.75	0.83	1.00	LEXYL2 protein
TC176398	1.32	2.67	4.50	0.76	Glucan endo-1,3-beta-D-glucosidase
TC176397	1.07	0.69	0.94	0.79	Alpha-N-acetylglucosaminidase
TC176376	1.03	0.41	0.42	1.02	Catalytic/coenzyme binding protein
TC176365	1.06	0.45	0.61	0.78	Putative oxidoreductase zinc-binding
TC176356	2.84	4.05	11.88	0.93	Basic PR-1 protein
TC176260	0.83	0.97	0.54	1.50	Glycerophosphoryl diester phosphodiesterase
TC176125	1.16	0.37	0.32	1.38	Globulin
TC176079	1.01	0.89	1.19	0.77	undetermined protein
TC176032	0.97	0.43	0.45	0.92	Photosystem II reaction center psb28 protein
TC176030	1.04	1.78	1.53	1.27	Subtilisin-like protease
TC176016	0.97	0.89	0.72	1.21	leucine-rich repeat disease resistance protein
TC175869	1.09	1.09	1.73	0.69	Cytochrome c
TC175639	1.00	0.47	0.51	0.93	sedoheptulose-1,7-bisphosphatase
TC175460	0.82	0.91	0.67	1.19	Thioredoxin H
TC175349	1.04	0.58	0.54	1.09	Apyrase 3
TC175288	0.72	1.07	0.53	1.42	Proteasome subunit alpha type-6
TC175234	1.20	0.90	1.12	1.00	Cytochrome c1-1, heme protein
TC175223	0.97	1.00	0.54	1.71	Nucellin
TC175191	1.19	0.45	0.56	0.95	Peroxisomal (S)-2-hydroxy-acid oxidase
TC175100	0.95	0.89	0.32	2.98	40S ribosomal protein S23
TC175030	1.43	0.55	0.83	0.88	Beta-1,3-1,4-glucanase
TC174920	1.01	1.13	0.93	1.29	Polygalacturonase inhibitor protein
TC174916	1.19	0.60	0.92	0.78	Thioredoxin
TC174843	0.87	0.94	0.83	0.98	undetermined protein
TC174793	0.98	1.16	0.82	1.38	Beta-D-glucan exohydrolase
TC174783	1.08	0.85	0.98	0.91	Putative disease resistance protein
TC174571	1.17	1.04	1.46	0.87	Monodehydroascorbate reductase
TC174335	1.15	0.52	0.64	0.93	Plastid Tic40

TC174300	0.84	0.35	0.33	0.91	Chaperonin-60 beta subunit precursor
TC174073	0.91	0.62	0.52	1.08	High mobility group protein
TC173874	1.19	0.75	0.81	1.12	Germin-like protein
TC173865	1.29	1.27	1.54	0.93	Glucan endo-1,3-beta-D-glucosidase
TC173836	1.25	1.36	n/a	n/a	Protein disulfide isomerase
TC173813	1.36	0.54	0.53	2.18	AGO1-1
TC173809	0.97	0.89	0.61	1.43	Photosystem I reaction center subunit
TC173769	1.38	0.61	1.18	0.73	Peptidyl-prolyl cis-trans isomerase
TC173720	1.07	1.71	2.06	0.90	Patatin-like protein 3
TC173665	0.91	0.92	0.85	0.98	Ubiquitin extension protein
TC173498	1.24	1.56	1.39	1.37	Peroxidase
TC173489	1.07	0.89	0.98	0.89	Cytosolic nucleoside diphosphate kinase
TC173455	1.14	0.55	0.76	0.81	Glutathione reductase
TC173338	1.30	0.58	1.26	0.54	glycine decarboxylase complex H-protein
TC173101	1.02	0.57	0.49	1.34	Putative acid phosphatase
TC173095	1.31	1.15	0.95	1.52	undetermined protein
TC173018	1.21	1.06	1.65	0.72	Osmotin-like protein
TC172995	1.06	0.99	0.94	1.16	Beta-D-glucosidase
TC172970	0.85	0.76	0.80	0.78	UDP-sulfoquinovose synthase chloroplast
TC172945	0.92	0.52	0.35	1.49	Pectin methyl esterase
TC172855	1.28	0.45	0.64	1.04	undetermined protein
TC172847	1.04	1.15	1.07	1.08	Beta-fructofuranosidase
TC172601	1.00	0.63	0.69	0.94	ferredoxin-thioredoxin-reductase
TC172593	1.16	0.79	0.97	0.97	Cysteine proteinase 3 precursor
TC172573	0.99	1.29	1.14	1.22	Polygalacturonase inhibitor protein
TC172573	0.65	1.41	0.50	2.02	Polygalacturonase inhibitor protein
TC172517	0.93	0.97	0.96	0.95	Translationally-controlled tumor protein
TC172502	1.03	0.70	0.50	1.46	CXE carboxylesterase
TC172434	1.43	1.10	1.71	1.00	Peroxidase
TC172430	1.15	0.34	0.49	0.77	Thioredoxin-X chloroplast precursor
TC172275	1.63	1.65	2.44	1.14	PR protein P2
TC172223	1.05	1.07	0.96	1.20	Phosphoenolpyruvate carboxylase
TC172201	1.04	0.66	0.93	0.78	Glutathione peroxidase
TC172190	1.09	0.66	0.53	1.33	Glutamine cyclotransferase-like
TC172172	0.85	0.83	0.64	1.10	Histone H1
TC171996	1.09	0.59	0.78	0.82	Thioredoxin
TC171930	1.02	0.69	0.66	1.08	Heparanase-like protein 2 precursor
TC171908	1.02	1.36	0.61	2.30	Glutamate decarboxylase
TC171722	1.36	1.79	1.46	1.76	undetermined protein
TC171721	1.01	1.10	0.93	1.20	HAD-superfamily hydrolase, subfamily IA
TC171679	1.56	6.61	13.62	0.75	Osmotin-like protein
TC171593	1.18	0.90	0.88	1.38	Sulfite reductase
TC171540	0.91	1.13	0.34	2.96	40S ribosomal protein S17-like protein
TC171499	1.24	1.76	3.80	0.52	Aspartate aminotransferase
TC171497	1.20	2.28	2.12	1.29	Inactive purple acid phosphatase 28
TC171399	0.90	1.27	0.75	1.46	undetermined protein
TC171351	0.96	0.67	0.70	0.93	Thylakoid lumenal 15 kDa protein 1
TC171341	1.06	0.76	0.87	0.94	PsbP family protein
TC171302	1.08	0.54	0.80	0.75	Glycerophosphodiesterase
TC171171	1.00	1.10	0.68	1.70	translation initiation factor 5A
TC171094	1.21	0.69	1.01	0.85	Monodehydroascorbate reductase
TC170985	1.06	0.88	0.76	1.22	undetermined protein

TC170945	1.38	0.61	0.65	1.31	Glycine rich protein-like
TC170792	1.02	0.81	1.65	0.60	AT-LS1 product
TC170624	1.17	1.50	1.87	0.92	Subtilisin-like protease
TC170554	1.02	0.82	1.02	0.84	Monodehydroascorbate reductase
TC170396	1.83	3.34	6.31	0.86	Pathogenesis related protein 1
TC170288	1.02	0.39	n/a	n/a	polypeptide-associated complex subunit
TC170266	1.24	18.71	25.16	0.91	Citrate binding protein
TC170244	1.26	0.69	0.99	0.90	Glutathione S-transferase
TC170121	1.09	1.01	0.97	1.13	Salicylic acid-binding protein 2
TC170111	1.07	1.79	1.67	1.19	ATP synthase subunit alpha
TC169998	1.00	0.63	0.74	0.85	Thioredoxin-like protein
TC169973	0.74	0.95	0.39	1.81	40S ribosomal protein S12
TC169893	1.63	1.11	1.98	0.86	Thaumatin-like protein
TC169870	1.27	1.04	1.41	0.98	Peroxidase
TC169869	1.24	2.00	1.46	1.71	L-lactate dehydrogenase
TC169850	0.97	0.33	0.26	0.96	Rubisco activase
TC169822	0.89	1.27	1.24	1.02	Putative beta-N-acetylhexosaminidase
TC169793	1.15	0.82	0.72	1.29	translation initiation factor 3 subunit
TC169727	0.93	0.78	0.74	1.01	Subtilisin-like protease-like protein
TC169550	1.28	0.55	0.65	1.13	Cysteine protease inhibitor 4
TC169531	0.96	3.32	13.74	0.26	Carbohydrate oxidase
TC169486	0.94	0.55	0.40	1.35	Pectin methyl esterase
TC169479	3.32	3.31	14.55	0.74	Basic PR-1 protein
TC169457	1.03	0.76	0.91	0.89	Xyloglucan endotransglycosylase LeXET2
TC169394	1.13	13.24	34.17	0.45	Kunitz-type protease inhibitor
TC169382	1.00	1.23	1.30	0.98	Ferredoxin--NADP reductase
TC169318	0.96	0.50	0.49	0.95	Glutamate synthase (Ferredoxin)
TC169293	0.78	1.15	0.61	1.50	Proteasome subunit alpha type
TC169284	1.08	1.10	0.82	1.46	Serine carboxypeptidase
TC169280	1.22	0.78	1.26	0.78	Superoxide dismutase [Fe] chloroplast
TC169082	0.95	0.15	0.17	0.86	Putative elongation factor P
TC169017	0.96	0.80	0.59	1.28	Alanine--glyoxylate aminotransferase 2
TC168961	0.94	0.68	0.81	0.73	UDP-sulfoquinovose synthase
TC168900	0.93	0.91	1.06	0.80	Prolyl carboxypeptidase like protein
TC168899	1.23	6.33	11.65	0.69	Beta-galactosidase precursor
TC168896	1.07	0.85	1.30	0.71	Superoxide dismutase
TC168794	0.96	2.52	4.31	0.57	Chitinase, class V
TC168736	1.05	0.74	0.76	1.01	Fructose-1,6-bisphosphatase
TC168700	1.20	2.36	5.14	0.72	NtPRp27-like protein
TC168675	0.99	0.72	0.82	0.88	Allyl alcohol dehydrogenase
TC168658	1.06	0.80	0.90	0.90	Thylakoid lumenal 17.4 kDa protein
TC168614	1.07	0.70	0.83	0.93	Thylakoid-bound ascorbate peroxidase 6
TC168590	0.78	0.90	n/a	n/a	mannose 6-phosphate reductase
TC168485	0.98	0.47	0.32	1.53	undetermined protein
TC168445	0.89	0.50	0.44	1.03	Photosystem I reaction center subunit IV B
TC168443	0.91	6.64	2.87	3.91	Pectin methlyesterase inhibitor protein 1
TC168437	1.01	0.95	1.49	0.64	Thioredoxin peroxidase
TC168435	1.18	1.84	5.87	0.36	Pectinesterase U1 precursor
TC168375	1.55	3.30	4.98	0.88	PR-1 protein
TC168321	1.10	1.54	1.80	0.96	Benzoquinone reductase
TC168318	1.41	0.98	2.56	0.68	Class II chitinase
TC168274	0.84	1.02	1.07	0.83	Late embryogenesis (Lea)-like protein

TC168267	0.61	0.83	0.47	0.97	Fructose-bisphosphate aldolase
TC168199	1.02	0.64	0.45	1.44	Polygalacturonase
TC168117	1.11	0.99	0.79	1.32	chloroplast nucleoid DNA binding protein
TC168098	0.84	0.70	0.60	0.98	Hydrolase
TC168083	1.08	0.50	0.44	1.29	Putative acid phosphatase
TC168055	0.95	0.75	0.69	1.07	Beta-mannosidase
TC167954	1.90	0.44	0.86	1.01	Aminopeptidase
TC167949	1.00	0.87	0.97	0.89	Beta-fructofuranosidase
TC167934	1.02	0.73	0.77	0.96	3-hydroxyisobutyryl-coenzyme A hydrolase
TC167892	1.19	1.18	1.57	0.90	Aconitase
TC167837	1.02	1.00	0.93	1.08	Cathepsin B-like cysteine proteinase
TC167735	1.22	1.45	2.17	0.83	Bacterial-induced peroxidase precursor
TC167718	1.03	1.20	1.14	1.08	Glutamine cyclotransferase-like
TC167648	1.03	1.06	1.67	0.66	Thioredoxin peroxidase
TC167619	1.32	4.12	3.35	1.67	Peroxidase
TC167578	1.06	0.46	0.48	1.01	Ribulose bisphosphate carboxylase
TC167569	1.01	0.40	0.55	0.72	Hydroxypyruvate reductase
TC167493	1.01	0.68	0.66	1.05	Methionine synthase
TC167456	1.39	1.02	0.98	1.34	purple acid phosphatase
TC167434	1.22	2.23	2.91	0.93	Peroxidase
TC167339	1.04	0.96	1.39	0.72	5'-nucleotidase surE
TC167231	1.08	0.66	0.77	0.95	Fasciclin-like arabinogalactan protein 9
TC167207	1.09	0.86	1.02	0.92	Polygalacturonase-inhibiting protein
TC167164	1.09	0.56	0.51	1.19	Thylakoid lumenal 19 kDa protein
TC167156	1.15	4.29	6.14	0.91	Benzoquinone reductase
TC167109	1.00	0.72	0.89	0.83	Malate dehydrogenase
TC167021	1.15	0.68	1.14	0.73	undetermined protein
TC167007	1.06	0.40	0.55	0.76	Hydroxypyruvate reductase
TC167003	1.09	2.46	2.26	1.21	Aspartyl-tRNA synthetase
TC166985	1.08	0.73	0.56	1.69	nascent polypeptide associated complex
TC166980	1.13	0.99	0.97	1.25	Ripening regulated protein DDTFR10-like
TC166903	1.29	0.73	0.79	1.28	Putative expansin
TC166895	1.13	0.83	0.91	1.00	BYJ15
TC166886	2.04	0.34	0.51	1.44	Cysteine protease inhibitor 7
TC166882	1.11	0.33	0.56	0.58	Plastocyanin
TC166879	1.04	0.85	0.98	0.90	Allyl alcohol dehydrogenase
TC166875	0.80	0.64	0.33	1.57	Ribosomal protein L1
TC166840	1.09	0.60	0.74	0.88	Thioredoxin
TC166795	1.37	0.82	1.13	0.98	Translationally-controlled tumor protein
TC166782	0.99	9.25	10.43	0.89	Peroxidase 1
TC166779	1.03	1.29	1.44	0.92	Secreted glycoprotein
TC166762	1.55	0.36	0.64	0.87	Cysteine protease inhibitor 1
TC166761	1.38	0.73	1.31	0.85	pathogenesis related protein 10
TC166752	1.02	0.70	0.79	0.92	Germin-like protein
TC166752	1.01	0.71	0.77	0.95	Germin-like protein
TC166643	0.88	0.88	0.58	1.32	undetermined protein
TC166625	0.93	0.80	0.48	1.59	carboxypeptidase
TC166486	1.72	0.54	0.75	1.17	Glyceraldehyde-3-phosphate dehydrogenase
TC166447	0.93	2.08	1.72	1.11	Subtilisin-like serine protease
TC166413	0.97	0.70	0.61	1.12	Glyceraldehyde-3-phosphate dehydrogenase
TC166407	0.98	1.26	1.75	0.80	Induced stolen tip protein TUB8
TC166362	0.97	1.27	1.17	1.04	Pectinacetylesterase

TC166307	1.23	0.84	1.13	0.91	Calmodulin-5/6/7/8
TC166277	1.19	5.63	5.83	1.18	Peroxidase
TC166276	0.95	0.76	0.79	0.94	Putative serine carboxylase II-2
TC166263	1.13	1.21	1.21	1.13	Peptidyl-prolyl cis-trans isomerase
TC166185	0.90	0.96	0.78	1.14	Heat shock cognate 70 kDa protein 2
TC166088	0.94	0.77	0.39	1.83	Pectin acetylesterase
TC166057	1.06	0.67	0.63	1.02	Photosystem II stability/assembly factor
TC166043	0.98	0.51	0.49	1.01	Inorganic pyrophosphatase
TC166036	0.89	1.18	1.14	0.99	CT099
TC165996	0.87	0.93	0.84	0.99	Cytochrome c oxidase subunit 6b-1
TC165993	0.98	0.85	0.66	1.21	Neutral leucine aminopeptidase preprotein
TC165969	1.11	0.76	0.73	1.15	Subtilisin-like protease
TC165960	0.97	0.59	0.72	0.80	Malate dehydrogenase
TC165914	0.92	0.76	0.67	1.10	Fructose-1,6-bisphosphatase
TC165908	1.30	1.10	1.35	0.95	Germin-like protein
TC165902	1.29	0.55	0.92	0.77	Putative lactoylglutathione lyase
TC165884	1.17	1.07	1.05	1.25	Peroxidase
TC165880	0.92	0.49	0.46	0.96	Chaperonin 21 precursor
TC165838	0.76	0.74	0.37	1.45	Histone H1E
TC165835	1.09	0.96	1.06	1.03	Remorin 1
TC165805	1.04	1.11	0.69	1.66	Alcohol dehydrogenase
TC165802	1.10	0.84	0.92	1.00	Putative disease resistance protein
TC165773	1.06	15.04	18.31	0.93	Peroxidase 1
TC165754	1.10	0.85	1.00	0.96	GDP-mannose-3' 5'-epimerase
TC165741	1.26	2.21	2.97	0.94	Peroxidase
TC165716	1.01	0.82	0.96	0.87	Pre-mRNA-splicing factor SLU7-A
TC165699	1.00	0.65	0.46	1.53	Dihydrolipoyl dehydrogenase
TC165660	0.99	0.98	0.67	1.50	oxygen-evolving complex protein
TC165600	1.20	0.47	0.75	0.79	Dehydroascorbate reductase
TC165584	0.98	0.82	0.64	1.25	Ripening regulated protein-like
TC165572	0.99	0.55	0.72	0.75	undetermined protein
TC165550	1.09	0.78	0.77	1.10	fasciclin-like arabinogalactan protein
TC165523	0.99	0.81	0.58	1.44	EBP1
TC165512	0.97	1.09	0.88	1.23	Glutamate dehydrogenase
TC165487	1.70	5.75	13.10	0.74	Osmotin-like protein
TC165481	0.88	0.91	0.70	1.24	Leucine-rich repeat plant specific
TC165366	0.84	0.73	0.67	0.91	Nucellin-like protein
TC165366	0.79	0.78	0.62	1.00	Nucellin-like protein
TC165307	1.31	1.25	0.80	1.87	ATP synthase subunit gamma
TC165209	1.08	0.82	0.83	1.06	Chaperone DnaK
TC165188	0.89	0.61	0.75	0.75	Mta/sah nucleosidase
TC165098	1.15	0.68	0.86	0.81	Putative glutathione S-transferase T5
TC165061	0.84	0.50	0.36	1.14	Photosystem I reaction center subunit IV
TC165048	1.02	0.69	0.37	2.02	50S ribosomal protein L12
TC165027	2.27	1.03	2.90	0.74	Succinyl-CoA ligase alpha 1 subunit
TC165011	0.92	0.64	0.88	0.67	lysosomal thiol reductase
TC165011	0.81	0.73	0.91	0.67	lysosomal thiol reductase
TC165002	0.77	0.53	0.50	0.86	Copper-containing amine oxidase
TC164986	1.25	0.57	0.80	0.84	Triosephosphate isomerase
TC164981	1.27	1.08	1.10	1.20	Light-induced protein
TC164943	1.20	1.01	0.91	1.57	Ripening regulated protein DDTFR10-like
TC164940	1.06	2.05	0.82	2.66	undetermined protein

TC164936	1.18	4.37	7.69	0.68	Endochitinase 2 precursor
TC164873	1.05	0.64	0.84	0.83	Putative carboxymethylenebutenolidase
TC164866	0.95	0.54	0.33	1.50	ALY protein
TC164848	1.16	0.47	0.74	0.73	Lactoylglutathione lyase
TC164825	1.19	0.64	0.79	0.99	24K germin like protein precursor
TC164766	1.24	7.25	12.61	0.74	Osmotin-like protein OSML15 precursor
TC164756	1.12	0.77	0.97	0.92	plastid-lipid associated protein
TC164705	1.07	0.58	0.49	1.26	Putative acid phosphatase
TC164698	0.93	0.64	0.20	4.32	Monothiol glutaredoxin-S2
TC164671	1.24	7.21	11.07	0.86	Endochitinase 4 precursor
TC164625	1.05	0.84	0.83	1.06	Patellin 1
TC164605	1.04	1.05	1.12	1.18	Phosphoribulokinase
TC164589	0.99	0.77	0.64	1.22	Glyceraldehyde 3-phosphate dehydrogenase
TC164579	1.22	0.97	1.07	1.22	Quinone reductase-like protein
TC164579	1.01	0.77	0.61	1.29	Quinone reductase-like protein
TC164504	1.71	2.35	5.75	0.43	Peroxidase
TC164491	0.99	1.75	1.38	1.16	undetermined protein
TC164460	1.31	0.70	n/a	n/a	Isopentenyl diphosphate isomerase
TC164452	1.15	0.67	0.82	1.00	Phosphoglycerate kinase
TC164447	1.20	5.05	5.22	1.20	Cationic peroxidase precursor
TC164409	1.02	0.76	0.88	0.88	Mta/sah nucleosidase
TC164402	1.16	1.15	1.70	0.77	Aspartate aminotransferase
TC164401	1.10	0.92	0.70	1.40	DNA binding protein precursor
TC164369	0.99	0.37	0.38	0.92	Putative alanine aminotransferase
TC164360	1.03	0.47	0.45	1.08	Chaperonin 21 precursor
TC164357	1.11	0.85	1.15	0.87	RAD23-like
TC164342	1.11	0.42	0.56	0.82	peroxisomal (S)-2-hydroxy-acid oxidase 2
TC164340	1.39	0.50	0.57	1.08	Glyceraldehyde-3-phosphate dehydrogenase
TC164338	1.23	0.46	0.60	0.97	Dehydroascorbate reductase-like protein
TC164333	1.00	0.63	0.44	1.46	Pre-pro-cysteine proteinase precursor
TC164318	1.06	4.58	6.77	0.72	Endochitinase precursor
TC164316	0.87	1.27	0.91	1.27	Enolase
TC164220	1.10	1.13	1.19	1.14	Enoyl-CoA hydratase/isomerase
TC164219	0.98	1.22	0.65	2.03	Phosphate-induced protein
TC164205	1.03	0.86	0.97	0.90	Proline-rich protein
TC164185	0.74	1.03	0.75	0.99	Histone H1
TC164183	1.03	0.98	0.82	1.31	Elongation factor-like protein
TC164182	1.05	0.68	0.71	1.01	Putative subtilisin-like serine proteinase
TC164168	1.17	0.49	0.45	1.31	undetermined protein
TC164145	0.81	0.34	0.44	0.66	Oxygen-evolving enhancer protein 1
TC164142	1.04	1.46	0.94	1.60	Elongation factor 1-alpha
TC164121	0.67	0.67	0.51	0.87	Fructose-bisphosphate aldolase
TC164093	1.02	0.98	1.29	0.79	Aconitase
TC164083	0.89	1.31	0.77	1.73	Phosphate-induced protein 1
TC164076	1.05	0.60	0.55	1.15	mitochondrial SBP40
TC164075	0.91	0.33	0.27	1.11	Chloroplast Drought-induced Stress Protein
TC164053	1.06	0.43	0.34	1.32	Chloroplast HSP70
TC164005	1.02	2.19	6.06	0.37	Pectin methyl esterase
TC164001	0.65	0.52	0.40	0.81	Oxygen-evolving enhancer protein 1
TC163967	0.90	0.79	0.76	0.97	Phosphoglycerate kinase
TC163961	0.97	0.32	0.31	1.04	Translation initiation factor IF-3
TC163950	0.90	1.50	0.38	3.58	Invertase inhibitor

TC163927	0.97	0.65	0.46	1.36	Erwinia induced protein 1
TC163885	1.07	0.68	0.75	1.00	Oxidoreductase
TC163877	1.16	0.35	0.45	0.88	peroxisomal (S)-2-hydroxy-acid oxidase
TC163860	1.08	1.01	0.76	1.74	NADH dehydrogenase
TC163835	0.90	1.07	0.58	1.72	Aldehyde dehydrogenase
TC163833	0.77	0.41	0.48	0.68	Copper amine oxidase
TC163804	1.39	0.61	0.69	1.13	Glyceraldehyde-3-phosphate dehydrogenase
TC163801	1.27	8.08	12.82	0.82	Osmotin-like protein
TC163787	1.19	0.64	1.05	0.73	Cysteine proteinase 3 precursor
TC163769	1.58	0.64	1.45	0.67	Acidic endochitinase
TC163713	0.86	1.15	1.51	0.66	Hydroxyproline-rich glycoprotein
TC163703	1.07	0.64	0.91	0.75	CT099
TC163668	0.85	1.79	0.89	1.82	Ripening regulated protein-like
TC163648	1.00	0.72	0.43	1.68	Serine hydroxymethyltransferase
TC163642	1.20	1.71	1.59	1.34	Peroxidase
TC163607	1.27	4.79	4.56	1.42	Peroxidase
TC163587	1.33	1.24	n/a	n/a	Phosphate-induced protein 1
TC163569	0.95	0.78	0.70	1.26	undetermined protein
TC163566	1.00	0.84	0.87	0.99	Nucleoid DNA-binding-like protein
TC163554	0.93	0.73	0.74	0.92	Heat shock 70 kDa protein
TC163544	1.08	0.95	1.63	0.66	Thioredoxin peroxidase
TC163512	0.85	0.72	0.62	0.97	Phosphoglycerate kinase
TC163506	1.56	0.47	0.81	0.83	Trisephosphate isomerase
TC163473	1.00	0.46	0.49	0.94	sedoheptulose-1 7-bisphosphatase
TC163459	0.99	0.64	0.57	1.12	Methionine synthase
TC163439	1.16	0.95	1.31	0.80	Triosephosphate isomerase
TC163429	1.44	0.96	1.61	0.87	Endochitinase
TC163384	0.75	0.49	0.48	0.76	Oxygen-evolving enhancer protein 1
TC163377	0.88	0.43	0.26	1.40	25 kDa protein dehydrin
TC163374	1.99	20.85	36.58	0.81	Osmotin-like protein
TC163367	1.11	0.50	0.86	0.62	Aminotransferase 2
TC163344	1.07	1.10	1.07	1.06	ATP synthase subunit beta
TC163337	0.94	0.75	0.63	1.16	Oxygen-evolving enhancer protein 2
TC163314	0.97	0.47	0.35	1.28	28 kDa ribonucleoprotein
TC163298	0.91	0.74	0.54	1.21	Chalcone isomerase
TC163292	0.96	1.35	0.73	1.78	Elongation factor 1-alpha
TC163250	1.04	0.64	0.49	1.37	Transketolase 1
TC163245	1.05	2.11	2.07	1.16	Phosphoglycerate mutase
TC163242	1.02	1.85	1.67	1.15	Alpha-1,4-glucan-protein synthase
TC163237	1.33	1.29	1.39	1.26	Protein disulfide isomerase
TC163234	1.32	3.58	4.76	0.92	Class I chitinase
TC163226	1.15	0.63	0.83	0.79	Glycine dehydrogenase [decarboxylating]
TC163215	0.98	0.88	0.97	0.90	Short chain dehydrogenase
TC163209	1.15	5.96	9.34	0.75	Endochitinase 1 precursor
TC163195	1.27	1.37	1.55	0.97	1,3-beta-D-glucan glucanohydrolase
TC163179	1.29	7.17	11.33	0.79	Glucan endo-1,3-beta-glucosidase
TC163174	1.21	0.96	1.86	0.68	peroxidase
TC163169	1.00	0.81	0.94	0.88	Malate dehydrogenase
TC163152	1.07	0.38	0.54	1.09	Ribulose bisphosphate carboxylase
TC163136	1.08	1.54	1.18	1.42	ATP synthase CF0 subunit I
TC163128	0.99	1.22	1.43	0.86	Succinyl CoA ligase beta subunit-like protein
TC163112	1.08	0.72	0.91	0.84	UTP-glucose-1-phosphate uridylyltransferase

TC163076	1.36	0.72	0.89	1.14	Leucine aminopeptidase
TC163071	1.04	0.82	1.04	0.83	Glucose-6-phosphate isomerase
TC163070	1.13	1.66	1.77	1.06	Subtilisin-like serine protease
TC163068	0.91	0.90	0.90	1.03	Acid invertase
TC163042	1.04	0.79	0.67	1.20	Phosphoenolpyruvate carboxylase
TC163028	0.86	0.71	0.26	2.33	Alpha-glucan water dikinase
EG016190	0.72	1.18	0.89	1.00	Multiprotein bridging factor 1b
EG015239	0.61	1.63	n/a	n/a	Small nuclear ribonucleoprotein
EG012093	1.15	1.83	1.40	1.50	60S ribosomal protein L12
DR037760	1.12	0.50	0.63	0.90	Glutaredoxin S12
DR036019	0.98	0.94	0.68	1.34	Serine-threonine protein kinase
DR034516	0.94	0.83	1.16	0.72	Lactoylglutathione lyase
DR034357	1.15	0.57	0.65	0.98	LL-diaminopimelate aminotransferase
DN941276	1.07	1.19	1.21	1.02	Expansin-like protein
DN941027	0.95	3.93	5.16	0.72	FAD-linked oxidoreductase 1
DN923306	1.06	0.77	1.10	0.75	Malate dehydrogenase
DN923306	1.05	0.80	1.07	0.79	Malate dehydrogenase
DN849126	1.25	0.42	0.91	0.56	Serine-glyoxylate aminotransferase
DN849126	1.11	0.46	0.82	0.61	Serine-glyoxylate aminotransferase
DN590764	1.08	1.75	1.04	1.76	undetermined protein
DN588905	1.00	1.07	0.83	1.35	Gamma-glutamyl transferase
CX700015	0.93	0.73	0.69	1.07	undetermined protein
CX161954	1.21	0.45	0.55	1.01	Aspartic protease inhibitor 10 precursor
CX161931	1.09	0.83	0.93	0.97	Reticuline oxidase-like protein precursor
CX161218	0.84	1.13	0.81	1.15	Histone H2B-like
CV504216	1.13	1.50	1.66	1.03	Serine protease
CV498942	1.03	0.66	0.50	1.36	Kunitz trypsin inhibitor
CV497134	0.92	0.92	0.69	1.16	PsbP domain-containing protein 3
CV475703	1.14	0.65	0.91	0.81	Glutathione-s-transferase theta
CV475452	1.15	5.17	7.99	0.75	Endochitinase 2 precursor
CV472133	1.00	1.15	1.01	1.14	leucine aminopeptidase preprotein
CV430199	0.93	0.83	0.80	0.97	ML domain protein
CO501950	1.27	1.11	n/a	n/a	Subtilisin-like protease
CN462008	1.06	1.08	2.11	0.55	Malate dehydrogenase
CN215097	0.95	0.67	0.58	1.10	Gamma-glutamylhydrolase 2
CN214633	1.18	0.85	1.28	0.78	Glycosyl hydrolase family 3 protein
CN212770	1.00	0.89	0.94	0.98	Polygalacturonase-inhibiting protein
CK863947	0.95	0.93	0.82	1.08	Xyloglucan-specific endoglucanase inhibitor
CK863886	0.94	0.78	0.62	1.24	Oxygen-evolving enhancer protein 2
CK276749	1.32	1.23	1.65	0.95	Subtilisin-like protease
CK263954	1.53	0.97	2.65	0.72	Class II chitinase
CK263509	0.97	0.86	1.02	0.84	undetermined protein
CK257172	0.69	0.93	0.45	1.46	Pyruvate dehydrogenase E1 component
BQ515024	1.24	1.22	1.06	1.36	Non-specific lipid-transfer protein
BQ511074	1.12	0.89	0.76	1.33	Peptidyl-prolyl cis-trans isomerase
BQ046779	1.12	1.16	0.65	2.15	Histone H2A
BQ046163	0.84	0.73	0.68	0.89	Pectin methylesterase 1
BQ046158	1.17	5.31	6.50	0.94	Cationic peroxidase
BQ046158	1.15	5.87	5.80	1.22	Peroxidase cevi16
BM112160	0.79	0.97	1.06	0.73	Vacuolar proton pump subunit F
BI178561	1.23	0.82	0.38	2.74	undetermined protein
BG599174	1.26	0.96	0.89	1.38	Thylakoid lumenal 25.6 kDa protein

BG597038	0.93	0.89	0.82	1.02	Serine-threonine protein kinase, plant-type
BG594905	1.04	0.59	0.96	0.66	Anthranilate synthase component I
BG097865	1.04	0.85	0.85	1.01	Periplasmic beta-glucosidase
BF188713	0.82	0.68	0.71	0.82	undetermined protein
BE472429	0.85	1.04	1.14	0.80	SBT4C protein
AM908242	0.97	0.63	0.50	1.16	Peptidyl-prolyl cis-trans isomerase
AM907060	1.13	3.35	4.32	0.92	Benzoquinone reductase
AM906296	1.09	1.16	1.42	0.88	undetermined protein

Appendix D. The 595 iTRAQ-Labeled Reproducible Proteins Identified in the Cytoplasmic Fractions

TC number	115/114	117/115	116/114	117/116	Annotation
TC194485	0.97	1.50	1.11	1.30	Coat protein
TC194369	1.14	1.06	0.91	1.34	RNA binding protein-like protein
TC194240	0.95	2.55	1.21	1.79	NADP-malic enzyme
TC194204	1.26	1.15	1.51	0.98	Aspartic protease inhibitor 1 precursor
TC194013	0.98	1.60	1.45	1.09	Hsp90-2-like
TC193534	0.98	0.74	0.79	0.92	50S ribosomal protein L12
TC193346	0.77	0.94	0.67	1.06	Glucose-1-phosphate adenylyltransferase
TC193180	1.08	3.14	3.16	1.17	Fructokinase
TC193170	1.04	1.49	1.38	1.06	Probable glutathione-S-transferase
TC193019	1.25	1.70	1.98	1.07	SGRP-1 protein
TC192386	1.11	0.88	0.89	1.10	Ferredoxin--NADP reductase
TC192329	1.05	1.60	1.57	1.18	Steroid binding protein
TC191617	0.95	0.86	0.91	0.89	Phosphoribulokinase
TC191591	1.25	0.54	0.45	1.40	Chloroplast 50S ribosomal protein L2
TC191536	1.14	1.04	1.12	1.09	SGRP-1 protein
TC191497	1.00	1.23	1.22	1.01	26S proteasome AAA-ATPase subunit RPT4a
TC191403	0.92	0.99	0.98	0.93	Putative thylakoid lumenal 16.5 kDa protein
TC191321	1.08	1.16	1.37	0.94	undetermined protein
TC191209	1.09	0.56	0.61	0.97	Glyoxisomal malate dehydrogenase
TC191208	0.94	1.34	1.07	1.13	Aldehyde dehydrogenase
TC191142	1.18	1.51	2.08	0.98	Class I chitinase
TC191055	1.07	1.07	1.20	0.91	ABC nickel/di-oligopepetide transporter
TC191045	1.10	1.16	1.25	1.03	Peptidyl-prolyl cis-trans isomerase
TC190989	0.61	1.70	1.41	0.66	Thaumatin-like protein
TC190712	1.01	1.58	1.68	0.94	Glutamine synthetase
TC190640	1.04	1.10	1.08	1.06	Ubiquitin-specific protease 15
TC190622	1.17	2.20	2.41	1.08	Cyanate lyase
TC190413	1.04	1.21	1.29	0.97	Pyruvate dehydrogenase E1 component
TC190200	1.30	0.54	0.55	1.38	GrpE protein homolog
TC190134	0.96	1.01	0.85	1.18	Glutathione S-transferase/peroxidase
TC190038	1.04	0.64	0.78	0.86	RuBisCO large subunit-binding protein
TC189862	1.34	0.86	0.56	1.80	Peroxiredoxin Q
TC189821	0.63	1.82	1.87	0.53	Thaumatin-like protein
TC189628	0.97	1.10	2.23	0.55	Heat shock protein 90
TC189480	0.86	1.38	0.94	1.25	Actin depolymerizing factor 3
TC189462	1.09	1.06	1.24	0.94	Glutathione S-transferase
TC189109	0.82	0.75	0.81	0.76	Dihydrolipoyl dehydrogenase
TC188798	1.14	0.88	1.08	0.95	3-beta hydroxysteroid dehydrogenase/isomerase
TC188621	1.38	1.34	1.26	1.47	Beta-subunit of K+ channels
TC188516	1.30	0.86	0.80	1.44	Kunitz-type protease inhibitor
TC188279	0.88	0.88	0.64	1.20	D-glycerate 3-kinase chloroplast precursor
TC188242	1.05	1.47	1.87	0.83	14-3-3 protein 9
TC188161	0.89	0.97	0.72	1.19	H-Protein
TC188093	0.98	7.05	9.28	0.75	Ethylene-responsive proteinase inhibitor
TC188051	0.89	0.98	1.18	0.76	Ubiquitin fusion protein
TC187943	0.95	0.42	0.39	1.06	Rubisco activase 2
TC187824	0.92	2.00	1.37	1.25	Aspartate aminotransferase
TC187760	1.26	0.52	0.71	0.90	H+-transporting two-sector ATPase
TC187651	0.98	2.24	1.81	1.17	Phenylacetaldehyde reductase

TC187437	1.10	n/a	n/a	0.71	Inositol monophosphatase family protein
TC187308	0.94	0.85	0.81	1.00	Glucose-1-phosphate adenylyltransferase
TC187295	1.05	1.36	1.81	0.78	Luminal-binding protein 5 precursor
TC187164	1.22	1.18	1.65	0.86	Protein Pop3
TC187144	0.96	0.76	0.75	0.99	Carbonic anhydrase
TC187080	1.01	0.85	0.87	0.97	Cysteine synthase
TC186926	1.24	1.73	1.84	1.17	Cysteine protease
TC186921	1.50	1.20	1.84	0.99	Glutathione S-transferase
TC186921	0.98	1.03	1.21	0.83	Glutathione S-transferase
TC186718	1.21	1.15	0.76	2.09	Peptidylprolyl isomerase
TC186600	1.78	0.89	1.11	1.44	60S acidic ribosomal protein P0
TC186583	1.58	0.73	1.06	1.03	Ribosome recycling factor
TC186398	0.94	0.96	1.14	0.79	Kinesin
TC186226	1.21	1.10	1.12	1.20	Thylakoid lumenal 20 kDa protein-like
TC185959	1.28	1.06	1.01	1.38	Glycine-rich RNA-binding protein
TC185943	1.03	1.26	1.49	0.90	Peptidyl-prolyl cis-trans isomerase
TC185934	1.03	1.19	1.13	1.09	Malate dehydrogenase
TC185914	1.21	1.33	1.45	1.12	Basic 30 kDa endochitinase precursor
TC185639	0.88	1.46	1.33	0.96	Molecular chaperone Hsp90-1
TC185610	1.22	1.49	1.53	1.13	1,3-beta-glucan glucanohydrolase
TC185563	1.13	1.07	1.35	0.91	glutamate/ornithine acetyltransferase
TC185345	0.95	1.25	1.21	0.98	Probable plastid-lipid-associated protein 13
TC185332	1.02	1.11	1.19	0.95	Dihydrolipoamide dehydrogenase precursor
TC185153	1.16	1.52	1.54	1.07	60S acidic ribosomal protein P
TC184969	1.00	0.79	0.69	1.12	Putative carbonyl reductase
TC184729	0.97	8.12	11.05	0.70	Ethylene-responsive proteinase inhibitor 1
TC184486	1.06	0.68	0.75	0.96	50S ribosomal protein L12
TC184334	1.14	4.53	3.57	1.37	Universal stress protein family protein
TC183941	1.32	1.13	1.28	1.16	Proteinase inhibitor 1
TC183932	1.12	1.63	1.72	1.06	Patellin 1
TC183428	1.31	0.81	1.26	0.82	Putative proline-rich protein
TC183342	1.76	2.01	4.20	0.79	3-ketoacyl-CoA thiolase 2
TC183181	1.12	1.32	1.26	1.16	Cystatin
TC183174	0.95	0.69	0.69	0.95	Chaperonin-60 beta subunit precursor
TC183052	0.94	1.81	1.76	0.99	Acyl-CoA-binding protein
TC182973	0.78	1.05	0.69	1.23	epimerase/dehydratase family protein
TC182555	1.17	0.67	0.80	0.98	50S ribosomal protein L12
TC182527	1.44	1.53	1.24	1.77	Wound-induced proteinase inhibitor 1
TC182443	0.99	1.10	1.01	1.06	Putative lactoylglutathione lyase
TC182432	1.09	0.87	0.95	1.00	Nucleoside diphosphate kinase 2
TC182140	1.03	0.49	0.49	1.08	MRNA binding protein precursor
TC182040	0.96	0.84	0.85	0.93	CP12 precursor
TC182026	0.94	1.60	1.51	0.99	Proteasome subunit beta type-2-A
TC181746	1.06	1.09	1.11	1.06	Phosphoglycerate kinase
TC181684	1.23	0.70	0.62	1.33	Chaperonin-60 beta subunit precursor
TC181617	0.82	0.91	0.71	1.04	Presequence protease 1
TC181534	0.62	2.02	0.94	1.25	Elongation factor EF-2
TC181436	0.64	1.62	1.05	0.97	Phosphoenolpyruvate carboxylase
TC181410	1.11	0.84	0.91	1.02	Putative glutathione S-transferase
TC181212	1.03	0.72	0.33	1.73	Ferredoxin I precursor
TC181183	0.84	0.87	0.82	1.01	glyceraldehyde-3-phosphate dehydrogenase
TC181073	1.13	1.03	1.01	1.23	Sn-1 protein

TC180977	1.00	1.03	0.98	1.06	Heme-binding protein
TC180730	1.34	1.29	1.67	0.97	60s acidic ribosomal protein-like protein
TC180568	1.27	1.27	1.80	0.90	Small molecular heat shock protein
TC180524	0.90	1.49	1.19	1.09	Hydrolase carbon-nitrogen family protein
TC180484	1.00	1.89	1.54	0.82	Glutamine synthetase
TC180423	1.40	1.10	2.15	0.74	Acidic ribosomal protein
TC179961	0.93	0.40	0.31	1.18	Elongation factor G
TC179956	1.06	0.76	0.63	1.30	Enzyme of the cupin superfamily
TC179884	1.02	0.64	0.61	1.07	NAD dependent epimerase/dehydratase
TC179723	1.01	0.58	0.70	0.84	CP12 precursor
TC179709	0.98	0.92	0.92	0.98	Acyl carrier protein precursor
TC179682	0.84	0.94	0.64	1.25	Aldehyde dehydrogenase
TC179575	0.84	1.07	0.71	1.32	Putative S-formylglutathione hydrolase
TC179525	1.25	2.28	2.03	1.35	Lignin-forming anionic peroxidase precursor
TC179248	1.01	0.57	0.50	1.14	4-nitrophenylphosphatase
TC179223	0.85	1.06	0.92	1.03	Malate dehydrogenase
TC179191	1.13	0.98	1.14	0.96	NAD-malate dehydrogenase precursor
TC179171	0.97	0.75	0.71	1.03	Glutamate-1-semialdehyde 2,1-aminomutase
TC179073	0.88	0.99	0.60	1.29	Chloroplast ferredoxin I
TC179063	1.00	1.23	1.44	0.91	40S ribosomal protein S2
TC179026	0.94	0.74	0.97	0.67	DJ-1 family protein
TC178939	1.16	2.08	0.58	4.18	Threonine dehydratase
TC178882	0.78	0.70	0.44	1.19	Solanesyl diphosphate synthase
TC178822	1.09	1.74	1.65	1.14	Oligopeptidase A
TC178648	1.09	1.57	1.58	1.08	Glutaredoxin
TC178639	1.03	1.20	1.15	1.09	Thioredoxin H-type 2
TC178608	1.44	1.54	1.51	1.49	40S ribosomal protein S16
TC178551	1.05	0.46	0.35	1.38	Chloroplast thioredoxin
TC178532	1.10	0.89	0.90	1.08	undetermined protein
TC178504	1.27	1.98	2.04	1.25	Subtilisin-like protease
TC178498	1.34	0.84	0.96	1.15	Sulfate adenylyltransferase
TC178467	0.88	0.66	0.54	1.11	Glutamine synthetase
TC178390	1.12	1.08	1.10	1.10	Glutathione peroxidase 5
TC178094	1.05	0.91	0.96	1.00	Putative ribose-5-phosphate isomerase
TC178042	1.12	1.18	1.51	0.87	Superoxide dismutase [Fe]
TC178018	1.00	1.24	1.21	1.02	Pit2 protein
TC177982	0.93	1.11	1.08	0.93	4-alpha-glucanotransferase
TC177676	1.21	1.54	2.06	0.90	NFU4 (NFU domain protein 4)
TC177601	0.99	1.66	1.65	0.99	Serpin-like protein
TC177499	1.41	1.25	1.74	1.01	Glutathione S-transferase
TC177484	1.24	0.63	0.55	1.37	Uroporphyrinogen decarboxylase
TC177451	1.06	0.94	0.80	1.25	Coproporphyrinogen III oxidase
TC177431	1.09	0.96	0.88	1.16	Fructose-bisphosphate aldolase
TC177357	0.89	0.99	0.90	0.97	ATP-dependent Clp protease
TC177316	1.15	1.15	1.33	1.00	Poly(A) polymerase
TC177289	0.92	1.21	1.08	1.02	Neutral leucine aminopeptidase
TC177278	1.25	1.08	1.44	0.97	Elongation factor Tu
TC177228	1.20	1.08	1.52	0.84	Peroxiredoxin
TC177202	1.10	1.59	2.19	0.81	CREG2-protein-like
TC177024	1.17	1.13	1.30	1.01	Succinyl-CoA ligase alpha 2 subunit
TC176976	1.40	1.73	2.15	1.11	Cathepsin B
TC176918	1.08	1.11	1.29	0.92	Cytochrome P450

TC176711	1.03	1.35	1.25	1.12	26S proteasome regulatory subunit 8
TC176693	1.25	0.66	0.87	0.93	Quinone oxidoreductase-like protein
TC176570	1.12	1.25	1.41	1.01	Glyceraldehyde-3-phosphate dehydrogenase
TC176570	1.00	1.26	0.99	1.33	Glyceraldehyde-3-phosphate dehydrogenase
TC176568	1.26	0.94	1.19	1.00	Protein kinase C inhibitor-like protein
TC176539	0.99	0.83	0.70	1.19	Aminomethyltransferase
TC176507	0.76	2.48	1.74	1.00	Plastid enolase
TC176501	1.06	1.36	1.60	0.90	Coatomer subunit delta-2
TC176495	0.79	1.04	0.91	1.11	glyceraldehyde-3-phosphate dehydrogenase
TC176436	1.02	1.39	1.52	0.93	Monodehydroascorbate reductase
TC176431	0.79	1.74	1.27	1.05	Cytosolic aconitase
TC176398	1.08	3.16	2.71	1.22	Glucan endo-1,3-beta-D-glucosidase precursor
TC176365	1.19	0.65	0.83	0.93	Putative oxidoreductase zinc-binding
TC176289	0.97	1.11	1.07	1.01	Ribosomal protein L27a-like protein
TC176180	0.95	0.50	0.43	1.21	MRNA binding protein precursor
TC176132	0.96	1.13	0.94	1.17	Thioredoxin-like protein
TC176045	1.12	0.82	0.88	1.06	Amino acid binding protein
TC176032	1.13	1.00	1.01	1.13	Photosystem II reaction center psb28 protein
TC175919	0.77	1.43	1.07	1.06	Glutathione S-transferase
TC175844	0.91	0.43	0.35	1.13	Peptidyl-prolyl cis-trans isomerase;
TC175736	0.94	0.54	0.40	1.20	Fructose-bisphosphate aldolase
TC175729	1.01	1.41	1.26	1.11	40S ribosomal protein S5
TC175639	0.94	0.55	0.49	1.07	sedoheptulose-1,7-bisphosphatase
TC175528	1.11	1.14	0.98	1.30	Thioredoxin
TC175400	1.23	1.41	1.57	1.09	60S ribosomal protein L18
TC175288	1.13	1.24	1.46	0.95	Proteasome subunit alpha type-6
TC175234	1.04	1.15	1.34	0.89	Cytochrome c1-1, heme protein
TC175213	0.96	1.23	1.25	0.81	Putative 60S ribosomal protein L35
TC175100	1.26	1.23	1.51	0.90	40S ribosomal protein S23
TC174954	1.33	0.82	1.02	1.09	Senescence-associated protein
TC174916	1.11	0.69	0.80	0.95	Thioredoxin
TC174912	1.14	1.59	1.46	1.23	Formate dehydrogenase
TC174803	0.94	1.09	1.00	1.01	Glutathione S-transferase
TC174571	1.01	1.30	1.40	0.94	Monodehydroascorbate reductase
TC174523	1.09	2.47	2.36	1.14	6-phosphogluconate dehydrogenase
TC174490	1.11	1.55	1.88	0.89	Copper chaperone
TC174426	1.25	0.91	0.91	1.24	undetermined protein
TC174407	0.95	1.01	0.83	1.15	Putative aminopeptidase
TC174256	1.03	0.91	0.69	1.35	erythritol 4-phosphate cytidylyltransferase
TC174142	1.02	0.85	0.85	0.96	ATP synthase gamma chain
TC173993	1.22	1.42	1.50	1.12	40S ribosomal protein S16
TC173981	1.05	1.07	1.09	1.04	Plastid fibrillin 2
TC173874	1.48	1.43	3.56	0.65	Germin-like protein
TC173865	1.82	1.71	2.81	0.85	Glucan endo-1,3-beta-D-glucosidase
TC173836	1.13	1.44	1.54	1.02	Protein disulfide isomerase
TC173795	0.82	1.45	1.15	1.04	Proteasome subunit beta type-4 precursor
TC173677	1.06	1.47	1.88	0.83	14-3-3 protein-like protein
TC173665	1.01	1.28	1.44	0.89	Ubiquitin extension protein
TC173522	0.87	1.12	0.83	1.19	Transcription regulator
TC173501	0.94	1.40	1.11	1.17	FAM10 family protein
TC173498	1.22	2.20	1.97	1.35	Peroxidase
TC173489	1.38	1.19	1.89	0.87	Cytosolic nucleoside diphosphate kinase

TC173468	1.12	1.04	1.29	0.88	S-adenosylmethionine synthetase 3
TC173455	0.88	1.08	0.75	1.23	Glutathione reductase
TC173383	1.13	1.42	1.58	1.03	Lactoylglutathione lyase
TC173338	0.92	1.01	0.78	1.17	glycine decarboxylase complex H-protein
TC173293	1.03	1.34	1.43	0.97	Salt tolerance protein
TC173194	1.05	0.97	0.99	1.03	L-isoaspartate-O-methyl transferase
TC173051	1.24	0.62	0.47	2.06	undetermined protein
TC173018	1.26	2.06	2.94	0.89	Osmotin-like protein
TC172980	1.09	1.43	1.40	1.11	Putative glutathione S-transferase
TC172946	0.92	0.70	0.74	0.88	50S ribosomal protein L4
TC172918	1.04	1.23	1.39	0.92	Proteasome subunit alpha type-6
TC172758	1.15	1.04	1.44	0.83	Nucleoside diphosphate kinase
TC172601	1.18	0.81	0.86	1.10	ferredoxin-thioredoxin-reductase precursor
TC172593	1.45	1.33	2.04	0.95	Cysteine proteinase 3
TC172566	1.28	0.49	0.53	1.20	Methionyl-tRNA synthetase
TC172552	0.91	1.03	0.95	0.99	ATP-dependent Clp protease
TC172517	0.93	1.19	1.29	0.96	Translationally-controlled tumor protein
TC172465	1.10	1.34	1.64	0.87	40S ribosomal protein S19-like
TC172434	1.52	1.68	2.38	1.25	Peroxidase
TC172430	1.17	0.51	0.57	0.98	Thioredoxin-X
TC172275	1.79	4.96	6.75	1.22	Pathogenesis-related protein P2
TC172266	1.10	1.12	1.25	0.96	undetermined protein
TC172263	1.05	0.82	0.89	0.98	Peroxiredoxin-2E
TC172228	1.24	1.19	1.20	1.26	Calmodulin cam-210
TC172201	1.27	0.77	0.96	1.02	Glutathione peroxidase
TC172096	1.43	0.81	0.89	1.41	Histidine triad (HIT) protein
TC171996	1.04	0.80	0.91	0.91	Thioredoxin
TC171993	0.96	1.28	1.39	0.88	NEDD8 RUB2
TC171850	1.07	0.78	1.03	0.80	ATP synthase gamma chain
TC171816	1.04	0.94	0.97	1.01	Putative RNA-binding protein
TC171679	1.24	8.59	8.36	1.26	Osmotin-like protein
TC171649	0.58	2.52	1.19	1.28	Pyruvate kinase
TC171633	0.81	0.93	0.65	1.18	Apospory-associated protein C-like
TC171540	1.22	1.40	1.75	0.90	40S ribosomal protein S17-like protein
TC171497	1.12	4.63	5.38	0.99	Inactive purple acid phosphatase 28
TC171451	1.15	1.13	1.31	0.99	dehydrogenase E1 beta subunit isoform 2
TC171351	1.06	1.06	1.13	0.99	Thylakoid lumenal 15 kDa protein 1
TC171341	1.26	0.90	0.66	1.76	Thylakoid lumenal 25.6 kDa protein
TC171271	1.24	0.63	0.83	0.93	RuBisCO subunit binding-protein
TC171135	1.07	1.15	1.72	0.73	Endoplasmin homolog precursor
TC171135	0.99	1.23	1.55	0.77	Endoplasmin homolog precursor
TC171094	0.94	1.08	1.24	0.83	Monodehydroascorbate reductase
TC171061	0.99	0.54	0.44	1.22	Heat shock protein precursor
TC171049	1.09	0.96	0.87	1.14	peptidase M1 family protein
TC171013	1.00	1.49	1.86	0.80	14-3-3-like protein 16R
TC170930	0.91	2.07	2.22	0.86	Superoxide dismutase [Cu-Zn] 2
TC170792	1.28	0.90	1.06	1.22	Light-inducible protein ATLS1
TC170791	1.27	0.57	1.19	0.63	Cytochrome b6-f complex iron-sulfur subunit
TC170770	0.93	1.10	1.01	1.02	Phosphoglucomutase
TC170708	1.08	1.09	1.01	1.17	Plastoglobulin-1
TC170604	0.95	0.41	0.30	1.30	2-deoxyglucose-6-phosphate phosphatase
TC170554	0.92	1.19	1.20	0.92	Monodehydroascorbate reductase

TC170396	1.68	5.23	4.84	1.58	Pathogenesis related protein 1
TC170370	0.99	1.17	1.35	0.84	Chaperonin CPN60-2
TC170348	1.06	1.85	2.10	0.95	glutathione peroxidase
TC170307	1.18	0.86	1.07	0.95	Nucleoside diphosphate kinase 2
TC170266	1.17	9.61	10.24	1.12	Citrate binding protein
TC170257	1.10	1.03	1.26	0.90	undetermined protein
TC170244	1.29	1.39	1.70	1.05	Glutathione S-transferase
TC170157	1.18	1.98	3.28	0.79	Calreticulin precursor
TC170111	1.19	1.25	2.43	0.65	ATP synthase subunit alpha
TC170091	1.13	1.35	1.83	0.86	Ribosomal protein S14-like
TC169912	1.07	1.28	1.31	1.04	Poly(A)-binding protein
TC169893	0.88	2.19	1.87	0.96	osmotin-like protein
TC169870	1.73	1.71	2.61	1.10	Peroxidase
TC169850	0.99	0.45	0.42	1.06	Rubiso activase
TC169768	0.78	0.64	0.46	1.03	Transketolase 1
TC169763	0.89	5.64	21.78	0.24	Miraculin-like protein
TC169619	1.10	0.75	0.73	1.18	3-isopropylmalate dehydrogenase
TC169550	1.30	1.10	1.25	1.16	Cysteine protease inhibitor 4
TC169479	1.81	7.53	9.97	1.30	Basic PR-1 protein
TC169399	0.81	0.82	0.63	1.12	N-acetyl-gamma-glutamyl-phosphate reductase
TC169394	0.81	7.59	12.06	0.70	Kunitz-type protease inhibitor
TC169366	1.05	1.29	1.24	1.07	P23 co-chaperone
TC169318	0.50	1.50	0.55	1.04	Glutamate synthase (Ferredoxin)
TC169280	1.17	1.32	1.70	0.89	Superoxide dismutase [Fe], chloroplast
TC169162	0.81	1.52	1.29	0.95	Hsp90-2-like
TC169081	1.24	1.21	1.88	0.90	Calcium ion binding protein
TC168971	1.05	1.11	1.08	1.02	6-phosphogluconate dehydrogenase
TC168961	0.80	0.87	0.65	1.05	UDP-sulfoquinovose synthase
TC168901	1.12	1.53	1.71	1.03	Cystatin-like protein
TC168900	1.13	1.60	2.06	0.87	Prolyl carboxypeptidase like protein
TC168896	1.12	1.26	1.61	0.86	Superoxide dismutase
TC168887	1.06	1.27	1.19	1.13	Ubiquitin carrier protein
TC168840	0.90	1.46	1.37	0.97	UDP-glucuronate decarboxylase 1
TC168794	1.41	3.40	5.08	0.93	Chitinase, class V
TC168700	1.21	3.58	4.52	1.03	NtPRp27-like protein
TC168658	1.13	1.14	1.39	0.92	Thylakoid lumenal 17.4 kDa protein
TC168584	0.88	1.03	0.75	1.19	epimerase/dehydratase
TC168485	1.43	1.02	1.28	1.13	undetermined protein
TC168445	1.19	0.87	1.20	0.86	Photosystem I reaction center subunit IV B
TC168439	1.06	1.25	1.57	0.85	Protein disulfide-isomerase precursor
TC168437	1.09	0.95	1.07	0.98	Thioredoxin peroxidase
TC168408	0.90	2.57	1.28	1.47	Methylenetetrahydrofolate dehydrogenase
TC168353	1.03	0.58	0.48	1.18	Ribulose bisphosphate carboxylase
TC168321	1.24	5.23	7.86	0.82	Benzoquinone reductase
TC168318	1.46	1.50	2.50	0.92	Class II chitinase
TC168274	1.21	1.42	2.50	0.67	Late embryogenesis (Lea)-like protein
TC168267	0.90	0.55	0.45	1.09	Fructose-bisphosphate aldolase
TC168258	2.06	0.95	1.23	1.54	Calmodulin-5/6/7/8
TC168258	0.96	1.98	1.26	1.55	Calmodulin
TC168185	0.92	1.09	0.94	1.08	Thylakoid-bound ascorbate peroxidase 6
TC168117	1.33	1.51	1.67	1.13	nucleoid DNA binding protein
TC168093	1.18	1.31	1.48	1.08	Elongation factor Tu

TC168088	0.76	1.14	1.02	0.77	Ferredoxin-thioredoxin-reductase
TC168061	1.20	1.57	1.69	1.06	Probable glutathione S-transferase
TC167947	1.07	0.70	0.87	0.96	2-deoxyglucose-6-phosphate phosphatase
TC167909	1.26	1.65	2.58	0.84	2-oxoglutarate dehydrogenase E2 subunit
TC167892	0.76	1.64	1.02	1.26	Aconitase
TC167875	1.00	1.03	1.06	0.97	Aspartate aminotransferase
TC167831	0.89	1.57	1.09	1.26	6-phosphogluconolactonase
TC167721	0.97	0.64	0.45	1.33	Triosephosphate isomerase
TC167648	1.01	1.00	1.17	0.87	Thioredoxin peroxidase
TC167602	1.14	1.48	2.39	0.74	Vacuolar H+-ATPase A1 subunit isoform
TC167578	0.94	0.61	0.50	1.15	Ribulose bisphosphate carboxylase
TC167569	0.91	0.63	0.63	0.86	Hydroxypyruvate reductase
TC167339	1.22	1.75	1.63	1.24	Putative stationary phase survival protein SurE
TC167306	1.13	1.20	1.33	1.04	Poly(A)-binding protein
TC167284	0.71	1.52	0.78	1.49	6-phosphogluconate dehydrogenase
TC167273	1.13	1.14	1.79	0.72	60S ribosomal protein L9
TC167231	1.15	1.22	2.01	0.71	Fasciclin-like arabinogalactan protein
TC167156	0.92	7.52	7.46	0.81	Benzoquinone reductase
TC167121	1.15	1.32	1.73	0.89	S-adenosyl homocysteine nucleosidase
TC167109	1.10	0.98	1.05	1.01	Malate dehydrogenase
TC167021	0.91	1.18	1.15	0.98	Putative asparate aminotransferase
TC166985	1.22	0.90	1.34	0.82	nascent polypeptide associated complex
TC166980	1.12	1.21	1.25	1.03	Ripening regulated protein DDTFR10-like
TC166952	1.08	1.34	1.39	1.04	Thioredoxin peroxidase 1
TC166921	1.21	1.19	1.96	0.78	Adenylate kinase B
TC166919	0.93	0.84	0.65	1.17	Monothiol glutaredoxin-S16
TC166915	1.35	1.02	1.43	0.94	Aspartic proteinase 2
TC166885	1.11	1.63	1.81	0.98	Putative oligopeptidase A
TC166882	1.02	0.70	0.76	0.86	Plastocyanin
TC166850	1.00	1.27	1.30	0.99	glutathione peroxidase
TC166840	1.06	0.72	0.80	0.95	Thioredoxin
TC166778	1.09	0.78	0.77	1.09	Aspartate aminotransferase
TC166762	1.46	0.79	0.70	1.63	Cysteine protease inhibitor 1
TC166761	1.26	1.80	2.14	1.06	pathogenesis related protein 10
TC166760	1.05	0.88	0.96	0.98	undetermined protein
TC166752	1.23	1.17	2.01	0.73	Germin-like protein
TC166702	0.99	1.41	1.15	1.22	Allene oxide cyclase
TC166558	1.01	3.79	6.19	0.63	undetermined protein
TC166554	1.05	1.30	1.19	1.21	40S ribosomal protein S10
TC166527	1.05	1.08	1.40	0.81	Superoxide dismutase
TC166486	0.97	0.74	0.77	0.95	Glyceraldehyde-3-phosphate dehydrogenase
TC166413	1.02	1.23	1.14	1.11	Glyceraldehyde-3-phosphate dehydrogenase
TC166362	0.92	5.12	3.77	1.24	Pectin acetylesterase
TC166345	1.44	0.73	0.72	1.07	Biotin carboxylase
TC166332	1.02	0.88	1.01	0.90	Stromal 70 kDa heat shock-related protein
TC166307	1.40	1.12	1.23	1.39	Calmodulin-5/6/7/8
TC166277	0.95	3.45	3.77	0.97	Peroxidase precursor
TC166263	1.18	1.49	1.30	1.39	Peptidyl-prolyl cis-trans isomerase
TC166220	1.05	1.09	1.05	1.13	Vacuolar processing enzyme-1b
TC166203	1.24	1.46	1.24	1.47	Peptidyl-prolyl cis-trans isomerase
TC166185	0.89	1.21	1.00	1.08	Heat shock cognate 70 kDa protein 2
TC166070	1.12	0.58	0.68	1.00	pentose-5-phosphate-3-epimerase

TC166057	1.09	1.28	1.68	0.84	Photosystem II stability/assembly factor HCF136
TC166043	1.01	0.54	0.46	1.20	Inorganic pyrophosphatase
TC166038	1.05	2.08	2.15	1.02	Desacetoxyvindoline 4-hydroxylase
TC166036	1.09	2.64	4.41	0.64	Copper ion binding protein
TC165969	0.96	1.14	1.04	1.05	Subtilisin-like protease
TC165960	1.11	0.75	0.81	1.01	Malate dehydrogenase
TC165952	0.99	1.40	1.09	1.26	1-aminocyclopropane-1-carboxylate oxidase
TC165919	0.41	2.40	0.86	1.19	Alpha-glucan phosphorylase
TC165914	0.84	0.96	0.77	1.03	Fructose-1,6-bisphosphatase
TC165902	0.84	1.18	0.97	1.01	Putative lactoylglutathione lyase
TC165880	1.14	0.71	0.82	0.98	Chaperonin 21 precursor
TC165870	0.89	1.90	1.71	0.95	3-isopropylmalate dehydrogenase
TC165867	1.11	1.34	1.36	1.03	60S ribosomal protein L4/L1
TC165835	1.24	2.25	4.53	0.61	Remorin 1
TC165819	1.27	1.43	1.57	1.01	Acidic ribosomal protein P1a-like
TC165793	1.20	1.34	1.50	1.15	60S ribosomal protein L1
TC165761	1.31	1.66	1.83	1.07	Ribosomal protein S13
TC165754	1.03	1.09	1.06	1.10	GDP-mannose-3' 5'-epimerase
TC165743	0.99	0.82	0.63	1.30	Glutamate-1-semialdehyde 2,1-aminomutase
TC165715	1.14	1.53	2.31	0.75	Vacuolar ATPase subunit B
TC165699	1.11	0.92	1.15	0.88	Dihydrolipoyl dehydrogenase
TC165690	0.72	1.07	0.67	1.10	alpha-glucan phosphorylase
TC165660	1.36	0.69	0.77	1.13	oxygen-evolving complex protein 3 precursor
TC165626	0.80	1.62	1.07	1.20	Cytosolic glutathione reductase
TC165600	1.04	0.84	0.83	1.04	Dehydroascorbate reductase
TC165578	0.97	1.42	1.64	0.84	14-3-3 protein 4
TC165572	1.03	1.50	2.36	0.63	undetermined protein
TC165550	1.08	1.17	1.14	1.11	fasciclin-like arabinogalactan protein
TC165535	1.00	1.28	1.04	1.23	Fructose-bisphosphate aldolase
TC165530	1.52	0.25	0.25	1.58	Adenylyl-sulfate reductase
TC165526	1.22	0.83	1.15	0.87	GrpE protein
TC165512	1.20	1.67	2.88	0.67	Glutamate dehydrogenase
TC165487	1.48	7.93	10.39	1.08	Osmotin-like protein
TC165467	1.45	n/a	1.67	n/a	Pyrroline-5-carboxylate reductase
TC165461	1.00	2.05	1.71	0.96	Annexin p34
TC165456	0.93	1.10	1.00	1.01	Putative dehydrogenase
TC165455	1.68	1.37	1.95	0.85	60S ribosomal protein L13
TC165407	1.13	1.44	1.58	1.03	RAD23, isoform I
TC165323	1.02	1.74	2.93	0.61	esterase
TC165315	0.97	1.29	1.22	1.04	Malate dehydrogenase
TC165279	0.86	1.37	1.23	0.96	Cyc07-like protein
TC165274	0.96	0.83	0.84	0.93	Protein THYLAKOID FORMATION1
TC165273	0.94	1.34	1.20	1.04	Actin
TC165237	1.45	0.88	1.17	1.05	BTF3-like transcription factor
TC165221	2.14	0.43	0.50	1.45	30S ribosomal protein S9
TC165209	1.11	0.78	0.94	0.93	Chaperone DnaK
TC165098	0.75	1.57	0.97	1.21	Glutathione S-transferase
TC165055	1.02	2.72	2.01	1.41	1-aminocyclopropane-1-carboxylate oxidase
TC165048	1.07	0.70	0.77	0.95	50S ribosomal protein L12
TC165047	1.18	0.35	0.42	1.03	Single-stranded DNA binding protein
TC165045	1.12	1.20	1.03	1.27	ABI3-interacting protein 1
TC165027	1.16	1.12	1.26	1.03	Succinyl-CoA ligase alpha 1 subunit

TC165011	0.95	1.06	1.17	0.90	lysosomal thiol reductase
TC165002	0.94	0.93	1.24	0.69	Copper-containing amine oxidase
TC164986	0.95	0.69	0.57	1.12	Triosephosphate isomerase
TC164981	1.14	1.02	1.34	0.91	Light-induced protein
TC164963	1.22	1.31	1.55	1.04	Fructose-bisphosphate aldolase
TC164953	1.00	1.05	1.25	0.84	26S proteasome regulatory subunit S5A
TC164936	1.14	4.35	3.98	1.37	Endochitinase 2 precursor
TC164886	0.96	0.72	0.62	1.12	Phosphoglucomutase
TC164877	1.15	0.40	0.44	1.16	Magnesium-chelatase subunit
TC164873	1.10	1.25	1.54	0.89	Putative carboxymethylenebutenolidase
TC164868	0.93	1.94	2.67	0.75	Xylose isomerase
TC164851	0.91	1.05	1.32	0.69	13-lipoxygenase
TC164848	0.92	0.84	0.76	1.03	Glyoxalase I putative
TC164832	1.13	0.89	0.69	1.43	Gamma hydroxybutyrate dehydrogenase
TC164825	1.32	0.70	0.96	0.96	24K germin like protein precursor
TC164815	1.11	0.74	0.77	1.06	Soluble inorganic pyrophosphatase 1
TC164770	1.04	1.08	0.85	1.31	Ribonucleoprotein 1
TC164767	0.84	1.24	0.97	1.07	Heat shock protein 70
TC164756	1.01	1.35	1.30	1.07	plastid-lipid associated protein
TC164695	1.03	1.36	1.66	0.84	14-3-3 protein
TC164678	0.88	1.16	1.10	0.93	Phosphoglycerate dehydrogenase
TC164671	1.17	4.76	2.27	2.46	Endochitinase 4 precursor
TC164666	0.78	1.89	1.37	1.05	Elongation factor EF-2
TC164637	0.99	1.22	1.10	1.14	Ribosomal protein L3
TC164625	1.03	2.31	1.96	1.23	Patellin 1
TC164589	1.07	1.29	1.34	1.03	Glyceraldehyde 3-phosphate dehydrogenase
TC164532	0.82	1.47	1.21	1.02	Heat shock cognate protein 80
TC164517	2.15	0.35	0.66	1.00	undetermined protein
TC164504	1.09	2.32	3.37	0.76	Peroxidase
TC164497	1.15	0.44	0.63	0.77	Thiamin biosynthetic enzyme
TC164491	1.07	1.37	0.84	1.82	Nucleic acid binding protein
TC164483	0.72	1.08	0.72	1.08	Ribosomal protein L3
TC164460	0.89	1.47	1.42	0.92	Isopentenyl diphosphate isomerase
TC164410	1.02	2.83	2.18	1.32	Isocitrate dehydrogenase [NADP]
TC164403	1.40	1.29	1.67	1.15	60S ribosomal protein L1
TC164402	0.99	1.13	1.14	0.98	Aspartate aminotransferase
TC164401	1.32	1.52	1.65	1.14	nucleoid DNA binding protein precursor
TC164387	0.95	1.15	0.88	1.25	Pyridoxine biosynthesis protein
TC164369	0.72	0.67	0.48	0.98	Alanine aminotransferase
TC164363	0.76	1.66	0.88	1.38	undetermined protein
TC164361	1.00	0.66	0.65	1.02	RuBisCO large subunit-binding protein
TC164360	1.12	0.77	0.88	0.98	Chaperonin 21 precursor
TC164357	1.14	1.30	1.42	1.03	RAD23-like
TC164342	1.04	0.61	0.65	0.97	peroxisomal (S)-2-hydroxy-acid oxidase 2
TC164340	0.94	0.80	0.79	0.97	Glyceraldehyde-3-phosphate dehydrogenase
TC164338	1.09	0.90	1.00	0.98	Dehydroascorbate reductase-like protein
TC164333	0.80	3.23	0.91	1.38	Pre-pro-cysteine proteinase precursor
TC164329	0.83	1.61	1.25	1.14	LeArcA1 protein
TC164318	1.00	7.42	6.12	1.12	Endochitinase precursor
TC164316	0.93	2.01	1.84	1.05	Enolase
TC164309	1.00	1.29	1.03	1.26	Fructose-bisphosphate aldolase
TC164307	0.92	0.54	0.45	1.07	Fructose-bisphosphate aldolase

TC164237	1.09	0.93	0.81	1.28	Cyclin delta-3
TC164233	0.95	1.29	0.87	1.43	Aspartate aminotransferase
TC164220	1.26	1.48	1.92	0.96	Enoyl-CoA hydratase/isomerase
TC164200	1.03	1.39	1.06	1.42	40S ribosomal protein S2
TC164183	1.11	1.07	1.23	0.95	Elongation factor-like protein
TC164182	0.81	1.57	1.13	1.11	Putative subtilisin-like serine proteinase
TC164175	1.08	1.25	1.55	0.85	Ribosomal protein L5
TC164171	0.90	1.00	0.73	1.21	Clp protease 2 proteolytic subunit precursor
TC164150	1.21	1.67	1.67	1.22	DS2 protein
TC164145	0.87	1.30	1.54	0.68	Oxygen-evolving enhancer protein 1
TC164121	0.90	0.56	0.45	1.09	Fructose-bisphosphate aldolase
TC164104	0.99	0.54	0.46	1.13	Fructose-bisphosphate aldolase
TC164094	0.90	0.51	0.47	0.99	Catalase isozyme 2
TC164093	0.78	1.73	1.13	1.14	Aconitase
TC164075	1.01	0.81	0.64	1.26	CDSP32 protein
TC164069	1.17	1.41	1.50	1.09	CXE carboxylesterase
TC164053	1.01	0.74	0.79	0.92	Chloroplast HSP70
TC164004	1.07	1.04	1.29	0.88	Phosphoribosylformylglycinamidine ligase
TC164001	1.08	1.03	1.55	0.68	Oxygen-evolving enhancer protein 1
TC163988	1.21	0.89	1.09	1.00	Elongation factor TuA, chloroplast precursor
TC163970	0.79	1.51	1.06	1.16	Ascorbate peroxidase
TC163967	0.97	0.70	0.64	1.05	Phosphoglycerate kinase
TC163934	1.01	1.33	1.27	1.06	26S protease regulatory subunit 6A homolog
TC163877	0.92	0.64	0.57	1.01	peroxisomal (S)-2-hydroxy-acid oxidase 2
TC163804	0.95	0.79	0.78	0.97	Glyceraldehyde-3-phosphate dehydrogenase
TC163771	0.95	1.00	1.07	0.92	Fructose-bisphosphate aldolase
TC163769	1.44	1.47	2.99	0.58	Acidic endochitinase
TC163763	1.01	1.60	1.75	0.91	Citrate synthase
TC163746	1.11	1.31	1.64	0.89	Auxin-induced protein
TC163703	1.03	1.28	1.37	0.95	CT099
TC163680	1.33	1.34	1.42	1.26	DS2 protein
TC163648	1.42	0.76	1.33	0.77	Serine hydroxymethyltransferase
TC163642	1.12	4.50	9.80	0.51	Peroxidase
TC163624	1.07	1.35	1.41	1.04	26S protease regulatory subunit 6B
TC163618	1.06	0.97	0.88	1.16	Diaminopimelate epimerase
TC163615	1.07	1.12	1.32	0.91	Adenosine kinase isoform 2S
TC163600	0.98	1.42	0.92	1.51	40S ribosomal protein S4
TC163599	0.87	1.09	1.82	0.62	Chlorophyll a-b binding protein 8
TC163589	1.18	0.99	1.36	0.85	Elongation factor TuB
TC163586	0.87	0.96	0.69	1.21	Peptide methionine sulfoxide reductase
TC163583	0.92	1.48	1.62	0.83	14-3-3 protein
TC163577	0.81	1.10	0.82	1.10	S-adenosylmethionine synthetase 2
TC163566	0.97	1.40	2.50	0.53	Nucleoid DNA-binding-like protein
TC163559	0.97	1.42	1.65	0.83	14-3-3 protein 10
TC163554	1.06	1.20	1.17	1.09	Heat shock 70 kDa protein
TC163544	0.96	0.95	0.96	0.97	Thioredoxin peroxidase
TC163533	0.97	1.67	1.14	1.33	Aluminum-induced protein-like
TC163500	0.95	0.61	0.46	1.20	Diaminopimelate decarboxylase 2
TC163499	1.15	0.59	0.62	1.10	Fruit protein PKIWI502
TC163473	0.94	0.59	0.51	1.08	Sedoheptulose-1 7-bisphosphatase
TC163469	0.80	1.04	0.83	1.02	S-adenosylmethionine synthetase
TC163459	0.95	1.31	1.26	0.99	Methionine synthase

TC163449	0.80	1.43	1.03	1.12	Cytosolic ascorbate peroxidase 1
TC163439	0.93	1.09	0.83	1.22	Triosephosphate isomerase
TC163414	0.91	1.94	1.98	0.80	Fasciclin-like arabinogalactan protein 14
TC163395	1.18	1.08	1.15	1.08	Fructose-1,6-bisphosphatase
TC163384	1.04	0.94	1.37	0.68	Oxygen-evolving enhancer protein 1
TC163381	1.07	1.15	1.34	0.93	14-3-3 protein
TC163377	1.36	0.96	0.98	1.37	25 kDa protein dehydrin
TC163374	0.98	8.19	8.05	1.07	Osmotin-like protein
TC163372	1.08	1.48	1.44	1.11	Eukaryotic initiation factor 4A-2
TC163367	0.74	0.82	0.58	0.95	Aminotransferase 2
TC163356	0.95	1.23	1.27	0.91	Actin
TC163344	1.30	1.22	2.52	0.65	ATP synthase subunit beta
TC163337	1.05	1.01	1.31	0.80	Oxygen-evolving enhancer protein 2
TC163316	1.06	0.72	0.58	1.34	Aldo-keto reductase
TC163314	1.00	0.77	0.87	0.94	28 kDa ribonucleoprotein
TC163302	0.98	0.92	0.98	0.96	Epoxide hydrolase
TC163292	1.40	1.28	1.98	0.92	Elongation factor 1-alpha
TC163269	1.24	1.38	1.26	1.36	Ribosomal protein S6-like protein
TC163250	0.78	0.59	0.41	1.09	Transketolase 1
TC163245	0.92	1.60	1.45	1.02	Phosphoglycerate mutase
TC163242	0.94	1.60	1.27	1.15	Alpha-1,4-glucan-protein synthase
TC163239	1.04	1.13	1.10	1.08	Cytosolic cysteine synthase
TC163237	1.22	1.42	2.07	0.83	Protein disulfide isomerase
TC163234	1.19	1.69	2.00	1.20	Class I chitinase
TC163226	0.69	0.91	0.60	1.05	Glycine dehydrogenase
TC163215	0.91	1.73	1.33	1.17	Short chain dehydrogenase
TC163212	0.96	1.48	1.74	0.82	14-3-3 protein
TC163210	1.06	1.50	2.49	0.65	Harpin binding protein 1
TC163209	0.96	3.62	2.49	1.42	Endochitinase 1 precursor
TC163195	1.82	1.94	2.62	1.19	1,3-beta-D-glucan glucanohydrolase
TC163179	1.23	7.94	8.23	1.19	Glucan endo-1,3-beta-glucosidase
TC163174	1.23	1.57	2.51	0.77	Suberization-associated anionic peroxidase
TC163169	1.04	1.04	1.12	0.96	Malate dehydrogenase
TC163152	0.81	0.70	0.44	1.18	Ribulose bisphosphate carboxylase
TC163139	0.93	1.15	1.40	0.78	Tubulin beta-1 chain
TC163136	1.19	0.56	0.80	0.80	ATP synthase CF0 subunit I
TC163128	1.06	1.20	1.20	1.05	Succinyl CoA ligase beta subunit
TC163112	0.86	1.14	0.97	1.01	UTP-glucose-1-phosphate uridylyltransferase
TC163104	0.79	1.06	1.21	0.71	Alpha-tubulin
TC163098	1.18	0.86	1.06	0.96	Asp
TC163092	1.01	4.30	2.79	1.54	Catalase
TC163076	1.01	1.28	0.98	1.36	Leucine aminopeptidase
TC163071	0.67	1.62	0.96	1.05	Glucose-6-phosphate isomerase
TC163054	0.53	3.68	2.19	0.91	Sucrose synthase 2
TC163042	0.50	1.85	0.88	1.04	Phosphoenolpyruvate carboxylase
TC163028	0.64	1.47	0.56	2.15	Alpha-glucan water dikinase
NP005933	0.85	1.38	1.13	1.04	actin
EG014698	1.04	1.34	1.58	0.85	Benzoquinone reductase
EG012093	1.18	1.29	1.57	0.98	60S ribosomal protein L12
EG009532	1.31	1.37	1.40	1.28	Ribosomal protein PETRP
DR037760	1.06	0.92	1.07	0.91	Glutaredoxin S12
DR036204	1.34	1.50	1.33	1.47	Aminotransferase

DR034516	1.09	1.20	1.48	0.87	Lactoylglutathione lyase
CX162516	0.98	1.51	0.95	1.42	Phytophthora-inhibited protease 1
CX161954	1.35	0.85	0.69	1.68	Aspartic protease inhibitor 10 precursor
CV504216	1.15	1.81	1.69	1.29	Serine protease
CV491918	1.10	1.22	1.28	1.02	Late embryogenesis-like protein
CV475703	1.06	0.90	1.05	0.92	Glutathione-s-transferase theta
CV472133	0.94	1.22	1.06	1.08	Neutral leucine aminopeptidase
CV470531	1.47	0.84	1.21	0.97	Elongation factor TuB
CK863803	1.20	2.43	2.79	1.03	Isocitrate dehydrogenase [NADP]
CK852345	1.05	1.42	1.56	0.94	Adenine phosphoribosyltransferase-like
CK276749	1.21	1.48	1.76	1.01	Subtilisin-like protease
CK275846	1.17	0.90	1.97	0.79	undetermined protein
CK263954	1.48	1.85	2.17	1.10	Class II chitinase
CK263733	0.93	0.38	0.30	1.18	Elongation factor G
CK260807	0.96	1.37	2.13	0.68	Hsc70
CK251632	1.05	2.42	2.13	1.23	Induced stolen tip protein TUB8
BQ510637	1.18	0.95	1.19	0.94	Endo-1,3-1,4-beta-d-glucanase
BQ506244	1.11	1.13	0.98	1.37	Serpin
BQ046158	1.05	3.14	4.47	0.74	Peroxidase
BM405677	0.96	0.75	0.48	1.06	Porphobilinogen deaminase
BM111091	1.02	0.49	0.46	1.07	Ribulose bisphosphate carboxylase
BG594905	1.07	1.23	1.42	0.93	Anthranilate synthase component I
BG592939	0.84	0.79	1.02	0.57	Haze protective factor 1 precursor
BE924235	1.37	0.95	0.87	1.49	Arginase 2
AM909595	0.95	1.65	1.63	0.97	Copper chaperone
AM907060	1.30	6.16	8.75	0.94	Benzoquinone reductase

Appendix E. *P. infestans* Proteins Identified from the Cell Wall and Cytoplasmic Fractions of Infected Phi-Treated and Infected Control Samples

Number/Protein Identification

| PITG_02687 | conserved hypothetical protein (107 aa)

| PITG_05636 | transaldolase (335 aa)

| PITG_07048 | superoxide dismutase, mitochondrial precursor (221 aa)

| PITG_15248 | catalase (523 aa)

| PITG_02853 | 3,2-trans-enoyl-CoA isomerase (283 aa)

| PITG_15045 | trans-2-enoyl-CoA reductase, putative (349 aa)

| PITG_07328 | manganese superoxide dismutase (214 aa)

| PITG_07048 | superoxide dismutase, mitochondrial precursor (221 aa)

| PITG_17406 | enoyl-CoA hydratase, mitochondrial precursor (261 aa)

| PITG_04315 | conserved hypothetical protein (339 aa)

| PITG_12682 | cytochrome c (113 aa)

| PITG_20402 | conserved hypothetical protein (145 aa)

| PITG_07098 | para-aminobenzoate synthase, putative (796 aa)

| PITG_08034 | conserved hypothetical protein (269 aa)

| PITG_11566 | conserved hypothetical protein (1001 aa)

| PITG_15504 | thioredoxin peroxidase, putative (209 aa)

| PITG_06265 | cysteine synthase, putative (357 aa)

| PITG_06595 | PATP synthase subunit beta, putative (473 aa)

| PITG_16080 |hypothetical protein (347 aa)

| PITG_20342 | conserved hypothetical protein (333 aa)

| PITG_16486 | glycoside hydrolase, putative (603 aa)

| PITG_02382 | conserved hypothetical protein (117 aa)

| PITG_13614 | malate dehydrogenase, mitochondrial precursor (336 aa)

| PITG_04457 | tripeptidyl-peptidase, putative (1365 aa)

| PITG_03473 | callose synthase, putative (2027 aa)

| PITG_10193 | ubiquitin, putative (157 aa)

| PITG_16048 | triosephosphate isomerase (280 aa)

| PITG_16663 | avr1 secreted RxLR effector peptide, putative (209 aa)

| PITG_14968 | cAMP-dependent protein kinase catalytic subunit alpha (448 aa)

| PITG_01253 | aldehyde dehydrogenase, mitochondrial precursor (519 aa)

| PITG_18772 | Mitochondrial Carrier (MC) Family (530 aa)

| PITG_03514 | DNA ligase, putative (972 aa)

| PITG_13614 | malate dehydrogenase, mitochondrial precursor (336 aa)

| PITG_02033 | alkylated DNA repair protein alkB 8 (641 aa)

| PITG_18398 | conserved hypothetical protein (309 aa)

| PITG_00730 | conserved hypothetical protein (425 aa)

| PITG_03571 | phosphatidylinositol kinase (PIK-L3) (4590 aa)

| PITG_08392 | FACT complex subunit SPT16, putative (1078 aa)

| PITG_18049 | chromosome segregation protein, putative (1212 aa)

| PITG_21071 | threonyl-tRNA synthetase (745 aa)

| PITG_10492 | lactation elevated protein 1 (423 aa)

| PITG_18001 | ubiquitin, putative (176 aa)

| PITG_07056 | isocitrate dehydrogenase, mitochondrial precursor (428 aa)

| PITG_14861 | conserved hypothetical protein (539 aa)

| PITG_01689 | hydroxyacylglutathione hydrolase, putative (309 aa)

| PITG_06906 |conserved hypothetical protein (590 aa)

| PITG_11252 | heat shock protein 70 (655 aa)

| PITG_11249 |heat shock 70 kDa protein (654 aa)

| PITG_14195 | enolase (458 aa)

| PITG_03879 | conserved hypothetical protein (2411 aa)

| PITG_01782 | conserved hypothetical protein (633 aa)

| PITG_06823 | conserved hypothetical protein (281 aa)

| PITG_00284 | phospholipase D, Pi-PXTM-PLD (1808 aa)

| PITG_16057 | enolase-like protein, putative (571 aa)

| PITG_18012 | aldehyde dehydrogenase, mitochondrial precursor (495 aa)

| PITG_11244 | heat shock 70 kDa protein (664 aa)

| PITG_00527 | luminal-binding protein 3 precursor (657 aa)

| PITG_02940 | phosphoglycerate mutase family (230 aa)

| PITG_23305 | hypothetical protein (281 aa)

| PITG_02527 | histone H2A (137 aa)

| PITG_01043 | 3-phosphoinositide-dependent protein kinase (486 aa)

| PITG_04640 | translation elongation factor 1-alpha, putative (444 aa)

| PITG_09218 | secreted RxLR effector peptide, putative (166 aa)

| PITG_00832 | conserved hypothetical protein (113 aa)

| PITG_14819 | hypothetical protein (484 aa)

| PITG_10922 | fatty acid synthase subunit alpha, putative (4048 aa)

| PITG_10926 | fatty acid synthase subunit alpha, putative (3847 aa)

| PITG_18025 | Pfatty acid synthase subunit alpha, putative (4124 aa)

| PITG_03550 | histone H2B (116 aa)

| PITG_02026 | succinyl-CoA ligase subunit alpha (340 aa)

| PITG_03549 | coatomer subunit gamma, putative (911 aa)

| PITG_03294 | 60S ribosomal protein L6, putative (221 aa)
| PITG_08023 | HECT E3 ubiquitin ligase, putative (2110 aa)
| PITG_17033 | Annexin (Annexin) Family (329 aa)
| PITG_09402 | phosphoglycerate kinase (243 aa)
| PITG_00941 | 60S ribosomal protein L21-1 (161 aa)
| PITG_22406 | conserved hypothetical protein (319 aa)
| PITG_11329 | Annexin (Annexin) Family (1275 aa)
| PITG_09431 | 40S ribosomal protein S19-3 (155 aa)
| PITG_09445 | conserved hypothetical protein (119 aa)
| PITG_04522 | peptidyl-prolyl cis-trans isomerase (172 aa)
| PITG_09540 | 60S ribosomal protein L19-1 (186 aa)
| PITG_12990 | glutathione transferase, theta class (227 aa)
| PITG_07328 | manganese superoxide dismutase (214 aa)
| PITG_07173 | 40S ribosomal protein S15 (156 aa)
| PITG_03486 | conserved hypothetical protein (118 aa)
| PITG_03477 | 60S ribosomal protein L7a-2 (264 aa)
| PITG_07400 | 2,3-bisphosphoglycerate phosphoglycerate mutase (261 aa)
| PITG_17261 | 60S acidic ribosomal protein P0 (319 aa)
| PITG_09345 | 40S ribosomal protein S5-2 (197 aa)
| PITG_03552 | histone H4 (104 aa)
| PITG_06415 | heat shock protein 90 (707 aa)
| PITG_02527 | histone H2A (137 aa)
| PITG_14850 | 40S ribosomal protein S7 (191 aa)
| PITG_11171 | conserved hypothetical protein (457 aa)
| PITG_11244 | heat shock 70 kDa protein (664 aa)
| PITG_03881 | histone H2A (140 aa)
| PITG_06427 | serine hydroxymethyltransferase (503 aa)
| PITG_10031 | lysosomal alpha-mannosidase, putative (1024 aa)
| PITG_06595 | ATP synthase subunit beta, putative (473 aa)
| PITG_18295 | conserved hypothetical protein (289 aa)
| PITG_14913 | 40S ribosomal protein S16 (159 aa)
| PITG_09610 | U6 snRNA-associated Sm-like protein (83 aa)
| PITG_06548 | conserved hypothetical protein (1289 aa)
| PITG_03294 | 60S ribosomal protein L6, putative (221 aa)
| PITG_02502 | T-complex protein 1 subunit zeta (858 aa)
| PITG_02197 | DNA topoisomerase, putative (718 aa)
| PITG_00527 | luminal-binding protein 3 precursor (657 aa)
| PITG_01922 | 40S ribosomal protein SA (284 aa)

| PITG_00156 | beta-tubulin (447 aa)
| PITG_02026 | succinyl-CoA ligase subunit alpha (340 aa)
| PITG_07098 | para-aminobenzoate synthase, putative (796 aa)
| PITG_11252 | heat shock protein 70 (655 aa)
| PITG_10193 | ubiquitin, putative (157 aa)
| PITG_20786 | lipase, putative (475 aa)
| PITG_13664 | conserved hypothetical protein (195 aa)
| PITG_00850 | thioredoxin-dependent peroxide reductase (378 aa)
| PITG_19999 | 40S ribosomal protein S14 (151 aa)
| PITG_09555 | ubiquitin-ribosomal fusion protein, putative (129 aa)
| PITG_19017 | 14-3-3 protein epsilon (250 aa)
| PITG_10931 | conserved hypothetical protein (555 aa)
| PITG_15786 | heat shock 70 kDa protein, mitochondrial precursor (634 aa)
| PITG_04457 | tripeptidyl-peptidase, putative (1365 aa)
| PITG_01770 | leukocyte receptor cluster member 8 (592 aa)
| PITG_11966 | chaperonin CPN60-1, mitochondrial precursor (598 aa)
| PITG_00229 | 26S protease regulatory subunit S10B (395 aa)
| PITG_23305 | hypothetical protein (281 aa)
| PITG_15504 | thioredoxin peroxidase, putative (209 aa)
| PITG_03698 | enolase (455 aa)
| PITG_14195 | enolase (458 aa)
| PITG_01711 | anthranilate synthase component I, putative (505 aa)
| PITG_17083 | Crinkler (CRN) family protein, pseudogene (405 aa)
| PITG_17243 | conserved hypothetical protein (853 aa)
| PITG_11247 | heat shock 70 kDa protein (654 aa)
| PITG_22103 | glyceraldehyde-3-phosphate dehydrogenase (334 aa)
| PITG_18001 | ubiquitin, putative (176 aa)
| PITG_08932 | conserved hypothetical protein (383 aa)
| PITG_13301 | H- or Na-translocating V-type and A-type ATPase (619 aa)
| PITG_07790 | peroxisomal (S)-2-hydroxy-acid oxidase, putative (383 aa)
| PITG_04640 | translation elongation factor 1-alpha, putative (444 aa)
| PITG_08761 | nucleoside diphosphate kinase B (222 aa)
| PITG_01689 | hydroxyacylglutathione hydrolase, putative (309 aa)
| PITG_18398 | conserved hypothetical protein (309 aa)
| PITG_15117 | actin-like protein (377 aa)
| PITG_12185 | 26S protease regulatory subunit 4 (446 aa)
| PITG_20264 | 40S ribosomal protein S13 (152 aa)
| PITG_19129 | ATP-dependent RNA helicase eIF4A, putative (412 aa)

| PITG_17130 | glyceraldehyde-3-phosphate dehydrogenase, putative (525 aa)
| PITG_12286 | ADP-ribosylation factor family (182 aa)
| PITG_07949 | alpha-tubulin, putative (455 aa)
| PITG_04709 | DNA ligase, putative (3897 aa)
| PITG_11369 | conserved hypothetical protein (480 aa)
| PITG_08764 | Voltage-gated Ion Channel (VIC) Superfamily (1682 aa)
| PITG_13614 | malate dehydrogenase, mitochondrial precursor (336 aa)
| PITG_15078 | actin-like protein (376 aa)
| PITG_22840 | peroxisomal (S)-2-hydroxy-acid oxidase, putative (329 aa)
| PITG_02940 | phosphoglycerate mutase family (230 aa)
| PITG_01469 | conserved hypothetical protein (1009 aa)
| PITG_22922 | secreted RxLR effector peptide, putative (489 aa)
| PITG_10860 | conserved hypothetical protein (269 aa)
| PITG_15618 | conserved hypothetical protein (705 aa)
| PITG_01550 | conserved hypothetical protein (1214 aa)
| PITG_15598 | conserved hypothetical protein (165 aa)
| PITG_02565 | protein kinase, putative (390 aa)
| PITG_06474 | conserved hypothetical protein (380 aa)
| PITG_03009 | conserved hypothetical protein (115 aa)
| PITG_11249 | heat shock 70 kDa protein (654 aa)
| PITG_06514 | calmodulin (150 aa)
| PITG_04910 | serine/threonine protein kinase (715 aa)
| PITG_04339 | secreted RxLR effector peptide, putative (241 aa)
| PITG_00613 | 26S protease regulatory subunit 8 (402 aa)
| PITG_15918 | conserved hypothetical protein (2212 aa)
| PITG_07212 | conserved hypothetical protein (446 aa)
| PITG_17516 | S-adenosylmethionine synthetase 2 (392 aa)
| PITG_16080 | hypothetical protein (347 aa)
| PITG_21150 | Folate-Biopterin Transporter (FBT) Family (518 aa)
| PITG_10757 | beta-glucan synthesis-associated protein, putative (725 aa)
| PITG_20212 | intraflagellar transport protein 172 (1783 aa)
| PITG_15530 | kinesin-like protein KIF9 (656 aa)
| PITG_11913 | heat shock cognate 70 kDa protein (787 aa)
| PITG_18446 | 26S protease regulatory subunit 6B (406 aa)
| PITG_00160 | conserved hypothetical protein (2625 aa)
| PITG_03432 | conserved hypothetical protein (1712 aa)
| PITG_10169 | 26S protease regulatory subunit 7 (439 aa)

| PITG_09009 | conserved hypothetical protein (386 aa)

| PITG_20342 | conserved hypothetical protein (333 aa)

| PITG_16048 | triosephosphate isomerase (280 aa)

| PITG_06982 | short chain dehydrogenase, putative (415 aa)

| PITG_02094 | dnaJ heat shock protein (308 aa)

| PITG_03152 | conserved hypothetical protein (1851 aa)

| PITG_16091 | conserved hypothetical protein (239 aa)

| PITG_18027 | histone acetyltransferase, putative (874 aa)

| PITG_08178 | conserved hypothetical protein (669 aa)

Appendix F. Copyright Agreement Letter

Title: Protein Profiling in Potato (*Solanum tuberosum* L.) Leaf Tissues by Differential Centrifugation

Author: Sanghyun Lim, Kenneth Chisholm, Robert H. Coffin, Rick D. Peters, Khalil I. Al-Mughrabi, Gefu Wang-Pruski, and Devanand M. Pinto

Publication: Journal of Proteome Research

Publisher: American Chemical Society
Date: Apr 1, 2012

PERMISSION/LICENSE IS GRANTED FOR YOUR ORDER AT NO CHARGE

This type of permission/license, instead of the standard Terms & Conditions, is sent to you because no fee is being charged for your order. Please note the following:

Permission is granted for your request in both print and electronic formats, and translations.
If figures and/or tables were requested, they may be adapted or used in part.
Please print this page for your records and send a copy of it to your publisher/graduate school.
Appropriate credit for the requested material should be given as follows: "Reprinted (adapted) with permission from (COMPLETE REFERENCE CITATION). Copyright (YEAR) American Chemical Society." Insert appropriate information in place of the capitalized words.
One-time permission is granted only for the use specified in your request.